

**MULTISCALE ANALYSES OF MICROBIAL POPULATIONS IN
EXTREME ENVIRONMENTS**

A Dissertation
Presented to
The Academic Faculty

by

Robert J. Martinez

In Partial Fulfillment
of the Requirements for the Degree
Doctor of Philosophy in the
School of Biology

Georgia Institute of Technology
August 2008

MULTISCALE ANALYSES OF MICROBIAL POPULATIONS IN EXTREME ENVIRONMENTS

Approved by:

Dr. Patricia A. Sobecky, Advisor
School of Biology
Georgia Institute of Technology

Dr. Thomas J. DiChristina
School of Biology
Georgia Institute of Technology

Dr. Jim C. Spain
School of Civil & Environmental
Engineering
Georgia Institute of Technology

Dr. Martial Taillefert
School of Earth & Atmospheric
Sciences
Georgia Institute of Technology

Dr. Ellery D. Ingall
School of Earth & Atmospheric
Sciences
Georgia Institute of Technology

Date Approved:

This dissertation is dedicated to Mom, Dad, John, and Tony. I'm not sure if words can explain how much your love and support have helped me through the years.

ACKNOWLEDGEMENTS

Without the help and understanding from numerous friends and colleagues, none of this work would have been possible. I would like to thank Patty Sobecky for giving me a chance in her laboratory and for always being available as an advisor and friend.

I thank my committee members: Tom DiChristina, Jim Spain, Martial Taillefert, and Ellery Ingall for their advisement. Additionally, I'd like to thank my committee members for taking the time to discuss aspects of microbial physiology and geochemistry. These discussions have been an invaluable resource for my research endeavors.

I would like to thank all of my friends at Georgia Tech for their support and interest in my work. I thank all my friends in the School of Biology, especially Tracy Hazen, David Giannantonio, Jason Landrum, Justin Burns, and the numerous undergraduate students that have passed through the Sobecky lab. Within the School of Earth and Atmospheric Sciences, I especially thank Melanie Beazley, Jud Partin, and Morris Jones.

Funding for this work was provided by the National Science Foundation and the U.S. Department of Energy.

TABLE OF CONTENTS

	Page
ACKNOWLEDGEMENTS	iv
LIST OF TABLES	xi
LIST OF FIGURES	xii
LIST OF SYMBOLS AND ABBREVIATIONS	xviii
SUMMARY	xxi
 <u>CHAPTER</u>	
1 INTRODUCTION	
1.1 Global sustainability	1
1.2 Extreme environments	6
1.2.1 Marine sedimentary systems	14
1.2.1.1 Cold seeps	15
1.2.1.2 Marine mud volcanoes	17
1.2.2 Terrestrial sedimentary systems	20
1.2.2.1 Shallow subsurface	22
1.2.2.2 Deep subsurface	24
1.3 Microbial detoxification mechanisms	29
1.3.1 Overview of metal detoxification mechanisms	30
1.3.2 Metal reductases	31
1.3.2.1 The <i>mer</i> operon	31
1.3.2.2 The <i>ars</i> operon	33
1.3.3 Metal efflux systems	35

1.3.4 Metal complexation	37
1.4 Dissemination of detoxification mechanisms by horizontal gene transfer	38
1.4.1 Overview of horizontal gene transfer	39
1.4.2 Horizontal gene transfer in marine systems	40
1.4.3 Horizontal gene transfer in terrestrial systems	41
1.5 Applications of microbial processes to global sustainability	43
2 PROKARYOTIC DIVERSITY AND METABOLICALLY ACTIVE MICROBIAL POPULATIONS IN SEDIMENTS FROM AN ACTIVE MUD VOLCANO IN THE GULF OF MEXICO	
2.1 Overview	50
2.2 Summary	51
2.3 Introduction	52
2.4 Results	54
2.4.1 Restriction fragment length polymorphism (RFLP) and rarefaction analyses of 16S rDNA and 16S crDNA GoM clone libraries	54
2.4.2 <i>Bacteria</i> community composition based on 16S rDNA sequence analyses	57
2.4.3 Phylogenetic diversity of metabolically active <i>Bacteria</i>	64
2.4.4 <i>Archaea</i> community composition based on 16S rDNA sequence analyses	65
2.4.5 Phylogenetic diversity of metabolically active <i>Archaea</i>	66
2.4.6 Quantitative PCR of ANME-2A and ANME-2C	67
2.5 Discussion	69
2.6 Experimental procedures	73
2.6.1 Site description and sampling	73
2.6.2 Preparation of reagents and materials used with RNA extractions	74

2.6.3	Nucleic acid isolation	74
2.6.4	Reverse transcription and amplification of rRNA	75
2.6.5	Polymerase chain reaction amplification of genomic DNA	76
2.6.6	Environmental clone library construction	77
2.6.7	Phylogenetic and rarefaction analysis	77
2.6.8	Quantitative PCR of ANME-2A and ANME-2C environmental rDNA	78
2.6.9	Data analysis	79
2.7	Conclusions	80
2.8	Acknowledgements	80
3	HORIZONTAL GENE TRANSFER OF P _{IB} -TYPE ATPASES AMONG <i>BACTERIA</i> ISOLATED FROM RADIONUCLIDE- AND METAL- CONTAMINATED SUBSURFACE SOILS	
3.1	Overview	81
3.2	Summary	82
3.3	Introduction	83
3.4	Results and discussion	86
3.4.1	Viable bacterial populations from contaminated soils and metal resistance phenotypes	86
3.4.2	Horizontal transfer of P _{IB} -type ATPases	88
3.4.3	Tolerance to uranium	96
3.5	Experimental procedures	100
3.5.1	Sample site	100
3.5.2	Strain isolation, determination of plasmids, and metal resistance	101
3.5.3	Uranium tolerance assays	103
3.5.4	PCR amplification of 16S rRNA and P _{IB} -ATPases	103

3.5.5 Sequencing and analyses	104
3.5.6 Nucleotide sequence accession numbers	105
3.6 Conclusions	105
3.7 Acknowledgements	106
4 AEROBIC URANIUM (VI) BIOPRECIPITATION BY METAL-RESISTANT BACTERIA ISOLATED FROM RADIONUCLIDE-AND METAL-CONTAMINATED SUBSURFACE SOILS	
4.1 Overview	107
4.2 Summary	107
4.3 Introduction	108
4.4 Results	110
4.4.1 Determination of phosphatase activity in subsurface strains	110
4.4.2 Molecular characterization of NSAPs	113
4.4.3 SDS-PAGE phosphatase activity assay	118
4.4.4 Aerobic biomineralization of U(VI) by microbial phosphate accumulation	119
4.4.5 Electron microscopy of biomineralized U(VI)	124
4.4.6 Anaerobic biomineralization of U(VI) by microbial phosphate accumulation	126
4.4.7 Aerobic hydrolysis of sodium tripolyphosphate	127
4.5 Discussion	129
4.6 Experimental procedures	134
4.6.1 Subsurface strains and growth conditions	134
4.6.2 Phosphatase activity assays	135
4.6.3 Nucleic acid isolation, NSAP primer design, and PCR amplification of genomic DNA	137
4.6.4 Selection of bacterial NSAP protein sequences	138

4.6.5 Phylogenetic analysis	140
4.6.6 Modeling of uranium speciation in simulated groundwater	140
4.6.7 Cell enumeration, phosphate, and uranium measurements	141
4.6.8 Electron microscopy	142
4.6.9 Data analysis	143
4.7 Conclusions	143
4.8 Acknowledgements	144
5 BIOTIC AND ABIOTIC CATALYZED PHOSPHATE HYDROLYSIS	
5.1 Overview	145
5.2 Summary	145
5.3 Introduction	146
5.4 Results	148
5.4.1 Contaminated soil slurry incubations	148
5.4.2 PhyloChip microarray analysis	149
5.4.3 Hydrous ferric oxide slurry incubations	150
5.5 Discussion	154
5.6 Experimental procedures	157
5.6.1 Sampling site	157
5.6.2 Hydrous ferric oxide synthesis	158
5.6.3 Subsurface strains and growth conditions	158
5.6.4 Phosphate measurement	159
5.6.5 Nucleic acid isolation, PCR amplification, and microarray analysis	159
5.7 Conclusions	160
5.8 Acknowledgements	160

6 CONCLUSIONS	161
6.1 Future directions	165
REFERENCES	168
VITA	204

LIST OF TABLES

	Page
Table 1.1: Microbial environments defined by extremes in pH, salinity, and temperature	13
Table 2.1: Representative archaeal and bacterial clones sequenced from both 16S rDNA and 16S crDNA clone libraries (Table illustrates sequences that appeared 4 or more times for each respective phylotype)	61
Table 2.2: Determination of anaerobic methane oxidizing archaeal ANME-2A and ANME-2C populations	68
Table 3.1: Oligonucleotide primers used during nested PCRs to amplify P _{IB} -type ATPases and number of isolates which yielded amplicons	90
Table 3.2: Support for acquisition of P _{IB} -type ATPases by HGT in subsurface isolates from radionuclide- and metal-contaminated soils	95
Table 3.3: Viable cell counts determined after washing and after 1 h of incubation at pH 4 either with or without 200 μ M uranyl acetate	97
Table 4.1: Oligonucleotide primers for PCR amplification of non-specific acid phosphatases	117

LIST OF FIGURES

	Page
Figure 1.1: Concentrations of atmospheric methane, nitrous oxide, and carbon dioxide measured over the past 50,000 years. Methane and nitrous oxide ice core data was obtained from the Greenland Ice sheet Project 2. Carbon dioxide ice core data was obtained from the Taylor dome on the East Antarctic ice sheet. Annual atmospheric methane, nitrous oxide, and carbon dioxide concentrations were sampled from Mauna Loa, Hawaii by the Commonwealth Scientific and Industrial Research Organisation, Australia.	3
Figure 1.2: Salt diapir driven formation of marine mud volcanoes. Migration of deep subsurface salt diapirs toward the seafloor deforms the overlying sedimentary strata (dotted lines) and ultimately forms the characteristic dome or conical topologies. Additionally, salt diapirism leads to the over pressurization and release of hydrocarbon pools on to the surrounding sediments and overlying water.	18
Figure 1.3: Gulf of Mexico cold seep research sites located within the Green Canyon (GC185 and GC 234) and Garden Banks (GB425) lease blocks. The GC185 and GC234 sites are defined by breaching methane hydrates and hydrocarbon seepage. The GB425 site (inset seafloor acoustic image) contains a mud volcano that releases gaseous hydrocarbons and brine on to the surrounding sediments and overlying water.	20
Figure 1.4: (A). The ORFRC S-3 wastes ponds with a storage capacity of 9.5 million liters and received uranium nitrate waste as well as sludge waste from other activities within the Oak Ridge reservation, Savannah River site, and the Idaho National Engineering Lab from 1951-1983. (B). The current site of S-3 ponds which underwent neutralization and denitrification prior to the construction of the multi-layer impermeable cap.	29
Figure 1.5: Depiction of microbial heavy metal detoxification systems driven by redox state, chemiosmotic transport, ATPase catalyzed transport and phosphate complexation.	35
Figure 1.6: Characterized microbe-metal interactions applicable to bioremediation strategies.	49
Figure 2.1: Rarefaction curves determined for different RFLP patterns of <i>Archaea</i> and <i>Bacteria</i> 16S rDNA clones (DNA-derived) and 16S crDNA clones (RNA-derived).	55

Figure 2.2: Phylogenetic tree of relationships of 16S rDNA and crDNA *Proteobacteria*-related clone sequences, as determined by distance Jukes-Cantor analysis, from sediments collected from Gulf of Mexico GB425 mud volcano (in boldface) to selected cultured isolates and environmental clones. Sequences derived from DNA templates are denoted by B, RNA templates by BR. Designations of environmental clone sequences: are API, Antarctic pack ice; AO, Arctic Ocean; BS, Black Sea; CM, Cascadia Margin; CR, chlorinated compound reduction; CSS, cold seep sediment; GB, Guaymas Basin; GoM, Gulf of Mexico; HS, hydrocarbon seep; HV, hydrothermal vent; JT, Japan Trench; NS, North Sea; SB, Santa Barbara Basin. GenBank accession numbers are in brackets. Bootstrap values represent 1,000 replicates and only values greater than 50% are reported. The scale bar represents 0.05 substitutions per nucleotide position. Stacked histograms denote rDNA and crDNA phylotypes with 4 or more representative clones detected at each of the following depths; 0-2 cm (□), 6-8 cm (■) and 10-12 cm (■).

56

Figure 2.3: Phylogenetic tree of relationships of 16S rDNA and crDNA non-*Proteobacteria* clone sequences, as determined by distance Jukes-Cantor analysis, from sediments collected from Gulf of Mexico GB425 mud volcano (in boldface) to selected cultured isolates and environmental clones. Designations of environmental clone sequences are: AD, anaerobic digester; CM, Cascadia Margin; DSS, deep subsurface; ES, estuarine sediment; GB, Guaymas Basin; GoM, Gulf of Mexico; JT, Japan Trench; MV, mud volcano; OC, Oregon coast; SBC, Santa Barbara Channel; SCS, South China Sea; SO, Sea of Okhotsk; SR, soil rhizosphere. GenBank accession numbers are in brackets. Bootstrap values represent 1,000 replicates and only values greater than 50% are reported. The scale bar represents 0.05 substitutions per nucleotide position. Stacked histograms denote rDNA and crDNA phylotypes with 4 or more representative clones detected at each of the following depths; 0-2 cm (□), 6-8 cm (■) and 10-12 cm (■).

58

Figure 2.4: Phylogenetic tree of relationships of 16S rDNA and crDNA archaeal clone sequences, as determined by distance Jukes-Cantor analysis from sediments collected from GB425 mud volcano to selected cultured isolates and environmental clones. Sequences derived from DNA templates are denoted by A, RNA templates are denoted by AR. Designations of environmental clone sequences are: CM, Cascadia Margin; DT, digestive tract (marine fish); ER, Eel River; GAB, Great Artesian Basin; GB, Guaymas Basin; GoM, Gulf of Mexico; HV, hydrothermal vent; MS, marine sediments; MT, Mariana Trench; SB, Santa Barbara Basin; SO, Sea of Okhotsk; SP, salt pond. GenBank accession numbers are in brackets. Bootstrap values represent 1,000 replicates and only values greater than 50% are reported. The scale bar represents 0.05 substitutions per nucleotide position. Stacked histograms denote rDNA and crDNA phylotypes with 4 or more representative clones detected at each of the following depths; 0-2 cm (□), 6-8 cm (■) and 10-12 cm (■).

62

Figure 2.5: (A). Frequency of bacterial phylogenetic lineages detected in 16S rDNA (DNA) and 16S crDNA (RNA) clone libraries derived from sediment depth intervals 0 to 2 cm, 6 to 8 cm and 10 to 12 cm. Calculations were based on the total number of clones associated with phylotypes from which a representative clone had been sequenced. (B). Frequency of archaeal phylogenetic lineages detected in 16S rDNA (DNA) and 16S crDNA (RNA) clone libraries derived from sediment depth intervals 0 to 2 cm, 6 to 8 cm and 10 to 12 cm. Calculations were based on the total number of clones associated with phylotypes from which a representative clone had been sequenced.

63

Figure 3.1: Neighbor-joining analysis of (A). 16S rDNA and (B). *zntA/cadA/prbA*-like sequences from either subsurface FRC isolates or from completed genomes. Accession numbers are in parentheses; § denotes FRC strain containing one or more plasmids. Subsurface isolates shown in shaded boxes and connected by a dotted line are positive for horizontal acquired P_{IB} -type ATPases related to *zntA/cadA/prbA*-loci. Bootstrap support >50% is shown. Scale bar for 16S rDNA and *zntA/cadA/prbA* phylogenies represent 0.1 changes per nucleotide position and 0.1 changes per amino acid position, respectively.

92

Figure 4.1: Media types used for identifying potential U-precipitating phosphatase phenotypes. Isolates that displayed a phosphatase-positive phenotype appeared either bright green on TPMG (Fig. 4.1A) or fluorescent when placed under UV light on TP-MUP (Fig. 4.1C). (A). TPMG (B). Tryptose phosphate-MUP (TP-MUP)/visible light (C). TP-MUP/UV light. Strains were streaked onto all three media types as follows: *Arthrobacter* spp. strain (1). X34, (2). V45, (3). AA20 (column 1); *Bacillus* spp. (4). Y7, (5). X18, (6). Y9-2 (column 2) and *Rahnella* spp. (7). Y9602, (8). Y4, (9). Y29 (column 3).

112

Figure 4.2:(**A-D**). PCR amplification of Classes A, B and C non-specific acid phosphatases (NSAPs). Agarose gel lanes are: L - 1-kb DNA ladder, N - no DNA template control, 1 - *Rahnella* sp. Y9602, 2 - *Enterobacter aerogenes* (Class A control), 3 - *Klebsiella pneumoniae* (Class A and B control), 4 - *Escherichia coli* MG1655 (Class B control), 5 - *Salmonella enterica* (Class B control), 6 - *Bacillus cereus* (Class C control), 7 - *Bacillus thuringiensis* (Class C control), 8 - *Bacillus* sp. Y9-2. Genomic DNA extracted from each strain was used as template with each clade- and species-specific NSAP primer sets denoted: (**A**). A(I), (**B**). B(I), (**C**). B(Kp), (**D**). C(I). NSAP phylogeny of bacteria most closely related to subsurface strains *Rahnella* sp. Y9602 and *Bacillus* sp. Y9-2. NCBI GenInfo identifier numbers are indicated in brackets. PCR primers targeted NSAP genes from bacteria belonging to: (**E**). clade A(I), within Class A, (**F**). clade B(I) and *Klebsiella pneumoniae* B(Kp) within Class B, (**G**). clade C(I) within Class C. 114

Figure 4.3:Neighbor-joining (NJ) amino acid phylogentic tree construction of (**A**). Class (A) NSAP and (**B**). Class B and Class C NSAP sequences. All NSAP sequences from were obtained by iterative PSI-BLAST searches of the NCBI protein database. NCBI GenInfo identifier numbers are indicated in brackets. The NSAP sequences for strains Y9602 and Y9-2 were obtained in this study by PCR amplification and sequence analysis. 115

Figure 4.4:Maximum parsimony (MP) amino acid phylogentic tree construction of (**A**). Class (A) NSAP and (**B**). Class B and C NSAP sequences. NCBI GenInfo identifier numbers are indicated in brackets. MP phylogeny is provided to support the robustness of observed NJ tree topology. 116

Figure 4.5:Renatured SDS-PAGE phosphatase activity analysis. Whole-cell lysates (25 µg of total protein/lane) of: **1** - *Klebsiella pneumoniae* ATCC 132 (Class A control), **2** - *Rahnella* sp. Y9602, **3** - *Bacillus cereus* ATCC 14579 (Class C control), **4** - *Bacillus* sp. Y9-2, **M** - molecular weight marker (masses are indicated in kDa). Arrows indicate the expected molecular mass of the the Class A and Class C NSAPs of 25 kDa and 30 kDa, respectively. All strains were grown in nutrient broth pH 5.5 to mid-log phase. 119

Figure 4.6:Synthetic groundwater (pH 5.5) amended with 10 mM G3P (as sole C and P source) and inoculated with either viable or heat-killed control *Rahnella* sp. Y9602 (squares) or *Bacillus* sp. Y9-2 (circles) or *Arthrobacter* sp. X34 (triangles). Abiotic controls were cell-free. Concentrations of: (**A**). Phosphate, (**B**). U(VI) and (**C**). CFU measured as a function of time. Arrow at 36 h denotes the addition of 200 µM U(VI). All incubations were performed under oxic conditions. Error bars denote standard deviation of triplicate experiments. 122

- Figure 4.7: Uranium (VI) speciation as a function of pH in synthetic groundwater (SGW). The open system model at 30°C calculated aqueous and solid phases at equilibrium using the concentrations of ions present in synthetic groundwater, $\text{UO}_2^{2+}(\text{aq}) = 200 \mu\text{M}$, $\text{PO}_4^{3-}(\text{aq}) = 200 \mu\text{M}$ and, $\text{P}_{\text{CO}_2} = 10^{-3.5} \text{ atm}$. Vertical dash-dot line indicates pH of experimental SGW incubations, dotted lines indicate aqueous phase U(VI) species, and solid lines indicate solid phase U(VI) species. 124
- Figure 4.8: Transmission electron micrographs of *Rahnella* sp. Y9602 following uranium biomineralization. **(A.)** Cells associated with extracellular uranium precipitate and **(B.)** cell surface localized uranium precipitate. Arrows in micrographs **(A.)** and **(B.)** indicate regions analyzed via energy dispersive X-ray (EDX) spectroscopy. Inset spectra identify elemental composition of uranium precipitate. 125
- Figure 4.9: Variable-pressure scanning electron micrograph of *Rahnella* sp. Y9602 biomineralized uranium **(A.)** EDX elemental mapping of uranium **(B.)**, phosphorus **(C.)**, and oxygen **(D.)**. 126
- Figure 4.10: Synthetic groundwater (pH 5.5) amended with 10 mM G3P (as sole C and P source) and inoculated with *Rahnella* sp. Y9602 (squares). Concentrations of: **(A.)** Phosphate, **(B.)** U(VI) and **(C.)** CFU measured as a function of time. Arrow at 36 h denotes the addition of 200 μM U(VI). All incubations were performed under anoxic conditions. Error bars denote standard deviation of triplicate experiments. 128
- Figure 4.11: Phosphate measurement of *Rahnella* sp. Y9602 incubated in synthetic groundwater (pH 5.5) amended with 10 mM glycerol (sole C source) and 3.33 mM sodium tripolyphosphate (sole P source). Abiotic controls were cell-free. Incubations were performed under oxic conditions. 129
- Figure 5.1: Area 3 soil slurry incubations of FWB120-06-00 (circles) and FWB120-08-00 (squares) core segments conducted in synthetic groundwater (pH 5.5) amended with 10 mM G3P (as sole C and P source). All incubations were performed under oxic conditions. Error bars denote standard deviation of triplicate experiments. 149
- Figure 5.2: Neighbor-joining analysis of all 16S rRNA genes obtained from FWB120-06-00 and FWB120-08-00 soil slurry incubations. The greengenes database (<http://greengenes.lbl.gov/cgi-bin/nph-index.cgi>) was used to construct the phylogenetic tree that identifies all phyla detected via PhyloChip microarray analysis. The scale bar indicates 0.10 change per nucleotide. 151

Figure 5.3:PhyloChip microarray analyses of microbial diversity present within replicate soil slurry incubations. Numbers above histogram bars indicate total phyla detected per incubation. 152

Figure 5.4:Hierarchical cluster analysis of soil slurry incubations. Soil slurries from each core segment were repeated in triplicate experiments and are represented as 06-1, 06-2, 06-3 for core FWB120-06-00 and 08-1, 08-2, 08-3 for FWB120-08-00. 153

Figure 5.5: Hydrous ferric oxide slurry incubations. Incubations were conducted in synthetic groundwater (pH 7.0) amended with 10 mM glycerol (sole C source) 3.33 mM sodium tripolyphosphate (as sole P source). All incubations were performed under oxic conditions. Incubations containing the *Rahnella* sp. were initiated with an inoculum cell density of 10^7 cells/ml. Abiotic control incubations were cell-free. Error bars denote standard deviation of duplicate experiments. 154

LIST OF SYMBOLS AND ABBREVIATIONS

16S	small subunit ribosome sedimentation coefficient
AD	anaerobic digester
AMD	acid mine drainage
ANME <i>Archaea</i>	anaerobic methane oxidizing <i>Archaea</i>
API	Antarctic pack ice
AO	Arctic Ocean
atm	atmosphere
ATPase	ATP-dependent enzyme
BS	Black Sea
CM	Cascadia Margin
CR	chlorinated compound reduction
crDNA	complementary ribosomal deoxyribonucleic acid
CS	cold seep environment
CSS	cold seep sediment
CTAB	cetyltrimethylammonium bromide
DAPI	4',6-diamidino-2-phenylindole
DEPC	diethyl pyrocarbonate
DNA	deoxyribonucleic acid
DNase-I	deoxyribonuclease I
dNTP	deoxyribonucleotide triphosphate
DOE	United States Department of Energy
DS	deep sea sediments

EDTA	ethylenediamine-tetraacetic acid
EDX	energy dispersive X-ray spectroscopy
ER	Eel river
G+C	guanine and cytosine
G3P	glycerol-3-phosphate
GAB	Great Artesian Basin
GB	Guaymas Basin
GoM	Gulf of Mexico
GWS	German Wadden Sea
HGT	horizontal gene transfer
HS	Hydrocarbon seep
HV	Hydrothermal vent
JDS	Japan deep sea sediments
JHV	Japan hydrothermal vent
JT	Japan Trench
kGy	kiloGray
MA	Mid-Atlantic Ridge
mbsf	meters below sea floor
MPME	Mediterranean planktonic
MT	Mariana Trench
MV	mud volcano
NS	North Sea
NSAP	non-specific acid phosphatase
OC	Oregon coast
OTU	operational taxonomic unit

PCR	polymerase chain reaction
PDP	phenolphthalein diphosphate
MMLV	moloney murine leukemia virus
RFLP	restriction fragment length polymorphism
RNA	ribonucleic acid
rRNA	ribosomal ribonucleic acid
RT-PCR	reverse transcription-polymerase chain reaction
SB	Santa Barbara Basin
SBC	Santa Barbara Channel
SDS-PAGE	sodium dodecyl sulfate polyacrylamide gel electrophoresis
SM	salt marsh
SO	Sea of Okhotsk
SP	salt pond
SR	soil rhizosphere

SUMMARY

Extreme environments arise as a result of natural and anthropogenic processes. These environments are characterized by physical and chemical extremes of temperature, pH, salinity, pressure, and ionizing radiation. Within these unique regions, a diverse group of microorganisms have been shown to harbor physiologies capable of catalyzing geochemical transformations that are environmentally beneficial on local and global scales. This work specifically examines the microbial transformations of methane and uranium [U(VI)] within aquatic and terrestrial sedimentary systems, respectively. Microbial transformations of methane and U(VI) are of immediate relevance to emerging global sustainability issues as they may influence climate change through greenhouse gas sequestration as well as contribute to the cycling of soluble metals in subsurface environments. The Gulf of Mexico (GoM) submarine mud volcano systems as well as the mixed metal and radionuclide contaminated subsurface of the Department of Energy's (DOE) Oak Ridge Field Research Center (ORFRC) represent unique aquatic and terrestrial extreme environments that harbor microbial communities capable of catalyzing geochemical transformations of methane and uranium, respectively. The microbial communities capable of contributing to carbon (methane) cycling in mud volcano sediments were characterized through 16S rRNA clone library analysis. Archaeal and bacterial 16S clone libraries generated from total DNA and ribosomal RNA extractions (i.e., 16S rDNA and crDNA libraries) were numerically dominated by methanotrophic (e.g., *γ-Proteobacteria* and anaerobic methane oxidizing *Archaea*), sulfate-reducing, and sulfur oxidizing species (e.g., *δ-Proteobacteria* and *ε-*

Proteobacteria). Within the ORFRC metal and radionuclide contaminated subsurface, microorganisms possessing both P_{IB}-type ATPase and NSAP ‘stress’ genes are hypothesized to have a selective advantage within the contaminated subsurface. A culture-dependent approach identified extensive horizontal gene transfer (HGT) of P_{IB}-type ATPase metal resistant genes within *Arthrobacter* and *Bacillus* spp. Additionally, nonspecific phosphohydrolase activity of ORFRC metal-resistant *Bacillus* and *Rahnella* isolates were shown to promote the biomineralization of up to 95% of total soluble U(VI). The present study is the first to: i) demonstrate the dominance of metabolically active ANME-2 euryarchaeotal, δ –, and γ -proteobacterial lineages within the sediments of a GoM cold seep mud volcano, ii) demonstrate the influence of HGT in disseminating P_{IB}-type ATPase metal resistance determinants to 20% of screened bacterial isolates obtained from the subsurface soils of the ORFRC, and iii) demonstrate the capability of ORFRC *Rahnella* and *Bacillus* strains to promoted the mineralization 73% and 95% of total soluble U(VI) during aerobic growth in synthetic groundwater with glycerol-3-phosphate as the sole carbon and phosphorus source. Findings from these studies demonstrate the prokaryotic diversity within aquatic and terrestrial sediments that are capable of sequestering carbon, metals, and radionuclides.

CHAPTER 1

INTRODUCTION

1.1 Global sustainability

In 1999, the National Research Council (NRC) published the report “Our Common Journey: A Transition Toward Sustainability” (NRC, 1999), which illustrated the need for fundamental changes in human activity that will be required to accommodate a predicted global population of 10 to 11 billion by the year 2100 (NRC, 1999). The most pressing issues facing Earth’s ability to sustain an increasing human population are the maintenance of clean water, clean air, and addressing human activities that contribute to ozone depletion and global climate change (NRC, 1999; Schlesinger, 2006). These issues are a result of technological advances which directly contribute to increasing greenhouse gas emissions as well as the release of organic and inorganic pollutants into the environment (Lloyd, 2002; Gavrilescu, 2004). In an effort to understand and mitigate the environmental issues of global sustainability, microbial diversity studies that examine the geochemical cycling of carbon, metals, and radionuclides provide great promise.

The natural regulation or radiative balance of earth’s climate is driven by the insulating effects of water vapor, carbon dioxide, and ozone within the atmosphere (Wolff and Spahni, 2007). Without such insulation, the surface temperature on earth would range from -18°C to -19°C rather than the current surface temperature range of 14°C to 15°C (Wolff and Spahni, 2007). From the turn of the industrial revolution to present day, the concentrations of atmospheric carbon dioxide, methane, and nitrous

oxide concentrations have risen 25%, 120%, and 9%, respectively and thus have changed atmospheric radiative forcing (Joos, 2008) (Fig. 1.1). Therefore, a better understanding of greenhouse sources and sinks are essential in determining the magnitude of global climate change when anthropogenic and natural emissions of such gases perturb radiative balance (Houghton, 2007; Reeburgh, 2007; Wolff and Spahni, 2007).

Equally important are the issues of organic and inorganic subsurface soil pollution as they directly relate to the health of humans and ecosystems. The most pronounced effects of pollution include: disease etiology, acute toxicity, loss of biodiversity, phytotoxicity, zootoxicity, and eutrophication (Philp, 2005). Unlike organic contaminants which can be transformed by microorganisms to less toxic forms and ultimately mineralized to carbon dioxide, inorganic contaminants, namely toxic metals must be detoxified through redox or complexation transformations (Philp, 2005). *In situ* remediation of subsurface soil contaminants are influenced by the local geochemistry. Because the mobility and fate of a given contaminant within soils can be enhanced or retarded by abiotic and biotic catalyzed geochemical transformations, remediation efforts aimed at the subsurface sequestration of inorganic contaminants must identify and constrain these factors.

In an effort to mitigate such pressing environmental issues, a greater understanding of the geochemical transformations driven by sedimentary prokaryotic communities is required. The roles aquatic and terrestrial microbial communities play in the geochemical cycling of carbon, nitrogen, phosphorus, sulfur, and metals continues to be elucidated. Most notably, prokaryotes play key roles in atmospheric chemistry and

aqueous geochemistry, which includes geological precipitation and weathering chemistries (Ehrlich, 1998; Newman and Banfield, 2002; Macalady and Banfield, 2003).

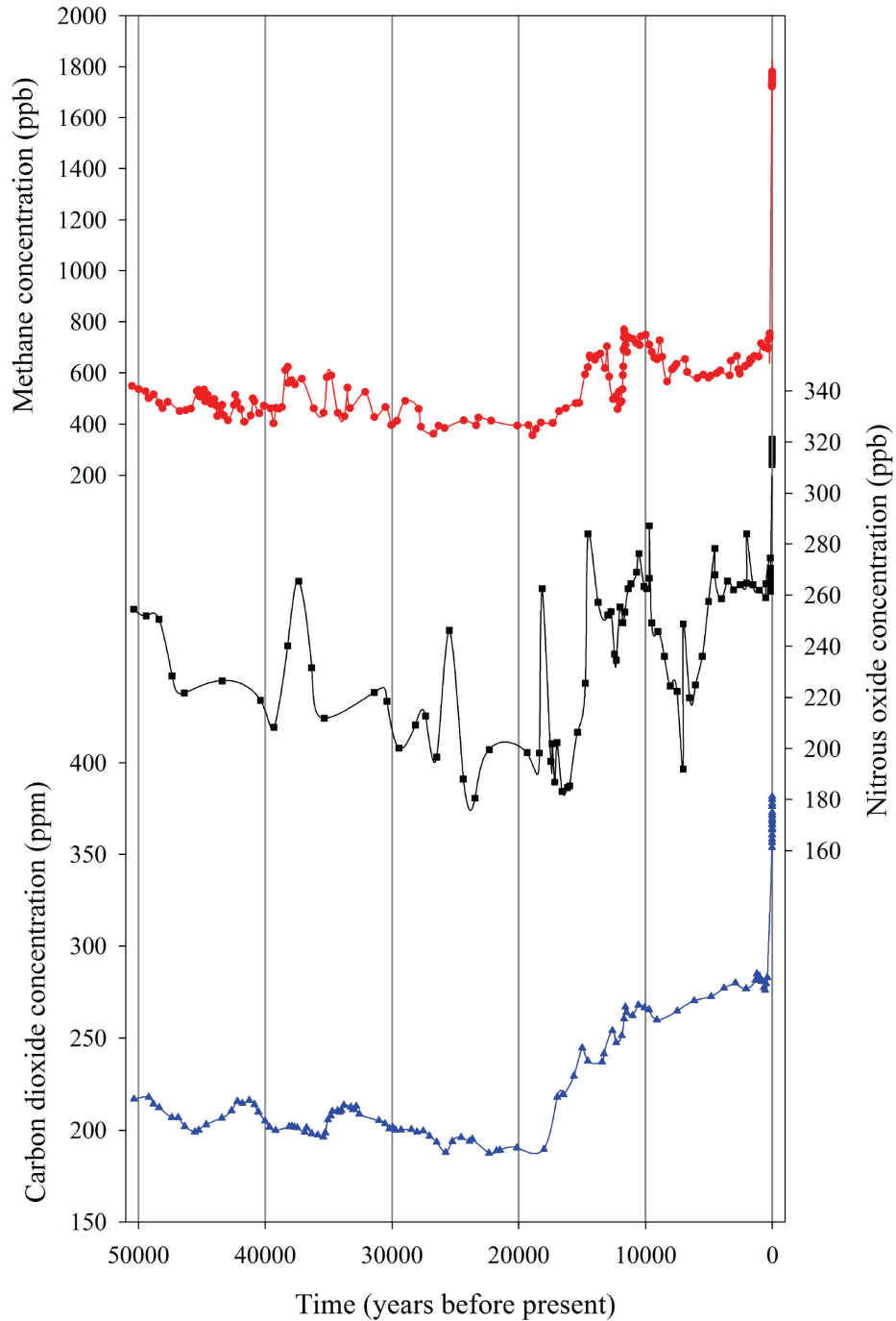


Figure 1.1. Concentrations of atmospheric methane, nitrous oxide, and carbon dioxide measured over the past 50,000 years. Methane and nitrous oxide ice core data was obtained from the Greenland Ice sheet Project 2 (Brook et al., 1996; Sowers et al., 2003). Carbon dioxide ice core data was obtained from the Taylor dome on the East Antarctic

ice sheet (Indermuhle et al., 1999 1203). Annual atmospheric methane, nitrous oxide, and carbon dioxide concentrations were sampled from Mauna Loa, Hawaii by the Commonwealth Scientific and Industrial Research Organisation, Australia (WDCGG, 2008).

Microbial catalyzed geochemical transformations are reported in all aquatic and terrestrial regions of the world, the exception being regions influenced by active volcanism (i.e., magmatic). Chemical and physical stresses such as extremes in temperature, pH, salinity, and pressure (i.e., extreme environments) do not inhibit microbial catalyzed geochemical transformations as microbial physiologies have evolved to allow unique lineages to thrive in environments defined by such parameters (Adams, 1993; Abe et al., 1999; Horikoshi, 1999; Oren, 1999; Baker-Austin and Dopson, 2007).

Prokaryotic and eukaryotic microorganisms have been shown to thrive in regions of the world previously believed to be devoid of life. The regions that pose the greatest challenge for organisms to thrive have been termed extreme environments. These regions include acidic, alkaline and saline environments; low temperature glacial and high temperature geothermal environments; and the high pressure regions of the deep-sea and deep subsurface (Table 1.1). Interdisciplinary research initiatives that focus on the characterization of prokaryotes present in extreme environments continue to be met with the fundamental hurdle of culturability.

Prior to the study of microbial diversity in extreme environments, the inability to culture all members of a given microbial community in non-extreme environments became apparent. Depending on the environment being studied (e.g., seawater, freshwater, activated sludge, sediments and soil) culturable prokaryotic cells can range from 0.0001% - 15% of total microscopic counts (Smalla, 2004). This has been termed

the “great plate count anomaly” (Staley and Konopka, 1985). The necessity to employ culture independent methods has been utilized to describe microbial diversity as well as identify metabolic activity. The use of such techniques as nucleic acid isolation and cloning; molecular fingerprinting; bromodeoxyuridine (BrdU); fluorescence *in situ* hybridization (FISH); stable isotope probing; marker and reporter gene tracking has facilitated culture-independent studies in both non-extreme and extreme environments (Smalla, 2004).

This study focuses on two separate sedimentary systems, 1) A Gulf of Mexico (GoM) cold seep mud volcano, and 2) Mixed waste acidic soils located at the Department of Energy’s (DOE) Oak Ridge Field Research Center (ORFRC). The factors that define the GoM site as an extreme environment are the low temperature (8°C) and high salinity (9.5% to 11%) present in the cold seep mud volcano sediments (Joye et al., 2005; Martinez et al., 2006a). The ORFRC can be defined as an extreme environment as a result of anthropogenic activity which has led to the occurrence of mixed metal and radionuclides, high concentrations of oxyanions and acidification (pH 4.0) of the soils and deep subsurface (Martinez et al., 2006b). Research efforts in the GoM and ORFRC sites have immediate relevance in better understanding and addressing issues of global climate change and the remediation of metal and radionuclide contaminants in soil and groundwater systems.

1.2 Extreme environments

Extremophiles, which have representative species in all 3 domains of life, are the organisms that thrive at the known physiological limits of temperature, pH, and salinity (Rothschild and Mancinelli, 2001; Pikuta et al., 2007). It is the unique regions of the planet defined by extremes in temperature, pH, and salinity that are considered extreme environments. The hypotheses ‘everything is everywhere’ and ‘the environment selects’ was originated by Dutch biologist Lourens G.M. Baas Becking (Quispel, 1998) and appropriately reflects the ability of microbial communities to adapt and thrive in virtually every environment that man has studied. In addition to pH, salinity, and temperature extremes listed on Table 1.1, select groups of microorganisms have been shown to possess physiologies capable of tolerating the physical extremes of dessication, ionizing radiation, and high pressure (Rothschild and Mancinelli, 2001; Pikuta et al., 2007). This section will highlight molecular mechanisms which have evolved in microorganisms for adaptation to varying physical and chemical conditions present in extreme environments.

For organisms that have not evolved mechanisms to cope with chemical and/or physical environmental extremes; the toxicity of temperature, pH, salinity, pressure, and ionizing radiation extremes are manifested in chemical changes of macromolecules. Such chemical changes include the hydrolysis and depurination of nucleic acids; lipid solidification or saponification; protein denaturation and hydrolysis (Cleaves and Chalmers, 2004). Therefore studies of microorganisms which have physiological adaptations that enhance the stability of nucleic acids, proteins, and lipids contribute to our understanding of the physical and chemical parameters that define the limits of life.

Unique molecular adaptations have been identified within prokaryotes isolated from low and high temperature environments. Within low temperature environments, physiological adaptations include maintenance of membrane fluidity by an increased incorporation of polyunsaturated fatty acids, production of ice crystal inhibiting antifreeze proteins, increase utilization of polar amino acids, and reduced hydrophobic protein subunit interactions (Cavicchioli et al., 2000; Russell, 2000). Molecular adaptations observed in thermophilic prokaryotes include heat stable membrane ether lipids, increased G+C content in the stem regions of RNA molecules, and increased DNA stability via the positive supercoiling activity of DNA gyrase (Kikuchi and Asai, 1984; Stetter, 1999).

Environments defined by extremes in pH also harbor prokaryotes with unique molecular adaptations. The maintenance of optimal intracellular pH (i.e., pH 4.6-7.0) in acidic environments continues to be an area of active research. Mechanisms by which prokaryotes extant within acidic environments maintain intracellular pH potentially include tetraether lipid membranes to maintain proton impermeability, increased expression of DNA and protein repair proteins, and increased intracellular potassium ion concentration to reduce proton motive force (i.e., maintain a Donnan potential) (Baker-Austin and Dopson, 2007). Conversely, alkaliphilic prokaryotes have been shown to maintain an intracellular pH from 7.5-8.5. Proposed mechanisms that maintain intracellular homeostasis are: negatively charged acidic cell wall polymers which enhance hydroxide ion repulsion; the utilization of a sodium motive force rather than a proton motive force for ATP generation, and the use of sodium/hydrogen or potassium/hydrogen antiporters for the maintenance of optimal intracellular pH (Horikoshi, 1999).

Within hypersaline environments membrane permeability requires enzymes to function under high salt concentration as cytoplasmic water loss causes elevated intracellular solute concentrations. Thus, enzymes rich in acidic amino acids have been shown to be a common attribute for the maintenance of activity under high salt concentrations (Oren, 1999). For microorganisms that lack salt-tolerant enzymes, the accumulation of high intracellular concentrations of compatible solutes (i.e., small organic molecules which include betaine, trehalose, glycerol, sucrose, proline, choline, carnitine, mannitol, glucitol, and ectoine) have been demonstrated to interact with salt sensitive enzymes and maintain activity under high salt concentrations (Oren, 1999; Beales, 2004).

Resistance to ionizing radiation has been identified in the *Actinobacteria*, *Bacteroides*, *Cyanobacteria*, *Euryarchaeota*, *Deinococcus-Thermus*, α -*Proteobacteria*, and γ -*Proteobacteria* prokaryotic phyla. To date, however, the majority of research has focused on the bacterial species *Deinococcus radiodurans* (Cox and Battista, 2005). Radioresistance in *D. radiodurans* was initially believed to be due to the efficiency of DNA repair proteins and the presence of 4-8 chromosome copies (Minton, 1994; Daly et al., 2004). Recent work has examined the intracellular recovery from elevated concentrations of reactive oxygen species prevalent following radiation exposure. The protective effect of cytosolic manganese granules has been demonstrated to contribute to the survival of *D. radiodurans* following irradiation (Daly et al., 2004; Ghosal et al., 2005). Further examination of manganese accumulating prokaryotes as well as poorly characterized radioresistant archaeal and bacterial phyla are required to determine the

potential diversity of mechanisms employed to resist the toxicity of exposure to ionizing radiation.

High pressure environments require microbial adaptations that control intracellular pH, protein folding, and membrane fluidity. Cytoplasmic acidification can become more prevalent with increasing hydrostatic pressure due to the ionization of intracellular weak acids (Abe et al., 1999). Studies examining the pressure-driven cytoplasmic acidification of *Saccharomyces cerevisiae* cells indicated a pH decrease that could affect intracellular enzyme activity (Abe and Horikoshi, 1998). Interestingly, studies examining a barotolerant *Streptococcus faecalis* mutant demonstrated increased intracellular ammonia accumulation as a result of increasing hydrostatic pressure, which can potentially aid in the neutralization of cytoplasmic acidification (Marquis and Bender, 1980). Within *Escherichia coli* cells exposed to an increase in hydrostatic pressure (i.e., 546 atm) total protein expression was shown to decrease. Conversely, the expression of heat shock and cold shock proteins increased with increased hydrostatic pressure which may be necessary in maintaining proper folding as pressure changes have been shown to affect the three dimensional structure of proteins and protein complexes (Weber and Drickamer, 1983; Welch et al., 1993). Lastly, increasing hydrostatic pressure contributes to membrane solidification as observed in low temperature environments, thus membrane fluidity is maintained by the incorporation of polyunsaturated fatty acids (Abe et al., 1999).

Microbial physiology studies of microorganisms present within extreme environments have contributed to our understanding of physical and chemical parameters that define the limits of life as well as the molecular adaptations that support the

metabolic activity in these unique regions. Furthermore, studies examining such molecular adaptations within microbial communities have directly contributed to our knowledge within the areas of astrobiology, evolution, biotechnology, and geochemistry.

The study of extreme environments has direct applications to the field of astrobiology. This field utilizes interdisciplinary research to understand life on earth as well as the potential for life on other planets. The diversity of microorganisms within earth's polar and geothermal heated regions as well as regions that possess extremes in pH has direct implications to the search for life within our solar system. Insight gained from the diversity of microorganisms present within earth's extreme environments has allowed for the postulation of life to occur on other planets in our solar system (Pikuta et al., 2007). The temperature and pH extremes present on Mars, Venus, and the moons of Saturn and Jupiter demonstrate possible regions to detect life (Pikuta et al., 2007). Thus, the goal for future space missions examining these regions is the detection of nucleic acid, protein, carbohydrate or lipid biomarkers indicative of metabolically active organisms.

The origin of life on earth continues to be a highly debated subject as observed in the multiple theories that have been proposed. The theories of panspermia (i.e., planetary seeding of microorganism), drying tidal pools, clay mineral surfaces, sulfide mineral surfaces, water vapor droplets, and deep-sea hydrothermal vents all propose explanations for the origin of life (Line, 2002; Cleaves and Chalmers, 2004). Currently, prokaryotic ribosomal RNA phylogeny indicates the deeply rooted (i.e., slowly evolved ancestral species) archaeal and bacterial species evolved from hyperthermophilic *Archaea* and either mesophilic or thermophilic *Bacteria* (Becerra et al., 2007). Analysis of rRNA

G+C content, protein disulfide oxidoreductase sequences, and orthologous protein sequences has lead several authors to develop hypotheses that indicate either a hyperthermophilic or mesophilic last common ancestor gave rise to the archaeal and bacterial domains of life (Galtier et al., 1999; Di Giulio, 2003; Pedone et al., 2004). Determination of a prokaryotic last common ancestor is further compounded by rampant horizontal gene transfer (HGT) in extant prokaryotes as observed by the vast archaeal contribution to the *Thermoanaerobacter tengcongensis* and *Thermotoga maritima* bacterial genomes (Pedone et al., 2004; Mongodin et al., 2005). Thus, defining a last common ancestor or last common community which roots in the tree of life remains an area of intense research (Javaux, 2006; Becerra et al., 2007). Although the origin of life remains highly debated, the environmental conditions on early earth resulted in the molecular adaptations that have been disseminated (i.e., through vertical and horizontal gene transfer) and are encoded by today's microbial communities present in non-extreme and extreme environments.

The discovery of molecular adaptations of microbial communities present in extreme environments has given rise to unique biotechnological and industrial applications. The study of thermophiles, psychrophiles, halophiles alkaliphiles and acidophiles has yielded insight in antibiotic discovery, thermostable and pH stable enzymes, and surfactants (Rothschild and Mancinelli, 2001). As 0.0001% to 0.3% of total prokaryotic cells within seawater and soils have been cultured, the vast majority of prokaryotes within these environments remain unculturable by current techniques (Smalla, 2004). Thus, the drive to understand the physiologies of currently unculturable

prokaryotes from both non-extreme as well as extreme environments remains an area of active research with great potential for novel biotechnological and industrial applications.

Microbial communities present within the deep sea, aquatic deep subsurface, and terrestrial deep subsurface environments encode unique physiologies for life under extremes in temperature, pressure and salinity. Moreover, the adaptive physiologies present in metabolically active microbial communities present within deep sea hydrothermal vent systems, hydrocarbon cold seep systems, and metal-contaminated deep subsurface environments have a great influence on the biogeochemical cycling of essential elements as well as metals and radionuclides (Newman and Banfield, 2002).

Table 1.1. Microbial environments defined by extremes in pH, salinity, and temperature. Adapted from (Pikuta et al., 2007)

Environment	pH	NaCl %(w/v)	Temperature °C	Representative microorganism	Reference
Freshwater psychrophile	5-7	0-1	<15	<i>Aquaspirillum arcticum</i>	(Butler et al., 1989)
Freshwater mesophile			15-60	<i>Shewanella amazonensis</i> ^a	(Venkateswaran et al., 1999)
Freshwater thermophile			>60	<i>Thermococcus waiotapuensis</i>	(Gonzalez et al., 1999)
Marine psychrophile	5-8	3-4	<15	<i>Colwellia psychrerythraea</i>	(Methe et al., 2005)
Marine mesophile			15-60	<i>Roseobacter denitrificans</i> ^a	(Shiba, 1991)
Marine thermophile			>60	<i>Pyrolobus fumarii</i> ^b	(Blochl et al., 1997)
Alkaliphilic psychrophile	9-11	0-1	<15	<i>Pseudomonas alcaliphila</i>	(Yumoto et al., 2001)
Alkaliphilic mesophile			15-60	<i>Alkalibacter saccharofermentans</i>	(Garnova et al., 2004)
Alkaliphilic thermophile			>60	<i>Bacillus</i> sp. strain TA2.A1	(Peddie et al., 2000)
Haloalkaliphilic psychrophile	9-10	3-25	<10	<i>Pseudoalteromonas antarctica</i>	(Bozal et al., 1997)
Haloalkaliphilic mesophile			15-60	<i>Halonatronum saccharophilum</i>	(Zhilina et al., 2001)
Haloalkaliphilic thermophile			>60	<i>Thermosediminibacter litoripruensis</i>	(Lee et al., 2005)
Halophilic psychrophile	8	3-30	<15	<i>Psychromonas antarcticus</i>	(Mountfort et al., 1998)
Halophilic mesophile			15-60	<i>Marinobacter aquaeolei</i> ^a	(Huu et al., 1999)
Acidophilic mesophile	0-4	0-2	15-60	<i>Ferroplasma acidiphilum</i>	(Golyshina et al., 2000)
Acidophilic thermophile			>60	<i>Sulfolobus solfataricus</i> ^a	(She et al., 2001)

^aMicroorganisms with genome sequence completed.

^bMicroorganisms with genome sequence in progress.

1.2.1 Marine sedimentary systems

The discovery of the Galapagos Rift hydrothermal vents and Florida escarpment cold seeps has only come about within the past 30 years (Lonsdale, 1977; Paull et al., 1984). Today, numerous hydrothermal vent and cold seep systems have been discovered and shown to occur in unique geological settings (Campbell, 2006). Hydrothermal vent systems are found within seafloor spreading zones, which allow for the mixing and chemical leaching of high temperature crustal rock with overlying seawater to produce superheated water enriched in metals and sulfidic compounds (Jannasch and Mottl, 1985). Conversely, cold seep systems are localized to both active and passive continental margins (Naehr et al., 2007). In passive margins where tectonic activity is minimal, salt tectonics drives the emission of liquid and gaseous hydrocarbons (MacDonald, 1998; Campbell, 2006). As both hydrothermal and cold seep systems exist below the photic zone, primary production is driven by chemosynthesis rather than photosynthesis. The energy requirements in these deep-sea locales are provided by hydrogen sulfide and/or methane. It is the oxidation of these molecules that provides the energy for the prokaryotic primary producers and eukaryotic chemosynthetic communities (Lonsdale, 1977; Paull et al., 1984; MacDonald, 1998; Van Dover et al., 2002; Campbell, 2006).

Within cold seep environments, hydrocarbons are present in gaseous, liquid and solid phases. It is these environmental conditions that provide the unique conditions that support eukaryotic (Kennicutt et al., 1985; Brooks et al., 1987; Freytag et al., 2001) and prokaryotic (Ahmad et al., 1999; Hinrichs et al., 1999; Boetius et al., 2000; Orphan et al., 2001a; Mills et al., 2005; Martinez et al., 2006a) chemosynthetic communities. The following section will highlight the geochemical and geophysical conditions present

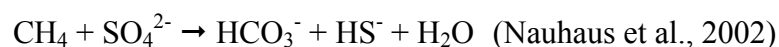
within deep sea cold seep systems as well as the molecular diversity of microbial communities inhabiting this unique extreme environment.

1.2.1.1 Cold seep systems

Deep-sea cold seep environments have been mapped throughout the world and it is within these locations that gaseous hydrocarbons can form hydrates (Kvenvolden, 1999; Milkov, 2000). Gas hydrates or methane hydrates, which are the main form of hydrates due to the high flux of methane in cold seeps are only formed under high pressure and low temperature environments that dominate the deep-sea environment (Kvenvolden, 1999). Methane hydrates are water ice cages (i.e., clathrates) that enclose gaseous methane with a methane to water ratio of 216:1 (vol:vol) (Kvenvolden, 1999; Sloan, 2003). Due to the large volume of methane sequestered in hydrates, a great deal of research has focused on cold seep environments for: i) the potential applications of gas hydrates as a fuel alternative, ii) the source of submarine hazards as a result of hydrate destabilization (Blake Ridge), and iii) the potential effect methane flux has on global climate change (Dickens et al., 1995; Kvenvolden, 1999; Kennett et al., 2000).

The origins of C₁-C₅ hydrocarbon gases within cold seep environments can be traced to abiotic (thermogenic) and biotic processes via carbon stable isotope analysis. Within biologically catalyzed reactions of organic molecules, the lighter ¹²C isotope is preferentially utilized, thus organic molecules (i.e., methane) of biogenic origin will have an isotopically lighter ratio of ¹³C/¹²C (Reeburgh, 2007). In general, ¹³C/¹²C less than -50‰ is considered biogenic in origin and a ratio greater than -50‰ is considered to be thermogenic in origin as referenced to Pee Dee belemnite ¹³C standard (Reeburgh, 2007).

Many characterized cold seep environments release methane that is of thermogenic and biogenic origins (Sassen et al., 1999; Orphan et al., 2001a; Michaelis et al., 2002). Abiotic or thermogenic production of hydrocarbon gases is a result of alkane degradation under high temperature and high pressure (Sassen et al., 1999), while biogenic hydrocarbon gases are produced by fermentative microbial communities (Hinrichs et al., 1999; Hinrichs et al., 2006). Isotopic analysis of authigenic carbonates present in many cold seep systems contain carbon with a depleted ^{13}C signature which suggests the microbial mediated oxidation of biogenic methane under anaerobic conditions (Hinrichs et al., 1999; Valentine and Reeburgh, 2000; Orphan et al., 2002). Several microbial community studies have demonstrated the presence and putative syntrophic relationship of anaerobic methane oxidizing *Archaea* and sulfate-reducing *Bacteria*. The anaerobic methane oxidizing *Archaea* are a distinct clade related to *Methanosarcina* spp. and the δ -*Proteobacteria* *Bacteria* are sulfate-reducing species closely related to *Desulfosarcina* spp. (Hinrichs et al., 1999; Orphan et al., 2001a; Jorgensen and Boetius, 2007). The summarized syntrophic relationship between the cold seep *Archaea* and *Bacteria* is theorized in the following equation:



Due to the fact that the thermodynamics of this relationship yields less than -25 kJ/mol, which is less than the minimum unit of biological energy (-20 kJ/mol) (Schink, 1997), alternative syntrophic relations have been theorized that involve the generation of an acetic acid or acetate intermediate product which increases the final energy yield (Valentine and Reeburgh, 2000).

The study of cold seep microbial consortia has focused on sediments associated with hydrocarbon seepage and breaching hydrate (Hinrichs et al., 1999; Boetius et al., 2000; Orphan et al., 2001a; Michaelis et al., 2002). Relatively, few studies have examined the microbial consortia present in cold seep mud volcano sediments. The cold seep mud volcanoes are unique in that the sediments are periodically or continuously exposed to brine fluids as well as high methane flux.

1.2.1.2 Marine mud volcanoes

Within cold seep environments, mud volcanoes are unique features that release liquid and gaseous hydrocarbons into the overlying seawater (Dimitrov, 2002). Typical tectonic driven volcanism arises from a break in the earth's crust which allows the release of molten rock. In contrast, mud volcanism is a result of sedimentary succession that is associated with active hydrocarbon generation. As a result of the hydrocarbon generation, pressurization of overlying sediments causes piercing and feeder channels allow for the flow of semi-fluid sediments (Dimitrov, 2002).

Within the Gulf of Mexico, cold seep systems and mud volcanism is driven by salt tectonics (Milkov and Sassen, 2001). During the Late Triassic-Middle Jurassic, thick Callovian salt deposits filled subbasins and gave rise to the salt diapirs present today in the Gulf of Mexico (Milkov and Sassen, 2001). Due to the greater buoyancy of salt diapirs relative to the overlying seafloor sediment, upward migration of the diapirs causes over pressurization of sediments. When migrating salt diapirs compress hydrocarbon reserves and deform the overlying sediments, the result is the formation of mud volcanoes (Fig. 1.2). Seafloor breaching of hydrocarbons as a result of salt diapir over

pressurization allows for overlying seawater to mix with deep salt deposits and ultimately gives rise to the unique high salinity fluids associated with marine mud volcano systems.

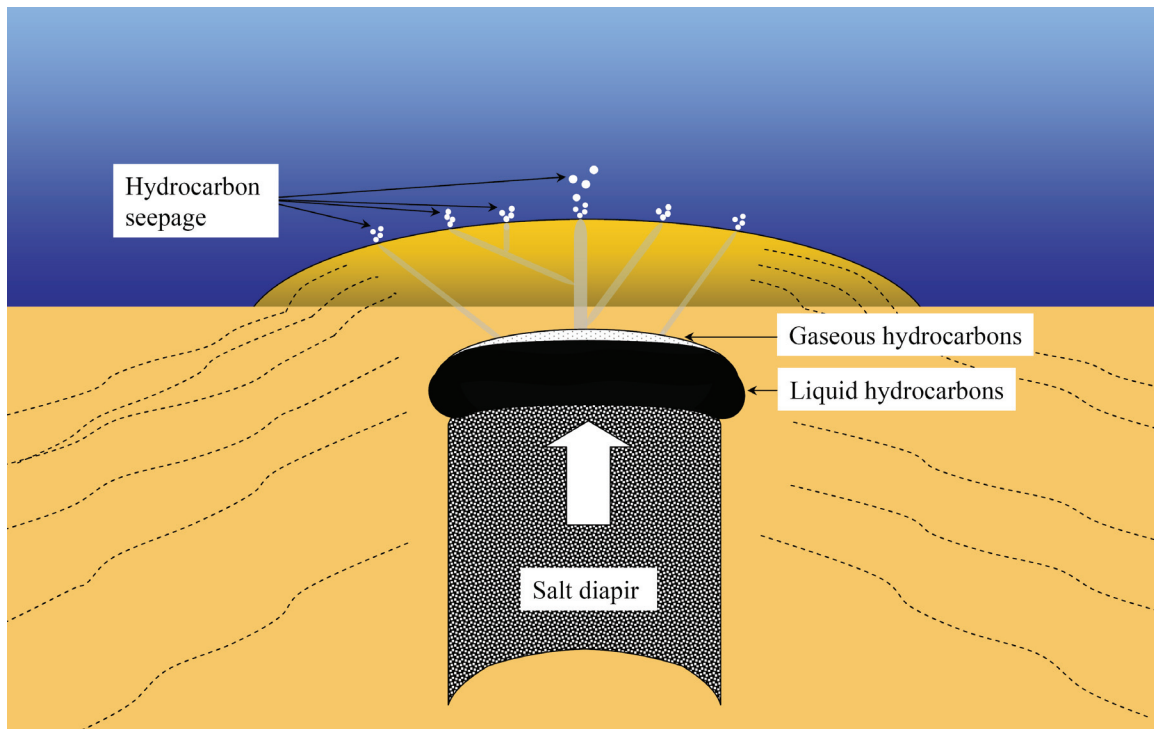


Figure 1.2. Salt diapir driven formation of marine mud volcanoes. Migration of deep subsurface salt diapirs toward the seafloor deforms the overlying sedimentary strata (dotted lines) and ultimately forms the characteristic dome or conical topologies. Additionally, salt diapirism leads to the over pressurization and release of hydrocarbon pools on to the surrounding sediments and overlying water.

The global distribution of mud volcanoes represents a significant conduit for atmospheric methane flux (Milkov, 2000; Dimitrov, 2002). Although mud volcanoes are present in both terrestrial and marine environments, the number of terrestrial mud volcanoes is in excess of 900 while the number of marine mud volcanoes is estimated to be between 10^3 - 10^5 (Milkov, 2000; Dimitrov, 2002).

Marine mud volcano methane emissions directly into the overlying water column are estimated to be 27 Tg year^{-1} (Milkov et al., 2003). The lack of long-term studies as well as the lack of monitoring equipment to properly measure marine methane flux into

the atmosphere has contributed to the large range in theorized emission range of 6 – 12.6 Tg year⁻¹ (Dimitrov, 2002; Etiope and Milkov, 2004; Milkov and Etiope, 2005). In addition to the flux of methane, recent studies conducted in the southern California and Gulf of Cadiz mud volcano systems demonstrated the accumulation of mercury within associated sediments, presumably as a result of rock leaching in underlying faults (Hein et al., 2006; Mieiro et al., 2007). These findings underline our current knowledge gap with regards to the global contributions of greenhouse gases and heavy metal release from marine mud volcano systems.

The study in Chapter 2 identified metabolically active anaerobic methane oxidizing *Archaea*, sulfate-reducing, and methane oxidizing *Bacteria* lineages within the sediments associated with the Gulf of Mexico mud volcano (GB425) (Fig. 1.3) (Martinez et al., 2006a). Additionally, studies in the Gulf of Cadiz and Haakon Mosby mud volcanoes have identified archaeal and bacterial lineages related to those identified in the Gulf of Mexico mud volcano system (Niemann et al., 2006a; Niemann et al., 2006b; Losekann et al., 2007). Interestingly, aerobic methane oxidation and anaerobic methane oxidation investigations conducted *ex situ* were shown to account for 1-3% and 37%, respectively for Haakon Mosby mud volcano sediment microbial communities (Niemann et al., 2006b). Thus, phylogenetic analysis of methane hydrate-bearing sediments and sediments associated with mud volcanoes demonstrate the ubiquitous presence of anaerobic methane oxidizing *Archaea*, sulfate-reducing, and methane oxidizing *Bacteria* lineages (Hinrichs et al., 1999; Boetius et al., 2000; Orphan et al., 2001a; Michaelis et al., 2002; Mills et al., 2003; Mills et al., 2004; Mills et al., 2005; Martinez et al., 2006a; Niemann et al., 2006a; Niemann et al., 2006b; Losekann et al., 2007). In summary,

archaeal methanotrophic influence on sea floor methane flux (i.e., anaerobic oxidation of 37% of total methane flux) and the concomitant ^{13}C depleted signature of cold seep authigenic carbonates potentially demonstrate a significant methane sequestration potential when considering the estimate of mud volcano methane emissions of 27 Tg year^{-1} (Milkov et al., 2003; Niemann et al., 2006b).

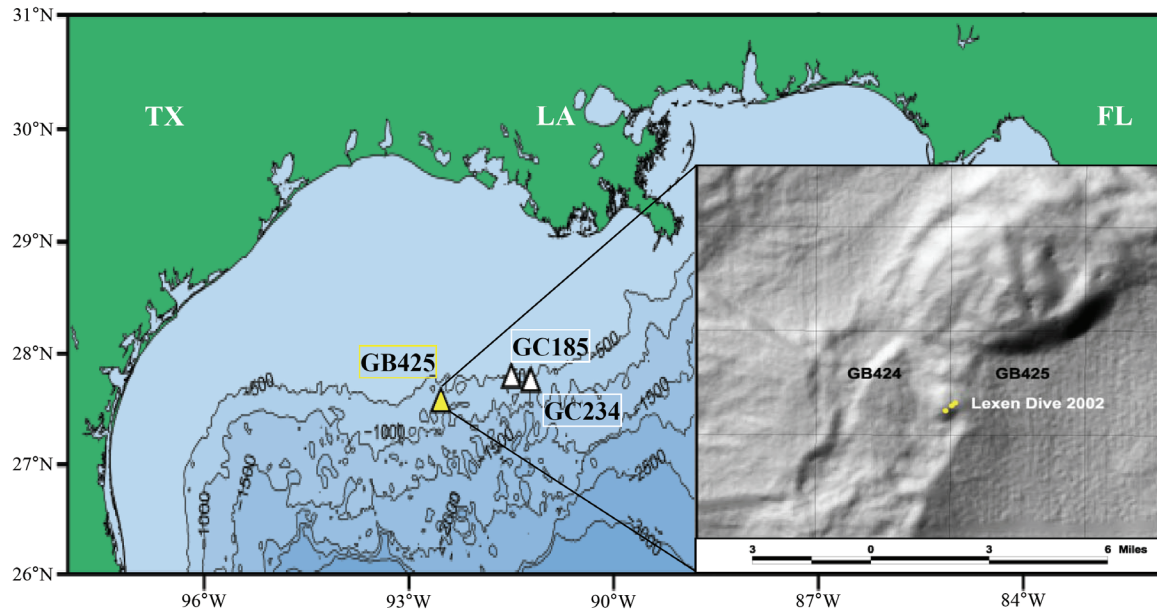


Figure 1.3. Gulf of Mexico cold seep research sites located within the Green Canyon (GC185 and GC 234) and Garden Banks (GB425) lease blocks. The GC185 and GC234 sites are defined by breaching methane hydrates and hydrocarbon seepage. The GB425 site (inset seafloor acoustic image) contains a mud volcano that releases gaseous hydrocarbons and brine on to the surrounding sediments and overlying water.

1.2.2 Terrestrial sedimentary systems

Terrestrial sedimentary systems or soils are defined by mineral particles, organic matter, living organisms, water, and gases that are present at the earth's surface and which at times may be submerged in 0.5 m of water (Schaetzl, 2005; Voroney, 2007). The formation of soil is driven by physical, chemical, and biological activity. As in

aquatic sedimentary systems, microbial activity within terrestrial systems catalyzes the transformation of both inorganic and organic compounds. The importance of soil microbiology was defined by the work of Sergei Winogradsky and Martinus Beijerinck in the late 1800's. These early soil microbiology studies examined nitrification, anaerobic nitrogen fixation, sulfur oxidation, microbial autotrophy and the development of enrichment cultures (Paul, 2007). The current fields of geomicrobiology and microbial ecology have evolved from the pioneering work of Winogradsky and Beijerinck.

The establishment of the field of soil microbiology in the early 20th century focused on studies that had direct applications to understanding agricultural nutrient cycling as well as contributing to a greater understanding of plant pathology (Atlas, 1993). Following World War II, advances in technology and population growth contributed to the contamination of soils and groundwater systems (Atlas, 1993). As soils provide a natural filtration system for groundwater, studies of deep subsurface soils have been driven by understanding the potential use of microorganisms in bioremediation applications and ultimately the maintenance of clean water (Amy, 1997).

It has been observed that every soil system on earth with the exception of soils directly influenced by volcanic activity, contain viable microbial communities (Standing, 2007). As a result, unique microbial communities have established themselves in terrestrial extreme and non-extreme environments. In addition to the previously described physical and chemical extremes experienced by microbial communities, subsurface microbial communities must also endure changes in water activity, adapt to environments with low carbon content, and overcome the toxicity posed by heavy metals and oxyanions (Krumholz, 2000; Senko et al., 2002). The following sections will

highlight the geophysical, geochemical, and microbial community structure of unique shallow and deep subsurface extreme environments.

1.2.2.1 Shallow subsurface

Unique regions of the world give rise to examples of terrestrial shallow subsurface extreme environments. Such shallow subsurface extreme environments include geothermally-heated rocks and soils, arid desert regions, and permafrost soils. Within these environments, microorganisms have evolved physiologies to cope with the physical and chemical stresses of temperature and pH. Several studies within these unique environments have examined the microbial community structure and adaptive physiologies. Microbial communities present within geothermally heated rocks and soils have been studied within Antarctica, Yellowstone National Park in Wyoming, and the Galápagos Islands (Llarch et al., 1997; Walker et al., 2005; Mayhew et al., 2007). Soils isolated from the fumaroles of Antarctica and the Galápagos Islands demonstrated unique microbial communities that are extant within a thermophilic and acidophilic environment. The limited number of microbial diversity studies within the Antarctica fumarole soils focused on characterizing the endospore-forming bacterial diversity which was found to be dominated by the *Bacillus* genera (Llarch et al., 1997; Logan et al., 2000). A culture-independent approach to examine microbial diversity within the low and high pH fumaroles of the Galápagos Islands identified *Acidobacteria*, *Cyanobacteria*, *Firmicutes*, and *Proteobacteria* phyla (Mayhew et al., 2007). The temperature and pH conditions present at the time of sampling for the Antarctica and Galápagos Islands undoubtedly selected for the microbial diversity detected in these studies. Interestingly, a geothermal

heating event within Yellowstone National Park in 1999 provided an opportunity to study the microbial community response to such a perturbation (Norris et al., 2002). A linear temperature gradient from 35°C to 65°C was examined by culture independent and culture-dependent methods. Denaturing gradient gel electrophoresis analyses indicated distinct shifts in microbial community structure as a result of high temperature perturbation. Additionally, soils samples that were geothermally heated demonstrated a 100-fold increase in culturable thermophiles. These data suggest that thermophilic microorganisms are ubiquitous in the Yellowstone soils but that thermal perturbations will periodically select these to be the dominant species.

Microbial diversity studies in arid desert sands and permafrost soils have expanded our current understanding of microbial community structure present within these regions of the world. In addition to the previously described extreme environment molecular adaptations, microbial communities subjected to periods of dessication within the shallow subsurface utilize spore formation, akinete development, and vegetative survival states to adapt to low water activity (Chanal et al., 2006). Recent studies within the arid Tunisia sands have demonstrated 31 culturable isolates representing 4 bacterial phyla. Interestingly, this study was the first to identify radiotolerant *α -Proteobacteria* that was able to survive irradiation of 2 kGy (Chanal et al., 2006).

Within the arctic and Antarctic permafrost environments, unique microenvironments have been characterized. Examples of these microenvironments include ice wedges (pure water ice), cryopegs (brine lenses), and taliks (unfrozen regions within permafrost environments) (Steven et al., 2006). The robust microbial diversity present within permafrost soils is reflected in the culturable isolates capable of

metabolisms that include aerobic and anaerobic heterotrophy, iron and sulfate reduction, methanogenesis, nitrification and nitrogen fixation (Steven et al., 2006). It is estimated that 14% of global organic carbon is sequestered within arctic permafrost (Metje and Frenzel, 2007). Similar to the deep sea cold seep environments, the permafrost regions of the world have been reported to contain stable methane hydrates (Kvenvolden, 1999; Steven et al., 2006). Due to changes in ambient temperature within arctic permafrost regions, the destabilization of methane hydrate has been observed (Buffett, 2000). Concomitant with hydrate destabilization is the increased methanogenic activity and soil respiration which can enhance methane and carbon dioxide atmospheric emissions (Houghton, 2007; Metje and Frenzel, 2007). Such positive feedback mechanisms could influence the atmospheric radiative balance and increase the rate of global warming.

1.2.2.2 Deep subsurface

Only within the last 20 years has the realization that metabolically active prokaryotes exist within the deep subsurface (Amy, 1997). Since then, deep subsurface studies have identified the microbial and metabolic diversity that exists within deep subsurface aquifers, a South African gold mine (reaching a depth of 4 km below land surface), and the deep subsurface of metal and radionuclide contaminated soils (Chapelle and Lovley, 1990; Fredrickson et al., 1995; BoivinJahns et al., 1996; Amy, 1997; Krumholz, 2000; Onstott et al., 2003; North et al., 2004; Lin et al., 2006; Trimarco et al., 2006; Akob et al., 2007).

The terrestrial deep subsurface is defined as the region that exists below the first few meters of soil (Paul, 2007). Within this region, the deepest depth to which microbial

activity can be supported is theorized to be approximately 3,500 m depth; this assumes 110°C is the thermal limit for life. Thus, as temperature increases at a rate of 25°C per 1000 m depth in the deep subsurface, a depth of 3,500 m would generate sufficient heat to establish a thermal threshold for microbial activity (Krumholz, 2000). Additionally, as pressure increases with depth, soil porosity decreases and contributes to the observed low carbon content (Krumholz, 2000; Wanger et al., 2006). As such, metabolic activity observed in the deep subsurface has redefined the limits of life in regions with low nutrient availability. Thus the term survival energy, which refers to the minimum energy a prokaryotic cell utilizes to maintain viability in starvation conditions is invoked to explain the persistence of cells in such extreme environments (Morita, 1997). In addition to low nutrient environments, low temperature (-40°C) glacial brine channels have been shown to harbor microorganisms with extremely low metabolic activities such that estimated mean generation times range from years to millenia (Price and Sowers, 2004; Jorgensen and Boetius, 2007).

Studies examining deep subsurface aquifers and clay formations have demonstrated the presence of metabolically active microorganisms potentially possessing mean generation times of hundreds to thousands of years. Such generation times would be required to sustain viable cells extant within regions of low carbon and low electron acceptor concentrations. Several studies have identified metabolically active microorganisms within subsurface samples ranging from 6-80 million years old (Chapelle and Lovley, 1990; Fredrickson et al., 1995; BoivinJahns et al., 1996). Interestingly, marine deep subsurface sediments (i.e., >400 mbsf) demonstrated the dominance of

bacterial over archaeal lineages in the deep and metabolic activity was only observed in bacterial lineages (Schipper et al., 2005).

Deep terrestrial subsurface microbial community research has been aided by the exploration of the world's deepest mines which occur within the Witwatersrand basin of South Africa (Wanger et al., 2006). The high temperature (55°C) and alkaline (pH 9) waters of the ancient aquifer have been estimated to be from 3-25 million years old. Although the aquifer has been isolated on a geological timescale; millimolar concentrations of hydrogen and methane were measured while oxygen, sulfate, acetate, and formate were present in micromolar concentrations (Lin et al., 2006). A study utilizing a culture-dependent enrichment for sulfate-reducing microorganisms within the aquifer water identified 21 operational taxonomic units (OTUs) representing α , β , and γ -*Proteobacteria*, *Actinobacteria*, *Firmicutes*, *Chloroflexi*, *Deinococcus-Thermus*, *Crenarchaeota*, and *Euryarchaeota* phyla (Trimarco et al., 2006). Although, the a potentially diverse sulfate-reducing community was surmised from the culturable isolates obtained, a later study employing a 16S rDNA high-density microarray culture-independent approach to assess microbial diversity within the aquifer identified a single *Firmicutes* phylotype as the dominant lineage present at the time of sampling (Lin et al., 2006).

The long term storage and bioremediation of metal and radionuclide wastes within the deep subsurface has benefited from microbial diversity studies. Diversity studies within the Russian Severnyi repository for liquid radioactive waste, Hanford National Laboratory (Washington) underground liquid waste containers, and the ORFRC (Tennessee) S-3 ponds have demonstrated the diversity of microorganisms capable of

tolerating extremes in pH, high concentrations of salts, oxyanions, metals, and radionuclides (Fredrickson et al., 2004; Nazina et al., 2004; North et al., 2004; Michalsen et al., 2007).

Within the Severnyi repository deep aquifer, microbial diversity studies were initiated to determine the potential for gas production as liquid nuclear waste is mixed with acetate, nitrate, and acetate (Nazina et al., 2004). Lipid extraction and analysis demonstrated the dominant lineages to be members of the *Actinobacteria* and *Firmicutes* phyla (Nazina et al., 2004). Additionally, within the Severnyi repository deep aquifer anaerobic denitrifiers, fermenters, sulfate-reducers, and methanogens were detected which verified the potential for overpressurization of the repository. Such overpressurization can contribute to the unexpected release of liquid waste into overlying soils and thus requires continuous monitor of aquifer gas concentrations.

The Hanford National Laboratory houses underground storage tanks which hold primarily radioactive cesium (^{137}Cs). Currently, it is estimated that 0.6 to 1.5 million gallons of this liquid radioactive waste has leaked out of the storage containers are migrating through the subsurface (Fredrickson et al., 2004). Culture-dependent microbial diversity studies conducted in the high pH, metal and radionuclide contaminated Hanford National Laboratory sediments aimed to identify microorganism capable of affecting the solubility of the subsurface contaminants. This study demonstrated the dominant culturable aerobic heterotrophic lineages to be members of the *Actinobacteria* and *Deinococcus-Thermus* phyla which demonstrated tolerance to dessication and ionizing radiation (Fredrickson et al., 2004). Within the contaminated soils, low water activity has

reduced microbial activity and thus minimized any effect on the present solubility of the subsurface contaminants.

Microbial diversity studies conducted on ORFRC deep subsurface sediments have focused on field-scale and laboratory-scale biostimulation under anoxic conditions to stimulate metal reducing microorganisms that catalyze the reductive precipitation of uranium (VI) to uranium (IV) (North et al., 2004; Wan et al., 2005; Michalsen et al., 2007). These culture-independent microbial diversity studies identified *Acidobacteria*, *Actinobacteria*, *Bacteroidetes*, *Chloroflexi*, *Firmicutes*, *Proteobacteria*, *Spirochaetes*, and *Verruomicrobia* as the dominant lineages present in clone libraries following glucose or ethanol enrichments. As these enrichment studies were culture-independent, the contributions each species play on uranium precipitation remains unknown. Only recently have microbial diversity studies of the Area 3 ORFRC deep subsurface sediments (Fig. 1.4) examined the aerobic microbial community. Culturable aerobic heterotrophic diversity of Area 3 ORFRC deep subsurface sediments indicated *Actinobacteria*, *Firmicutes*, and *Proteobacteria* to be the dominant phyla (Martinez et al., 2006b). Additionally, phosphate-mediated biomineralization of uranium was demonstrated to precipitate up 95% of total soluble uranium via the non-specific acid phosphatase (NSAP) activity of isolates belonging to *Firmicutes*, and *Proteobacteria* phyla (Beazley et al., 2007; Martinez et al., 2007).



A.



B.

Figure 1.4. (A). The ORFRC S-3 wastes ponds, with a storage capacity of 9.5 million liters, received uranium nitrate waste as well as sludge waste from other activities within the Oak Ridge reservation, Savannah River site, and the Idaho National Engineering Lab from 1951-1983. (B). The current site of S-3 ponds which underwent neutralization and denitrification prior to the construction of the multi-layer impermeable cap (Brooks, 2001; DOE, 2006).

1.3 Microbial detoxification mechanisms

Microorganisms are continually subjected to changing environmental conditions, thus the ability to sense and respond to toxic compounds is essential to cell survival. Compounds such as bacteriocides (including antibiotics, antiseptics, bacteriocins, and disinfectants) and heavy metals demonstrate toxicity through membrane disruption, inhibition of enzyme function, and oxidative damage. As a result, molecular mechanisms have evolved to detoxify such compounds through chemical modification and/or efflux from the cell cytoplasm. The following section will focus on microbial metal detoxification mechanisms.

1.3.1 Overview of metal detoxification mechanisms

The transition metals cobalt, copper, zinc, manganese, molybdenum, nickel are essential for bacterial and archaeal enzyme function, oxidative stress response and environmental sensory (Madigan, 2003; Tottey, 2007). In contrast, the heavy metals arsenic, cadmium, chromium, lead, mercury, tellurium, thallium and silver have not been demonstrated to be required by microbial cells but rather demonstrate toxicity (Rosen, 2002; Lloyd, 2003; Silver and Phung, 2005). The toxicity of heavy metals and high concentrations of essential metals are manifested through improper ion substitution within metalloproteins, disruption of electron transport, disruption of ion transport, and catalysis of redox chemistry that promotes oxidative stress (Harrison et al., 2007). Therefore, multiple resistance mechanisms have evolved within prokaryotes to combat the toxicity of heavy metals and essential metals when either of these species approaches a minimum inhibitory concentration (Rosen, 2002; Silver and Phung, 2005). Mechanisms for metal resistance include ATP-driven efflux, chemiosmotic efflux, metal reduction, intracellular metal sequestration [Fig. 1.5., (Rosen, 2002; Lloyd, 2003; Silver and Phung, 2005; Remonsellez et al., 2006; Tottey, 2007)].

Microbial reduction of arsenic, chromium, cobalt, gold, mercury, molybdenum, palladium, silver, selenium, vanadium, neptunium, technetium, plutonium, and uranium have been demonstrated to be catalyzed by reductases, cytochromes, and hydrogenases (Lloyd, 2003). Furthermore, the reduction of chromium, gold, neptunium, palladium, selenium, uranium, and vanadium by metabolically active microbial species has been shown to facilitate precipitation via transition to a less soluble valence state or enhancing ligand binding as a result of a change in valence state.

Studies investigating chromium resistance in *Pseudomonas aeruginosa* and *Cupriavidus metallidurans* CH34 (formerly *Ralstonia metallidurans* CH34, *Ralstonia eutropha* and *Alcaligenes eutrophus*) the chromium resistance determinant ChrA permease identified in works synergistically with an unidentified cytoplasmic reductase (Nies et al., 1989; Ishibashi et al., 1990). Detoxification of chromate [Cr(VI)] is facilitated by the efflux of chromium in the reduced valance state [i.e., Cr(III)].

Within the species *Desulfovibrio vulgaris* and *Desulfovibrio desulfuricans*, studies examining purified cytochrome c_3 as well as mutational studies of this cytochrome have demonstrated the mechanism by which these sulfate-reducing species are capable of reducing U(VI) to U(IV) (Lloyd, 2003). Currently, the cytochrome-mediated reduction of uranium by *Desulfovibrio* spp. is the only characterized enzymatic mechanism for actinide reduction (Lloyd, 2003).

Although cytochrome, hydrogenase, and non-specific cytoplasmic reductases play important roles in detoxifying toxic metals, the following sections will focus on the well characterized mercury (mer operon) and arsenic (ars operon) reductase systems.

1.3.2 Metal reductases

1.3.2.1 The mer operon

Although mercury is naturally released into the environment through the weathering of mercuric minerals, hydrothermal vent and volcanic processes; the anthropogenic release accounts for 75% of all mercury introduced into the environment (Barkay et al., 2003; Mieiro et al., 2007). The toxicity of mercury arises from the high affinity interactions of cysteine disulfide bridges and subsequent inactivation of mercury

bound protein (Barkay et al., 2003). Consequently, prokaryotic mercury resistance genes are among the most prevalent metal resistance determinants occurring in both bacterial and archaeal lineages (Barkay et al., 2003; Silver and Phung, 2005; Simbahan et al., 2005).

The *mer* operon was first identified in the 1950's in a clinic strain of *Shigella flexneri* harboring the R100 plasmid which contained the Tn21 transposon (Nakaya, 1960). The mechanisms of mercury detoxification have been well characterized in gram-negative and gram-positive bacterial strains. The regulation of mercury resistance genes is achieved by the MerR transcriptional activator which drives the expression of the periplasmic-localized inorganic mercury binding MerP protein; inner membrane MerT, MerC, and MerF transport proteins; organomercurial lyase MerB and mercuric reductase MerA. The transport of oxidized mercury (Hg^{2+}) from the extracellular environment into the cytoplasm is driven by cysteine binding motifs in both the periplasmic (MerP) and inner membrane (MerT, MerC, and MerF) proteins (Barkay et al., 2003; Silver and Phung, 2005). Since ATP binding motifs are not associated with any of the proteins within the *mer* operon, transfer from among cysteine binding motifs or the membrane potential are believed to drive transport of mercury into the cell cytoplasm.

Organomercurial detoxification is achieved by two proteins, MerG and MerB. Within most bacterial strains, organomercurial compounds are believed to be sufficiently nonpolar and pass through the lipid membrane but studies utilizing *Pseudomonas* plasmid pMR26 have demonstrated the ability of MerT and MerP to facilitate the transport of select organomercurials such as phenylmercuric acetate (PMA) (Uno, 1997; Barkay et al., 2003). There have been limited studies focusing on the periplasmic localized MerG

protein. To date, studies utilizing the *Pseudomonas* plasmid pMR26 have only demonstrated that the MerG protein enhances resistance to PMA (Kiyono, 1999). Once organomercurials enter the cytoplasm, MerB, facilitates the reduction of the carbon bound mercury atom which releases ionized inorganic mercury (Barkay et al., 2003; Silver and Phung, 2005). The Hg^{2+} ion is then reduced by MerA and volatilized zero-valent mercury escapes the cell and enters the atmosphere (Barkay et al., 2003).

1.3.2.2 The *ars* operon

Similar to mercury, arsenic is naturally released into the environment through the weathering of arsenic bearing minerals but the anthropogenic releases via acid mining, antimicrobial feed additive in the poultry industry and the burning of coal are globally significant sources (Mukhopadhyay et al., 2002). The toxicity of arsenic is due to the similarity of arsenate and phosphate ions. This similarity allows for arsenate transport via Pit and Pst phosphate transport systems (Mukhopadhyay et al., 2002). The uncharged arsenite compound is transported into the cell cytoplasm via aqua-glyceroporins (Sanders, 1997).

The *ars* operon regulates the detoxification of arsenic and antimony via ATPase (i.e. arsenite efflux ArsAB complex), diffusion transporter and reductase expression (Busenlehner et al., 2003). The existence of efflux systems for both arsenate As(V) and arsenite As(III) is believed to be due to the emergence of oxygen 3.8 billions years ago. Prior to an oxygenated atmosphere, efflux of As(V) was probably not as necessary as As(III) efflux and thus As(III) efflux systems are believed to be the more ancient arsenic detoxification system (Mukhopadhyay et al., 2002).

The control of gene expression within the *ars* operon is achieved by transcriptional activator ArsR. The detoxification of As(III), As(V), and Sb(III) is driven by the ArsA and ArsB efflux proteins and the ArsC reductase (Carlin, 1995; Silver and Phung, 2005). Interestingly, arsenic efflux can be achieved via chemiosmotic transport, expression of only ArsB or ATP-driven efflux via the ArsAB complex (Mukhopadhyay et al., 2002).

Arsenic in the form of As(III) has been found to be 100 times more toxic than As(V) (Neff, 1997). As such, the arsenite oxidase encoded by the *aoxA* and *aoxB* must be considered when discussing arsenic resistance systems. The arsenite resistance system does not contain the complexity observed in the *ars* operon but the presence of *aoxA* and *aoxB* genes have been demonstrated to enhance microbial survival. Specifically, studies comparing the resistance of As(III) between wild type *Alcaligenes faecalis* strains and knockout mutants (i.e., lacking *aoxA* and *aoxB*) demonstrated a two-fold increase in sensitivity to decrease in resistance when exposed to soluble As(III) (Muller et al., 2003).

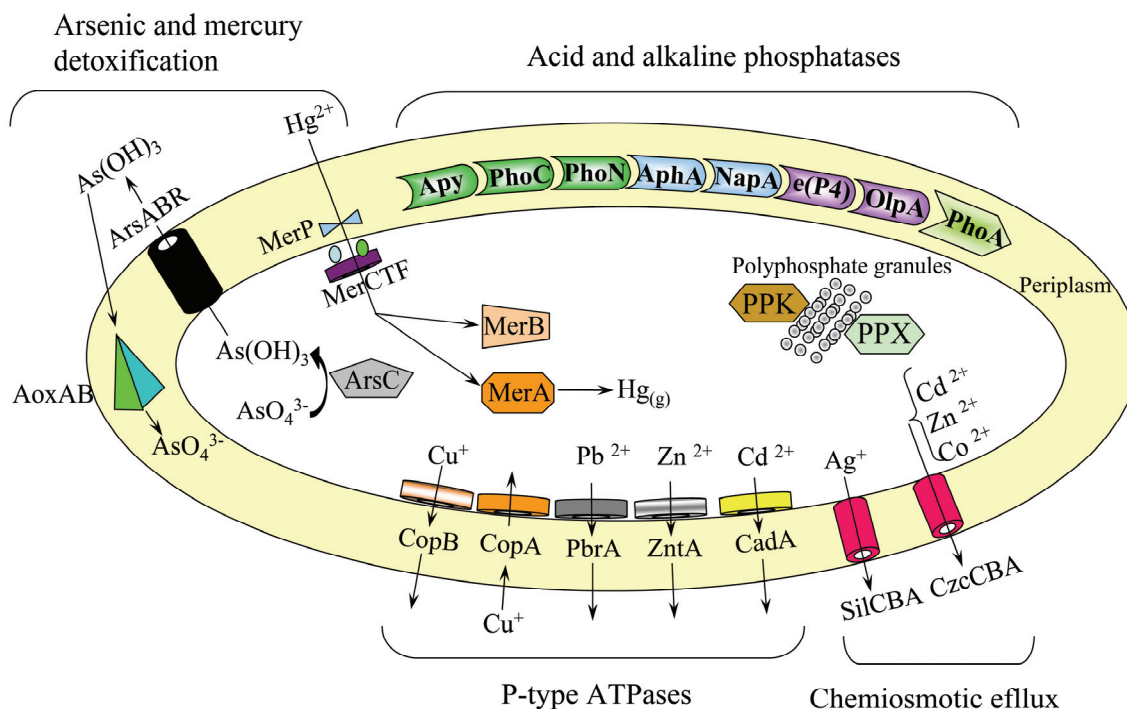


Figure 1.5. Depiction of microbial heavy metal detoxification systems driven by redox state, chemiosmotic transport, ATPase catalyzed transport and phosphate complexation. Adapted from (Silver and Phung, 2005).

1.3.3 Metal efflux systems

Heavy metal efflux systems in prokaryotes are categorized by two unique modes of transport: 1) Chemiosmotic coupled efflux of metal ions and 2) ATP-driven efflux systems (Silver and Phung, 2005). Chemiosmotic transport systems are further subdivided into the Major Facilitator Superfamily, Cation Diffusion Facilitator family, Resistance Nodulation Cell Division Superfamily, chromate efflux, and arsenite efflux systems (Haney et al., 2005; Silver and Phung, 2005).

The ATP driven efflux systems of metal ions are carried out by the inner membrane-anchored P-type ATPases. The superfamily of P-type ATPases has been shown to efflux the ions of hydrogen, sodium, potassium, calcium, cadmium, copper,

lead, nickel, silver, zinc as well as sugars, amino acids, and lipids (Kuhlbrandt, 2004). All P-type ATPases share four common structural features: 1.) 8 transmembrane helical domains, 2.) ATP-binding domain, 3.) phosphorylation domain, and 4.) dephosphorylation domain (Tsai et al., 2002; Kuhlbrandt, 2004; Silver and Phung, 2005). The divalent metal P_{1B}-type ATPases differ from all other P-type ATPases in that they contain an intracellular cysteine metal binding motif (Tsai et al., 2002). It is the intracellular metal binding motif that specifically allows for the efflux of cytoplasmic-accumulating cadmium, copper, lead, nickel, silver, zinc (Rosen, 1996; Nies, 2003; Silver and Phung, 2005).

In contrast to P-type ATPase metal efflux systems, chemiosmotic systems function as ion antiporters which efflux periplasmic accumulating metals (Nies, 2003; Silver and Phung, 2005). Chemiosmotic metal detoxification systems function by coupling the uptake of hydrogen ions to the efflux of heavy metals which include cadmium, cobalt, nickel, silver, and zinc (Nies, 2003). Metal detoxification via P-type ATPases and chemiosmotic efflux occurs by decreasing cytoplasmic and periplasmic metal concentrations, respectively. To examine the potential synergy between the P-type ATPases CadA, ZntA, and the CzcCBA chemiosmotic metal efflux systems in *Cupriavidus metallidurans* strain CH34, knockout studies were recently conducted (Legatzki et al., 2003). Deletion of *zntA* and *cadA* P-type ATPases demonstrated that CzcCBA was able to detoxify micromolar concentrations of cadmium and zinc. Resistance to millimolar concentrations of cadmium and zinc, observed in the wild-type strain, required either ZntA or CadA in addition to CzcCBA (Legatzki et al., 2003). Thus, the combination of cytoplasmic and periplasmic efflux systems provide enhanced

resistance without the need for enzymatic metal transformations (i.e., redox and methylation transformations).

1.3.4 Metal complexation

The intracellular and extracellular immobilization of toxic metals has been observed in plants, fungal, bacterial, and archaeal strains (Klaus-Joerger et al., 2001; Malik, 2004; LeDuc and Terry, 2005; Silver and Phung, 2005). Fortuitious metal complexation as a result of microbial respiration has been observed in sulfate-reducing bacteria. Phosphate complexation of divalent metals and radionuclides has been demonstrated in polyphosphate granule-accumulating bacteria and in bacterial strains overexpressing of NSAPs (Macaskie et al., 1992; Renninger et al., 2004; Suzuki and Banfield, 2004; Martinez et al., 2007).

Sulfate-reducing microbial communities have been shown to biomineralize cadmium, cobalt, chromium, copper, manganese, nickel, selenium, and zinc as sulfide precipitates (White, 1998). Unfortunately, the introduction of oxygen into these reduced systems fosters sulfur oxidizing microorganisms and ultimately resolublizes the metal sulfide precipitates. Thus phosphate biomineralization approaches are attractive as they are not sensitive to changes in redox potential.

Phosphate mediated complexation can reduce the local cellular concentration of toxic metals and radionuclides via intracellular sequestration or extracellular precipitation. Polyphosphate overexpressing *Arthrobacter* strains isolated from a uranium tailing was observed to sequester uranium intracellularly via polyphosphate complexation (Suzuki and Banfield, 2004). This intracellular sequestration along with an observed

enhanced tolerance to acidic uranium solutions demonstrate the potential benefit polyphosphate granule accumulation may have in cell survival. The complexation of metals and radionuclides has been shown to be facilitated by acid and alkaline phosphatase organophosphate hydrolysis (Macaskie et al., 1992; Powers et al., 2002; Appukuttan et al., 2006; Martinez et al., 2007). Gram-negative and gram-positive bacteria isolated from the ORFRC demonstrated overexpression of NSAPs (Martinez et al., 2007). Interestingly, addition of 200 μM soluble uranium to an actively dividing *Rahnella* sp. culture resulted in 10^6 -fold decrease in culturable cells 12 h post uranium addition. A return to culturability was observed 36 h post uranium addition concomitant with the precipitation of over 80% of soluble uranium. As NSAP knock-out mutants were not compared in growth experiments with uranium supplementation, the extent to which microbial phosphatase activity contribute to cell survival under metal and radionuclide stress conditions remains to be elucidated. Undoubtedly, complexation reactions alleviate the oxidative stress faced by microbial communities from metals and radionuclides.

1.4 Dissemination of detoxification mechanisms by horizontal gene transfer

The acquisition of genetic information via horizontal gene transfer (HGT) event(s) can provide the recipient cell a competitive growth advantage by rapidly providing resistance to antibiotics and heavy metals, virulence capabilities, and expanding the metabolic capabilities of the host cell (Frost et al., 2005). The following sections will highlight the influence of HGT within marine and terrestrial environments.

1.4.1 Overview of horizontal gene transfer

The transfer of genetic material between dividing cells, either prokaryotic or eukaryotic is considered vertical transmission. It is the vertical transfer of genetic material that is the mode by which successive generations of a given species are perpetuated. In contrast, horizontal gene transfer (HGT) is the exchange of genetic material between two related or unrelated species. Dissemination of genetic information via HGT is facilitated by mobile genetic elements which include bacteriophage, plasmids, genomic islands, integrons, transposons, and insertion sequences as well as the integration of naked DNA translocated from the extracellular environment to the cell cytoplasm (i.e., transformation)(Sorensen et al., 2005).

The mosaic nature of microbial genomes, as observed in the inconsistencies of microbial phylogenetic topologies, reflects the influence of HGT on microbial genome innovation (Doolittle, 1999; Gogarten and Townsend, 2005). Furthermore, the evidence of HGT in eukaryotic genome evolution has been observed in comparative analysis of archaeal, bacterial, and eukaryotic genomes (Choi and Kim, 2007; Rivera, 2007).

Archaea and *Bacteria* have been identified as contributing to distinct portions of the eukaryotic genome. Transcription, translation and other functionally similar genes within eukaryotic cells have been shown to be more closely related to orthologous genes within *Archaea* while genes involved in biosynthesis of amino acids and lipids have been shown to be more closely related to orthologous genes of *Bacteria* (Rivera et al., 1998; Rivera and Lake, 2004). Thus, HGT can significantly influence microbial evolution and diversification on short timescales by providing a selective growth advantage or contributing to the innovation of prokaryotic and eukaryotic genomes.

Although the genotypes and phenotypes indicative of HGT can be identified, the mechanisms that specifically control HGT events are not well understood and thus remain an area of active research (Zatyka and Thomas, 1998). HGT events provide recipient cells with a selective advantage in ever changing environments with varying stressors (i.e. nutrients, antibiotics, heavy metals, predators, etc.). As the diversity of nutritional requirements, tolerance/resistance to toxic compounds, and the presence of predators vary in mixed microbial communities, it is not possible to identify one stressor that promotes HGT (Johnsen and Kroer, 2007). Recent studies examining stressors such as nutrient availability, antibiotics, and induction of the DNA repair 'SOS regulatory system' have been shown to enhance HGT rates (van Elsas and Bailey, 2002; Beaber et al., 2004; Springael and Top, 2004; Lopez et al., 2007). Furthermore, nitrates and actinides (present in Cold war legacy contaminated subsurface soils) have been demonstrated to induce DNA damage through hydrolysis and alkylation (Dykhuizen et al., 1996; Miller et al., 2002; Craft et al., 2004; Lundberg et al., 2004). Therefore, within environments contaminated with oxidants such as heavy metals, radionuclides and oxyanions DNA damage is likely and in response HGT rates may be enhanced.

1.4.2 Horizontal gene transfer in marine systems

Within the aquatic environment, recent horizontal gene transfer and the mobile genetic element studies have focused on the occurrence and diversity of plasmid and bacteriophage (Sobecky et al., 1997; Sobecky et al., 1998; Edwards and Rohwer, 2005; Lindell et al., 2005 1117; Comeau et al., 2006; Zhang et al., 2006). Recent studies investigating microbial diversity in Marianas trench deep sea sediments, Antarctic deep

sea water column, and prokaryotes associated with the East Pacific Rise hydrothermal vent tubeworm (*Alvinella pompejana*) have revealed evidence for horizontal gene transfer between archaeal species, between bacterial species, and between archaeal and bacterial species (Tamegai et al., 2004; Moreira et al., 2006; Moussard et al., 2006). These investigations relied on the analysis of PCR amplified gene products and metagenomic DNA. Evidence of HGT in these deep sea environments was determined by differences in gene organization within a *nar* gene cluster of a *Pseudomonas* strain obtained from the Marianas trench (Tamegai et al., 2004). Examination of metagenomic DNA from a novel myxobacterial related δ -proteobacterial strain in the Antarctic water column revealed evidence for HGT via comparative protein sequence analysis. An acetyltransferase gene present in the δ -proteobacterial metagenomic DNA demonstrated high identity with a low G+C *Bacillus cereus* acetyltransferase (Moreira et al., 2006). HGT between archaeal lineages within the hydrothermal vent system was demonstrated by atypical base composition in the gene encoding the putative translation factor Sua5, while nucleotide deletions present within a putative permease demonstrated evidence for bacterial to archaeal HGT (Moussard et al., 2006). In contrast to coastal HGT studies, the diversity of mobile genetic elements in the deep sea environment has not been examined to any extent and further studies are needed.

1.4.3 Horizontal gene transfer in terrestrial systems

Horizontal gene transfer studies in terrestrial environments have largely focused on the study of human and plant pathogenic bacteria, soil microbes harboring catabolic genes applicable to organic bioremediation, and soil microbes harboring toxic metal

resistance determinants (Silver and Misra, 1988; Frost et al., 2005). This section will focus on the horizontal gene transfer of metal resistance determinants.

Bacterial metal resistance determinants can occur on chromosomes, plasmids and transposons. The mobile gene pool, namely plasmids, has representatives that encode one or multiple metal resistant determinants and all known metal resistance determinants have been shown to be encoded on plasmids. Additionally, the linkage of antibiotic and metal resistance determinants has been well characterized in gram-negative and gram-positive bacteria (Silver and Misra, 1988; Nies, 1992; Baker-Austin et al., 2006).

Metal resistance determinants for mercury, arsenic, antimony, cadmium, chromium, copper, nickel, and zinc have been well characterized in the Tn21 subtype of Tn3-like transposons and plasmids from *Staphylococcus* spp., *Cupriavidus metallidurans* CH34 (Yoon et al., 1991; Rosenstein et al., 1992; Liebert et al., 1999; Mergeay et al., 2003; Vandamme and Coenye, 2004).

Chemiosmotic as well as ATP-driven efflux systems have been identified on mobile genetic elements (i.e., plasmids and transposons) present in both gram-positive (Nucifora et al., 1989; Nies, 1992; Lebrun et al., 1994; O'Sullivan et al., 2001) and gram-negative bacteria (Nies, 1992; Larbig et al., 2002; Mergeay et al., 2003). A recent study examining 22 archaeal and 188 bacterial genomes provided evidence for the horizontal gene transfer of P_{IB}-type ATPases (Coombs and Barkay, 2005). Only 7% of the species examined demonstrated evidence of HGT. The authors suggested that P_{IB}-type ATPase HGT has a minimal affect on microbial genome innovation. This claim was based on evidence that 8 % of the isolates obtained from uncontaminated deep subsurface soils demonstrated HGT of P_{IB}-type ATPases and 7% of the prokaryotic species with

completed genome sequences demonstrated HGT of P_{IB}-type ATPase (Coombs and Barkay, 2004, 2005). In contrast, the Sobecky laboratory demonstrated that 20% of the culturable isolates from metal- and radionuclide-contaminated soils had evidence for the HGT of P_{IB}-type ATPases [discussed further in Chapter 3 (Martinez et al., 2006b)]. HGT within the metal- and radionuclide-contaminated soils was demonstrated to be a recent event as indicated by a lack of nucleotide base amelioration (Martinez et al., 2006b). The contradiction between the extent of HGT in isolates obtained from uncontaminated environments to those obtained from contaminated environments suggests: i) HGT of P_{IB}-type ATPases within contaminated environments has a greater impact on microbial genome innovation than previously considered or ii) HGT of P_{IB}-type ATPases prior to the introduction of soil contaminants has driven the structure of the present microbial community.

1.5 Applications of microbial processes to global sustainability issues

The introduction of metals and radionuclides into the environment occurs via natural release mechanisms (i.e., volcanic activity, expulsions of hydrothermal vent fluids, and the dissolution of metal bearing minerals) and anthropogenic release (i.e., mining, industry, nuclear power and weapons development (Lloyd, 2002; Newman and Banfield, 2002; Gavrilescu, 2004; Mieiro et al., 2007)). Within the United States, it is estimated that cleanup of metal and radionuclide contamination, as a result of the United States nuclear weapons research program, will cost \$300 billion (DOE, 2000).

During the years 1942-1992, the United States nuclear weapons research program maintained research and manufacturing facilities in 36 states, this amounted to 120 unique sites requiring remediation of organic, metal and radionuclide contaminants (DOE, 1997). In 1997, an estimated 75 million cubic meters of contaminated soil and more than 470 billion gallons of contaminated groundwater required remediation (DOE, 1997).

Although a recent DOE report highlighted the closure of 86 Cold War era nuclear weapon facilities, sites such as Hanford, Savannah River, Idaho and Oak Ridge national laboratories still require extensive cleanup efforts for the safe decommissioning of these sites (DOE, 2007). Currently, the Field Research Center at the Oak Ridge National Laboratory (Oak Ridge, Tennessee) supports an interdisciplinary effort comprised of academic and government laboratory researchers focusing on both chemical (abiotic) and microbial mediated *in situ* sequestration of co-contaminating metals and radionuclides. The insight gained from studying the microbial and geochemical constraints involved in metal and radionuclide sequestration will ultimately be applied to the remaining DOE Cold War legacy sites requiring cleanup.

In attempts to address metal and radionuclide contaminated soils and groundwater, the use of various physical and chemical remediation strategies have yielded limited success. Methods such as excavation, pump and treat, adsorption to mineral phases (zero valent iron), ion exchange, mineral precipitation (hydroxyapatite, bone char) and organic complexation (inositol-6-phosphate) are plagued with high cost and short-term effectiveness (Bruno et al., 1995; Sato et al., 1997; Nash et al., 1998; Barlow, 2005). In contrast to the proven success of excavation for the treatment of

petroleum contaminated soils; the excavation, transportation, and storage of metal and radionuclide contaminated soils simply moves the contaminants from one location to another without effectively treating the contaminants (Barlow, 2005). Furthermore, the hazard of excavation of metal and radionuclide contaminated soils is predominantly the dispersal of toxic dust during all stages of the process.

Chemical treatment methods such as zero valent iron and phosphate mineral reactive barriers have had limited success due to the fact that metals and radionuclides, when present in high concentrations, precipitate and/or adsorb in such high quantities that subsurface groundwater flow paths are diverted. This localized change in hydraulic conductivity of subsurface soils exacerbates subsurface containment issues by increasing the region influenced by the contaminant plume. Thus, a bioremediation approach or the *in situ* stimulation of microbial communities that can promote the dissolution of metals and radionuclides is an attractive alternative that can circumvent issues associated with chemical treatment methods.

Bioremediation is defined as the use of plants and microbes to detoxify contaminants present in the environment (Philp, 2005). Prior to bioremediation activities in metal and/or radionuclide contaminated sites, an understanding of the local geology and geochemistry is necessary. The geochemical parameters of redox potential and pH are required to determine the solubility of reduced or complexed metals. Specifically, the elements chromium, mercury, and uranium have marked changes in solubility and bioavailability when the valence state transitions from the oxidized to reduced state. The reduced valence state for these elements has been demonstrated to be less toxic as well as greatly decreasing solubility (Barkay et al., 2003; Lloyd, 2003). Equally important is the

pH of the contaminated environment. In addition to redox changes, pH will also determine the solubility of metals and radionuclides (Langmuir, 1997). Defining these parameters in uranium contaminated subsurface is vital for successful bioremediation strategies.

Within the subsurface, local geochemistry and microbial activity can influence changes in *Eh* and pH which will ultimately affect uranium solubility. Changes in uranium oxidation will dictate changes in solubility as the +VI valence state is soluble and the +IV valence state is insoluble at pH 7 (Banaszak et al., 1999). In the absence of complexing ligands, low pH environments enhance uranium solubility as does a high pH carbonate-rich environment. Thus, strategies that focus on reductive precipitation or biomineralization of uranium must consider the pH and redox potential of the environment as well as the pH optima to promote growth of the strain(s). Microbial metal interactions which catalyze the reductive precipitation, biosorption, bioaccumulation, and biomineralization are mechanisms by which *in situ* sequestration of metals and radionuclides can be facilitated (Fig. 1.6).

Studies examining the metal-reducing genera *Desulfovibrio*, *Geobacter*, *Pseudomonas* and *Shewanella* have demonstrated great promise for applications focusing on the reductive precipitation or volatilization of toxic metals and radionuclides (Lovley et al., 1991; Wade and DiChristina, 2000; Payne et al., 2002; Barkay et al., 2003; Lloyd, 2003). Due to the required low redox potential for the reductive precipitation of transition metals and radionuclides, the introduction of oxygen and oxyanions can re-oxidize and re-mobilize the reduced element. Additionally, metal reducing microorganisms can remobilize metal species. This is exemplified during the

volatilization of mercury via microbial mercuric reductase enzymes. Reduced zero-valent mercury is not sequestered but rather volatilized and transported into the atmosphere where it can soon become oxidized and become deposited in a new environment (Barkay et al., 2003). This cycle of microbial reduction and atmospheric oxidation is repeated and perpetuates the cycle of environmental mercury contamination.

Cell surface adsorption and intracellular bioaccumulation have been studied as potential strategies for metal and radionuclide immobilization. The ionizable carboxyl and phosphate functional groups present on prokaryotic cell surfaces support the binding of metals (Haas et al., 2001). Studies examining the adsorptive capabilities of *Arthrobacter*, *Bacillus*, *Lactobacillus*, and *Streptomyces* spp. have demonstrated the removal of up to 95% of soluble uranium and thorium (Tsuruta, 2004, 2006). Although bioadsorption has proved an effective method for the removal of radionuclide bearing solutions, these studies have used solutions with less than 1 mM uranium or thorium and therefore this approach appears to be best suited as a polishing treatment step to address micromolar concentrations of liquid radionuclide waste.

The overexpression of the polyphosphate accumulating *ppk* gene has been shown to immobilize divalent metals and radionuclides within growth media and within the cell cytoplasm (Boswell et al., 2001; Pan-Hou et al., 2002; Renninger et al., 2004). Overexpression of the *ppk* gene in *Pseudomonas aeruginosa* was demonstrated to accumulate 100 times more phosphate than the unengineered *P. aeruginosa* strain and under carbon-limiting conditions, polyphosphate granules depolymerized resulting in the extracellular precipitation of 80% of the 1mM soluble uranium (Renninger et al., 2004). The chelating properties of polyphosphates have been indicated to be the mechanism for

intracellular accumulation of mercury by *Escherchia coli* overexpressing the *Klebsiella aerogenes ppk* gene (Pan-Hou et al., 2002).

Aerobic biomineralization of metals and radionuclides has not been as extensively studied as the approach employing reductive precipitation. In lieu of this fact, metal phosphate and metal sulfide biomineralization have demonstrated promise as bioremediation approaches (Macaskie, 1991; Macaskie et al., 1992; Macaskie et al., 1997; White, 1998). The geochemical stability of insoluble metal- and radionuclide-phosphates allows for *in situ* sequestration in environments that having changing redox potential and changing pH. In contrast, the stability of reductively precipitated metals and radionuclides are challenged by changes in microbial community composition, oxygen concentration, oxyanion concentrations, and mineral interactions (Liu et al., 2002; Wan et al., 2005; Brodie et al., 2006; Moon et al., 2007).

The hydrolysis of organophosphate molecules through the enzymatic activities of NSAPs provides a phosphate-mediated metal and radionuclide biomineralization strategy. Extensive studies on the gram-negative *Serratia* sp. NCIMB 40259 (formerly *Citrobacter* species) which overexpresses a Class C NSAP have demonstrated the isolates metal precipitating capabilities. Specifically, the *Serratia* sp. NCIMB 40259 strain was shown to precipitate divalent metals, actinides, as well as demonstrate the ion exchange potential of uranyl phosphate minerals to remove cooccurring heavy metals (Macaskie et al., 1992; Macaskie et al., 1994; Paterson-Beedle et al., 2006). The study in Chapter 4 demonstrates the uranium precipitating capabilities of *Bacillus* and *Rahnella* spp. isolated from the ORFRC metal and radionuclide contaminated deep subsurface. The *Bacillus* and *Rahnella* spp. were shown to foster the precipitation of uranium as a

uranyl phosphate mineral through the activities of Class A and Class C of NSAPs, respectively (Beazley et al., 2007; Martinez et al., 2007).

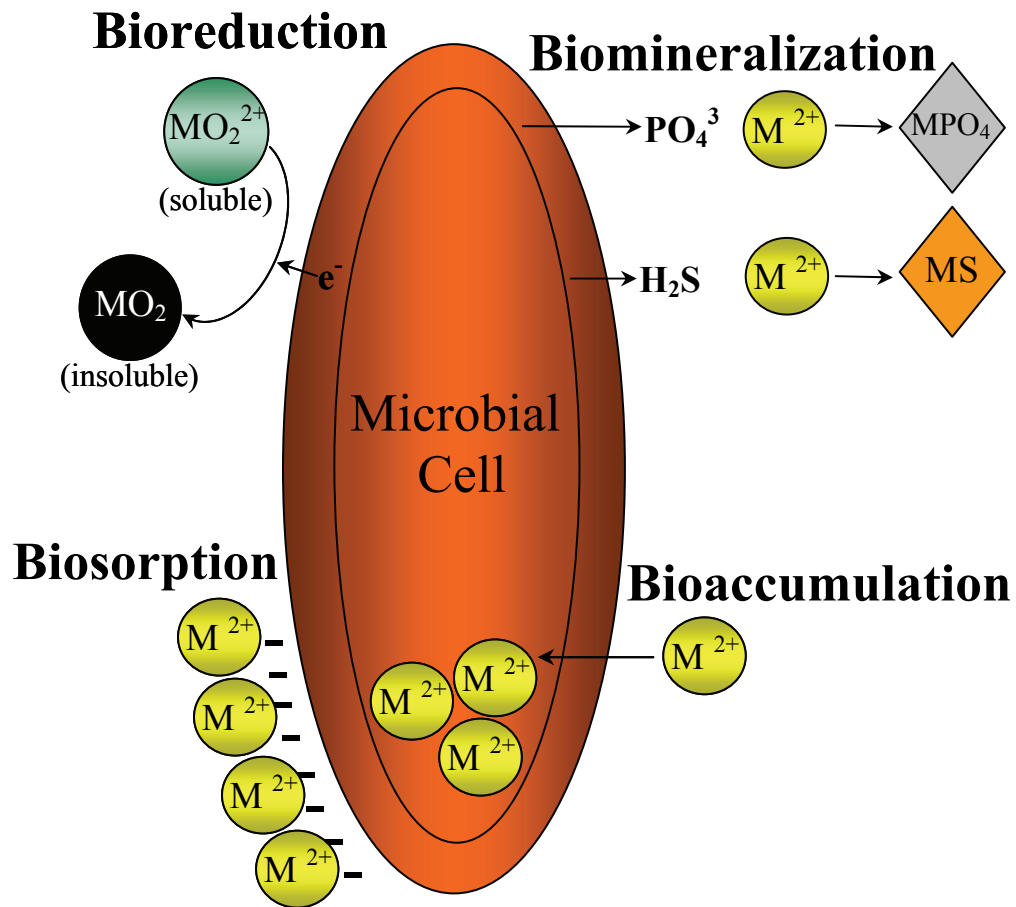


Figure 1.6. Characterized microbe-metal interactions applicable to bioremediation strategies. Adapted from (Lloyd, 2005)

CHAPTER 2

PROKARYOTIC DIVERSITY AND METABOLICALLY ACTIVE MICROBIAL POPULATIONS IN SEDIMENTS FROM AN ACTIVE MUD VOLCANO IN THE GULF OF MEXICO

2.1 Overview

The studies in this chapter examine cold seep marine sediment microbial diversity, specifically sediments associated with a Gulf of Mexico (GoM) marine mud volcano. Marine mud volcanoes have been estimated to release 27 Tg of methane per year into the water column; as such, marine mud volcano systems represent a globally significant source of methane. Therefore, identification of the methane oxidizing prokaryotic communities associated with these sediments is necessary to understand marine methane fluxes and their potential influence on global climate. Previous studies examining prokaryotic diversity in cold seep sediments have relied on total DNA extractions. As starvation conditions have been shown to enhance 16 rRNA degradation, the isolation of total 16S rRNA from mud volcano sediments can delineate differences between metabolically active microbial communities and total microbial diversity. To determine the metabolically active prokaryotic community within GoM mud volcano sediments, we extracted total archaeal and bacterial DNA as well as rRNA. A PCR-based approach was employed to identify total prokaryote diversity (DNA clone libraries) and diversity of metabolically active prokaryotes (rRNA clone libraries).

2.2 Summary

In this study, ribosomes and genomic DNA were extracted from three sediment depths (0 to 2, 6 to 8, and 10 to 12 cm) to determine the vertical changes in the microbial community composition and identify metabolically active microbial populations in sediments obtained from an active seafloor mud volcano site in the northern Gulf of Mexico. Domain-specific *Bacteria* and *Archaea* 16S PCR primers were used to amplify 16S rDNA gene sequences from extracted DNA. Complementary 16S ribosomal DNA (crDNA) was obtained from rRNA extracted from each sediment depth that had been subjected to reverse transcription-polymerase chain reaction-PCR amplification. Twelve different 16S clone libraries, representing the three sediment depths, were constructed and a total of 154 rDNA (DNA-derived) and 142 crDNA (RNA-derived) *Bacteria* clones and 134 rDNA and 146 crDNA *Archaea* clones obtained. Analyses of the 576 clones revealed distinct differences in the composition and patterns of metabolically active microbial phylotypes relative to sediment depth. For example, ϵ -*Proteobacteria* rDNA clones dominated the 0 to 2 cm clone library whereas γ -*Proteobacteria* dominated the 0 to 2 cm crDNA library suggesting γ -*Proteobacteria* to be among the most active *in situ* populations detected at 0 to 2 cm. Some microbial lineages, although detected at a frequency as high as 9% or greater in the total DNA library (i.e., *Actinobacteria*, α -*Proteobacteria*), were markedly absent from the RNA-derived libraries suggesting a lack of *in situ* activity at any depth in the mud volcano sediments. This study is one of the first to report the composition of the microbial assemblages and physiologically active

members of archaeal and bacterial populations extant in a Gulf of Mexico submarine mud volcano.

2.3 Introduction

Mud volcanoes are areas of focused active fluid seepage occurring both terrestrially and in undersea locales (Milkov and Sassen, 2001; Dimitrov, 2002; Kopf, 2003; Etiope and Milkov, 2004). Submarine mud volcanoes are seafloor diaper structures that exhibit seepage of mud and fluid [i.e., water, brine, oil and gas (predominately methane)] with episodic eruptions into the surface strata and overlaying water column (MacDonald et al., 2000; Milkov, 2000; Dimitrov, 2002). Although the mechanisms promoting mud volcano formation are varied (Dimitrov, 2002), the global distribution of seafloor mud volcanoes, estimated to be in the range of 10^3 - 10^5 , represents a considerable and still largely unexamined source of carbon input to the overlaying sediment, water column and atmosphere (Eichhubl et al., 2000; Milkov, 2000; Kopf, 2003; Etiope and Milkov, 2004). In recent years, an increasing number of studies have attempted to address the fate of methane originating from these undersea mud volcanoes, its potential impact on the global carbon cycle (Sassen et al., 2003) and the role of benthic marine microbial communities on the consumption (i.e., oxidation) of this greenhouse gas (Hinrichs et al., 1999; Boetius et al., 2000; Orphan et al., 2001b).

The northern continental slope of the Gulf of Mexico (GoM), a hydrocarbon seep region with documented mud volcanoes (MacDonald et al., 2000), contains vast reservoirs of oil and gas deposits, areas of active gas venting and gas hydrate mounds

occurring as outcrops on the seafloor. In contrast to the extensive efforts to characterize the geochemical and microbiological parameters of methane rich cold seeps including shallow and deeper water sites in the GoM (Lanoil et al., 2001; Zhang, 2002; Mills et al., 2003; Joye et al., 2004), fewer studies have attempted to investigate the microbial community composition of seafloor mud volcano systems. Although microbial community structure and potential function have recently been characterized from mud volcanoes located in Eastern Mediterranean Ridge and Norwegian continental slope (Pimenov, 1999; Pancost et al., 2000; Pimenov et al., 2000), to date none of these studies have attempted nucleic acid-based characterizations of these microbial populations.

A previous characterization of the GoM mud volcano site examined in this study, seafloor depth of 600 m, indicated the presence of high-molecular-weight hydrocarbons while gas sampling of the fluid indicated the composition was >99% methane (MacDonald et al., 2000). No attempts, however, were made to characterize the extant microbial communities associated with this GoM mud volcano system. In the present study, sediments were collected from the mud volcano site designated GB425 using a manned research submersible. The objectives were to characterize the diversity of microbial populations through sediment depth profiles by a culture-independent DNA-based approach and determine the composition of metabolically active members of the microbial community by a culture-independent RNA-based method. Total DNA and RNA were extracted from mud volcano sediment samples and 16S clone libraries generated from PCR and reverse transcription-polymerase chain reaction (RT-PCR) amplification products, respectively. This is one of the first molecular-based

characterizations of metabolically active members of a sediment microbial community associated with a submarine mud volcano system.

2.4 Results

2.4.1 Restriction fragment length polymorphism (RFLP) and rarefaction analyses of 16S rDNA and 16S crDNA GoM clone libraries

The composition of the *Bacteria* and *Archaea* community in a mud volcano site in the Gulf of Mexico (GoM) was determined by 16S rRNA phylogenetic analyses of clone libraries derived from RNA and DNA extracted from three different sediment depths. Twelve different 16S rRNA libraries were constructed representing a total of 154 *Bacteria* 16S rDNA clones (DNA-derived), 142 *Bacteria* 16S complementary rDNA clones (RNA-derived, denoted crDNA), 134 *Archaea* 16S rDNA clones and 146 *Archaea* 16S crDNA clones. All clones were grouped according to restriction fragment length polymorphism (RFLP) patterns. Rarefaction analysis was conducted to determine if a sufficient number of clones from each of the libraries were screened to estimate diversity within each of the clone libraries sampled (Fig. 2.1). Curves reached saturation for *Archaea* clones obtained from DNA and RNA (Fig. 2.1). Thus, a sufficient number of clones were sampled representative of the *Archaea* diversity of the DNA and RNA-derived libraries. In contrast, curves did not reach saturation for the *Bacteria* rDNA and crDNA libraries (Fig. 2.1). Although additional sampling of the *Bacteria* rDNA clones would be needed to reveal the full extent of the diversity, numerous dominant RFLP groups were obtained. Specifically, one dominant group of clones from each of the

Bacteria rDNA (02B-9; Fig. 2.2) and crDNA (12BR-1; Fig. 2.2) libraries comprised 36% and 15% of all clones, respectively.

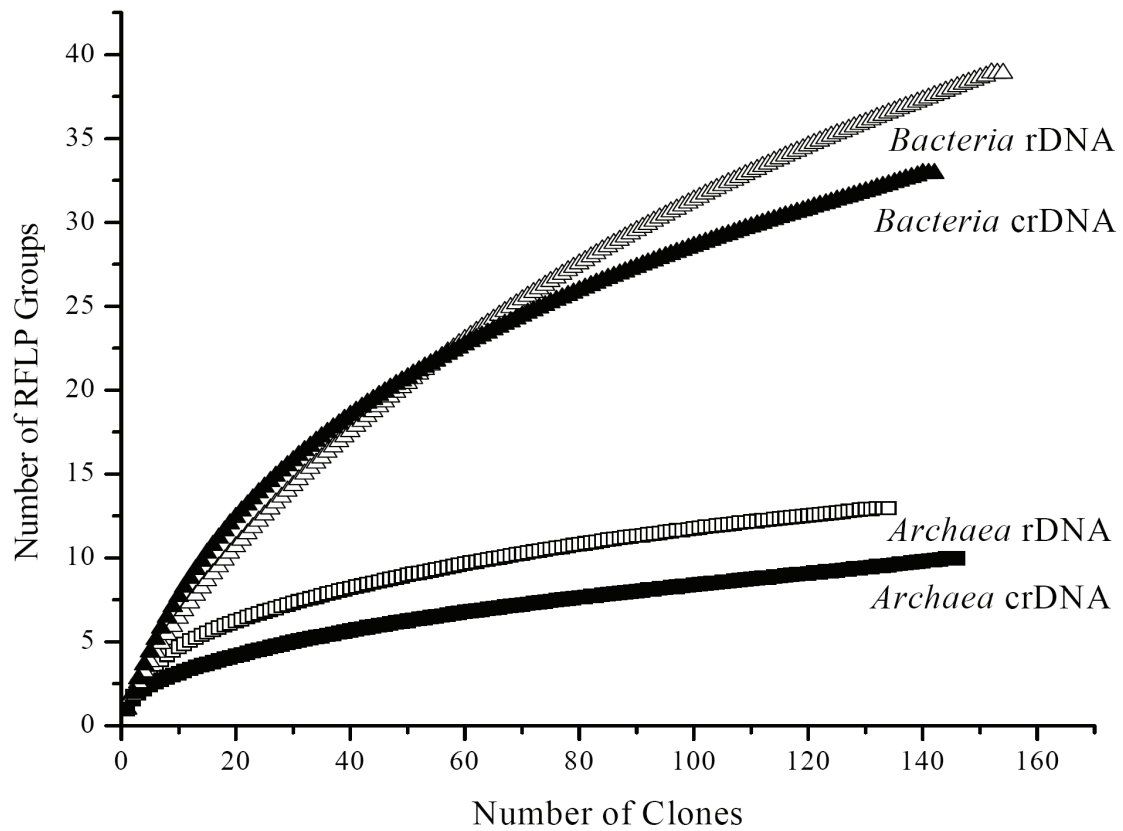


Figure 2.1 Rarefaction curves determined for different RFLP patterns of *Archaea* and *Bacteria* 16S rDNA clones (DNA-derived) and 16S crDNA clones (RNA-derived).

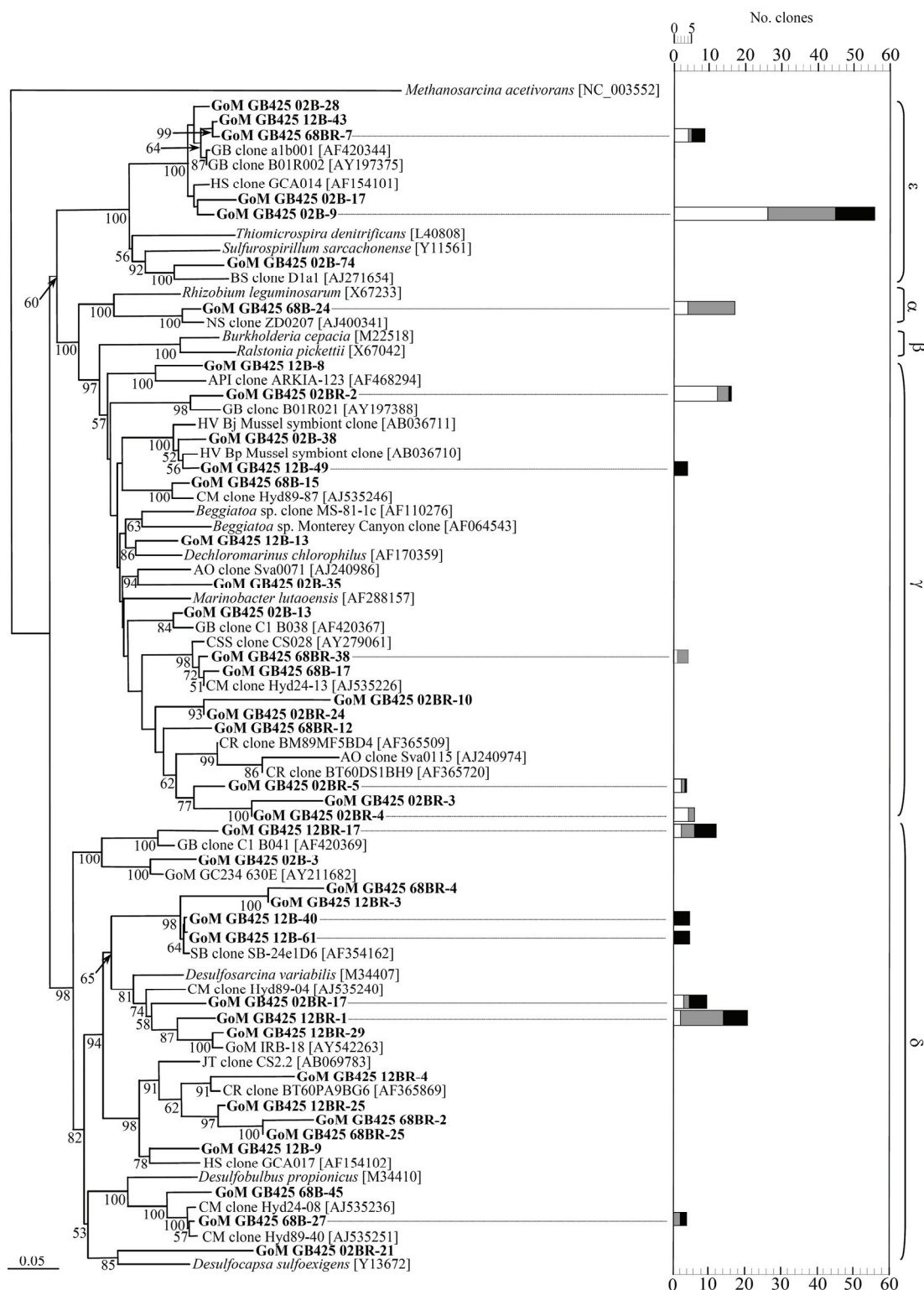


Figure 2.2 Phylogenetic tree of relationships of 16S rDNA and crDNA *Proteobacteria*-related clone sequences, as determined by distance Jukes-Cantor analysis, from sediments

collected from Gulf of Mexico GB425 mud volcano (in boldface) to selected cultured isolates and environmental clones. Sequences derived from DNA templates are denoted by B, RNA templates by BR. Designations of environmental clone sequences: are API, Antarctic pack ice; AO, Arctic Ocean; BS, Black Sea; CM, Cascadia Margin; CR, chlorinated compound reduction; CSS, cold seep sediment; GB, Guaymas Basin; GoM, Gulf of Mexico; HS, hydrocarbon seep; HV, hydrothermal vent; JT, Japan Trench; NS, North Sea; SB, Santa Barbara Basin. GenBank accession numbers are in brackets. Bootstrap values represent 1,000 replicates and only values greater than 50% are reported. The scale bar represents 0.05 substitutions per nucleotide position. Stacked histograms denote rDNA and crDNA phylotypes with 4 or more representative clones detected at each of the following depths; 0-2 cm (□), 6-8 cm (■) and 10-12 cm (■).

2.4.2 *Bacteria* community composition based on 16S rDNA sequence analyses

Analysis of the 154 rDNA *Bacteria* clones indicated the greatest phylogenetic diversity relative to the other clone libraries (Fig. 2.1, Fig. 2.2 and Fig 2.3). With few exceptions the *Bacteria* clones obtained were most related to as yet uncultured lineages. A total of 40 distinct RFLP patterns representing ten distinct phylogenetic lineages were detected (data not shown). A vast majority of the sequenced clones (113 of 143) belonged to the *Proteobacteria* (Table 2.1 and Fig. 2.2). Of these, 55% were related to the ϵ -*Proteobacteria*, including the most numerically dominant phylotype, 02B-9, most similar to a cold-seep clone from Guaymas Basin (Table 2.1). This phylotype comprised 36% of the total rDNA clone library and was detected at all three depths, most frequently at 0 to 2 cm (Fig. 2.2). Overall, the frequency of the ϵ -related clones decreased with sediment depth with some phylotypes not detected at either the 6 to 8 cm or 10 to 12 cm (Fig. 2.2 and 2.5A). Phylogenetic analyses indicated that the ϵ -related rDNA clones clustered tightly with other environmental clones from other cold seep sediments (Fig. 2.2).

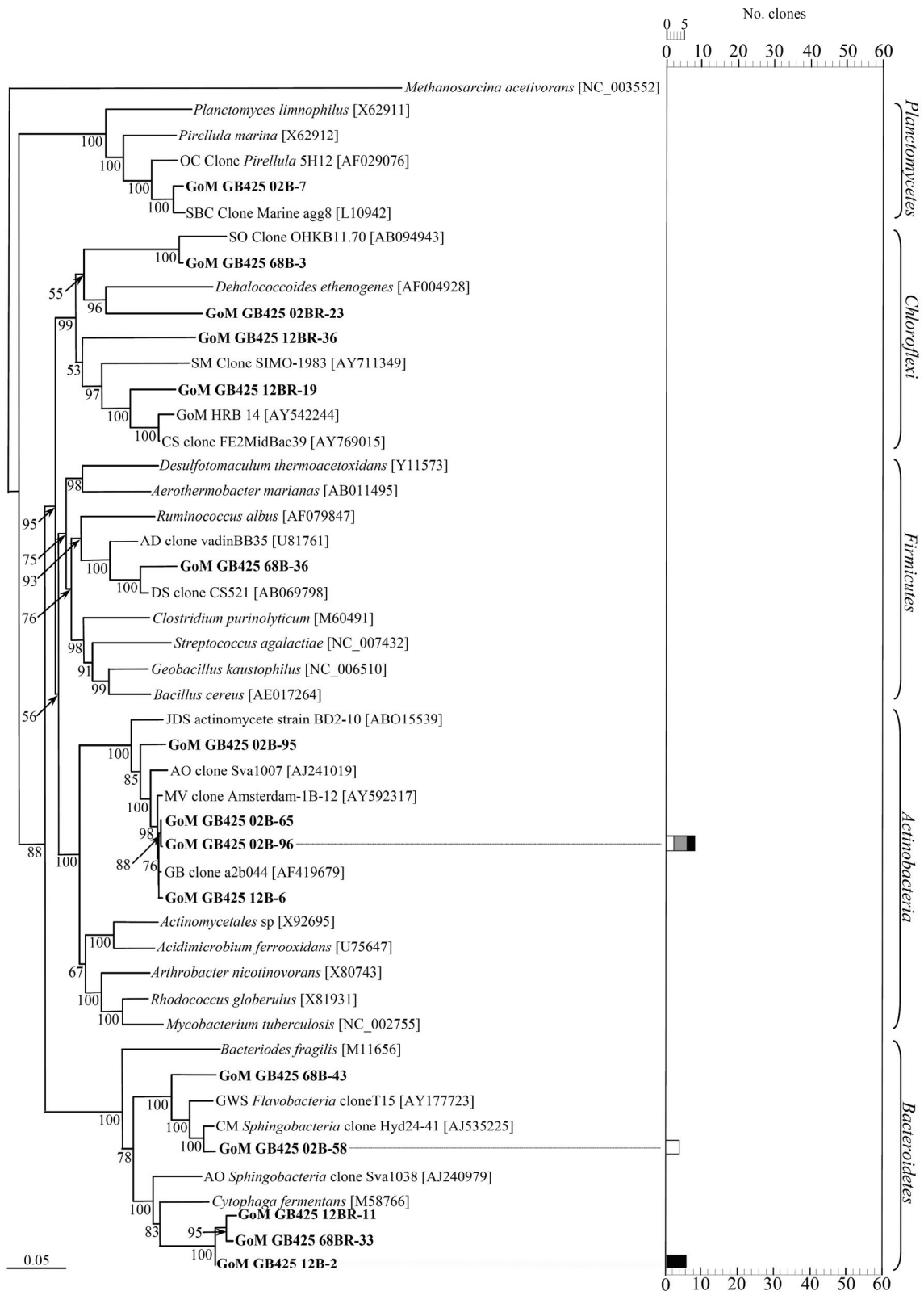


Figure 2.3 Phylogenetic tree of relationships of 16S rDNA and crDNA non-Proteobacteria clone sequences, as determined by distance Jukes-Cantor analysis, from

sediments collected from Gulf of Mexico GB425 mud volcano (in boldface) to selected cultured isolates and environmental clones. Designations of environmental clone sequences are: AD, anaerobic digester; CM, Cascadia Margin; DSS, deep subsurface; ES, estuarine sediment; GB, Guaymas Basin; GoM, Gulf of Mexico; JT, Japan Trench; MV, mud volcano; OC, Oregon coast; SBC, Santa Barbara Channel; SCS, South China Sea; SO, Sea of Okhotsk; SR, soil rhizosphere. GenBank accession numbers are in brackets. Bootstrap values represent 1,000 replicates and only values greater than 50% are reported. The scale bar represents 0.05 substitutions per nucleotide position. Stacked histograms denote rDNA and crDNA phylotypes with 4 or more representative clones detected at each of the following depths; 0-2 cm (□), 6-8 cm (■) and 10-12 cm (■).

The remaining proteobacterial lineages (α , δ , and γ) comprised between 14 and 16% of the total 16S rDNA library. The sole GoM α -phylotype, most closely related to a North Sea environmental sequence (Table 2.1) (Zubkov et al., 2002) represented 26% of the total clones detected at 6 to 8 cm (Fig. 2.2 and 2.5A). With the exception of this α -related phylotype, no one phylotype numerically dominated these DNA clone libraries (Table 2.1 and Fig. 2.2). Overall, the γ - and δ -phylotypes exhibited the greatest phylogenetic diversity relative to all proteobacterial lineages detected (Fig. 2.2). The number of δ -related clones detected was highest at 10 to 12 cm (Fig. 2.5A) and only one phylotype (68B-27; Table 2.1), most similar to an environmental sequence from Cascadia Margin (Knittel et al., 2003), was detected at more than one depth. Similarly, γ -*Proteobacteria* related clones increased numerically in abundance with increasing depth (Fig. 2.5A). The remaining 30 sequenced clones were related to non-*Proteobacteria* lineages including *Actinobacteria* and *Bacteroidetes* (Table 2.1). *Actinobacteria* represented 9% of all rDNA clones detected. Four distinct RFLP patterns were observed (data not shown) and all of the *Actinobacteria*-related phylotypes were most similar (Table 2.1) to a cold seep environmental sequence from Guaymas Basin (Teske et al., 2002) (Fig. 2B) and to several Mediterranean mud volcano clones (unpublished). Similar

percentages of these clones were detected for each of the depth profiles (Fig. 2.5A). There may be depth-restricted phylotypes, though these clones occurred infrequently ($n < 4$) in the clone library (Fig. 2.3). The *Bacteroidetes*-related clones represented 8% of the total rDNA *Bacteria* library and clones 12B-2 and 02B-58 (Table 2.1) exhibited potential similar depth restricted pattern as some of the *Actinobacteria*-related clones (Fig. 2.3). These two phylotypes are also phylogenetically distinct from each other (Fig. 2.3). *Chloroflexi*, *Firmicutes*, and *Planctomycetes*-related clones were observed, however, these clones occurred infrequently ($n < 4$) (Fig. 2.3). Clones related to *Firmicutes*, *Planctomycetes* and *Chloroflexi* each comprised 4% or less of the total rDNA clones (Fig. 2.5A).

Table 2.1

Representative archaeal and bacterial clones sequenced from both 16S rDNA and 16S crDNA clone libraries (Table illustrates sequences that appeared 4 or more times for each respective phylotype).

Domain	Phylogenetic Group	Clone Designation	Nearest Relative	Similarity (%)
<i>Archaea</i>	Marine Benthic Group B	GoM GB425 02A-2	GoM GC234 001R	93
	Unclass. <i>Euryarchaeota</i>	GoM GB425 02A-11	GB Clone AT_R040	89
	ANME-2A	GoM GB425 02A-7	ER Clone BA2H11fin	97
		GoM GB425 02A-21	SB Clone SB-24a1F10	98
		GoM GB425 12AR-3	ER Clone BA2H11fin	99
		GoM GB425 02AR-18	ER Clone BA2H11fin	99
	ANME-2B	GoM GB425 02A-3	ER Clone Eel-36a2A4	98
		GoM GB425 68AR-4	ER Clone Eel-36a2A4	100
	ANME-2C	GoM GB425 02AR-1	ER Clone Eel-36a2A1	99
		GoM GB425 02AR-21	ER Clone Eel-36a2A1	98
<i>Bacteria</i>	α - <i>Proteobacteria</i>	GoM GB425 68-B24	NS Clone ZD0207	95
	γ - <i>Proteobacteria</i>	GoM GB425 12B-49	Bj Mussel Symbiont	97
		GoM GB425 02BR-2	GB Clone B01R021	95
		GoM GB425 02BR-4	<i>Beggiatoa</i> sp. clone MS-81-1c	89
		GoM GB425 02BR-5	AO Clone Sva0115	90
		GoM GB425 68BR-38	CSS Clone CS028	97
	δ - <i>Proteobacteria</i>	GoM GB425 12B-61	SB Clone SB-24e1D6	99
		GoM GB425 68B-27	CM Clone Hyd24-08	99
		GoM GB425 12B-40	SB Clone SB-24e1D6	97
		GoM GB425 02BR-17	CM Clone Hyd89-04	96
		GoM GB425 12BR-1	GoM IRB-18	96
		GoM GB425 12BR-17	GB Clone C1 B041	98
	ε - <i>Proteobacteria</i>	GoM GB425 02B-9	GB Clone a1b001	97
		GoM GB425 68BR-7	GB Clone a1b001	98
	<i>Actinobacteria</i>	GoM GB425 02B-96	GB Clone a2b044	98
	<i>Bacteroidetes</i>	GoM GB425 12B-2	<i>Cytophaga fermentans</i>	88
		GoM GB425 02B-58	CM Clone Hyd24-41	96

digestive tract (marine fish); ER, Eel River; GAB, Great Artesian Basin; GB, Guaymas Basin; GoM, Gulf of Mexico; HV, hydrothermal vent; MS, marine sediments; MT, Mariana Trench; SB, Santa Barbara Basin; SO, Sea of Okhotsk; SP, salt pond. GenBank accession numbers are in brackets. Bootstrap values represent 1,000 replicates and only values greater than 50% are reported. The scale bar represents 0.05 substitutions per nucleotide position. Stacked histograms denote rDNA and crDNA phylotypes with 4 or more representative clones detected at each of the following depths; 0-2 cm (□), 6-8 cm (■) and 10-12 cm (■).

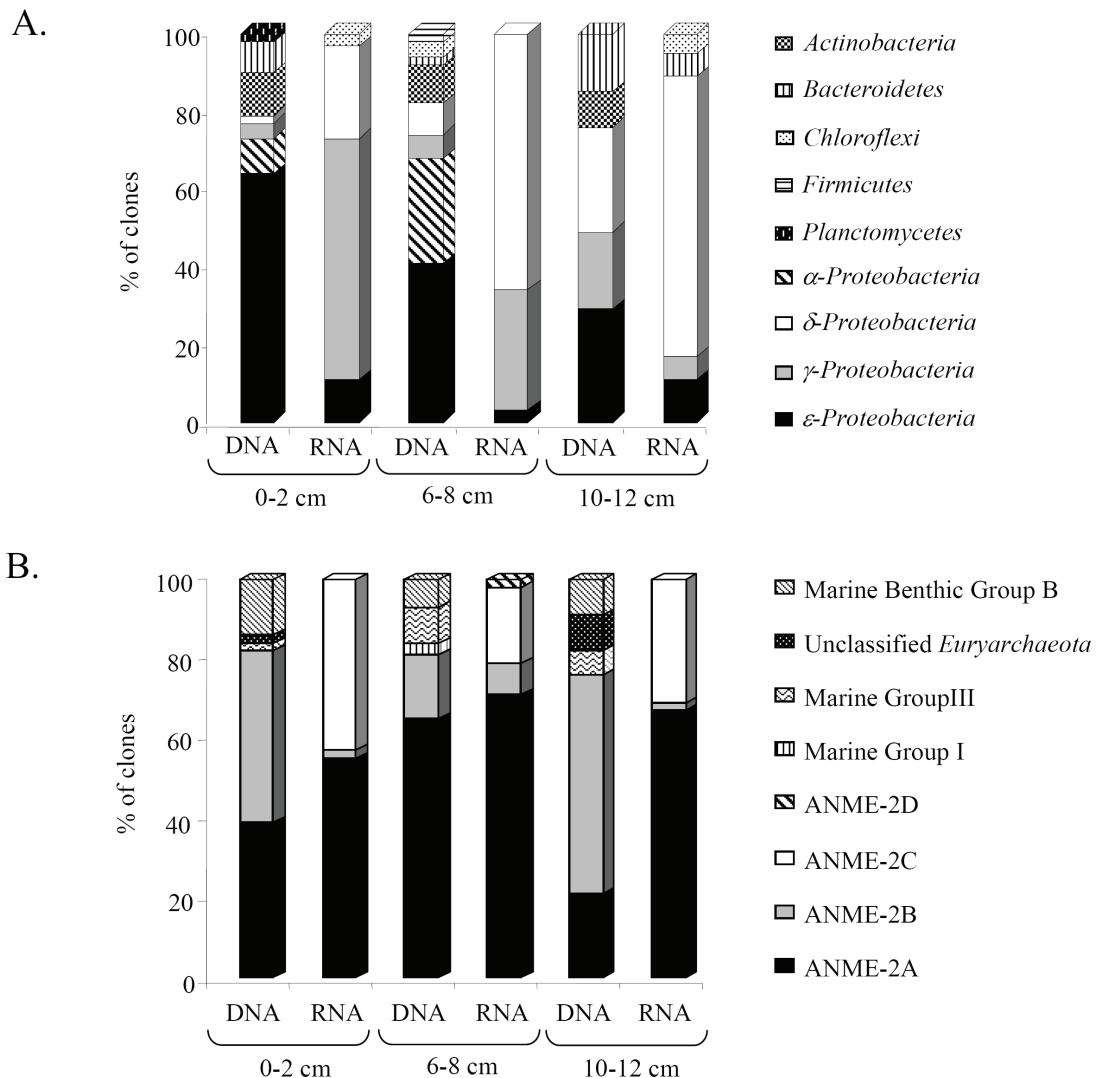


Figure 2.5. (A). Frequency of bacterial phylogenetic lineages detected in 16S rDNA (DNA) and 16S crDNA (RNA) clone libraries derived from sediment depth intervals 0 to 2 cm, 6 to 8 cm and 10 to 12 cm. Calculations were based on the total number of clones associated with phylotypes from which a representative clone had been sequenced. **(B).**

Frequency of archaeal phylogenetic lineages detected in 16S rDNA (DNA) and 16S crDNA (RNA) clone libraries derived from sediment depth intervals 0 to 2 cm, 6 to 8 cm and 10 to 12 cm. Calculations were based on the total number of clones associated with phylotypes from which a representative clone had been sequenced.

2.4.3 Phylogenetic diversity of metabolically active *Bacteria*

Analysis of the 142 *Bacteria* crDNA clones (RNA-derived) revealed a lower diversity relative to the *Bacteria* rDNA library (Fig. 2.1, 2.2, and 2.3) and again included predominately uncultured bacterial lineages (Table 2.1). A total of 33 RFLP patterns representing seven distinct phylogenetic lineages were detected (data not shown). The vast majority of the sequenced clones (100 of 111) were representative of the *Proteobacteria* (Fig. 2.2). Of these, 50% were δ -related, including the most numerically dominant phylotype, 12BR-1 (Table 2.1 and Fig. 2.2). This phylotype was most closely related to an environmental clone sequence recently obtained from Gulf of Mexico sediments associated with seafloor-breaching gas hydrates located 105 to 131 kilometers to the east of GB425 (Mills et al., 2003; Mills et al., 2005). The percentage of δ -related crDNA clones detected increased with increasing depth (Fig. 2.5A). A similar trend was observed with the δ -related rDNA-derived clones (Fig. 2.5A). The three most numerically dominant δ -related phylotypes were detected at all three depths (Fig. 2.2). The δ -related phylotypes exhibited considerable phylogenetic relatedness as evidenced by the occurrence of several distinct GoM clades (Fig. 2.2). The remaining 44 *Proteobacteria*-related crDNA clones represented the γ - and ϵ -lineages with γ representing the second most frequently detected metabolically active lineage (Fig. 2.2). Eight distinct γ -related phylotypes, comprising 32% of the total crDNA library, were

detected with the most numerically dominant phylotype, 02BR-2, most similar to an environmental sequence from Guaymas Basin (Fig. 2.2 and Table 2.1). In contrast to the δ -related crDNA clones, γ -related clones were detected most frequently at 0 to 2 cm (Fig. 2.5A). The sole ε -related phylotype, 68BR-7, most similar to a cold seep clone sequence from Guaymas Basin (Table 2.1) (Teske et al., 2002), was detected at all depths (Fig. 2.2).

The remaining crDNA clones were related to the non-*Proteobacteria* phyla, *Bacteroidetes* and *Chloroflexi* (Fig. 2.3). *Bacteroidetes*-related crDNA clones were most closely related to *Cytophaga fermentans* (Fig. 2.3). Neither of the two *Bacteroidetes*-related phylotypes were detected at 0 to 2 cm. *Chloroflexi*-related crDNA clones were only detected at the 0 to 2 cm and 10 to 12 cm depths.

2.4.4 Archaea community composition based on 16S rDNA sequence analyses

Analysis of the 134 *Archaea* rDNA clones revealed lower diversity relative to the *Bacteria* rDNA library (Fig. 2.1 and 2.4) and included only uncultured archaeal lineages. A total of 14 RFLP patterns representing six distinct phylotypes were detected (data not shown). The majority of the *Archaea* clones (107 of 134) belonged to the order *Methanosarcinales* (Fig. 2.4). Of these clones, 49% were related to the ANME-2B clade, including the most numerically dominant phylotype 02A-3. This phylotype was most closely related to an environmental clone sequence obtained from a marine cold seep (Table 2.1) (Orphan et al., 2001b). The second most dominant phylotype, 02A-7, was most closely related to an environmental clone sequence within the ANME-2A clade (22% of the total library) (Hinrichs et al., 1999) and comparable numbers were detected

at all depths (Fig. 2.4). Clones related to anaerobic methane oxidizing archaeal populations (i.e., ANME-2A and 2B; Table 2.1) were detected at all three depths (Fig. 2.5B). However, phylotype 02A-21 was detected more frequently at 6 to 8 cm (Fig. 2.4). In contrast, the most dominant phylotype, 02A-3, occurred less frequently at the 6 to 8 cm depth (Fig. 2.4).

The remaining eight phylotypes, comprising 27 rDNA clones, were related to non-methanogenic lineages including Marine Groups I and III (van der Maarel et al., 1998; Lanoil et al., 2001; Benlloch et al., 2002; Inagaki et al., 2003; Mills et al., 2003), Marine Benthic Group B (Mills et al., 2003) and unclassified *Euryarchaeota* (Teske et al., 2002). The most numerically dominant phylotype, 02A-2, comprised 10% of the total library and was distantly related (Table 2.1) to environmental clone GoM GC234 001R previously isolated from hydrate-bearing cold seep sediments in the northern GoM (Fig. 2.4) (Mills et al., 2003). This phylotype was detected at all depths with similar frequency (Fig. 2.5B). A total of 5 phylotypes (n=8 clones) clustered with the Marine Group III (Fig. 2.4). With the exception of 02A-9, clones related to this group were detected only at 6 to 8 cm and 10 to 12 cm. Similarly, phylotype 02A-11 comprising 4% of the total library and only distantly related to an environmental clone sequence (Table 2.1) (Zhang, 2002) was most frequently detected at 10 to 12 cm (Fig. 2.4).

2.4.5 Phylogenetic diversity of metabolically active *Archaea*

Analysis of the 144 *Archaea* crDNA (i.e., RNA-derived) clones revealed lower diversity relative to the *Bacteria* crDNA library (Fig. 2.1) and included only uncultured lineages related to putative anaerobic methane oxidizers from other cold seep locales

(Table 2.1). A total of 8 RFLP patterns comprising four distinct phylotypes were detected (data not shown) from the metabolically active archaeal populations. All of the sequenced clones were representatives of the order *Methanosarcinales* (Table 2.1 and Fig. 2.4). Of these, 65% were related to the ANME-2A clade, including the most numerically dominant phylotype denoted 12AR-3 (61% of the total crDNA library; Table 2.1). This phylotype was most closely related to the cold seep environmental sequence Ba2H11fin from California continental margin hydrate-containing sediments (Table 2.1) (Hinrichs et al., 1999). This phylotype occurs at comparable frequency at all three depths (Fig. 2.4). The second most metabolically active lineage was related to ANME-2C and was detected approximately 2-fold more frequently at 0 to 2 cm and 10 to 12 cm (Fig. 2.5B). ANME-2C-related phylotype 02AR-1 comprised 27% of the total crDNA library and was most closely related to an environmental sequence (Table 2.1) (Hinrichs et al., 1999). In contrast to the ANME-2C lineage, the remaining two metabolically active lineages related to ANME-2B and ANME-2D, 68AR-4 and 68AR-18, respectively, were most frequently detected at 6 to 8 cm.

2.4.6 Quantitative PCR of ANME-2A and ANME-2C

A number of environmental studies have reported discrepancies between RNA-derived and DNA-derived clone libraries, specifically clones detected only in crDNA libraries (Nogales et al., 1999; Nogales et al., 2001; Mills et al., 2005; Moeseneder et al., 2005). Although ANME-2A clones were detected in both libraries, we were unable to detect ANME-2C clones in any of the DNA-derived libraries (Fig. 2.5B). To determine if the lack of ANME-2C rDNA clones detected in this study was perhaps due to either

low cellular abundance yet high metabolic activity or to methodological issues, the 16S rDNA copy number per gram of sediment of the dominant ANME-2 clades detected in the RNA libraries (i.e., ANME-2A and ANME-2C) was determined. Primers for ANME-2A amplification, designed in this study, and ANME-2C-specific primers previously reported (Girguis et al., 2003) were tested against all ANME-2 clades from GoM libraries and *Methanosarcina acetivorans*. No cross-reactivity with either ANME-2C- or ANME-2A-specific primers was observed in non-quantitative PCR reactions (data not shown). SYBR-based quantitative PCR results indicated minimal ANME 2A- and 2C-primer cross-reactivity (i.e., four orders of magnitude less per unit template, only detected in the last 2 to 3 cycles of the reaction) only between ANME-2B and ANME-2A, respectively (data not shown). Estimated 16S rDNA copy number per gram sediment of ANME-2A and ANME-2C populations indicated a significant increase (ANOVA, $P < 0.001$) with depth (Table 2.2). Sediments did, however, have considerable ANME-2C 16S rDNA copies ranging from 2.35×10^4 to 4.74×10^5 per gram, abundances that were in some cases greater than measured ANME-2A copy number (Table 2.2).

Table 2.2

Determination of anaerobic methane oxidizing archaeal ANME-2A and ANME-2C populations

Sediment depth (cm)	Mean no. of ANME-2A 16S rDNA/g of sediment \pm SE	Mean no. of ANME-2C 16S rDNA/g of sediment \pm SE
0 to 2	$1.64 \times 10^4 \pm 2.64 \times 10^2$	$2.35 \times 10^4 \pm 3.64 \times 10^2$
6 to 8	$2.58 \times 10^5 \pm 1.82 \times 10^2$	$4.74 \times 10^5 \pm 3.32 \times 10^2$
10 to 12	$1.33 \times 10^5 \pm 8.53 \times 10^1$	$4.51 \times 10^4 \pm 2.89 \times 10^2$

Data are based on four independent sample analyses.

SE, standard error.

2.5 Discussion

This study is the first to report the composition of the microbial assemblages (based on DNA-derived libraries) as well as the metabolically active members of the archaeal and bacterial populations (based on rRNA-derived libraries) extant in a seafloor mud volcano in the northern Gulf of Mexico. Moreover, this is also one of the first descriptions of the metabolically active archaeal and bacterial populations from a seafloor mud volcano as determined by RT-PCR of 16S rRNA along a sediment depth profile. Marine methane seep systems have repeatedly been shown to harbor uncultured and frequently novel microbial lineages (Hinrichs et al., 1999; Boetius et al., 2000; Orphan et al., 2001b; Nauhaus et al., 2002; Girguis et al., 2003; Mills et al., 2003; Mills et al., 2004; Mills et al., 2005). In contrast, less is known with regard to microbial community structure in submarine mud volcano systems.

Metabolically active microbial communities were detected at all depths sampled within the GoM mud volcano sediments. A 4- and 6.8-fold higher RNA:DNA ratio was observed for 0 to 2 cm depth relative to 6 to 8 cm and 10 to 12 cm respectively. As cell numbers were comparable at each depth perhaps other factors may be influencing metabolic activity (e.g., salinity). In the current study, a limited coincidence of overlapping 16S rDNA and rRNA clones was detected. It is tempting to speculate that this result is due (largely) to the differences in the abundance versus the metabolically active fraction of the mud volcano sediment community. However, it is well recognized, that DNA- and RNA-based molecular based approaches to characterize microbial communities are subject to inherent technical biases (Baker et al., 2003 238). Such

biases include differential and/or incomplete cell lysis, differences in nucleic acid extraction and recovery as well as primer biases that can affect the overall microbial diversity estimation. As methodology for the extraction of RNA from soil and sediments suitable for enzymatic manipulation has improved (Alm and Stahl, 2000; Hurt et al., 2001), an increasing number of studies have attempted to characterize the metabolically active bacterial and archaeal populations from diverse habitats (Miskin et al., 1999; Nogales et al., 1999; Nogales et al., 2001; Inagaki et al., 2002; Mills et al., 2004; Moeseneder et al., 2005). However, fewer studies have conducted corresponding DNA and RNA analyses on the same samples (Teske et al., 1996; Nogales et al., 1999; Nogales et al., 2001; Mills et al., 2005; Moeseneder et al., 2005). As has been reportedly previously, microbial growth rates correlate strongly with rRNA content (Nomura et al., 1984). Therefore, when attempting to compare DNA-derived clone libraries to comparable RNA-derived libraries differing levels of metabolic activity (e.g., concentrations of ribosomes per cell) may affect the relative frequencies of clones observed in each library (Nogales et al., 2001; Koizumi et al., 2003; Moeseneder et al., 2005).

Analyses of the 12 *Bacteria* and *Archaea* clone libraries representing three different sediment depths (0 to 2, 6 to 8 and 10 to 12 cm) revealed distinct differences in the patterns of metabolically active bacterial and archaeal fractions relative to their respective DNA-derived libraries obtained from the same sediment depth. For example, direct comparison of *Bacteria* crDNA and rDNA libraries from the 0 to 2 cm depth indicated that ϵ -*Proteobacterial* rDNA clones dominated the clone library. However, the γ -*Proteobacteria*, rather than the ϵ group, dominated the RNA-derived library in this

study thus indicating γ to be among the most active *in situ* populations detected at 0 to 2 cm. The γ -*Proteobacteria* populations subsequently decreased in activity with increasing sediment depth suggesting environmental conditions less favorable to cell growth and metabolic activity. These findings are in contrast to the results observed for the δ lineage wherein both the DNA and RNA libraries show an increase in relative abundance of δ -related clones with respect to increasing sediment depth. This is not unexpected as the phylotypes associated with this proteobacterial class are likely involved in sulfate reduction, a process generally restricted to anoxic niches. We have observed similar trends for the γ , ϵ and δ classes in comparable sediment depth profiles associated with *Beggiatoa* sp. mat communities as well as sediments (0 to 2 cm depth) associated with surface-breaching gas hydrate mounds located in northern Gulf of Mexico cold seep systems (Mills et al., 2003).

Some microbial lineages, although detected at a frequency as high as 9% or greater in the total DNA library (i.e., *Actinobacteria*, α -proteobacteria), were markedly absent from the RNA-derived libraries suggesting a lack of *in situ* activity in the mud volcano sediments. A similar trend was observed with the non-methanogenic lineages (i.e., Marine Groups I and III, Marine Benthic Group B and the unclassified *Euryarchaeota* group). Although these four lineages were detected at all sediment depths by DNA analyses, none of these groups appeared to be metabolically active *in situ*. Although the ANME-2B lineage dominated at the 0 to 2 cm and 10 to 12 cm depth based on DNA analyses, the ANME-2A and ANME-2C populations were the most metabolically active *in situ*. It is interesting to note that although we detected ANME-2A in rDNA and crDNA clone libraries, we failed to detect ANME-2C in our DNA-derived

library. This result may indicate that GoM ANME-2C related *Archaea*, while perhaps less abundant, are more metabolically active relative to ANME-2B. The occurrence of metabolically active anaerobic methane oxidizing and sulfate reducing populations suggests a highly favorable environment for the anaerobic oxidation of methane in GoM mud volcano sediments. However, corroborating geochemical data will need to be obtained to substantiate our hypothesis.

Numerous studies have reported the characterization of the microbial community structure from marine cold seep sedimentary systems (Hinrichs et al., 1999; Boetius et al., 2000; Orphan et al., 2001b; Nauhaus et al., 2002; Girguis et al., 2003; Knittel et al., 2003; Mills et al., 2003; Mills et al., 2004; Mills et al., 2005), including efforts describing a possible bacterial and archaeal partnership(s) promoting the anaerobic oxidation of methane (Boetius et al., 2000; Orphan et al., 2001a; Michaelis et al., 2002; Kallmeyer, 2004). However, to date, only a limited number of studies have addressed the microbiology of marine mud volcano systems (Pancost et al., 2000; Pimenov et al., 2000; Yakimov, 2002). Seafloor mud volcanoes, sites of vast gas seepage, have been proposed to play a significant role in atmospheric greenhouse gas (methane) emissions (Dimitrov, 2002; Kopf, 2003; Sassen et al., 2003; Etiope and Milkov, 2004). A previous study had suggested, based on stable isotope and biomarker analyses, that methanogenic microorganisms can readily consume the majority of methane released from mud volcano sediments in the Mediterranean (Pancost et al., 2000). While anaerobic methane oxidizing microbial populations were the (only) metabolically active archaea detected in our study, direct evidence for the oxidization of released methane from GB425 is lacking. Thus, to better understand the microbially mediated contributions to carbon (methane)

cycling and regulation in methane-rich sedimentary systems such as Gulf of Mexico mud volcanoes locales, information on the composition, activity and geochemistry of mud volcano-associated microbial communities is needed.

2.6 Experimental procedures

2.6.1 Site description and sampling

The study site sampled is located in the northern GoM continental slope province. The site, GB425 (600 m water depth) is located at 27°33'N, 92°32'W. A description of the geology and chemistry of this 'mud lake' has been previously reported (MacDonald et al., 2000). Mud samples, fluidized in hypersaline brine (approx. 133‰ salinity), were saturated with methane (MacDonald et al., 2000). A manned submersible (*Johnson Sea-Link*) was used during a July 2002 cruise to retrieve sediment cores and fluids. Multiple sediment core samples (2.9 cm OD, 12-15 cm length) were collected and immediately processed on shipboard. The length of the retrieved core represents the average sample depth that could be recovered from the submersible. Cores were aseptically processed and sectioned into 2 cm intervals and immediately stored in liquid N₂. Salinity values for 0 to 2, 6 to 8, and 10-12 cm depths were 95‰, 104‰, and 110‰, respectively. Microbial cell counts per gram (wet weight) of sediment were comparable at all depths sampled (0 to 2, 6 to 8 and 10 to 12 cm) and ranged from 6.2 to 9.6 x 10⁹.

2.6.2 Preparation of reagents and materials used with RNA extractions

Prior to shipboard handling or laboratory-based nucleic acid extractions, potential contaminating RNases were removed from all solutions. All stock solutions and water were treated with 0.1% diethylpyrocarbonate (DEPC) overnight at 37°C and autoclaved. All glassware and non-plastics were baked as described in (Hurt et al., 2001). All surfaces and plastics were cleaned with RNase Erase (ICN) to remove contaminating RNases during shipboard and laboratory manipulations.

2.6.3 Nucleic acid isolation

Total ribonucleic acids were extracted essentially as described in Hurt *et al.* (2001) from 10 g (wet weight) of sediment sampled in triplicate from each sediment depth (0 to 2, 6 to 8, and 10 to 12 cm). In brief, sediment samples stored in liquid N₂ were repeatedly thawed by physically grinding in the presence of a denaturing solution (4 M guanidine isothiocyanate, 10 mM Tris-HCl [pH 7.0], 1 mM EDTA, 0.5% 2-mercaptoethanol) and refrozen by immersion in liquid N₂. The sediment samples were incubated for 30 min at 65°C in pH 7.0 extraction buffer (100 mM sodium phosphate [pH 7.0], 100 mM Tris-HCl [pH 7.0], 100 mM EDTA [pH 8.0], 1.5 M NaCl, 1% hexadecyltrimethylammonium bromide [CTAB], and 2% sodium dodecyl sulfate [SDS]) and centrifuged (1,800 × g, 10 min). The supernatants from three separate extractions were pooled, extracted with 24:1 (vol/vol) chloroform-isoamyl alcohol, and centrifuged (1,800 × g, 20 min). RNA was precipitated at room temperature (30 min) in isopropyl alcohol. Samples were pelleted by centrifugation (16,000 × g, 20 min) and resuspended in DEPC-treated water. The corresponding genomic DNA fractions from each depth

were extracted, pooled and purified from triplicate sediment samples as described in Mills *et al.* (2003). The integrity of total nucleic acids and DNase I treated RNA were visualized via agarose (1.0%) gel electrophoresis. The concentration of recovered RNA and DNA respectively at each depth was 85.2 and 42.8 µg/g (0 to 2 cm), 22.2 and 45.3 µg/g (6 to 8 cm) and 18.1 and 60.9 µg/g (10 to 12 cm). Corresponding RNA:DNA ratios indicated the highest value, 1.99, occurred at 0 to 2 cm and ratios decreased with depth, i.e., 0.49 (6 to 8 cm) and 0.29 (10 to 12 cm).

2.6.4 Reverse transcription and amplification of rRNA

Aliquots of rRNA were reverse transcribed with Moloney murine leukemia virus (MMLV) reverse transcriptase according to manufacturer's instructions (Invitrogen). DNaseI-treated purified RNA was initially denatured by heating (65°C) for 10 min. The reverse transcription reaction mix consisted of 5 µM of a 16S rRNA reverse primer amplifying either domain-specific *Bacteria*, i.e., DXR518 (5'-CGTATTACCGCGGCTGCTGG-3') (Nogales et al., 1999) or *Archaea*, i.e., Arch958R (5'-YCCGGCGTTGAMTCCAATT-3') (DeLong, 1992), 50-100 ng of denatured RNA and 200 µM dNTP mix. The mixture was incubated for 5 min at 65°C and 2 min at 4°C followed by the addition of 1 × first-strand buffer (50 mM Tris-HCl [pH 8.3], 75 mM KCl, 3 mM MgCl₂) and heating at 37°C for 2 min. A 200-U aliquot of MMLV was added prior to a 50 min incubation at 37°C that resulted in transcription of the RNA into complementary 16S ribosomal DNA (crDNA). The crDNA end product was used as the template for a standard PCR reaction. Possible DNA contamination of RNA templates was routinely monitored by PCR amplification of aliquots of RNA that were not reverse

transcribed. No contaminating DNA was detected in any of these reactions. The primers used for standard PCR amplification included the above reverse primers (DXR518 and Ar958R) and 16S rDNA forward domain-specific *Bacteria*, 27F (5'-AGAGTTTGATCCTGGCTCAG-3') and *Archaea*, A341F (5'-CCTAIGGGGIGCAICAG-3') primers (Johnson, 1994; Watanabe et al., 2002). The PCR mix contained 10 to 50 ng of crDNA, 1× PCR buffer (Stratagene), 1.5 mM MgCl₂, 200 μM of each dNTP, 0.25 μM of each forward and reverse primer, and 1.7 Units Taq polymerase (Takara Bio). Amplicons were analyzed on 1.0% agarose gels run in TBE buffer stained with ethidium bromide and UV illuminated.

2.6.5 Polymerase chain reaction amplification of genomic DNA

The amplification of *Bacteria* 16S rDNA using 27F (5'-AGAGTTTGATCCTGGCTCAG-3') and 1522R (5'-AAGGAGGTGATCCARCCGCA-3') (Johnson, 1994) and of *Archaea* 16S rDNA using Arch21F (5'-TTCCGGTTGATCCYGCCGGA-3') and Arch958R (5'-YCCGGCGTTGAMTCCAATT-3') (DeLong, 1992) from purified extracted sediment community DNA was followed as previously described in Mills *et al.* (2003). Amplified products were analyzed on 1.0% agarose gels run in TBE buffer, stained with ethidium bromide, and UV illuminated. Amplicons were subsequently pooled from three to five reactions and purified with the Qiaquick gel extraction kit (Qiagen).

2.6.6 Environmental clone library construction

16S amplicons, derived from RNA (crDNA) and DNA samples (rDNA), were subsequently pooled from three to five reactions and cloned into the TOPO TA cloning vector pCR2.1 according to manufacturer's instructions (Invitrogen). To prevent amplification of *Escherichia coli* host 16S rDNA, M13F and M13R primers were used to amplify inserts from *Bacteria* crDNA and rDNA and *Archaea* crDNA clones and *Archaea* rDNA clones were amplified with Arch21F and Arch958R primers (DeLong, 1992). PCR products from both *Bacteria* and *Archaea* rDNA libraries were digested with MspI. PCR products from *Bacteria* and *Archaea* crDNA libraries were digested with MspI/HhaI and RsaI/HhaI, respectively. Clones were grouped according to restriction fragment length polymorphism (RFLP) banding patterns, unique clones identified and sequenced as described in Mills *et al.* (2003). Multiple (e.g., two or more) representative clones were sequenced from RFLP groups containing five or more members. Sequencing was performed at the Georgia Tech core DNA facility using a BigDye Terminator v3.1 Cycle sequencing kit on an automated capillary sequencer (model 3100 Gene Analyzer, Applied Biosystems).

2.6.7 Phylogenetic and rarefaction analysis

Briefly, multiple sequences of individual inserts were initially aligned using the program 'BLAST 2 Sequences' (Tatusova and Madden, 1999) available through the National Center for Biotechnology Information and assembled with the program BioEdit v5.0.9 (Hall, 1999). Sequences were checked for chimeras using Chimera Check from Ribosomal Database Project II (Maidak et al., 1999). Sequences from this study and

reference sequences were subsequently aligned using CLUSTAL X (Thompson et al., 1997). An average of at least 550 nucleotides were included in the phylogenetic analyses of bacterial and archaeal clones. Bootstrapped neighbor-joining trees (Saitou and Nei, 1987) with 1,000 samplings were created in MEGA3 (Kumar et al., 2004) using the Jukes-Cantor model (Jukes, 1969). Rarefaction analysis was performed using equations as previously described in (Heck et al., 1975). Standard calculations were used to produce the curve using the total number of clones obtained compared to the number of clones representing each unique RFLP pattern. The 44, 16S rDNA and 34, 16S crDNA gene nucleotide sequences have been deposited in the GenBank database under accession numbers AY542549-AY542626.

2.6.8 Quantitative PCR of ANME-2A and ANME-2C environmental rDNA

Primers specific for ANME-2A were designed by aligning previously published ANME-2A 16S rDNA sequences (Orphan et al., 2001b) with ANME-2A 16S rDNA sequences obtained from this study using CLUSTAL X (Thompson et al., 1997). Specificity of ANME-2A primers was determined by nBLAST nucleotide homology analysis (<http://www.ncbi.nlm.nih.gov/BLAST/>) and by PROBE_CHECK from the Ribosomal Database Project (<http://rdp.cme.msu.edu/index.jsp>). Cross-reactivity testing of ANME-2A primers was determined with *Methanosarcina acetivorans* genomic DNA, partial ANME-2B 16S rDNA gene sequences and partial ANME-2C 16S crDNA gene sequences. Quantification of ANME-2A and ANME-2C 16S rDNA genes was conducted using clones GoM GB425 02A-7 (ANME-2A) and GoM GB425 02AR-1 (ANME-2C) cloned into TOPO TA cloning vector pCR2.1. Serial dilutions of plasmids

bearing ANME-2A and ANME-2C cloned 16S rDNA sequences were used to generate standard curves for quantification. Environmental DNA from 0.5 g (wet weight) sediment isolated as previously described (Mills et al., 2003) was used as the template DNA with ANME-2A specific primers AR429F (5'-TCATTTGTTAGCAAGGGCCG-3') and AR805R (5'-AAACACGGTCGCACCGTGT-3') designed in this study and ANME-2C specific primers AR468F (5'-CGCACAAGATAGCAAGGG-3') and AR736R (5'-CGTCAGACCCGTTCTGGTA-3') (Girguis et al., 2003). Amplification of environmental 16S rDNA sequences were conducted using 1X Platinum SYBR Green (Invitrogen) containing 0.375 U of Platinum Taq DNA polymerase, 200 µM each of dATP, dGTP, dCTP and dUTP, 3mM MgCl₂, 250 µM AR429F and AR805R (ANME-2A-specific) or AR468F and AR736R (ANME-2C-specific) and 0.25 U uracil-N-glycosylase. SYBR Green quantitative PCR assays were run as follows: initial 95°C for 10 min and 40 cycles at 95°C for 1 min, 60°C for 1 min and 72°C for 1 min. The expected PCR product size of 377 bp (ANME-2A) and 274 bp (ANME-2C) was verified on a 1.0 % agarose gel.

2.6.9 Data Analysis

A one-way analysis of variance (ANOVA) was performed in SYSTAT 9 to determine the significance of ANME-2A and ANME-2C 16S rDNA copy numbers along the depth of the sediment profile.

2.7 Conclusions

This is the first study to identify metabolically active prokaryotes within marine mud volcano sediments via rRNA extraction. Our data identified δ -, γ -, and ε -*Proteobacteria* as the dominant metabolically active bacterial lineages. Analysis of metabolically active archaeal lineages identified ANME-2A and ANME-2C as the dominant anaerobic methane oxidizing clades.

2.8 Acknowledgements

This material is based upon work supported by NSF grant OCE-0085549 and NSF grant DBI-0304606. The U.S. Department of Energy and the National Undersea Research Program provided support for submersible operations. We thank the crews of the *R/V Seward Johnson* and the *Johnson Sea Link* for their invaluable assistance with sample collection.

CHAPTER 3

HORIZONTAL GENE TRANSFER OF PIB-TYPE ATPASES AMONG *BACTERIA* ISOLATED FROM RADIONUCLIDE- AND METAL-CONTAMINATED SUBSURFACE SOILS

3.1 Overview

This chapter examines the culturable aerobic heterotrophs isolated from radionuclide- and metal-contaminated mixed waste subsurface soils obtained from the U.S. Department of Energy's (DOE) Field Research Center (FRC) in Oak Ridge, TN. Within the FRC contaminated soils, microorganisms must tolerate the low pH and high radionuclide and metal concentrations that resulted from the unregulated waste dumping during the U.S. nuclear weapons development program. Thus, metal resistance genes are a necessity for microorganisms to survive in such environments. Horizontal gene transfer (HGT) of metal resistance determinants such as P_{IB}-type ATPases can enhance the survival of microbial communities present in mixed waste sites. Here we examined 400 culturable isolates that were obtained from the contaminated subsurface soils and screened for resistance to cadmium, chromium, lead, and mercury. A subset of metal resistant isolates, which were dominated by *Arthrobacter*, *Bacillus*, and *Rahnella* spp., were screened for the presence of P_{IB}-type ATPases as well as evidence that these genes were disseminated via HGT.

3.2 Summary

Aerobic heterotrophs were isolated from subsurface soils sampled from the U.S. Department of Energy's (DOE) Field Research Center (FRC) located in Oak Ridge, Tenn. The FRC represents a unique and extreme environment consisting of highly acidic soils, co-occurring heavy metals, radionuclides and high nitrate concentration. Four hundred isolates from contaminated soils were assayed for heavy metal resistances and a smaller subset for tolerance to uranium. The vast majority of the isolates were gram-positive and belonged to the high G+C and low G+C genera *Arthrobacter* and *Bacillus*, respectively. Genomic DNA from a randomly chosen subset of 50 Pb-resistant (Pb^{r}) isolates was amplified with PCR primers specific for P_{IB} -type ATPases (i.e., *pbrA/cadA/zntA*). A total of 10 *pbrA/cadA/zntA* loci exhibited evidence for acquisition by horizontal gene transfer. A remarkable dissemination of these horizontally acquired P_{IB} -type ATPases was supported by unusual DNA base compositions and phylogenetic incongruence. Numerous Pb^{r} P_{IB} -type ATPase-positive FRC isolates belonging to the genus *Arthrobacter* tolerated toxic concentrations of soluble U(VI) (UO_2^{2+}) at pH 4. These unrelated, yet synergistic, physiological traits observed in *Arthrobacter* isolates residing in the contaminated FRC soils may contribute to their survival in such an extreme environment. This study is, to the best of our knowledge, the first study to report the broad horizontal transfer of P_{IB} -type ATPases in contaminated subsurface soils and is among the first studies to report uranium tolerance of aerobic heterotrophs obtained from the acidic soils at the DOE FRC.

3.3 Introduction

The remediation of hazardous mixed-waste sites, particularly those co-contaminated with heavy metals and radionuclides, remains one of the most costly environmental challenges currently faced by the U.S. and other countries. Interactions between microorganisms, radionuclides and metals that promote their precipitation and immobilization *in situ* are promising strategies for treatment and cleanup of the contaminated subsurface (Fredrickson et al., 2000; Anderson et al., 2003). At mixed-waste sites where concentrations of metal contaminants can reach toxic levels, the metal resistance of indigenous microbial populations could be critical for the success of *in situ* biostimulation efforts. For example, while a number of microbes can carry out reductive precipitation of radionuclides (e.g., *Desulfovibrio* sp., *Geobacter* sp., *Shewanella* sp.) (Lovley et al., 1991; Wade and DiChristina, 2000; Payne et al., 2002), the sensitivity of these organisms to heavy metals could possibly limit their *in situ* activities. Thus, the metal sensitivity of some radionuclide-reducing microbes suggests that the acquisition of metal resistance traits (e.g., P_{IB}-type ATPases that regulate the transport of heavy metals) might be conducive to facilitating and/or enhancing microbial metabolism during subsequent biostimulation activities in metal- and radionuclide-contaminated subsurface environments.

The P-type ATPases represent a chromosomally-encoded superfamily of ion translocating proteins present in all three domains of life (Axelsen and Palmgren, 1998). The prokaryotic heavy metal-translocating P_{IB}-type ATPases detoxify the cell cytoplasm by catalyzing the efflux of divalent ions (i.e., cadmium, cobalt, lead, nickel and zinc)

(Rensing et al., 1999; Axelsen and Palmgren, 2001; Nies, 2003). The P_{IB}-type ATPases represent one of three mechanisms for promoting microbial heavy metal resistance or tolerance: 1) metal reduction (Lovley et al., 1991), 2) metal complexation (Macaskie et al., 1992) and 3) ATP-dependent metal efflux (Nies, 1999). In previous studies workers have also determined the presence of P_{IB}-type ATPase genes encoded on mobile genetic elements (i.e., plasmids and transposons) present in both gram-positive (Nucifora et al., 1989; Lebrun et al., 1994; O'Sullivan et al., 2001) and gram-negative bacteria (Larbig et al., 2002; Mergeay et al., 2003).

Analysis of completed microbial genomes has indicated that horizontal gene transfer (HGT) continues to be an important factor contributing to the innovation of microbial genomes (Nakamura et al., 2004; Beiko et al., 2005; Gogarten and Townsend, 2005). HGT driven by mobile genetic elements such as plasmids (Frost et al., 2005), insertion sequences (Mahillon and Chandler, 1998), integrons (Nemergut et al., 2004) transposons (Pearson et al., 1996), and phages (Canchaya et al., 2003) has been shown to provide microbes with a wide variety of adaptive traits for microbial survival and proliferation (e.g., antibiotic and heavy metal resistance, diverse metabolic capabilities, including xenobiotic degradation and virulence). While point mutations contribute to microbial adaptation, the horizontal dissemination of genes has proven to be more critical in promoting rapid genomic flexibility and microbial evolution (Thomas and Nielsen, 2005). However, HGT among some microbial populations, particularly those present in the deep subsurface, has been postulated to be unlikely to occur owing to the low cell densities and the low permeability of the soil strata (van Waasbergen et al., 2000). Recently, detectable HGT of bacterial P_{IB}-type ATPases in bacterial isolates from a deep

subsurface environment free of heavy metal contamination has been reported (Coombs and Barkay, 2004). Although the HGT of P_{IB}-type ATPases was detected in only a few isolates, the extent of HGT may have been underestimated due to the close relatedness of the bacterial lineages studied (Coombs and Barkay, 2004).

In the present study, we examined the extent of horizontally transferred P_{IB}-type ATPases in bacterial isolates cultured from subsurface soils with a history of radionuclide and heavy metal contamination. The isolates were obtained from soil samples from the Department of Energy (DOE) Field Research Center (FRC) located in the Oak Ridge National Laboratory Reservation (Oak Ridge, TN). The FRC subsurface is an extreme geochemical environment that places a number of stresses on the extant microbial community, including low pH (e.g., < 4), nitrate concentrations that can exceed 100 mM, and the cooccurrence of heavy metals and radionuclides (U and other actinides) (<http://www.esd.ornl.gov/nabirfrc>) (Petrie et al., 2003). Our main objective was to examine the role of HGT in the evolution of metal homeostasis by performing phylogenetic analyses of sequences of *zntA/cadA/copA*-like genes amplified from the genomes of 50 lead-resistant (Pb^r) subsurface bacteria. The P_{IB}-type ATPases were amplified from genomic DNA using a previously described set of PCR primers specific for this subfamily of ATPases (Coombs and Barkay, 2004). Analyses of 28 amplified *zntA/cadA/pbrA*-like loci revealed evidence for their horizontal transfer among 10 Pb^r *Arthrobacter* spp. and *Bacillus* spp strains. Our results indicate that the dissemination of P_{IB}-type ATPases by HGT has occurred recently among isolates representing the *Actinobacteria*, *Firmicutes* and *Proteobacteria* phyla present in metal- and radionuclide-contaminated soils of the FRC.

3.4 Results and Discussion

3.4.1 Viable bacterial populations from contaminated soils and metal resistance phenotypes

Cultivation-based methods were used to isolate aerobic heterotrophs present in radionuclide- and heavy metal-contaminated subsurface soils at the U.S. DOE FRC. In the current study, the numbers of heterotrophic bacteria recovered from the contaminated FRC soils were low, ranging from $< 10 \text{ CFU g}^{-1}$ to 10^4 CFU g^{-1} . All four types of media utilized in this study yielded similar CFU counts. Comparable low population densities for aerobic heterotrophs, isolated on the same media types used in this study, have been previously reported for contaminated soils from a high-level waste plume at the Hanford Site (Fredrickson et al., 2004). While enrichment-based studies targeting Fe(III)-reducing populations from FRC soils have also reported similar low population densities (Petrie et al., 2003), fewer studies have reported data for aerobic populations from the FRC. Such information is particularly relevant as areas within contaminated FRC sites are already oxygenated and/or can become re-oxygenated during rain-driven recharge events. Moreover, microorganisms maintaining metabolic activity in the presence of oxygen may play key roles in sequestration and immobilization of toxic radionuclides such as U(VI) via bioprecipitation processes (Lovley and Coates, 1997; Barkay and Schaefer, 2001). These biologically mediated processes could represent alternative remediation strategies as recent studies have reported the enzymatic and/or abiotic reoxidation of bio-reduced U (Finneran et al., 2002; Elias et al., 2003). Additionally, previous kinetic studies have also shown that, in the presence of electron shuttles, Fe(III)

and Mn(IV) oxides promoted the abiotic oxidation of U(IV) to U(VI) (Nevin and Lovley, 2000; Liu et al., 2002).

The majority (392 of 400) of the FRC isolates recovered from contaminated soils were gram-positive and belonged to the high G+C and low G+C genera *Arthrobacter* and *Bacillus*, respectively. As many as 40% of all cultured isolates recovered from FRC soil were related to *Arthrobacter* based on 16S rDNA analysis (data not shown). Gram-negative isolates recovered from the FRC sediments were most closely related to *Rahnella* (Fig. 3.1). As the acidic FRC soils are co-contaminated with heavy metals (Brooks, 2001), it was of interest to determine the metal resistance phenotypes of the isolates, particularly as it has been postulated that *Arthrobacter* sp. (Suzuki and Banfield, 2004) and *Bacillus* sp. (Merroun et al., 2005) could be important in promoting the remediation of uranium either through intracellular sequestration or bioadsorption mechanisms. The percentage of FRC isolates (n = 400) that were resistant to the heavy metals cadmium, chromium, lead, and mercury were 10%, 11%, 44%, and 49%, respectively. The majority of the FRC isolates also exhibited resistance to two or more metals (data not shown). A comparison of metal resistances between gram-positive FRC isolates and gram-positive strains previously isolated from saturated deep subsurface sediments at the DOE's Hanford and Savannah River (SRS) sites revealed marked differences in resistance phenotypes (Benyehuda et al., 2003). Higher percentages of isolates from Hanford and SRS than of isolates from the FRC (11%) were shown to be resistant to chromium [38% and 37% respectively; (Benyehuda et al., 2003)]. The percentages of Hanford and SRS gram-positive strains resistant to lead were 48% and 20%, respectively (Benyehuda et al., 2003). While 49% of the FRC gram-positive

isolates were resistant to mercury, only 8% of the SRS isolates were mercury resistant (Benyehuda et al., 2003). Cadmium resistance was not determined for the Hanford or SRS isolates in the previous study (Benyehuda et al., 2003). It is important to note that the isolates from Hanford and SRS were cultured from uncontaminated soils from deeper saturated strata, whereas FRC isolates were recovered from the contaminated subsurface. Such site and depth variation could have contributed to the observed differences in metal resistance phenotypes among subsurface bacteria isolated from SRS, Hanford, and FRC sites.

3.4.2 Horizontal transfer of P_{IB}-type ATPases

A cellular enzymatic detoxification mechanism to remove toxic metals is the efflux pumping of mono- and divalent cations via chromosomally-encoded metal homeostasis genes [e.g., P-type ATPases (Kuhlbrandt, 2004)]. Mobile genetic elements, including broad-host-range conjugative plasmids, also encode resistance determinants thus promoting their horizontal transfer to unrelated microorganisms (Mergeay et al., 2003). Recently, Coombs and Barkay (Coombs and Barkay, 2004) investigated the role of HGT in the evolution of lead resistance (Pb²⁺) among 105 deep subsurface strains from uncontaminated Hanford and SRS saturated soils. Using nested PCR primers designed to specifically amplify P_{IB}-type ATPases (e.g., *zntA/cadA/pbrA* -like), this study produced evidence for HGT of *zntA/cadA/pbrA*-related loci among gram-negative *Proteobacteria*. A total of 48 amplicons were obtained from 105 Pb²⁺ isolates though only 4 of these amplicons, belonging to the genera *Acinetobacter*,

Comamonas, and *Ralstonia*, exhibited criteria (phylogenetic incongruency, G+C content) indicative of acquisition by HGT.

To trace the possible evolutionary path(s) of the metal homeostasis genes in FRC bacteria from the contaminated subsurface, ATPase genes derived from the genomic DNA of 50 randomly chosen Pb^r isolates was amplified using a nested PCR approach with the same primer sets used by Coombs and Barkay (Coombs and Barkay, 2004) (Table 3.1); 33 and 28 FRC isolates yielded PCR products in reactions 1 and 2, respectively (Table 3.1). The 28 amplicons obtained in reaction 2, (i.e., *zntA/cadA/pbrA* loci), represented a similar frequency as reported by Coombs and Barkay (Coombs and Barkay, 2004). Sequences for 26 of the 28 amplicons were subsequently obtained; two of the 26 strains yielded products with two different primer sets (Table 3.1). Sequence analyses of these 26 amplicons revealed the presence of numerous signature regions of P_{IB} -type ATPases, including phosphorylation and ATP-binding domains (Lutsenko and Kaplan, 1995), thus demonstrating the utility of these particular primer sets. Seventeen of the 26 amplicons were selected for further sequence analyses as all contained complete regions of the signature domains and it was only these isolates that were subjected to 16S

Table 3.1
Oligonucleotide primers used during nested PCR to amplify P_{IB}-type ATPases and number of isolates which yielded amplicons

PCR	Primer ^c	Primer sequence	Target genus/genera	Annealing temp (°C)	No. of Pb ^r isolates that yielded a PCR product
1 ^a	79JC	5' TGA CTGGCGAATCGGTBCCBG 3'	<i>Bacillus, Acinetobacter, Pseudomonas</i>	59	8
	84JC	5' GGAGCATCGTTAATDCCTCDCC 3'			
	132JC	5' CTA ACTGGCGAATCAGTCCC 3'	<i>Arthrobacter</i>	55	25
	84JC	5' GGAGCATCGTTAATDCCTCDCC 3'			
2 ^b	81JC	5' GGATGTCCTTGTGCTYTART 3'	<i>Bacillus, Acinetobacter, Pseudomonas</i>	49	5
	84JC	5' GGAGCATCGTTAATDCCTCDCC 3'			
	133JC	5' CCCTCACCTTGTGCTGTGG 3'	<i>Arthrobacter</i>	49	23
	84JC	5' GGAGCATCGTTAATDCCTCDCC 3'			

^a Expected product size, approximately 1.2 kb.

^b Expected product size, approximately 0.75 kb.

^c See Coombs and Barkay, 2004 for specific thermocycling parameters.

rRNA gene sequencing. The remaining nine amplicons were not long enough for phylogenetic analyses due to truncations in one or more of the expected domain sequences (possibly due to insertions, deletions, or other recombination events). The only gram-negative strains from the 50 randomly chosen *Pb*^r strains that had amplifiable P_{IB}-type ATPases were isolates FRC X7 and FRC Y9602. These isolates had PCR amplifiable *copA*-related P_{IB}-type ATPases (data not shown) along with the expected *zntA/cadA/prbA* loci (Fig. 3.1). This result is not surprising given the limited number of control strains tested in the initial primer sets for the P_{IB}-type *zntA/cadA/prbA*-specific ATPases (Coombs and Barkay, 2004). Overall, the neighbor-joining and maximum likelihood tree analyses of the *zntA/cadA/prbA*-like deduced amino acid sequences (e.g., 500 to 600 bp) resulted in a tree with remarkable incongruency between the 16S rRNA and ATPase gene phylogenies (Fig. 3.1). Seven of the 17 amplicons exhibited no unusual or unexpected incongruencies, which would have been suggestive of HGT, such as atypical G+C content or phylogenetic incongruency [Fig. 3.1 and Table 3.2, (Lawrence and Ochman, 1997)]. However, all seven of the *zntA/cadA/prbA*-like sequences derived from *Arthrobacter* isolates exhibited evidence of recent acquisition by HGT. Specifically, the *zntA/cadA/prbA*-like gene sequences amplified from FRC isolates V45 and Z8, belonging to the phylum *Actinobacteria*, as determined by 16S phylogeny, (Fig. 3.1) grouped in one of the two bifurcated nodes within the *Firmicutes* (Fig. 3.1). In addition, the V45 and Z8 isolates contained *zntA/cadA/prbA*-like genes with a G+C content much lower than expected for other *Arthrobacter* spp. [35 to 36 mol% instead of 59 to 70 mol% (Keddie, 1986); Table 3.2]. A second set of P_{IB}-type ATPases in FRC

Figure 3.1 Neighbor-joining analysis of (A) 16S rDNA and (B) *zntA/cadA/prbA*-like sequences from either subsurface FRC isolates or from completed genomes. Accession

numbers are in parentheses; § denotes FRC strain containing one or more plasmids. Subsurface isolates shown in shaded boxes and connected by a dotted line are positive for horizontal acquired P_{IB}-type ATPases related to *zntA/cadA/prbA*-loci. Bootstrap support >50% is shown. Scale bar for 16S rDNA and *zntA/cadA/prbA* phylogenies represent 0.1 changes per nucleotide position and 0.1 changes per amino acid position, respectively.

isolates AA1, AA20, AA21 and AA25, also belonging to the phylum *Actinobacteria* (Fig. 3.1), clustered with ZntA/CadA/PbrA-like sequences most closely related to the second bifurcated node within the *Firmicutes* (Fig. 3.1). These four isolates also exhibited unusual G+C contents (38 mol%; Table 3.2). The ATPase-related sequences amplified from FRC isolates X11, Y7 and Y22, belonging to the phylum *Firmicutes*, clustered within one distinct γ -*Proteobacteria* ZntA/CadA/PbrA-like clade (Fig. 3.1). Horizontal acquisition of these ATPase genes is also supported by unusual DNA base compositions, as indicated by the G+C content (Table 3.2). Strains, FRC-X11, FRC-Y7 and FRC-Y22, contained *zntA/cadA/pbrA*-like genes with a G+C content of 58 to 59 mol% (Table 3.2). This content varied considerably from the most closely related culturable isolate, *Bacillus cereus* which has a 32 mol% G+C (Claus, 1986). Together, such phylogenetic incongruencies and unusual G+C content provides strong evidence for the horizontal acquisition of these P_{IB}-type ATPases genes. As determined by 16S rDNA gene analysis, *Bacillus* spp. isolates FRC-X11, FRC-Y7 and FRC-Y22 exhibited more than 96% identity, and the ATPase sequences amplified from these isolates exhibited more than 97% amino acid identity (data not shown). Interestingly, the γ -*Proteobacteria*-related ATPase amino acid sequences from isolates FRC-X34 and FRC-Y22 (*Arthrobacter* and *Bacillus* spp., respectively) (Fig. 3.1) exhibited 98% identity but represent two distinct phyla via 16S rDNA sequence (*Actinobacteria* and *Firmicutes*) (Fig. 3.1). Although the G+C content of the *zntA/cadA/pbrA*-like sequence (59 mol%) amplified from isolate

FRC-X34 is similar to the reported G+C content of other *Arthrobacter* spp., many γ -*Proteobacteria* have comparable G+C contents (range, 38 mol% to 63 mol%) (Krieg, 1984). Thus, horizontal transfer of the *zntA/cadA/pbrA*-like gene to isolate FRC-X34 may still be supported by our results, however we have denoted it here as a “maybe” for the purposes of this study (Table 3.2).

The FRC isolates were also screened for the presence of plasmids (Fig. 3.1). Of the 10 strains that fulfilled the criteria that the P_{IB}-type ATPases may have been acquired by HGT, 8 contained plasmids of sufficient size to encode such genes and to be either mobilizable and/or self-transmissible (data not shown). Studies are being conducted to determine whether plasmid-encoded ATPase genes are indeed present in these isolates. Taken together, all of these findings are highly suggestive of a considerably broad and remarkable dissemination of horizontally acquired P_{IB}-type ATPase genes from both the *Firmicutes* and *Proteobacteria* phyla to bacteria isolated from contaminated soils (Fig. 3.1 and Table 3.2). However, it is important to note that one cannot conclude, based on this current study, whether or not such HGT events occurred prior to or following FRC soil contamination. Indeed, a host of other biological and/or environmental factors likely contribute to such horizontal gene exchanges (Sorensen et al., 2005; Thomas and Nielsen, 2005).

Table 3.2
Support for acquisition of P_{IB}-type ATPases by HGT in subsurface isolates from radionuclide- and metal-contaminated soils

Genus	Strain	Phylogenetic incongruence	G+C content (%)	Support for HGT ^a	Most closely related P _{IB} -type ATPase
<i>Arthrobacter</i>	FRC-AA1	+	38	+	<i>Firmicutes</i>
	FRC-AA20	+	38	+	<i>Firmicutes</i>
	FRC-AA21	+	38	+	<i>Firmicutes</i>
	FRC-AA25	+	38	+	<i>Firmicutes</i>
	FRC-V45	+	36	+	<i>Firmicutes</i>
	FRC-X34	+	59	Maybe	<i>γ-Proteobacteria</i>
	FRC-Z8	+	35	+	<i>Firmicutes</i>
<i>Bacillus</i>	FRC-AA22	-	38	-	<i>Firmicutes</i>
	FRC-N65	-	38	-	<i>Firmicutes</i>
	FRC-X11	+	59	+	<i>γ-Proteobacteria</i>
	FRC-X18	-	38	-	<i>Firmicutes</i>
	FRC-X26	-	38	-	<i>Firmicutes</i>
	FRC-Y7	+	58	+	<i>γ-Proteobacteria</i>
	FRC-Y22	+	58	+	<i>γ-Proteobacteria</i>
	FRC-Z41	-	38	-	<i>Firmicutes</i>
<i>Rahnella</i>	FRC-X7	-	59	-	<i>γ-Proteobacteria</i>
	FRC-X7 (<i>copA</i>)	-	59	-	<i>γ-Proteobacteria</i>
	FRC-Y9602	-	59	-	<i>γ-Proteobacteria</i>
	FRC-Y9602 (<i>copA</i>)	-	59	-	<i>γ-Proteobacteria</i>

^a The evidence for HGT was supported by analysis of both phylogenetic incongruence and the G+C content.

3.4.3 Tolerance to uranium (U)

In addition to the heavy metals, microorganisms in the FRC subsurface are subjected to other contaminants including radionuclides and organic solvents (<http://www.esd.ornl.gov/nabirfrc>). Thus, to determine whether the heterotrophic FRC strains isolated in this study were capable of tolerating toxic concentrations of U, tolerance assays were conducted under acidic conditions with numerous isolates representing the most commonly isolated genera (e.g., *Arthrobacter*, *Bacillus* and *Rahnella*).

The isolates that were the least tolerant of both the acidic pH and U toxicity (i.e., 200 μ M uranyl acetate) assay conditions were the FRC *Bacillus* spp. (Table 3.3). A similar result was reported for other *Bacillus* spp. previously isolated from an acidic inactive open-pit U mine (Suzuki and Banfield, 2004). The exception was *Bacillus* sp. strain FRC-X18, which maintained viability at pH 4 (Table 3.3) and exhibited the least reduction in cell number in the presence of U (Table 3.3). Strains FRC-N65, FRC-X18, and FRC-Y9-2 exhibited greater tolerance to the acidic pH conditions relative to the other *Bacillus* strains (Table 3.3). The gram-negative *Rahnella* sp. strain FRC-Y9602 exhibited only a slight decrease in cell viability (Table 3.3) due to pH conditions but a >100-fold loss of viability upon exposure to U(VI). The *Arthrobacter* strains exhibited the greatest tolerance to the low-pH and U conditions (Table 3.3). Of the six *Arthrobacter* strains tested, the *A. histidinolovarans* control strain exhibited the greatest decrease in cell viability during incubation at pH 4 with or without U (Table 3.3). In contrast, the FRC strains exhibited little to no decrease in cell viability (Table 3.3). A similar tolerance to acid has also been reported for two other *Arthrobacter* spp. from the

Table 3.3
Viable cell counts determined after washing and after 1 h of incubation at pH 4 either with or without 200 μ M uranyl acetate^a.

Genus	Strain	CFU (washed) ^b	CFU (without U) ^c	CFU (with U)
<i>Arthrobacter</i>	FRC-AA1	$(1.79 \pm 0.48) \times 10^{8d}$	$(1.59 \pm 0.49) \times 10^8$	$(1.45 \pm 0.49) \times 10^8$
	FRC-AA21	$(1.53 \pm 0.37) \times 10^8$	$(7.78 \pm 0.20) \times 10^7$	$(6.45 \pm 0.38) \times 10^7$
	FRC-AA25	2.31×10^8	1.39×10^8	$(9.20 \pm 0.49) \times 10^7$
	FRC-V45	$(1.67 \pm 0.40) \times 10^8$	$(9.13 \pm 0.15) \times 10^7$	$(6.85 \pm 0.18) \times 10^7$
	FRC-X34	1.83×10^8	1.71×10^8	1.07×10^8
	<i>A. histidinolovorans</i> ATCC 11442	$(1.57 \pm 0.13) \times 10^8$	$(6.10 \pm 0.49) \times 10^7$	$(4.35 \pm 1.04) \times 10^7$
<i>Bacillus</i>	FRC-N65	2.99×10^8	$(1.12 \pm 0.38) \times 10^8$	$<1 \times 10^4$
	FRC-X18	$(1.87 \pm 0.50) \times 10^8$	$(3.51 \pm 1.14) \times 10^7$	4.03×10^5
	FRC-Y9-2	$(2.55 \pm 0.64) \times 10^7$	$(3.12 \pm 1.05) \times 10^6$	$<1 \times 10^4$
	<i>B. cereus</i> ATCC 14579	$(9.70 \pm 0.52) \times 10^7$	$<1 \times 10^4$	$<1 \times 10^4$
<i>Escherichia</i>	<i>E. coli</i> JM109	$(8.00 \pm 0.37) \times 10^7$	$(4.65 \pm 0.30) \times 10^7$	$<1 \times 10^4$
<i>Rahnella</i>	FRC-Y9602	1.10×10^8	$(5.40 \pm 0.40) \times 10^7$	$(1.54 \pm 0.92) \times 10^6$

^a At pH 4 U(VI) occurs primarily as uranyl ion (UO_2^{2+}).

^b All strains were plated immediately following two washes with 0.1M NaCl at pH 4.

^c Strains were incubated for 1 h at pH 4.

^d Standard deviations greater than 10% are shown.

open-pit U mine (Suzuki and Banfield, 2004). All five *Arthrobacter* FRC strains maintained cell viability following exposure to U. Similarly, two of the three high G+C microorganisms previously isolated from the open-pit U mine site exhibited a comparable tolerance to a toxic concentration of U (Suzuki and Banfield, 2004).

The tolerance to U exhibited by gram-positive and gram-negative microorganisms may be explained by several different cellular mechanisms, as previously reported by other investigators (Macaskie et al., 1992; Renninger et al., 2004; Suzuki and Banfield, 2004). One mechanism, bioadsorption, has recently been hypothesized to occur in a well-characterized *Arthrobacter* type strain, *A. nicotianae* (Tsuruta, 2002). In this particular study as much as 80% of the uranyl ions were removed from aqueous solution at pH 4 (Tsuruta, 2002); however, cellular U localization was not determined. A second mechanism, U sequestration, shown to occur in the *Arthrobacter* isolate S3Y (Suzuki and Banfield, 2004), resulted in an intracellular accumulation of uranium precipitates perhaps as a means to limit U toxicity. In this case, the authors used TEM and EDX analysis to identify the co-precipitation of U with phosphorus- and calcium-rich granules (Suzuki and Banfield, 2004). Interestingly, strain S3Y exhibited no evidence of bioadsorption (Suzuki and Banfield, 2004) thus suggesting that *Arthrobacter* species such as *A. nicotianae* may also be capable of intracellular U accumulation. Studies are currently underway to determine whether intracellular U sequestration promotes the tolerance to U that has been observed in *Arthrobacter* strains isolated from heavy metal- and radionuclide-contaminated subsurface soils.

Among some of the most promising strategies for remediation of the contaminated subsurface are the bioimmobilization of metals and radionuclides by microbial processes

and their metabolic products (Barkay and Schaefer, 2001). Numerous microbes carry out reductive processes that result in decreased solubility, and thus bioavailability and toxicity, of metals and radionuclides (Lovley et al., 2004). Recent efforts to stimulate microbial communities to remove U from contaminated aquifers and groundwater by promoting the *in situ* activity of dissimilatory metal-reducing organisms highlight the important role of microbial processes in the subsurface (Anderson et al., 2003; North et al., 2004). In these studies, biostimulation strategies for subsurface remediation resulted in significant increases in *Geobacter* spp. and sulfate-reducing bacterial populations. As these populations are expected to function in environments that are affected by mixed wastes, the presence of toxic heavy metals and nitrates that cooccur in sites such as the FRC (Finneran et al., 2002; Petrie et al., 2003) could potentially limit their activities. For example, *Desulfovibrio desulfuricans* G20, a model organism for the immobilization of metals as metal sulfides has been shown to be susceptible to micromolar concentrations of heavy metals including Cu(II), Zn(II) and Pb(II) (Sani et al., 2003), while mixed cultures of sulfate reducers were inhibited by Cr(VI) (Smith and Gadd, 2000), Cu(II) and Zn(II) (Utgikar et al., 2003). Likewise some heavy metals including Cr(VI) have also been shown to negatively affect growth of *Shewanella* spp., which have been studied for their role in immobilizing metals and radionuclide by their reduction to insoluble forms (Viamajala et al., 2004). Thus, the (heavy) metal sensitivity of some radionuclide-reducing microorganisms indicates that acquiring metal resistance(s) could be highly conducive to facilitating and/or enhancing microbial metabolism in metal contaminated subsurface environments. Such enhancement could be achieved by stimulating the transfer of metal resistance broad-host-range metal resistance plasmids to metal- and

radionuclide-reducing microbes in treated subsurfaces and/or promoting the efficient transformation and incorporation of key genes for adaptation via transformation- or transduction-mediated processes (Frost et al., 2005). To the best of our knowledge, this study is among the first to report the heavy metal resistance phenotypes and U tolerance of *Arthrobacter* spp. isolated from an acidic contaminated subsurface environment. These unrelated, yet synergistic, physiological traits observed in *Arthrobacter* isolates resident in contaminated FRC soils may contribute to their survival in such an extreme environment. Thus, *Arthrobacter* species, particularly those resident in contaminated soils such as the FRC, may represent as yet a largely untapped group of microorganisms with considerable bioremediation potential.

3.5 Experimental procedures

3.5.1 Sampling site

Contaminated soils were collected from the DOE Natural and Accelerated Bioremediation Field Research Center located in the Oak Ridge National Laboratory Reservation at Oak Ridge, Tenn. The contaminated soils are adjacent to an asphalt parking area that covers three former waste ponds (S-3 ponds) used during weapons production activities. The waste ponds and surrounding soils contain uranium (U) and other radionuclides, nitric acid, organics solvents and heavy metals (<http://www.lbl.gov/NABIR/>). Soil cores (3.75 cm diameter, approximately 180 cm in length) were collected on 18 to 20 February 2003 as described in Petrie et al. (Petrie et al., 2003). In this study, contaminated subsurface soil samples were obtained from the

saturated zone, where elevated U and nitrate concentrations have been reported (<http://www.lbl.gov/NABIR/>). Soil core samples were obtained boreholes FB058 and FB059 (Area 1; maximum depth, 19ft); FB051, FB053 and FB054 (Area 2; maximum depth, 26ft); and FB055 and FB057 (Area 3; maximum depth, 19ft). These samples were handled aseptically and preserved under an argon atmosphere. Cores were shipped chilled overnight to Georgia Institute of Technology and processed for chemical and microbiological analysis immediately. Dry/wet ratio values ranged from 0.8 to 0.88. The soil pH, as determined by McLean (McLean, 1982), ranged from a low of 4.0 (Area 3) to a high of 7.5 (Area 2). Redox potential of groundwater proximal to subsurface cores ranged from +111 mV- +375 mV. Detailed geology, chemistry and site descriptions are available on the DOE NABIR website (September 2005, <http://www.lbl.gov/NABIR/>).

3.5.2 Strain isolations, determination of plasmids and metal resistance

Aerobic chemoheterotrophs were isolated by homogenizing triplicate 3-g soil samples (e.g., sampled over the length of the intact sub-sectioned core, n=3) in sterile saline and plating serial dilutions onto a variety of media including full-strength (100%) PTYG, which contained (per liter) 5 g peptone, 5 g typtone, 5 g yeast extract, 10 g glucose, 0.6 g $\text{MgSO}_4 \cdot 7\text{H}_2\text{O}$, 0.06 g CaCl_2 , 1% PTYG, 1% tryptone, which contained 10 g tryptone per liter, and R2A, which contained (per liter) 0.5 g yeast extract, 0.5 g proteose peptone, 0.5 g Casamino acids, 0.5 g glucose, 0.5 g soluble starch, 0.3 g sodium pyruvate, 0.3 g K_2HPO_4 , 0.05 g $\text{MgSO}_4 \cdot 7\text{H}_2\text{O}$ (Becton Dickinson) and 15 g agar (Sigma). Areas 1 and 2 yield the highest number of isolates and Area 3, soils with the highest nitrate and uranium concentrations (<http://www.esd.ornl.gov/nabirfrc/>), yielded

the lowest number of isolates. Due to the heterogeneous nature of the soil samples and low CFU counts, triplicate samples were used to obtain as many culturable isolates as possible. Plates were incubated for 1-5 days at 25°C and 30°C. Strains were purified by repeatedly streaking onto the same agar used for initial isolation. The Gram reaction of each of the 400 isolate was determined as described by Powers (Powers, 1995). PCR amplification of 16S rDNA genes from each isolate was performed as previously described (Mills et al., 2003). Isolates were grouped on the basis of the restriction fragment length polymorphism (RFLP) banding patterns of their 16S rRNA amplicons after digested with MspI and HhaI as described by Mills et al. 2003. Multiple representatives from each RFLP group were subjected to 16S rRNA sequence analysis. Long-term storage of the FRC isolates was in dimethyl sulfoxide/glycerol at -80°C. Nutrient broth (NB) (3 g beef extract per liter, 5 g peptone per liter) was used for the maintenance of the purified FRC strains. Isolates were screened for the presence of plasmids as previously described in Reyes et al. (Reyes et al., 1999). For determination of resistances to the metal salts cadmium chloride, potassium chromate, lead citrate and mercuric chloride, 400 FRC isolates were assayed as previously described (Reyes et al., 1999; Benyehuda et al., 2003). The following concentrations of metals tested: 500 nmol $(C_2H_3O_2)_2Pb \cdot 3H_2O$, 50 nmol Hg_2Cl_2 , 2 μ mol K_2CrO_4 , and 500 nmol $CdCl_2 \cdot 5/2H_2O$. Metal-resistant and -sensitive control strains were used as described in Benyehuda et al. (Benyehuda et al., 2003) to confirm metal resistance phenotypes.

3.5.3 Uranium tolerance assays

Tolerance to uranium (U) at pH 4 was determined as previously described (Suzuki and Banfield, 2004) using 200 μ M uranyl acetate, 50 ppm U(VI). Five-milliliter overnight broth cultures of FRC isolates and control strains (*Arthrobacter histidinovorans* ATCC 11442, *Bacillus cereus* ATCC 14579 and *Escherichia coli* JM109) were diluted 1:100 and grown to mid-log phase at either 25°C in nutrient broth (FRC isolates and control strains) or 37°C in Luria-Bertani (LB) broth (*E. coli*). Three 1-ml aliquots of mid-log phase cells were centrifuged (10 min, 10,000 x g), cell pellets washed twice with 0.1M NaCl, pH 4 and each aliquot was assayed as follows: (i) diluted into sterile saline and immediately plated on nutrient agar; (ii) incubated 1 h in 0.1M NaCl (pH 4); and (iii) incubated 1 h in 0.1M NaCl, (pH 4) containing 200 μ M U(VI). Following incubation, cells were serially diluted in sterile saline, plated on either LB or NB agar, incubated 24-48 h, and enumerated. Triplicate assays were conducted and all data were analyzed for statistical significance.

3.5.4 PCR amplification of 16S rRNA and P_{IB}-ATPases

Genomic DNA was isolated from FRC isolates by a rapid boiling method (Holmes and Quigley, 1981). Briefly, FRC isolates were incubated in NB for 6 h at 30°C. A 100- μ l cell suspension was centrifuged, the pellet resuspended in 20 μ l sterile distilled water and heated (100°C for 10 min). Lysates were centrifuged, and the supernatants decanted and transferred to sterile tubes for storage at -20°C prior to use. PCR amplification of 16S rDNA genes were performed as previously described (Mills et al., 2003) and PCR amplification of the P_{IB}-type ATPase genes was also performed as

previously described (Coombs and Barkay, 2004). Specifically, PCR primers used in reaction 1 target conserved sequences found in all P-types ATPases for the target genera indicated in Table 3.1. The PCR primers used in reaction 2 target domain sequences that are found only in heavy-metal transporting (P_{IB} -type) ATPases (Table 3.1) (Coombs and Barkay, 2004)].

3.5.5 Sequencing and analyses

Sequencing of the *zntA/cadA/pbrA*-like and 16S rDNA amplicons at the School of Biology Genome Center (Georgia Institute of Technology) using a BigDye Terminator v3.1 cycle sequencing kit on an automated capillary sequencer (model 3100 Gene Analyzer, Applied Biosystems). The primers used to sequence the P_{IB} -type ATPase loci are listed in Table 3.1, primers 27f and 1522r (Mills et al., 2003) were used for 16S rDNA PCR products. Multiple sequences of PCR products were initially aligned using the program BLAST 2 Sequences (Tatusova and Madden, 1999) available through the National Center for Biotechnology Information and were assembled with the program BioEdit v5.0.9 (Hall, 1999). Sequences from this study and reference sequences, as determined by BLAST analysis, were aligned using ClustalX v1.81 (Thompson et al., 1997). Neighbor-joining trees were created from these alignments. On average, of 780 and 560 nucleotides were included in the phylogenetic analyses of 16S rDNA and P_{IB} -ATPase sequences, respectively. Tree topologies of 16S rDNA phylogenies were identical when analyzed using maximum likelihood and maximum parsimony. Similar analyses of P_{IB} -ATPase amino acids sequences resulted in some tree topologies differences but did not alter the outcome of the data generated by neighbor joining. The

bootstrap data indicate percentages for 1000 samplings. The final trees were viewed using NJPlot (Perriere and Gouy, 1996) and TreeView v1.6.6 available at <http://taxonomy.zoology.gla.ac.uk/rod/treeview.html>.

3.5.6 Nucleotide sequence accession numbers

The 17 16S rRNA nucleotide sequences have been deposited in the GenBank database under accession numbers DQ224387 to DQ224403 and the 19 P_{IB}-ATPase nucleotide sequences have been deposited in the GenBank database under accession numbers DQ234600 to DQ234618.

3.6 Conclusions

Horizontal gene transfer of P_{IB}-type ATPases was detected in 20% of the screened metal resistant isolates. As uranium resistance has not been attributed to a defined molecular mechanism, we tested the metal resistant isolates for tolerance to uranium U(VI) under low pH. FRC *Arthrobacter* and *Rahnella* spp. demonstrated the greatest tolerance to U(VI). The least tolerant to U(VI) and low pH were the *Bacillus* strains. This is the first study to demonstrate the broad dissemination of P_{IB}-type ATPase genes within the contaminated subsurface of the FRC.

3.7 Acknowledgements

We thank Cassie Black, Mike Humphrys, Kerri Lafferty and Kristin Tuttle for providing excellent technical assistance and Dave Watson for providing FRC soil cores. This research was supported by the Natural and Accelerated Bioremediation Research (NABIR) program, Office of Science (BER), U.S. Department of Energy (Grants DE-FG02-99ER62864 and DE-FG02-04ER63906).

CHAPTER 4

AEROBIC URANIUM (VI) BIOPRECIPITATION BY METAL RESISTANT BACTERIA ISOLATED FROM RADIONUCLIDE- AND METAL-CONTAMINATED SUBSURFACE SOILS

4.1 Overview

This chapter examines metal resistant *Arthrobacter*, *Bacillus*, and *Rahnella* spp. obtained from the contaminated subsurface at the U.S. Department of Energy's (DOE) Oak Ridge Field Research Center (ORFRC). In an effort to identify radionuclide- and metal-resistant aerobic heterotrophs that can affect uranium U(VI) solubility, ORFRC *Arthrobacter*, *Bacillus*, and *Rahnella* spp. culture collection for strains were screened for constitutive acid phosphatase expression. Previous studies that characterized bacterial acid phosphatases focused on clinically relevant species. The following study employed a PCR-based approach to screen our environmental strains for one or more of the characterized non-specific acid phosphatase (NSAP) genes (i.e., Classes A, B, or C). The ORFRC *Rahnella* and *Bacillus* spp. not only possessed constitutively-expressed NSAP genes, but these strains were also shown to promote the precipitation of soluble U(VI).

4.2 Summary

In this study, the immobilization of toxic uranium [U(VI)] mediated by the intrinsic phosphatase activities of naturally occurring bacteria isolated from contaminated subsurface soils was examined. The phosphatase phenotypes of strains belonging to the

genera, *Arthrobacter*, *Bacillus* and *Rahnella*, previously isolated from subsurface soils at the U.S. Department of Energy's (DOE) Oak Ridge Field Research Center (ORFRC) were determined. The ORFRC represents a unique, extreme environment consisting of highly acidic soils with co-occurring heavy metals, radionuclides, and high nitrate concentrations. Isolates exhibiting phosphatase-positive phenotypes indicative of constitutive phosphatase activity were subsequently tested in U(VI) bioprecipitation assays. When aerobically grown in synthetic groundwater (pH 5.5) amended with 10 mM glycerol-3-phosphate (G3P), phosphatase-positive *Bacillus* and *Rahnella* spp. strains Y9-2 and Y9602 liberated sufficient phosphate to precipitate 73% and 95% of total soluble U added as 200 μ M uranyl acetate, respectively. In contrast, an *Arthrobacter* sp. X34 exhibiting a phosphatase-negative phenotype did not liberate phosphate from G3P or promote U(VI) precipitation. This study provides the first evidence of U(VI) precipitation via the phosphatase activity of naturally occurring *Bacillus* and *Rahnella* spp. isolated from the acidic subsurface at the DOE ORFRC.

4.3 Introduction

The treatment of hazardous waste sites, particularly those co-contaminated with radionuclides and heavy metals remains one of the most costly environmental challenges currently faced by the U.S. and other countries. The disposal of radioactive waste has traditionally involved underground storage tanks, shallow land burial pits, and trenches (Riley, 1992; DOE, 1995). When leaks occur, these wastes come into contact with surrounding geologic media allowing for migration of radiological pollutants into nearby soils and groundwater. The mobility and solubility of radionuclides such as uranium (U),

technetium (Tc) and other toxic metals [e.g., cadmium (Cd), lead (Pb), chromium (Cr)] are dependent upon their oxidation state and chemical speciation (Kotegov, 1968; Suzuki and Banfield, 1999). Microbial processes that promote the precipitation of radionuclides and metals show promise for the remediation of contaminated soils, groundwater and waste streams (Lovley and Coates, 1997; Stephen and Macnaughton, 1999; Gadd, 2000; Barkay and Schaefer, 2001).

A number of studies have demonstrated the enzymatically catalyzed precipitation of insoluble phases of U (Lovley et al., 1991; Lovley and Phillips, 1992; Wade and DiChristina, 2000), Tc (Lloyd et al., 1999b; Lloyd et al., 1999a), Cr (Tucker et al., 1998; Turick, 1998; Smith and Gadd, 2000), and selenium (Cantafio et al., 1996; Tucker et al., 1998) by microbial reduction processes. In addition to this reductive bioprecipitation process, insoluble mineral forms of radionuclides and metals can also be immobilized through interactions between microbially produced sulfide (White, 1998; Lebranz, 2000), phosphate (Boswell, 1999; Jeong, 1999; Macaskie et al., 2000; Mire et al., 2004) or through bacterial iron oxidation (Banfield et al., 2000) in a process termed biomineralization. In contrast to microbial reductive precipitation, which requires anaerobic conditions, biomineralization can occur aerobically, making this process a possible remediation strategy for radionuclides in contaminated groundwater and oxygenated subsurface zones.

In this study, an experimental approach was designed to determine if phosphatase activity extant in bacteria previously isolated from contaminated subsurface soils collected from the Department of Energy's (DOE) Field Research Center (ORFRC) located in the Oak Ridge National Laboratory Reservation (Oak Ridge, TN) could

promote U immobilization by biogenic phosphate mineral production. Previous studies have demonstrated the efficacy of nonspecific acid phosphohydrolase (NSAP)-mediated radionuclide and metal precipitation (Boswell, 1999; Jeong, 1999; Macaskie et al., 2000; Mire et al., 2004). Bacterial NSAPs are a broad class of phosphohydrolases (phosphatases) which contain highly conserved amino acid motifs and exhibit optimal hydrolysis of a number of structurally unrelated phosphoester substrates in acidic to neutral pH conditions (Rossolini et al., 1998). In addition to their role in P acquisition, phosphohydrolases regulate cellular metabolism, are involved in signal transduction and may also be critical to bacterial pathogenicity (Reilly et al., 1996; Wanner, 1996; Berlutti et al., 1998). Using a phenotypic-based screening approach, a number of the subsurface bacterial isolates tested displayed phosphatase activity (i.e., cell surface or secreted). In the presence of an organophosphate or inorganic phosphate substrate, this phosphatase activity was sufficient to promote the hydrolysis of sufficient orthophosphate to promote the biomineralization of U(VI) as a U-phosphate mineral in aerobic and anaerobic synthetic groundwater designed to mimic ORFRC conditions. Additionally, electron microscopy studies were conducted to determine the localization of biomineralized U(VI).

4.4 Results

4.4.1 Determination of phosphatase activity in subsurface strains

Previously, aerobic heterotrophs isolated from radionuclide- and metal-contaminated subsurface soils collected from the ORFRC were tested for resistance to a

number of heavy metals [e.g., Cd (II), Cr(VI), Pb(II) and Hg(II)] (Martinez et al., 2006b). The majority of the isolates were Gram-positive and belonged to the high G+C and low G+C genera *Arthrobacter* and *Bacillus*, respectively. Gram-negative isolates were most closely related to the genus *Rahnella*. A number of the metal resistant strains were shown to encode P_{IB}-type ATPases that detoxify the cell cytoplasm by catalyzing the efflux of divalent metal ions (Martinez et al., 2006b). In the present study a subset of these subsurface isolates were assayed for traits that would suggest the presence of a phosphatase-mediated mechanism that could protect cells from the toxic effects of radionuclides (Macaskie et al., 1992; Gadd, 2004; Mire et al., 2004; Renninger et al., 2004 537) (Fig. 4.1).

Initial screening of 135 metal resistant isolates for phosphatase activity on tryptose methyl green agar (TPMG) (Riccio et al., 1997) indicated a majority (75 of 135) exhibited a phosphatase-positive phenotype. However, 33 of the 135 subsurface isolates (e.g., *Arthrobacter* and *Bacillus* spp.) did not grow on TPMG (Fig. 4.1A). Thus, a modified medium, TP-MUP (tryptose-phosphate 4-methylumbelliferyl phosphate,

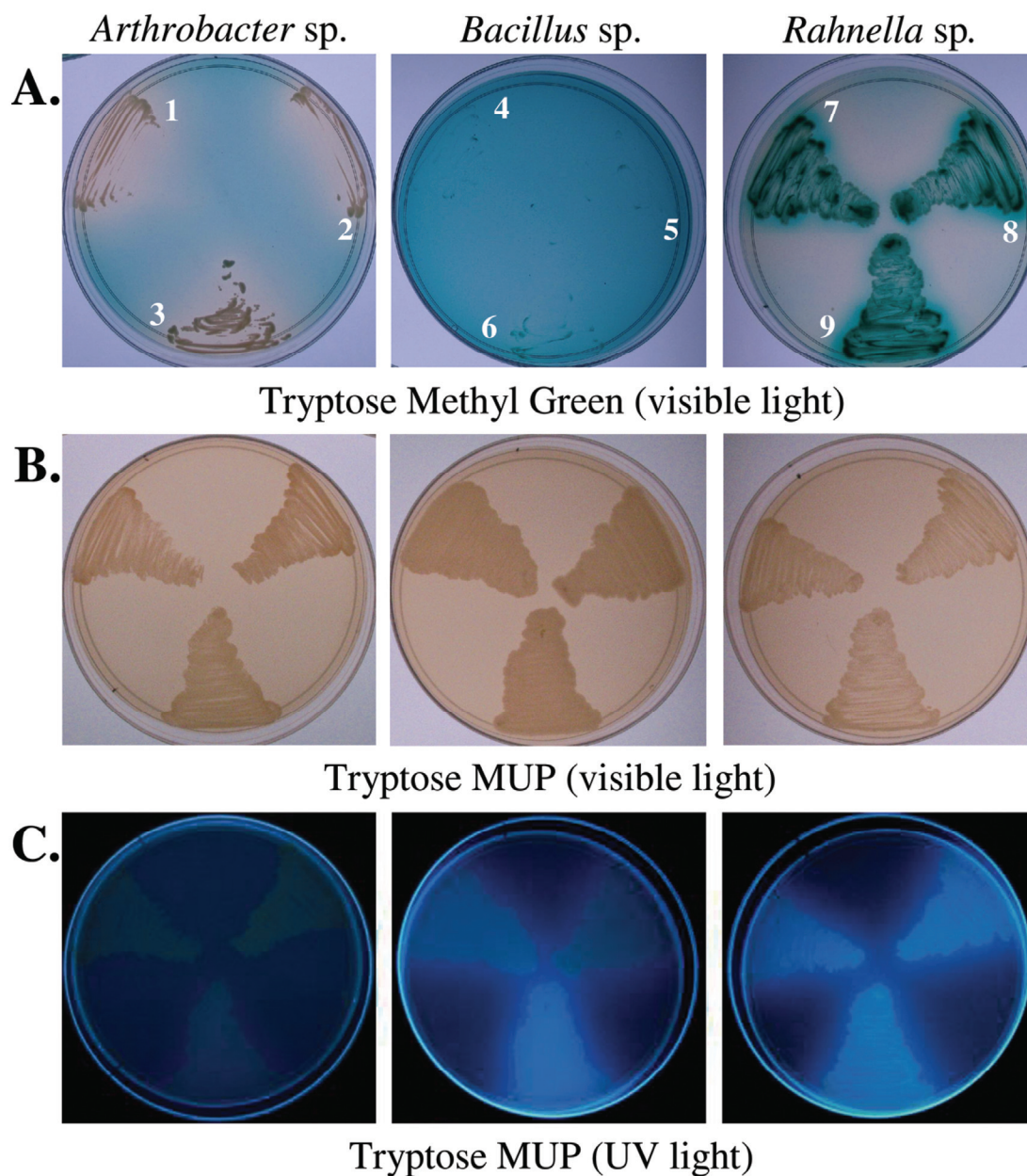


Figure 4.1. Media types used for identifying potential U-precipitating phosphatase phenotypes. Isolates that displayed a phosphatase-positive phenotype appeared either bright green on TPMG (Fig. 4.1A) or fluorescent when placed under UV light on TP-MUP (Fig. 4.1C). **(A).** TPMG **(B).** Tryptose phosphate-MUP (TP-MUP)/visible light **(C).** TP-MUP/UV light. Strains were streaked onto all three media types as follows: *Arthrobacter* spp. strain (1). X34, (2). V45, (3). AA20 (column 1); *Bacillus* spp. (4). Y7, (5). X18, (6). Y9-2 (column 2) and *Rahnella* spp. (7). Y9602, (8). Y4, (9). Y29 (column 3).

disodium agar), was used in addition to TPMG to screen for phosphatase-positive phenotypes. The TP-MUP medium promoted robust growth of all three genera types tested (Fig. 4.1B) and 10 of the 33 isolates that failed to grow on TPMG initially were phosphatase positive (data not shown). A representative subset of 9 Pb resistant (Pb^r) *Arthrobacter*, *Bacillus* and *Rahnella* isolates (3 per genera) with either phosphatase-positive or negative phenotypes are shown (Fig. 4.1A and 4.1C). Four of the 9 Pb^r isolates exhibited phosphatase phenotypes suggestive of the ability to bioprecipitate metals (Y9-2, Y4, Y29, Y9602).

4.4.2 Molecular characterization of NSAPs

Previous work has shown that a constitutively expressed non-specific acid phosphatase (NSAP) belonging to the Class A NSAPs has been involved in promoting the precipitation of U(VI) by the liberation of phosphate from glycerol-2-phosphate (Macaskie et al., 1992; Yong and Macaskie, 1995). A PCR based approach was designed to assay subsurface isolates for the presence of one or more classes of the characterized NSAP genes (i.e., Classes A, B and C) (Fig. 4.2A-D) (Martinez et al., 2006b). As there is an appreciable divergence of nucleotide sequences among NSAP genes, designing PCR primers to amplify the genes from each respective NSAP Class from phylogenetically diverse microbial lineages was not pursued (Fig. 4.3 and 4.4). Instead, a series of PCR primer sets were designed to amplify nearly full length acid phosphatase genes (Table 4.1) from species most closely related to the FRC subsurface strains examined in this study based on 16S rRNA phylogeny. To confirm the specificity of the designed primers, NSAP genes belonging to each molecular class (i.e., A, B and C) were amplified from

genomic DNA of control strains containing either one or more of the targeted phosphatase genes (i.e., positive controls) (Fig. 4.2A-D). Each primer pair was specific as only the expected acid phosphatase gene for the respective molecular class was obtained from the positive control(s). To validate the ability of each of the PCR primer

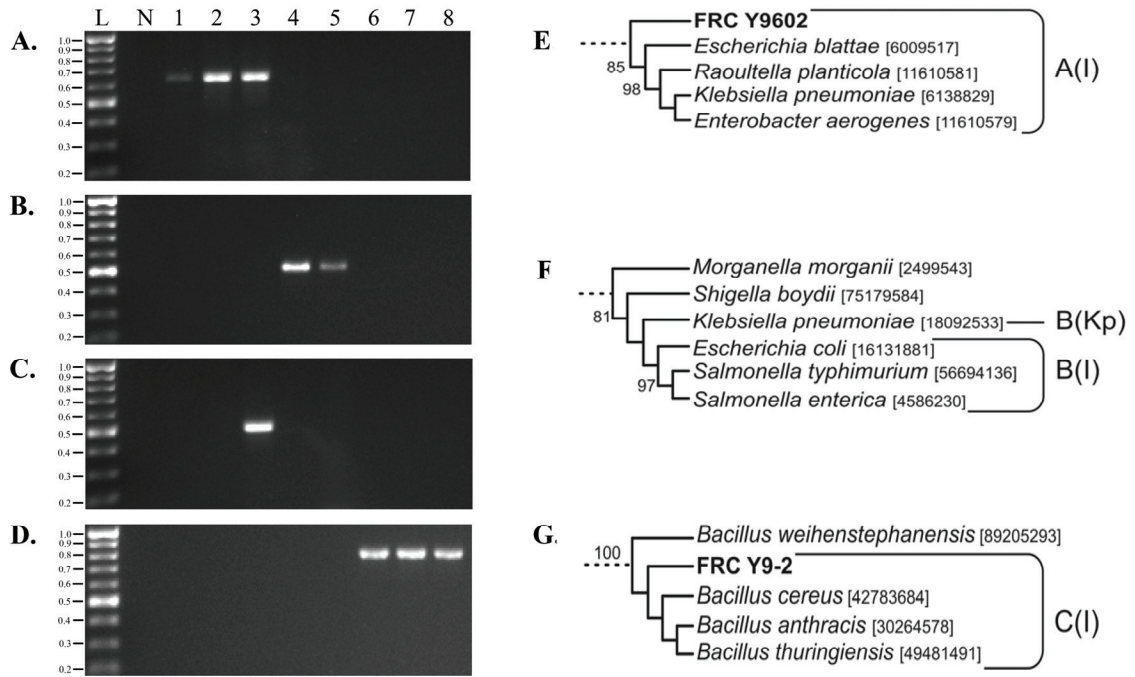


Figure 4.2 (A-D). PCR amplification of Classes A, B and C non-specific acid phosphatases (NSAPs). Agarose gel lanes are: L - 1-kb DNA ladder, N - no DNA template control, 1 - *Rahnella* sp. Y9602, 2 - *Enterobacter aerogenes* (Class A control), 3 - *Klebsiella pneumoniae* (Class A and B control), 4 - *Escherichia coli* MG1655 (Class B control), 5 - *Salmonella enterica* (Class B control), 6 - *Bacillus cereus* (Class C control), 7 - *Bacillus thuringiensis* (Class C control), 8 - *Bacillus* sp. Y9-2. Genomic DNA extracted from each strain was used as template with each clade- and species-specific NSAP primer sets denoted: (A). A(I), (B). B(I), (C). B(Kp), (D). C(I). NSAP phylogeny of bacteria most closely related to subsurface strains *Rahnella* sp. Y9602 and *Bacillus* sp. Y9-2. NCBI GenInfo identifier numbers are indicated in brackets. PCR primers targeted NSAP genes from bacteria belonging to: (E). clade A(I), within Class A, (F). clade B(I) and *Klebsiella pneumoniae* B(Kp) within Class B, (G). clade C(I) within Class C.

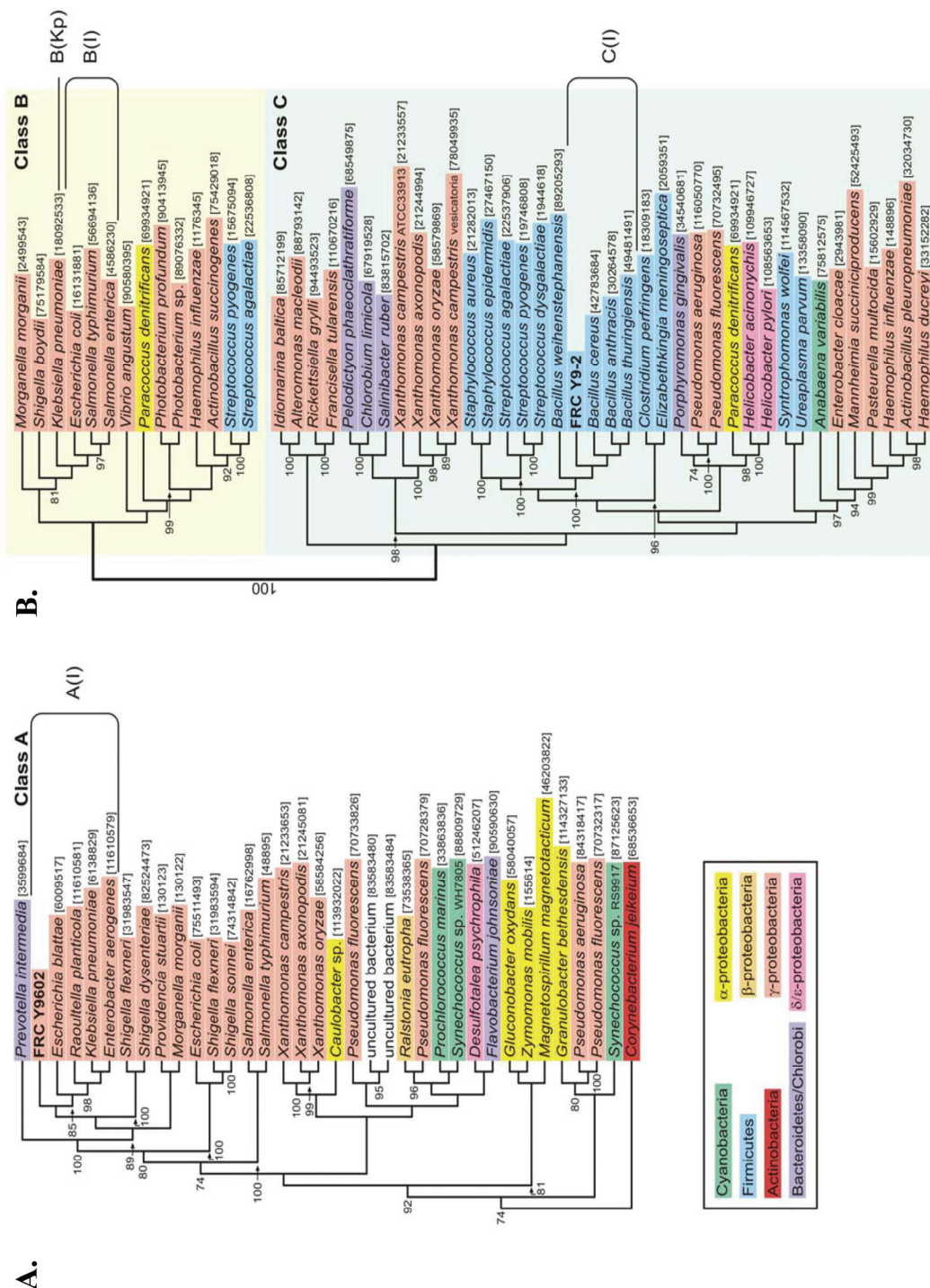


Figure 4.3 Neighbor-joining (NJ) amino acid phylogenetic tree construction of (A). Class A NSAP and (B). Class B and Class C NSAP sequences. All NSAP sequences from were obtained by iterative PSI-BLAST searches of the NCBI protein database. NCBI GenInfo identifier numbers are indicated in brackets. The NSAP sequences for strains Y9602 and Y9-2 were obtained in this study by PCR amplification and sequence analysis.

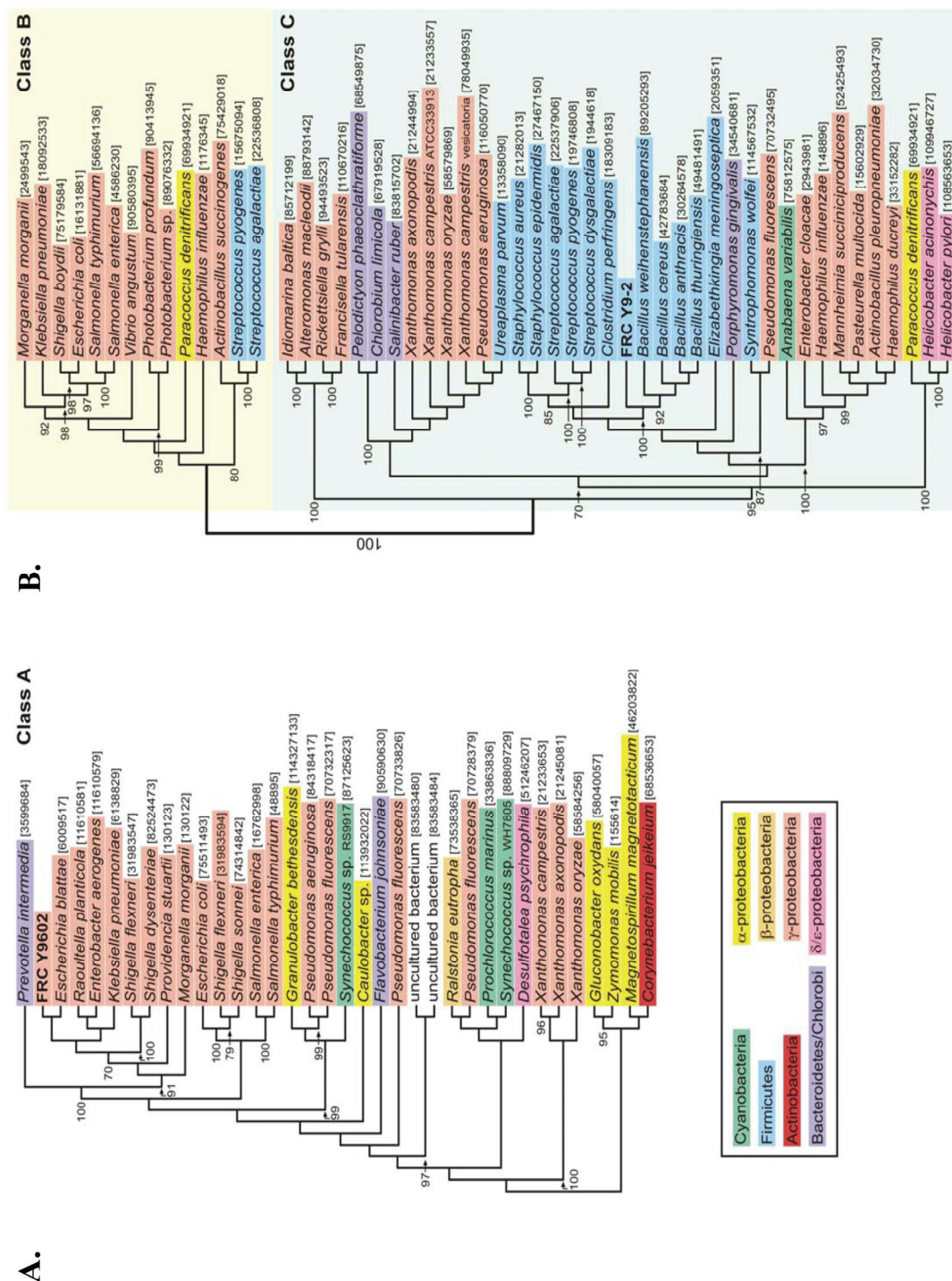


Figure 4.4 Maximum parsimony (MP) amino acid phylogenetic tree construction of (A). Class A NSAP and (B). Class B and C NSAP sequences. NCBI GenInfo identifier numbers are indicated in brackets. MP phylogeny is provided to support the robustness of observed NJ tree topology.

Table 4.1
Oligonucleotide primers for PCR amplification of non-specific acid phosphatases

Primer set	Primer sequence	NSAP class	NSAP target (clade/species)	Annealing temperature (°C)	Expected product size (bp)
Cl _a F	5' ACCACSAARCCSGATCTCTA 3'	A	A(I) ^a	59	635
Cl _a R	5' TTBGCTTTCTGTGCAACTGCTG 3'				
Cl _b K _p F	5' ATTGAGAACAGCCTGCTGGG 3'	B	B(K _p) ^b	65	499
Cl _b K _p R	5' GCTTATAGGAGGAGTTGGCGG 3'				
Cl _b F	5' CATTGGGTYTCKGTCGCMCA 3'	B	B(I) ^c	57	498
Cl _b R	5' CGCGCAGRATGCCGRATACCRCG 3'				
Cl _c F	5' CCACTTTATTAATCTGTAGC 3'	C	C(I) ^d	46	771
Cl _c R	5' CGGATTTTATCTTTTCTGC 3'				

^a Gene length of control strains 747 bp.

^b Gene length of control strain 714 bp.

^c Average gene length of control strains 817 bp.

^d Gene length of control strains 828 bp.

sets to discriminate between the various phosphatase genes, denoted here as clades A(I), B(I), C(I) or species B(Kp) (Fig. 4.2E-G), genomic DNA from each of the control strains was used as template and amplified with all of the other primer sets (Table 4.1). Cross-reactivity was not observed with any of these 'non-target' PCR primer sets, as amplicons were not obtained (Fig. 4.2A-D). Acid phosphatase genes belonging to clades A(I) and C(I) were obtained from genomic DNA extracted from the *Rahnella* Y9602 and *Bacillus* Y9-2 strains, respectively (Fig. 4.2E and 4.2G). Acid phosphatase genes were not amplified when genomic DNA extracted from *Arthrobacter* sp. X-34 was tested (data not shown). These results validate the use of a PCR-based approach to characterize NSAP genes present in environmental strains.

4.4.3 SDS-PAGE phosphatase activity assay

Following the phosphatase phenotypic and genotypic analysis of the FRC *Rahnella* sp. Y9602 and a *Bacillus* sp. Y9-2, whole-cell lysates of *Rahnella* sp. Y9602, *Bacillus* sp. Y9-2, *Klebsiella pneumoniae* ATCC 132 (Class A control) and *Bacillus cereus* ATCC 14579 (Class C control) were analyzed via denaturing polyacrylamide gel electrophoresis. Renaturation and incubation of separated proteins at pH 5.5 with 5 mM phenolphthalein diphosphate demonstrated that the FRC *Rahnella* sp. Y9602 and a *Bacillus* sp. Y9-2 possessed the expected 25 kDa and 30 kDa NSAPs, respectively (Fig. 4.5).

4.4.4 Aerobic biomineralization of U(VI) by microbial phosphate accumulation

A series of experiments were conducted to determine whether or not FRC strains that exhibited a positive phosphatase phenotype had the potential to bioprecipitate soluble U(VI). We selected three representative FRC subsurface strains, a *Rahnella* sp. strain Y9602 and a *Bacillus* sp. strain Y9-2, and *Arthrobacter* sp. X34 for further characterization. Strains Y9602 and Y9-2 exhibited a phosphatase positive phenotype while strain X34 was phosphate negative (Fig. 4.1A-C). Whole cell phosphatase activity of *Arthrobacter* sp. X34, *Bacillus* sp. Y9-2, and *Rahnella* sp. Y9602 was 0.9 ± 0.1 , $8.8 \pm$

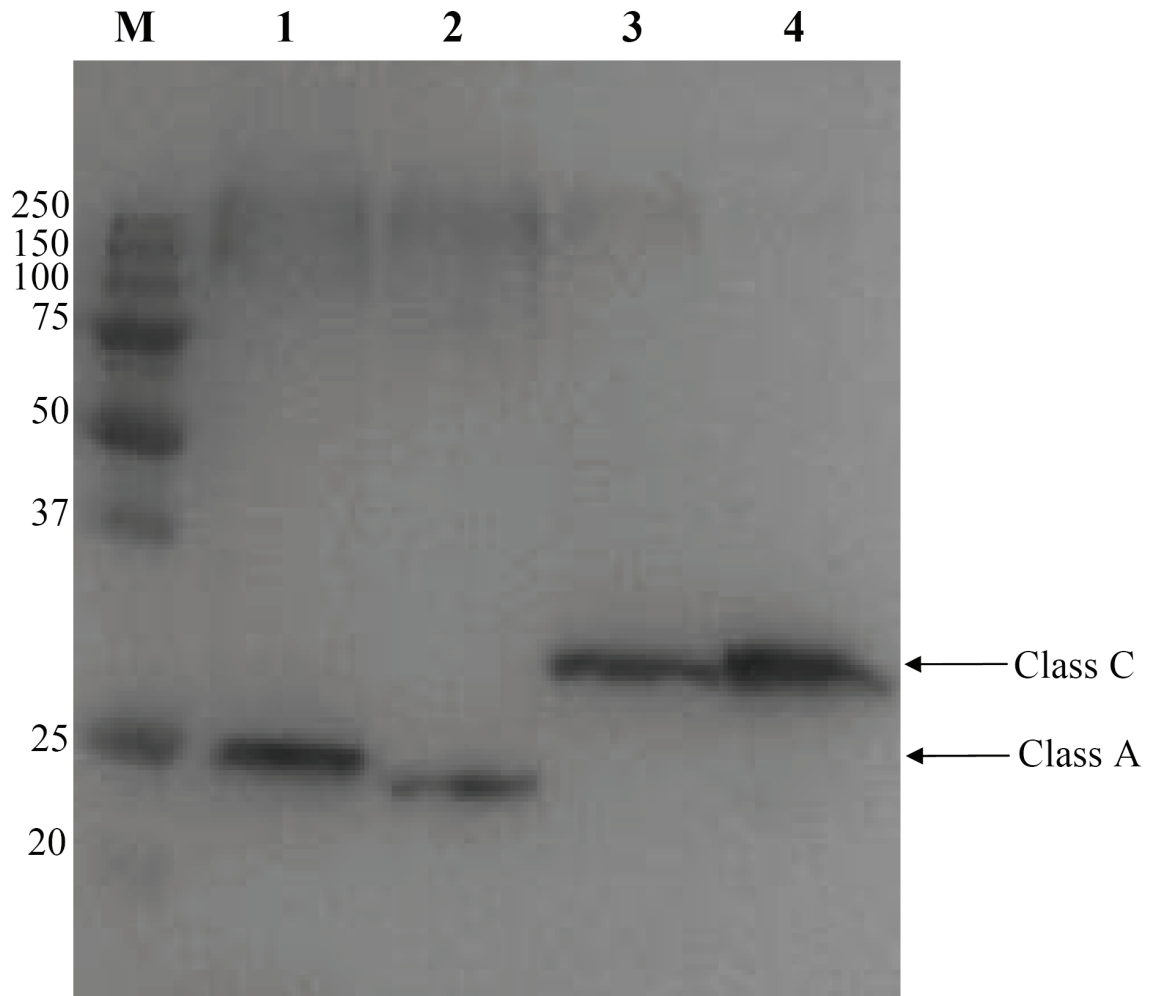


Figure 4.5 Renatured SDS-PAGE phosphatase activity analysis. Whole-cell lysates (25 µg of total protein/lane) of: **1** - *Klebsiella pneumoniae* ATCC 132 (Class A control), **2** -

Rahnella sp. Y9602, **3** - *Bacillus cereus* ATCC 14579 (Class C control), **4** - *Bacillus* sp. Y9-2, **M** - molecular weight marker (masses are indicated in kDa). Arrows indicate the expected molecular mass of the Class A and Class C NSAPs of 25 kDa and 30 kDa, respectively. All strains were grown in nutrient broth pH 5.5 to mid-log phase.

0.8, and 10.4 ± 1.3 nmol/min, respectively. Whole-cell phosphatase activity assays identified a pH optima of 5.5 (data not shown). In synthetic groundwater medium *Rahnella* exhibited enhanced phosphatase activity relative to the *Bacillus* while no activity was observed with the phosphatase negative *Arthrobacter* (Fig. 4.6A). Inorganic phosphate accumulated in the medium of strains Y9602 and Y9-2 in the presence of a model dissolved organophosphorus compound, glycerol-3-phosphate (G3P) provided as the sole carbon and phosphorus source (Fig. 4.6A). In contrast, phosphate did not accumulate in medium inoculated with the phosphatase negative *Arthrobacter* sp. X34 (Fig. 4.6A). A 3.6-fold greater phosphate accumulation occurred in incubations with viable *Rahnella* sp. (i.e., 939 μ M) as compared to viable *Bacillus* spp. (i.e., 263 μ M) (Fig. 4.6A) in the absence of U(VI). The enhanced phosphate accumulation observed with *Rahnella* sp. Y9602 resulted in a 10-fold greater concentration of reactive phosphate by the end of the 120 h incubation relative to *Bacillus* sp. Y9-2 (Fig. 4.6A). In contrast, less than 50 μ M phosphate was measured in either the cell-free (abiotic) or heat-killed controls during the course of incubation (Fig. 4.6A). Upon addition of 200 μ M U(VI) at 36 h, there was a statistically significant decrease ($P < 0.05$) in reactive phosphate concentrations for both the *Rahnella* and *Bacillus* spp. relative to their viable controls without U(VI).

Precipitation of soluble U(VI) as a U-phosphate mineral was predicted to occur thermodynamically in the experimental assay conditions tested [i.e., pH 5.5 and 200 μ M

U(VI)] (Fig. 4.7). To determine whether the concentration of bio-accumulated phosphate was sufficient to promote the removal of U(VI) by precipitation, total soluble U was measured. Within the first hour of U(VI) addition, *Rahnella* and *Bacillus* spp. removed 34% and 31% of total soluble U(VI), respectively. By the end of the 120h incubation, a significant difference in the amount of U(VI) precipitated ($P < 0.05$) was detected with 95% and 73% of the added U(VI) removed by *Rahnella* and *Bacillus*, respectively, relative to the abiotic and heat-killed controls (Fig. 4.6B). In contrast, U(VI) was not precipitated in viable or heat-killed *Arthrobacter* sp. amendments (Fig. 4.6B). The precipitation of U(VI) was mediated by microbial activity as less than 5 μM soluble U(VI) was removed either from the abiotic or the heat-killed cell controls following U(VI) addition (Fig. 4.6B). Thus, the loss of U(VI) is not due to bioadsorption or abiotic chemical interactions (Fig. 4.6B).

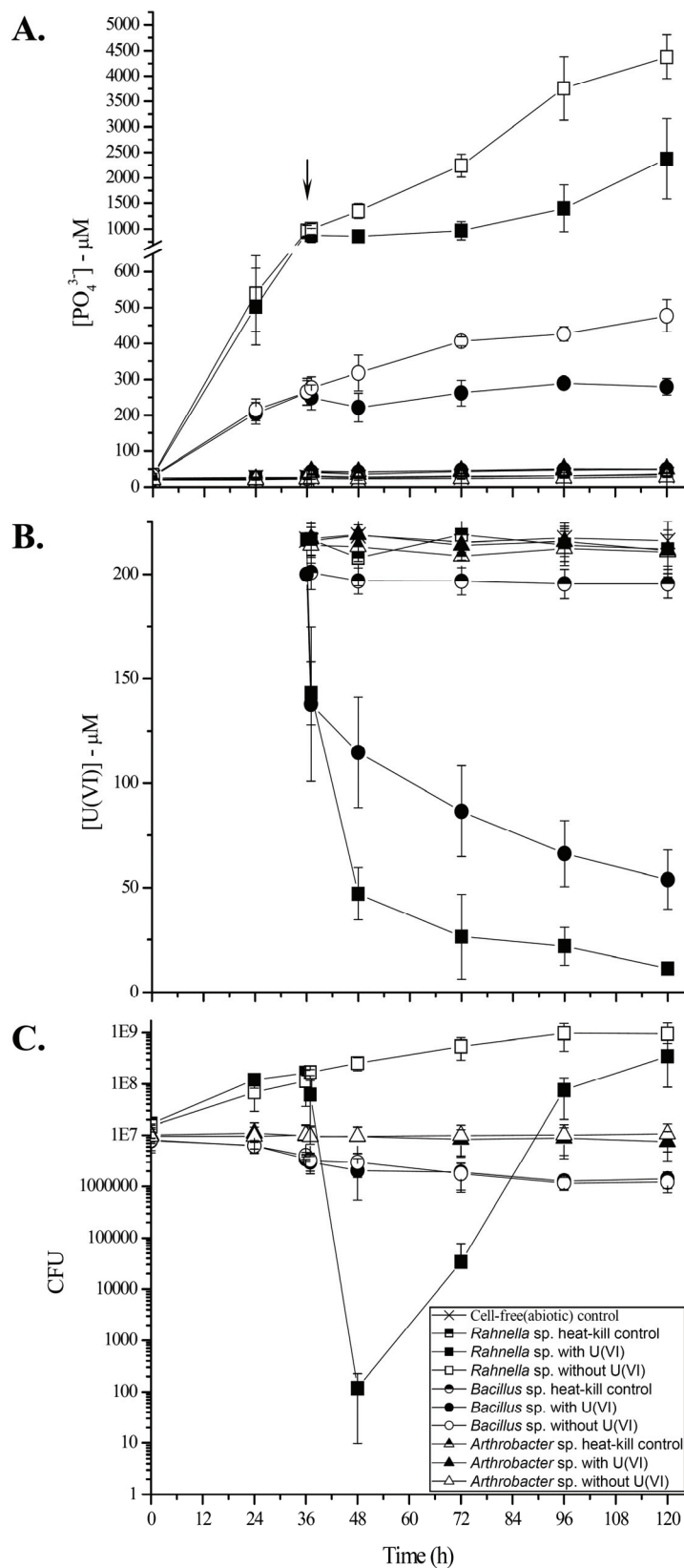


Figure 4.6 Synthetic groundwater (pH 5.5) amended with 10 mM G3P (as sole C and P

source) and inoculated with either viable or heat-killed control *Rahnella* sp. Y9602 (squares) or *Bacillus* sp. Y9-2 (circles) or *Arthrobacter* sp. X34 (triangles). Abiotic controls were cell-free. Concentrations of: (A). Phosphate, (B). U(VI) and (C). CFU measured as a function of time. Arrow at 36 h denotes the addition of 200 μ M U(VI). All incubations were performed under oxic conditions. Error bars denote standard deviation of triplicate experiments.

Colony Forming Units (CFU) were determined to identify the affect soluble U(VI) has on cell viability (Fig. 4.6C). *Rahnella* sp. Y9602 CFU counts increased approximately 2 log during the 120 h incubation without U(VI) (Fig. 4.6C). However, upon U(VI) addition, *Rahnella* cell viability was dramatically affected as evidenced by a 10^6 -fold decrease in CFU counts (Fig. 4.6C). The decrease in CFU counts did not appear to be due to significant cell lysis as cell counts were greater than 10^7 per ml when determined by direct microscopy (data not shown). Interestingly, *Rahnella* cell viability subsequently increased exponentially and by the end of the 120 h incubation the CFU counts were comparable to that of the control without U(VI) (Fig 4.6C). The exponential increase in CFU counts coincided with a decrease in U(VI) from solution. In contrast, CFU counts of *Arthrobacter* sp. X34 and *Bacillus* sp. Y9-2 with or without U(VI) did not demonstrate a significant difference (Fig. 4.6C). The differential growth response observed between the three strains is likely due to the inability of the Y9-2 and X34 to grow on G3P as a sole carbon source as we observed a 2 log increase in CFU when the strains were grown in synthetic groundwater medium amended with 0.2% yeast extract (data not shown). However, the intrinsic activity of the phosphatase positive Y9-2, even in the absence of appreciable cell growth, was sufficient to promote significant U(VI) precipitation (Fig. 4.6B).

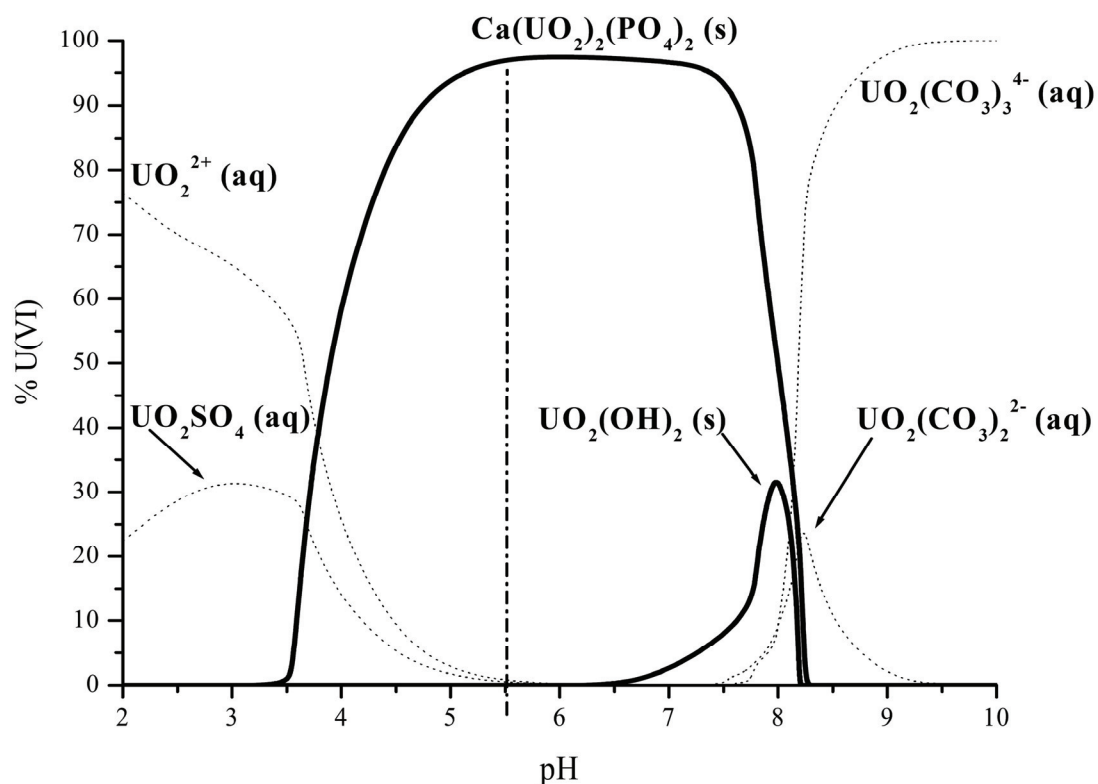


Figure 4.7 Uranium (VI) speciation as a function of pH in synthetic groundwater (SGW). The open system model at 30°C calculated aqueous and solid phases at equilibrium using the concentrations of ions present in synthetic groundwater, $\text{UO}_2^{2+}(\text{aq}) = 200 \mu\text{M}$, $\text{PO}_4^{3-}(\text{aq}) = 200 \mu\text{M}$ and, $P_{\text{CO}_2} = 10^{-3.5} \text{atm}$. Vertical dash-dot line indicates pH of experimental SGW incubations, dotted lines indicate aqueous phase U(VI) species, and solid lines indicate solid phase U(VI) species.

4.4.5 Electron microscopy of biomineralized U(VI)

Transmission electron microscopy of *Rahnella* sp. Y9602 following biomineralization assays indicated extensive extracellular uranium precipitation as well as cell surface localized precipitation (Fig. 4.8A and B). Energy dispersive X-ray (EDX) spectroscopy of the extracellular and cell surface electron dense regions indicated by the arrows in (Fig. 4.8A and B) demonstrated the composition of uranyl phosphate components (i.e., uranium, phosphorous, and oxygen).

Variable-pressure scanning electron microscopy of the uranium associated cell pellet lacking fixation and metal sputter coating indicated an amorphous mineral that was composed of uranium, phosphorous, and oxygen when EDX elemental mapping was performed (Fig. 4.9A-D).

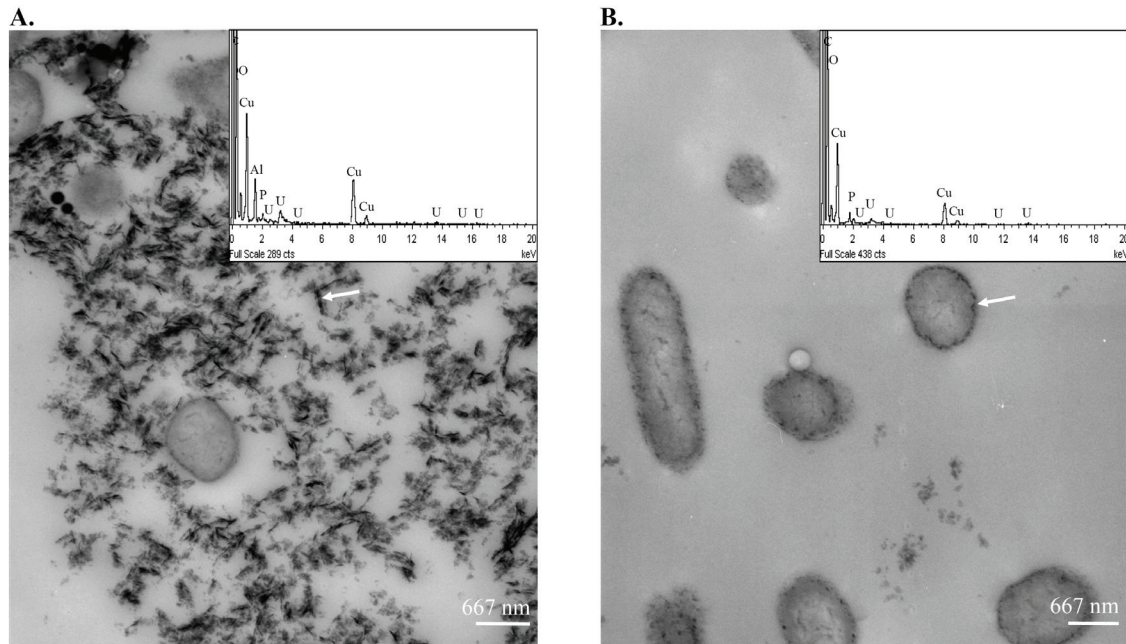


Figure 4.8 Transmission electron micrographs of *Rahnella* sp. Y9602 following uranium biomineralization. **(A.)** Cells associated with extracellular uranium precipitate and **(B.)** cell surface localized uranium precipitate. Arrows in micrographs **(A.)** and **(B.)** indicate regions analyzed via energy dispersive X-ray (EDX) spectroscopy. Inset spectra identify elemental composition of uranium precipitate.

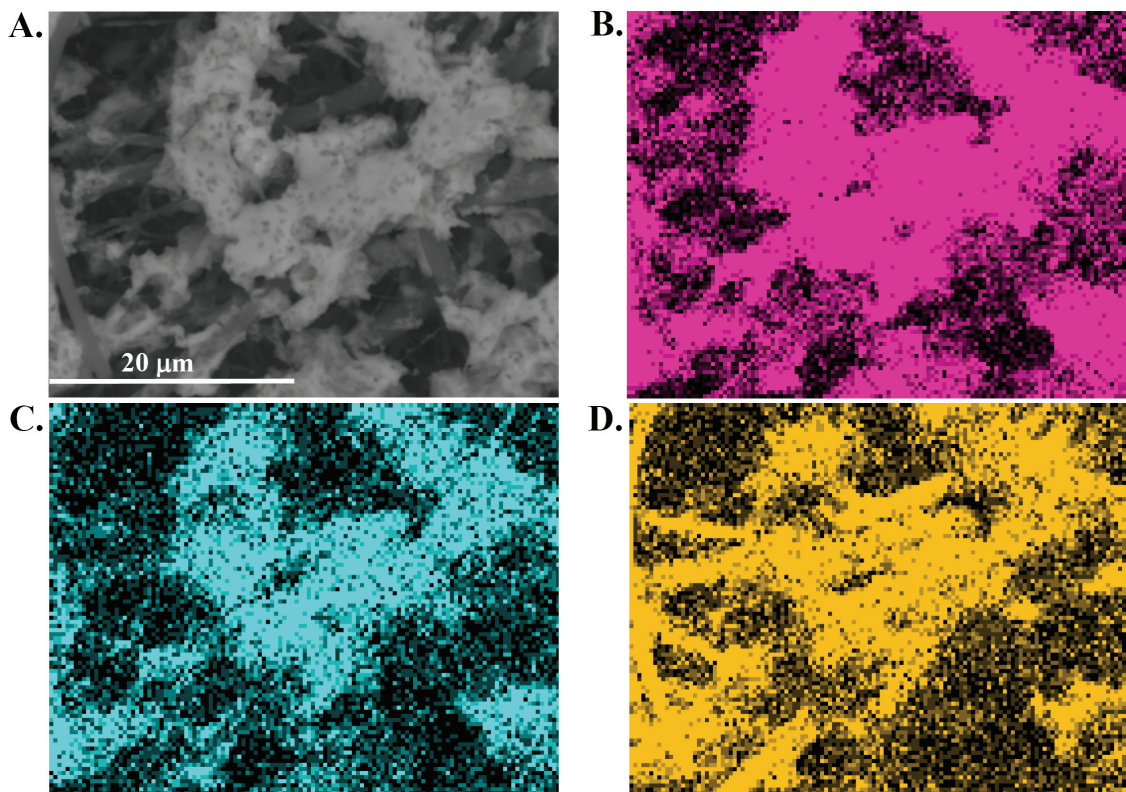


Figure 4.9 Variable-pressure scanning electron micrograph of *Rahnella* sp. Y9602 biomineralized uranium (A.) EDX elemental mapping of uranium (B.), phosphorus (C.), and oxygen (D.).

4.4.6 Anaerobic biomineralization of U(VI) by microbial phosphate accumulation

During a nitrate reduction screening assay, of FRC *Rahnella* sp. Y9602, *Bacillus* sp. Y9-2, and *Arthrobacter* sp. X34 only the *Rahnella* sp. Y9602 exhibited the capability of respiring on nitrate as a terminal electron acceptor (data not shown). The *Rahnella* sp. was then incubated in the previously described SGW under anoxic conditions that required soluble nitrate to be utilized as the terminal electron acceptor. Inorganic phosphate accumulated during anoxic incubations with glycerol-3-phosphate (G3P) provided as the sole carbon and phosphorus source (Fig. 4.10A). Upon addition of 200

μM U(VI) at 36 h, greater than 75% of total U(VI) precipitated within 1 h and over 95% of total U(VI) precipitate upon completion of the 120 h incubation (Fig. 4.10B). Viable cell counts of the *Rahnella* sp. incubated without U(VI) exposure did not surpass the initial cell density of 10^7 cells/ml (Fig. 4.10C). Similar to the aerobic biomineralization assays, uranium exposure resulted in a loss of culturability of the *Rahnella* sp. (i.e., greater than a 10^5 decrease in culturability). Upon completion of the 120 h assay, culturability increased by a factor of 10^4 (Fig. 4.10C).

4.4.7 Aerobic hydrolysis of sodium tripolyphosphate

Incubations of the *Rahnella* sp. Y9602 in SGW with 10 mM glycerol (sole C source) and 3.33 mM sodium tripolyphosphate (sole P source) yielded complete hydrolysis as 10 mM orthophosphate was measured in solution following 72 h. The abiotic control did not demonstrate phosphate hydrolysis of the tripolyphosphate substrate indicating the requirement for enzymatic hydrolysis to liberate 10 mM orthophosphate within a 72 h period. (Fig. 4.11).

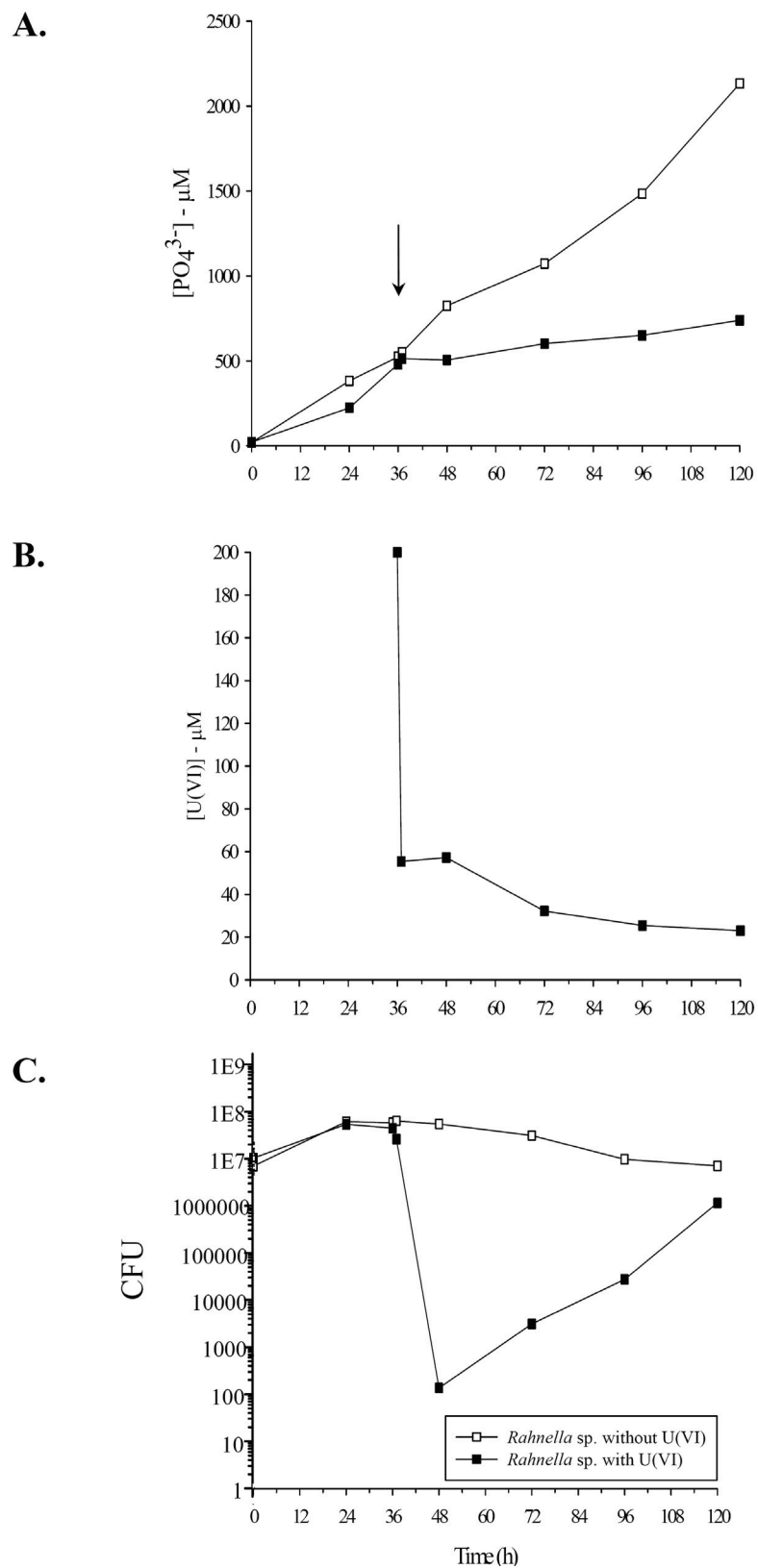


Figure 4.10 Synthetic groundwater (pH 5.5) amended with 10 mM G3P (as sole C and P

source) and inoculated with *Rahnella* sp. Y9602 (squares). Concentrations of: (A). Phosphate, (B). U(VI) and (C). CFU measured as a function of time. Arrow at 36 h denotes the addition of 200 μ M U(VI). All incubations were performed under anoxic conditions.

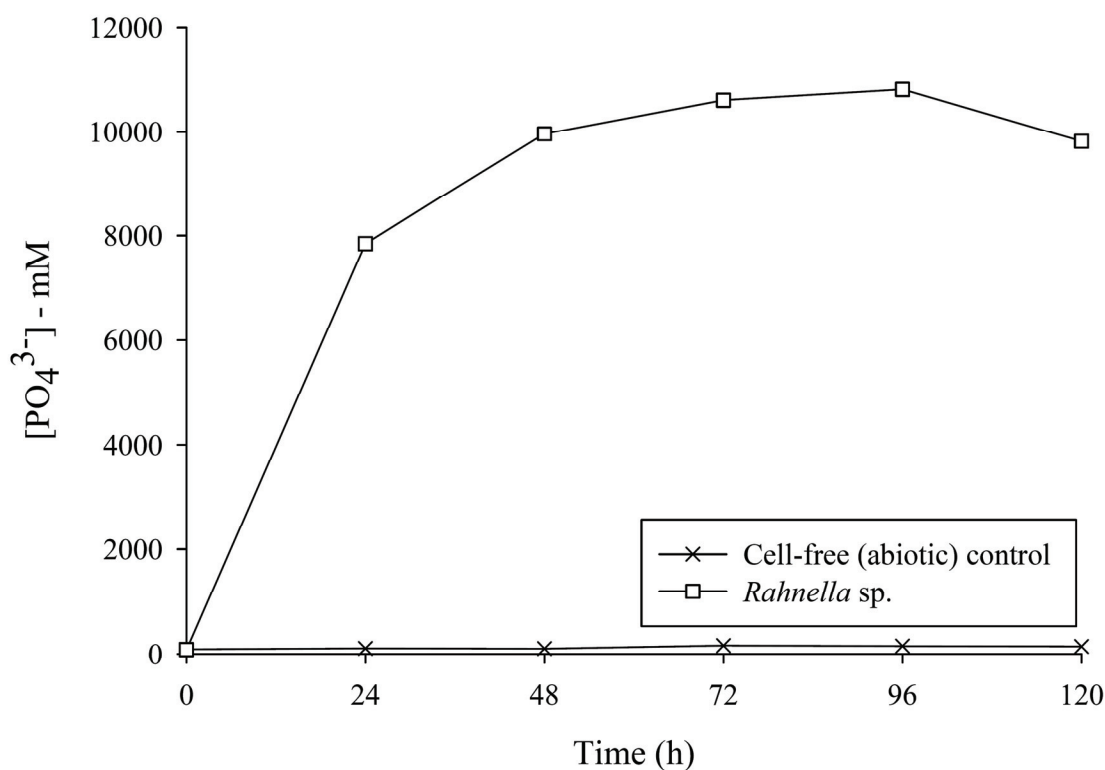


Figure 4.11 Phosphate measurement of *Rahnella* sp. Y9602 incubated in synthetic groundwater (pH 5.5) amended with 10 mM glycerol (sole C source) and 3.33 mM sodium triphosphate (sole P source). Abiotic controls were cell-free. Incubations were performed under oxic conditions.

4.5 Discussion

The cleanup of U contaminated groundwater and soils by methods such as pump-and-treat and excavation can be costly and disruptive to ecosystems. *In situ* remediation

strategies, particularly those mediated by microorganisms, that stabilize U by sorption or by incorporation into low solubility solid phases are attractive alternatives as they are generally more cost-effective and less invasive than other options (Nash et al., 1998; Arey et al., 1999; Bostick et al., 1999). U solubility is dependent upon its oxidation state [i.e., U(VI)_{aq} and U(IV)_{s}]. In anaerobic conditions, dissimilatory metal- and sulfate-reducing bacteria have been shown to reduce U(VI) in either a growth-dependent or independent manner (Gadd, 2004; Wall and Krumholz, 2006). The removal of U from contaminated systems by bioreduction may be effective as the reduced U(IV) product is in the form of uraninite [$\text{UO}_{2(\text{s})}$], an insoluble mineral above pH 5 (Rai et al., 1990). In aerobic conditions, U is usually present as the highly soluble uranyl ion (UO_2^{2+}) (Suzuki and Banfield, 1999). Thus, U precipitation in oxic conditions must be driven by a redox-independent mechanism. In the case of bacterially mediated U precipitation in oxygenated zones, proposed strategies have mainly focused on enzymatic precipitation of U as complexes of phosphate (Macaskie et al., 1988; Macaskie et al., 1992; Yong and Macaskie, 1995)].

In the present study, phosphate immobilization of U(VI) mediated by the intrinsic phosphatase activities of bacteria isolated from radionuclide- and metal-contaminated subsurface soils at the ORFRC was examined. In the aerobic subsurface, U is present as U(VI) and thus microorganisms may, we theorize, precipitate U by liberating phosphate as a means to prevent or limit U toxicity. Moreover, FRC isolates belonging to common soil genera (*Arthrobacter*, *Bacillus* and *Rahnella*) are resistant to a number of co-occurring heavy metals including Pb, Cd, and Hg (Martinez et al., 2006b). Sensitivities to co-occurring metals such as Pb and Cd rather than the radiological toxicity of actinides

such as U have been shown to severely limit the growth of some bacteria proposed for use in the bioremediation of mixed waste sites (Ruggiero et al., 2005). Thus, one might expect that a mechanism that could provide cellular protection from actinide stress would likely confer a competitive advantage to microbes in similarly contaminated subsurface soils. Further, testing the phosphatase activities of subsurface strains that are Pb^{II} is supported by previous studies using the Pb^{II} soil isolate *Citrobacter* sp. N14 [renamed *Serratia* sp. N14 (Pattanapitpaisal et al., 2002)]. The activity of a NSAP constitutively expressed by strain N14, was directly implicated in the precipitation of greater than 90% of U(VI) from solution as a uranyl phosphate precipitate (Macaskie et al., 1994). A number of studies have subsequently demonstrated comparable U-phosphate precipitation with diverse genera including *Deinococcus*, *Escherichia*, and *Pseudomonas* (Basnakova et al., 1998; Powers et al., 2002; Appukuttan et al., 2006). However, such activity only occurred following the introduction of recombinant acid [*phoN* (Basnakova et al., 1998; Appukuttan et al., 2006)] or alkaline [*phoA* (Powers et al., 2002)] phosphatase genes.

Our study provides the first evidence of U precipitation via the endogenous phosphatase activity of naturally occurring strains belonging to the genera *Bacillus* and *Rahnella* isolated from radionuclide- and metal-contaminated soils. We theorize that acid rather than alkaline phosphatases are most likely to be involved in detoxification processes in phosphatase positive strains, as the contaminated soils from which the strains were isolated are acidic (Martinez et al., 2006b). The role of NSAPs is also supported by the fact that whole cell as well as whole cell lysate phosphatase activities of the *Bacillus* and *Rahnella* strains indicated a pH optimum of 5.0-5.5. Interestingly, the small molecular weight NSAPs were the only phosphatases demonstrating activity

following renaturation in the polyacrylamide gel. The amino-terminal and internal regions of the constitutively expressed phosphatase of *Serratia* sp. N14 demonstrate significant similarities to Class A NSAPs based on partial amino acid sequence analysis (Jeong et al., 1998). To verify the presence of NSAP genes in our phosphate-liberating strains, PCR primer sets were designed to amplify genes belonging to the known molecular classes of NSAPs. Sequence analysis of PCR amplicons revealed Class A and Class C NSAP genes were obtained from *Rahnella* Y9602 and *Bacillus* Y9-2 strains, respectively.

Although the *Bacillus* and *Rahnella* strains liberated different concentrations of inorganic phosphate as a result of the hydrolysis of G3P, significant amounts (i.e., 73-95%) of U were precipitated. This phosphate accumulation was in addition to that required for cellular metabolic activity, as G3P was the sole carbon and phosphorus source. In contrast to *Bacillus* Y9-2 viability, *Rahnella* Y9602 exhibited a significant (and sharp) decrease in culturability upon exposure to 200 μ M U(VI). One explanation for the observed difference between *Bacillus* and *Rahnella* cell culturability is that *Rahnella* Y9602 may have entered a period of non-culturability due to the uranium stress. A similar culturability response has been reported for *Pseudomonas* sp. S8A isolated from metal-contaminated acidic soil upon exposure to the heavy metals cadmium and lead (Kassab and Roane, 2006). Alternatively, active metabolism (i.e., growing cells) may be required for U(VI) to inhibit cell culturability as we did not detect any change in CFU in the non-growing *Bacillus* strain. However, when *Bacillus* Y9-2 was supplemented with a carbon source that promoted cell growth (i.e., yeast extract) only a slight decrease in CFU (i.e., 5-fold) was observed upon exposure to U(VI). Thereafter,

Bacillus CFU remained constant for the duration of the incubation (data not shown). Another explanation is that differences in cell walls between the gram-negative *Rahnella* and gram-positive *Bacillus* may also influence cell sensitivity to U(VI). Although G3P was the only substrate used for U(VI) biomineralization studies, the *Rahnella* sp. Y9602 was capable of hydrolyzing sodium tripolyphosphate. Further indicating the broad range of substrates hydrolyzed by NSAPs (e.g., nucleoside phosphates, hexose-, pentose-, and glycerol-phosphates) (Rossolini et al., 1998). These substrates could occur in appreciable amounts suitable for promoting U precipitation as a result of *in situ* biostimulation events designed to increase microbial biomass and stimulate metabolic activity (Istok et al., 2004; Hwang et al., 2006; Wu et al., 2006). Our findings suggest that microbial phosphatase activity may provide a secondary barrier for immobilizing radionuclides in aerobic conditions. Uranium phosphate precipitation may aid in immobilizing contaminants when reductively precipitated U becomes soluble as a result of changes in redox state. Furthermore, our data demonstrates that strains such as the *Rahnella* sp. Y9602 that can respire on nitrate in anoxic environments can continue to promote the precipitation of U(VI).

Thermodynamic modeling of the U-phosphate precipitate likely formed in the synthetic groundwater conditions is calcium autunite $[\text{Ca}(\text{UO}_2)_2(\text{PO}_4)_2]$ (Fig. 4.7). Analysis of the U-phosphate precipitate via electron microscopy further supported thermodynamic modeling as uranium precipitate contained phosphorus and oxygen. Extended X-ray absorption fine structure measurements have recently confirmed these findings (Beazley et al., 2007). As U precipitation was measured for only 84 h, the continued accumulation of $\text{Ca}(\text{UO}_2)_2(\text{PO}_4)_2$ appears to be kinetically controlled and,

given additional time, complete removal of soluble U(VI) is expected. Calcium autunite, which can be formed from the ion exchange of chernikovite $[(\text{UO}_2)\text{H}(\text{PO}_4)]$ with calcium (Sowder et al., 1996), may prove to facilitate the removal of co-occurring heavy metals. Biogenically precipitated chernikovite has, in fact, already been shown to catalyze the removal of Ni(II), Co(II), Sr(II), and Cs(I) by an ion exchange mechanism (Basnakova and Macaskie, 2001; Paterson-Beedle et al., 2006). Autunite-group minerals are biogenically precipitated (Basnakova and Macaskie, 2001; Paterson-Beedle et al., 2006) and *in situ* microbial phosphatase activity may play an important role in U stabilization. In addition, autunite minerals control U mobility in contaminated soils at the Fernald, Ohio and the Oak Ridge National Laboratory K25 sites (Buck et al., 1996; Roh et al., 2000). However, it is important to note that the microbial contribution to autunite formation in these sites has yet to be determined.

4.6 Experimental procedures

4.6.1 Subsurface strains and growth conditions

The metal resistant subsurface strains *Arthrobacter* spp. X34, V45, AA20; *Bacillus* spp. Y7, X18, Y9-2 and *Rahnella* spp. Y9602, Y4, Y29 were previously isolated from radionuclide- and metal-contaminated subsurface soils collected from the ORFRC as described (Martinez et al., 2006b). Detailed geology, chemistry, and site descriptions are available on the DOE Environmental Remediation Sciences Program website (<http://www.esd.ornl.gov/nabirfrc/>). Strains were isolated from soil core samples as described in Martinez *et al.* (2006) from sites where the saturated zones contained

elevated U, other radionuclides, and heavy metals (Brooks, 2001). Strain identification was previously confirmed by 16S rDNA phylogeny (Martinez et al., 2006b). Media used to identify strains with constitutive phosphatase activity were Tryptose-phosphate methyl green agar (TPMG) (Riccio et al., 1997) and Tryptose-phosphate 4-methylumbelliferyl phosphate, disodium agar (TP-MUP) modified from (Adcock and Saint, 2001). The modified TP-MUP consisted of 20 g tryptose, 5 g sodium chloride, 2.5 g disodium phosphate, 2 g dextrose, 85 mg 4-methylumbelliferyl phosphate, and 15 g agar per liter. Plates were incubated at 30°C for 24 h with the exception of TPMG (36 h). Cells were grown in pH buffered synthetic groundwater (SGW) consisting of 50 mM MES (pH 5.5), 2 μ M FeSO₄, 5 μ M MnCl₂, 8 μ M Na₂MoO₄, 0.8 mM MgSO₄, 7.5 mM NaNO₃, 0.4 mM KCl, 7.5 mM KNO₃, 0.2mM Ca(NO₃)₂. Media containing glycerol-3-phosphate (Sigma) as the sole carbon and phosphorus source utilized a final concentration of 10 mM. Media containing glycerol (Sigma) as the sole carbon source and sodium tripolyphosphate (Sigma) as the sole phosphorus source utilized final concentrations of 10 mM and 3.33 mM, respectively. Nutrient broth (NB) agar (3 g beef extract, 5 g peptone, 15 g agar per liter) was used for the maintenance of the strains. All strains were incubated at 30°C and liquid cultures were shaken at 200 rpm under aerobic growth conditions (open to atmospheric gas). Anaerobic growth conditions were performed at 30°C under an atmosphere of 1% H₂ with the balance N₂.

4.6.2 Phosphatase activity assays

Whole cell phosphatase activity was estimated by monitoring the hydrolysis of *p*-nitrophenyl phosphate (*p*NPP) (Sigma). FRC strains were grown to mid-log phase in

nutrient broth (pH 5.5), harvested by centrifugation (10,000g, 10 min), washed twice with 100 mM sodium acetate (pH 5.5). Phosphatase activity was initiated by the addition of 10^9 cells to 5 mM *p*NPP in 100 mM sodium acetate buffer (pH 5.5) at 30°C in a reaction volume of 0.5 ml. Reactions were terminated after 30 min by the addition of 0.5 ml of 0.02 M NaOH. Accumulation of *p*-nitrophenol (*p*NP) was measured spectrophotometrically at 405 nm.

Whole-cell lysates for SDS-PAGE phosphatase activity assays were obtained from 500 ml cultures grown to mid-log phase in NB media pH 5.5. Cultures were pelleted by centrifugation at 10, 000 g for 10 min and washed twice with sterile 0.85% saline. Washed cell pellets were then resuspended in 3.5 ml of 10 mM Tris-HCl pH 7.4 and passed through a French press twice at 25,000 psi. Triton X-100 was then added to cell lysates at a final concentration of 2%. DNA in cell lysates were sheared by 3 passages through a 25G needle and the insoluble fraction was removed by centrifugation at 10, 000 g for 10 min. Soluble protein concentrations were obtained by the bicinchoninic acid assay (Pierce). Soluble proteins (25 µg/lane) were separated via electrophoresis on 15% denaturing (Bio-Rad). Following electrophoresis, proteins within SDS polyacrylamide gels were renatured for 4 h in renaturation buffer (10 mM Tris-HCl pH 7, 1% Triton X-100 (vol/vol), 2 mM magnesium chloride, 0.05 mM zinc chloride) with buffer changes every 30 min. Gels were then incubated for 1 hr at 37°C in equilibration buffer (5 mM magnesium sulfate, 100 mM sodium acetate buffer pH 5.5). Equilibrated gels were then incubated in equilibration buffer containing 5 mM PDP (Sigma) and 0.05 mg/ml methyl green (ICN Biomedicals) for 16 h. Excess methyl green was then washed from polyacrylamide gels with equilibration buffer for 1 h.

4.6.3 Nucleic acid isolation, NSAP primer design, and PCR amplification of genomic DNA

Genomic DNA for PCR-based analyses was isolated from subsurface isolates by either a rapid boiling method as previously described (Martinez et al., 2006b) or a bead mill homogenization method (Miller et al., 1999). The sequences of primers and PCR reaction conditions used for the amplification of *Bacteria*-specific 16S rDNA from isolated genomic DNA were followed as previously described (Mills et al., 2003). The Class A, B and C NSAP primers used in this study were designed to amplify the respective genes in bacteria bearing close relatedness (based on 16S rRNA phylogeny) to the FRC *Rahnella* and *Bacillus* strains. The programs CLUSTAL X (Thompson et al., 1997) and BioEdit v5.0.9 (Hall, 1999) were used to align and visualize the NSAP nucleotide sequences of type strains related to the studied FRC strains. The primers used for standard PCR amplification of Class A, B and C NSAPs are listed in Table 4.1. These PCR primer sequences allowed for greater than 60% of each respective gene class to be amplified. Genomic DNA isolated from the following type strains: *Enterobacter aerogenes* ATCC 13048 (Class A control), *Klebsiella pneumoniae* ATCC 132 (Class A and B control), *Escherichia coli* MG1655 ATCC 47076 (Class B control), *Salmonella enterica* ATCC 14028 (Class B control), *Bacillus cereus* ATCC 14579 (Class C control) and *Bacillus thuringiensis* ATCC 13366 (Class C control) were used as positive controls to confirm the specificity of the designed NSAP primers (Fig. 4.4). Additionally, the PCR primer set targeting *Klebsiella pneumoniae* Class B NSAP denoted B(Kp) was designed after sole use of the Class B primer targeting clade B(I) failed to amplify this strain. The PCR mix contained 20 ng of genomic DNA, 1× PCR buffer (New England

Biolabs), 1.5 mM MgCl₂, 200 μM of each dNTP, 0.25 μM of each forward and reverse primer (Integrated DNA Technologies), and 1.0 Units Taq polymerase (New England Biolabs). The thermocycling conditions are as follows: 1 cycle for 10 min at 95°C followed by 25 cycles of 95°C for 30 s, annealing temperature as listed in Table 4.1 for the specific class of NSAP for 30 s, followed by 72°C for 45 s, and 1 cycle for 10 min at 72°C.

Amplified products were analyzed on 1.0% agarose gels run in TBE buffer, stained with ethidium bromide, and UV illuminated. Amplicons were purified with the Qiaquick gel extraction kit (Qiagen) and cloned into pDrive cloning vector according to manufacturer's instructions (Qiagen). Cloned NSAPs were PCR amplified from lysed colonies with M13F (5'-GTAAAACGACGGCCAG-3') and M13R (5'-CAGGAAACAGCTATGAC-3') and sequenced at the Georgia Tech genomics core facility using a BigDye Terminator v3.1 Cycle sequencing kit on an automated capillary sequencer (model 3130 Gene Analyzer, Applied Biosystems).

4.6.4 Selection of bacterial NSAP protein sequences

In order to collect bacterial protein sequences of putative NSAPs from biological databases, a multi-step procedure, specifically designed to cope with the significant number of erroneous annotations that exist in current databases was followed (Devos and Valencia, 2001; Valencia, 2005). First, we retrieved all the protein sequences of bacterial NSAPs whose enzymatic activities have been experimentally characterized and used them as query sequences in PSI-BLAST (Altschul et al., 1997) searches against the nr database. Successive PSI-BLAST iterations were performed until convergence was

reached (i.e., until new sequences were not found), using a very stringent Expect-value threshold for inclusion of new sequences of 10^{-20} . After removing the redundant sequences, we constructed two preliminary multiple sequence alignments (MSAs), one for Class A NSAPs and another for NSAPs belonging to the molecular Classes B and C using CLUSTAL W version 1.83 (Thompson et al., 1994) with default parameters.

Because highly similar sequences may not always share the same detailed biochemical function (Tian and Skolnick, 2003), we excluded all putative NSAP sequences lacking conservation in the active site residue positions from the MSAs. We obtained the following active site residue information for class A NSAPs from the X-ray structure of a NSAP of *Escherichia blattae* (Ishikawa et al., 2000): Lys115, Arg122, Ser148, Gly149, His150, Arg183, His189 and Asp193. For class B NSAPs, we considered the active site residues: Asp44, Asp46, Thr48, Arg114, Asp167 and Asp171, inferred from the crystallographic structure of AphA of *Escherichia coli* (Calderone et al., 2004). As a structure for class C members is not available, we generated a theoretical model of the *Haemophilus influenzae* e (P4) acid phosphatase (Green et al., 1991) using the protein comparative modeling server TASSER-Lite (Pandit et al., 2006). By analyzing the three-dimensional alignment of the e (P4) structural model to the AphA crystallographic structure, we proposed the following active site residues for class C NSAPs: Asp84, Asp86, Thr88, Arg146, Asp201 and Asp205 (using the numbering of the e (P4) sequence).

In addition to the active site residue conservation condition to keep a candidate NSAP sequence, we also required the EC number of the putative NSAP to be predicted as EC 3.1.3.2 (i.e., acid phosphatase according to the IUBMB Enzyme Nomenclature) by

the highly precise EFICAz algorithm (Tian et al., 2004). We only imposed this requirement to putative Class A and Class B NSAPs because Class C NSAP sequences were not available during the training of the current version of EFICAz.

4.6.5 Phylogenetic analysis

Using CLUSTAL W version 1.83 with default parameters, we prepared class A and classes B/C MSAs of the experimentally characterized NSAPs and the putative NSAPs protein sequences that passed all the filters. We used the PHYLIP version 3.66 (Felsenstein, 2006) package of programs to perform the phylogenetic analysis of the NSAPs. We employed the Protpars program to generate maximum parsimony trees, the Protdist program to compute the evolutionary distance matrices (corrected by the Jones-Taylor-Thornton model) and the Neighbor program to generate the distance based trees. We used the Seqboot and the Consense programs to assess the statistical significance of the trees by performing 100 bootstrap resamplings.

Sequence analysis of the nearly full length Y9602 Class A and Y9-2 Class C phosphatases utilized 636 and 773 nucleotides, respectively. The Y9-2 16S rDNA sequence and NSAP gene sequences for Y9602 and Y9-2 NSAP have been deposited in the GenBank database under accession numbers EF158823-EF158825.

4.6.6 Modeling of uranium speciation in simulated groundwater

Thermodynamic equilibrium modeling of uranium in SGW was conducted using MINEQL+ v. 4.5 (Schecher and Software:, 2001) with the Nuclear Energy Agency's updated thermodynamic database for uranium (Guillaumont and Grenthe, 2003). The

open system model of pH-dependent uranium speciation at 30°C utilized the Davies equation with the following SGW parameters: $\text{UO}_2^{2+}{}_{(\text{aq})} = 200 \mu\text{M}$, $\text{PO}_4^{3-}{}_{(\text{aq})} = 200 \mu\text{M}$, $P_{\text{CO}_2} = 10^{-3.5} \text{ atm}$.

4.6.7 Cell enumeration, phosphate, and uranium measurements

Triplicate flasks containing 250 ml SGW (pH 5.5) amended with 10 mM glycerol-3-phosphate (as sole C and P source) were inoculated with approximately 10^7 cells ml^{-1} of each strain. Prior to inoculation in SGW, FRC strains were grown overnight at 30°C in NB (pH 6.8) from frozen stocks (-80°C). The next day, cells from solid agar were grown 16-18 h in NB broth (pH 5.5) and subsequently diluted 1/50 into fresh NB (pH 5.5) and grown to mid-log phase. Cells were harvested by centrifugation (10,000g, 10 min), washed twice with isotonic saline (8.5 g l^{-1} NaCl), and gently resuspended in SGW (pH 5.5). Cells resuspended in SGW were sub-aliquoted into flasks for (a) viable cell activity or (b) non-viable cell activity (i.e., heat-killed cells). Heat-killed cells were held at 30 min at 85°C and cooled to room temperature prior to inoculation. A second control was set-up to monitor for abiotic, chemical interactions (e.g., no viable or heat-killed cell inoculum was added). All flasks were incubated at 30°C, 200 rpm. Subsamples were aseptically removed to determine (i) culturable cell counts, (ii) inorganic phosphate concentration, (iii) pH and (iv) soluble U concentrations, measured after the addition of 200 μM uranyl acetate at 36 h of incubation. Cell count, phosphate and pH measurements, were obtained immediately after cell inoculation, at 24 h intervals for 5 days and 1 hr after U(VI) addition. Viable cell counts were determined by serially diluting 1 ml aliquots in sterile saline and plating onto NB agar. For determination of

phosphate and uranium concentrations, triplicate subsamples were removed and filtered (0.2 μm pore size, AcetatePlus; GE Water and Process Technologies). Phosphate concentrations were determined by spectrophotometry (Murphy and Riley, 1962). Dissolved uranium concentrations were measured by inductively coupled plasma-mass spectrometry (ICP-MS) with an Agilent 7500a Series system. Samples acidified with 2% nitric acid (trace metal grade, Fisher) were diluted in Nanopure water (Barnstead). Uranium standards and samples contained holmium and bismuth (SPEX certiPrep) as internal standards. Blanks, calibration check standards (95-105% recovery), and River Water Certified Reference Material for Trace Metals (SLRS-4, National Research Council Canada, Ottawa, Canada) containing internal standards were analyzed for quality controls. The analytical error on triplicate samples was $< 3\%$ RSD (Relative Standard Deviation).

4.6.8 Electron microscopy

Upon completion of *Rahnella* sp. Y9602 uranium biomineralization assays, 40 ml of culture was harvested by centrifugation (10,000g for 10 min), supernate was decanted and cell pellets were fixed in 1 ml of 2.5% glutaraldehyde in 0.1M cacodylate pH 7.3). Cells were embedded in SPURR resin. Following resin polymerization, embedded cells were cut into 100 nm thick sections with a Leica Ultracut S microtome. Note: the only source of electron density came from the uranium added during the biomineralization assays. The commonly used metals of osmium tetroxide, lead citrate, and uranyl acetate which provide electron density for transmission electron microscopy (TEM) were not added. A Hitachi H7600T TEM equipped with an Oxford INCA Energy 200 energy-

dispersive X-ray spectrometer was used to visualize the embedded cells and conduct elemental analysis of electron dense regions.

Analysis of *Rahnella* sp. Y9602 biomineralized uranium was also conducted with a Hitachi S3500N variable-pressure scanning electron microscope (VP-SEM) equipped with an Oxford INCA Energy 200 energy-dispersive X-ray spectrometer with an accelerating voltage of 20 kV and a chamber pressure of 20 Pa was used for all analyses. Upon completion of uranium biomineralization assays, 300 μ l of the uranium-associated cell pellet was placed on a glass fiber filter and visualized. Note: the uranium-associated cell pellet was not fixed or sputter coated with any heavy metals for visualization.

4.6.9 Data analysis

The Wilcoxon's signed ranks test was used analyzing the differences in reactive phosphate and soluble U(VI) concentrations. All statistical analyses were done in the software package SYSTAT 9.

4.7 Conclusions

Liquid cultures of metal-resistant ORFRC *Bacillus* and *Rahnella* spp. were shown to hydrolyze G3P which promoted the precipitation of 73% and 95% of U(VI), respectively, when supplemented at a final concentration of 200 μ M uranyl acetate. Similarly, anaerobic incubations of the *Rahnella* spp. supplemented with 200 μ M U(VI) were shown to hydrolyze G3P and promote the precipitation of 95% U(VI) as a uranyl phosphate mineral. Transmission electron microscopy and variable pressure

scanning electron microscopy coupled with an energy dispersive X-ray spectrometer indicated that the aerobically precipitated uranium also contained phosphorus and oxygen within the mineral phase. The precipitate was most likely an autunite-type mineral which was predicted in our thermodynamic modeling. This is the first study to demonstrate ORFRC *Bacillus* and *Rahnella* spp. can promote the mineralization of U(VI) as a uranyl phosphate mineral when grown in synthetic groundwater containing G3P as the sole carbon and phosphorus source.

4.8 Acknowledgements

This research was supported by the Office of Science (BER), U.S. Department of Energy Grant No. DE-FG02-04ER63906. We would like to thank Hong Yi (Emory University) and Dr. Joan Hudson (Clemson University) for advice and assistance with electron microscopy studies.

CHAPTER 5

BIOTIC AND ABIOTIC CATALYZED PHOSPHATE HYDROLYSIS

5.1 Overview

This chapter examines the contribution of organophosphate hydrolysis by microbial communities extant within the contaminated subsurface soils at the U.S. Department of Energy's (DOE) Oak Ridge Field Research Center (ORFRC) in Oak Ridge, TN. Additionally, we demonstrate inorganic phosphate hydrolysis via the soil analog hydrous ferric oxide (HFO). As a complementary approach to bioreduction of U(VI) to U(IV), microbially-mediated phosphoester and phosphoanhydride hydrolysis can promote the *in situ* sequestration of soluble U(VI) as an insoluble uranyl phosphate mineral. Utilization of high-density 16S rRNA microarrays were able to rapidly identify the microbial community that was enriched by glycerol-3-phosphate (G3P) supplementation. Furthermore, the abiotic hydrolysis of inorganic phosphate (i.e., sodium tripolyphosphate) demonstrates an added source of reactive orthophosphate for metal and radionuclide precipitation in the contaminated subsurface.

5.2 Summary

In this study, the microbial and chemical hydrolysis of G3P was examined in soil slurry incubations. Our previous studies indicated that *Bacillus* and *Rahnella* strains isolated from subsurface soils at the U.S. Department of Energy's (DOE) Oak Ridge Field Research Center (ORFRC) exhibited phosphatase activity sufficient to promote the biomineralization of up 95% uranium [U(VI)], at a final concentration of 200 μM .

Therefore, soil slurry incubations of two different ORFRC Area 3 subsurface samples were conducted to determine the potential organophosphate hydrolyzing capabilities of the *in situ* microbial community and to identify the bacterial taxa present following G3P supplementation. G3P hydrolysis was demonstrated over 10 day soil slurry incubations as up to 9.1 mM orthophosphate was measured in solution. Microbial diversity assessed by high-density 16S rRNA microarray analysis identified a total of 1084 taxa present within the two different soil samples used for the slurry incubations. Aerobic hydrous ferric oxide (HFO) slurries containing the *Rahnella* sp. Y9602 aerobically grown in synthetic groundwater (pH 7.0) amended with 3.33 mM sodium tripolyphosphate and 10 mM glycerol liberated 3.5 mM orthophosphate. Abiotic HFO slurries liberated 0.8 mM orthophosphate. This study provides the first evidence of robust microbial diversity present within ORFRC Area 3 subsurface soils capable of growing aerobically with G3P as the sole C and P source. Additionally, HFO studies demonstrate the contributions metal oxides may play in phosphoanhydride hydrolysis within the subsurface.

5.3 Introduction

The United States nuclear weapons research program maintained research and manufacturing facilities in 36 states which ultimately amounted to 120 unique sites requiring remediation of organic, metal and radionuclide contaminants (DOE, 1997). In 1997, the U.S. DOE estimated that 75 million cubic meters of contaminated soil and more than 470 billion gallons of contaminated groundwater required remediation (DOE, 1997). The scale of metal and radionuclide contamination within DOE contaminated

sites requires cost-effective strategies to address the mobility and fate of these contaminants within the deep subsurface. *In situ* sequestration of uranium via microbially mediated reductive precipitation and/or complexation are viewed as economically feasible strategies to address subsurface contamination. However, within the vadose zone changing redox potential does not support the stable formation of uraninite (i.e., U(IV) insoluble mineral). Therefore, approaches that employ phosphate complexation can effectively promote *in situ* sequestration of uranium as an insoluble uranyl phosphate mineral.

In addition to microbially mediated organophosphate and inorganic phosphate hydrolysis; metal oxides, actinides, and lanthanides have been shown to promote phosphoester and phosphoanhydride hydrolysis (Baldwin et al., 1995; Baldwin et al., 1996; Moss et al., 1997; Baldwin et al., 2001; Franklin, 2001; Inman et al., 2001; Yazzie et al., 2003; Torres et al., 2005). Thus, the contribution of phosphoester and phosphoanhydride hydrolysis within metal and radionuclide contaminated subsurface soils may provide an abiotic source of reactive orthophosphate for the sequestration of soluble uranium.

In this study, we examined the naturally occurring microbial communities present within contaminated ORFRC soils following organophosphate stimulation as a potential strategy for *in situ* metal and radionuclide sequestration. Additionally, we examined the phosphoanhydride hydrolyzing potential of HFO.

5.4 Results

5.4.1 Contaminated soil slurry incubations

During soil slurry incubations, G3P phosphoester hydrolysis as indicated by increasing orthophosphate concentrations was used as a proxy for microbial activity. Starting phosphate concentrations within the FWB120-06-00 and FWB120-08-00 soil slurries ranged from 17 μM to 22 μM (Fig. 5.1). At the 96 h time point, phosphate concentrations increased by a factor of two and continued to increase over the 240 h incubation. The end of the 240 h incubation demonstrated phosphate concentrations that ranged from 1320 μM to 9100 μM (Fig. 5.1).

Prior to soil slurry incubations, direct cell counts demonstrated that FWB120-06-00 and FWB120-08-00 soils contained $<10^4$ cells/g. Various DNA extraction methods were performed on soils prior to slurry incubations but failed to yield DNA concentrations above 1 ng/g soil (data not shown). Following soil slurry incubations, DNA extractions for FWB120-06-00 ranged from 186 ng to 977 ng per gram soil (wet weight) and FWB120-08-00 yielded DNA concentrations of 209 ng to 440 ng per gram soil (wet weight).

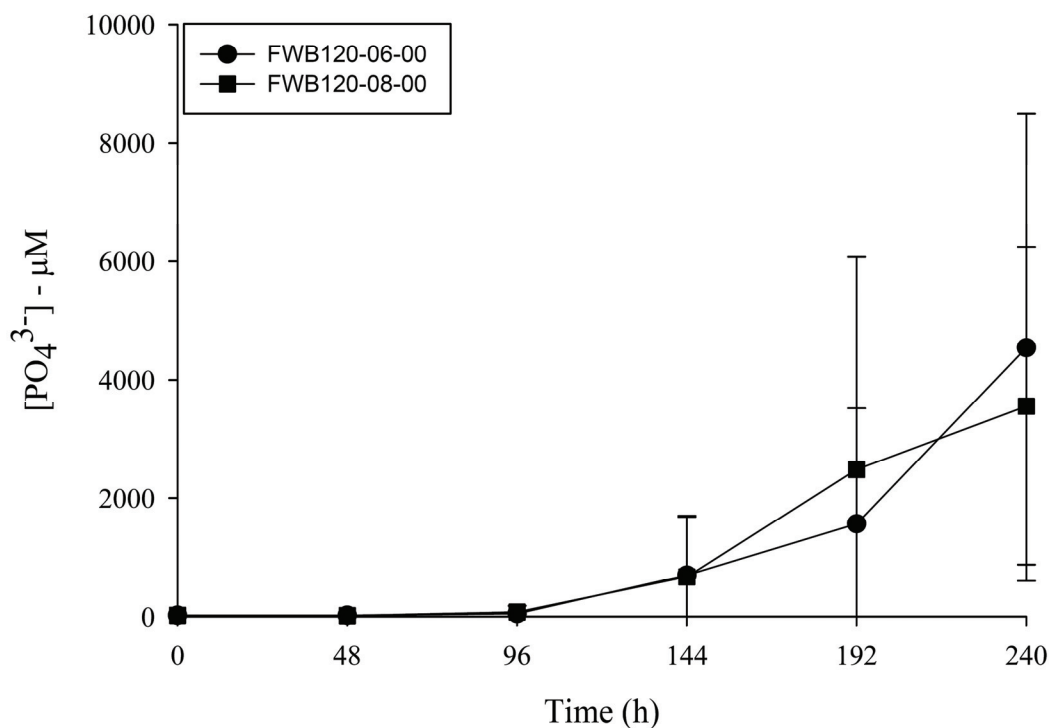


Figure 5.1 Area 3 soil slurry incubations of FWB120-06-00 (circles) and FWB120-08-00 (squares) core segments conducted in synthetic groundwater (pH 5.5) amended with 10 mM G3P (as sole C and P source). All incubations were performed under oxic conditions. Error bars denote standard deviation of triplicate experiments.

5.4.2 PhyloChip microarray analysis

Microarray analyses of FWB120-06-00 and FWB120-08-00 soil slurries demonstrated robust diversity as a total of 1084 unique phyla were detected (Fig. 5.2). Differences in diversity of phyla detected among replicate slurries from FWB120-06-00 and FWB120-08-00 soils ranged from 418 to 772 OTUs (Fig. 5.3). Comparisons of incubations by hierarchical cluster analysis further demonstrated differences in the diversity of phyla stimulated following G3P amended soil slurries (Fig. 5.4). The differences among soil slurries from each core segment prevented the clustering of bacterial phyla within replicate incubations.

5.4.3 Hydrous ferric oxide slurry incubations

Hydrous ferric oxide (HFO) slurry incubations conducted cell-free (abiotic) or inoculated with the acid phosphatase over-expressing *Rahnella* sp. Y9602 demonstrated hydrolysis of sodium tripolyphosphate (Fig. 5.5). For the cell-free and *Rahnella* sp. incubations, soluble phosphate concentrations were below detection at the beginning of the 120 h incubation. At the 48 h time point, the cell-free incubations on average accumulated 10 μM phosphate. Incubations containing the *Rahnella* sp. on average accumulated 11 μM phosphate at the 24 h time point. By the end of the 120 h incubation, cell-free and *Rahnella* sp. slurry incubations on average accumulated 830 μM and 3526 μM phosphate, respectively.

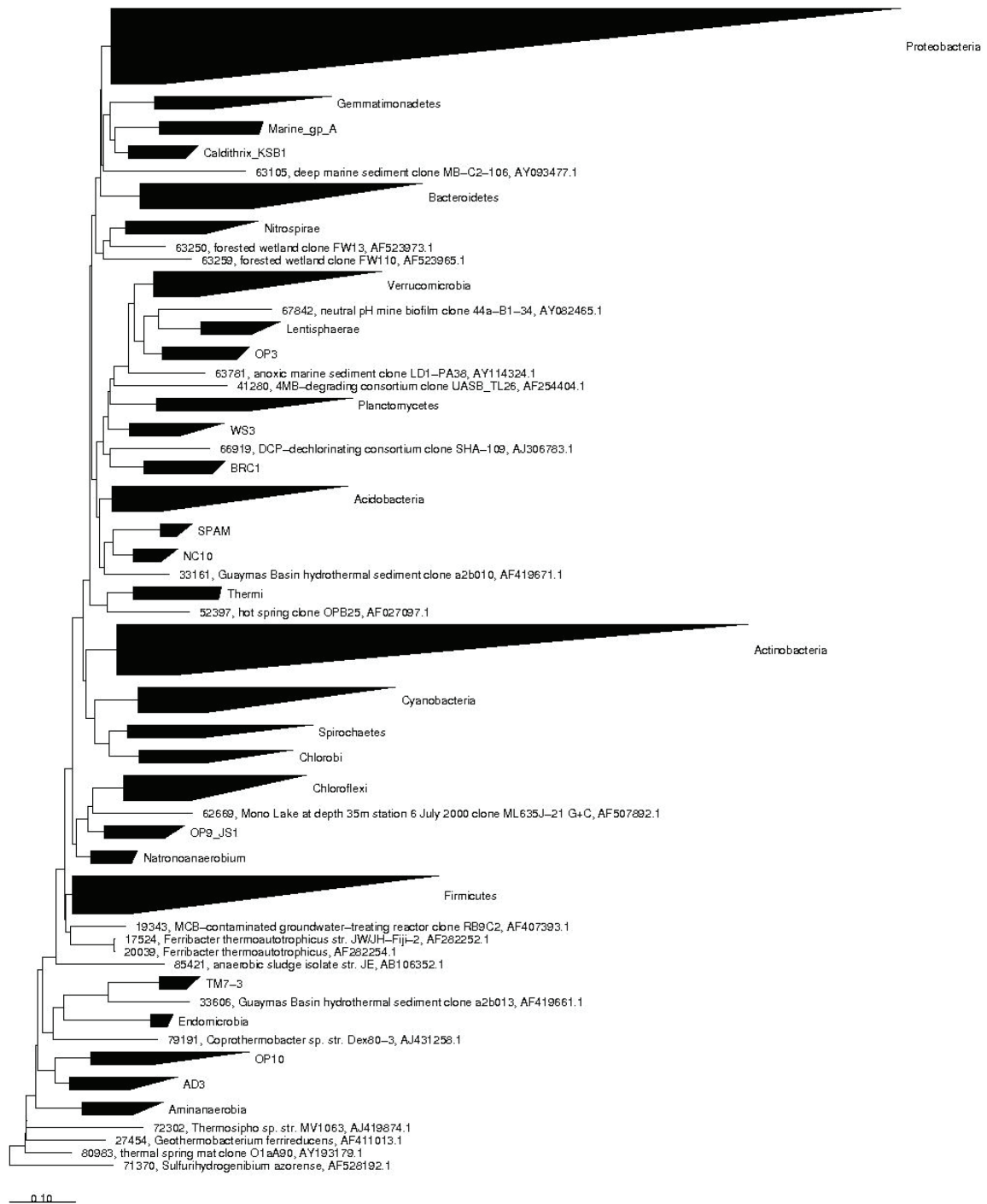


Figure 5.2 Neighbor-joining analysis of all 16S rRNA genes obtained from FWB120-06-00 and FWB120-08-00 soil slurry incubations. The greengenes database (<http://greengenes.lbl.gov/cgi-bin/nph-index.cgi>) was used to construct the phylogenetic tree that identifies all phyla detected via PhyloChip microarray analysis. The scale bar indicates 0.10 change per nucleotide.

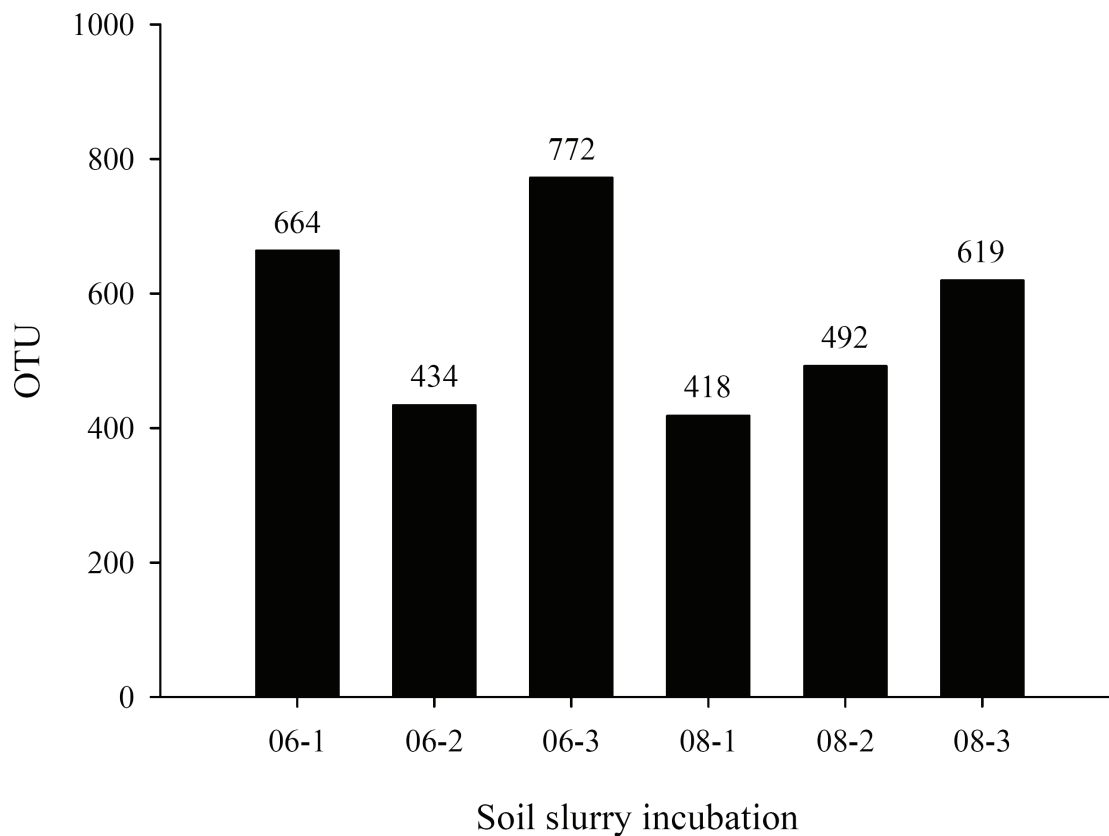


Figure 5.3 PhyloChip microarray analyses of microbial diversity present within replicate soil slurry incubations. Numbers above histogram bars indicate total phyla detected per incubation.

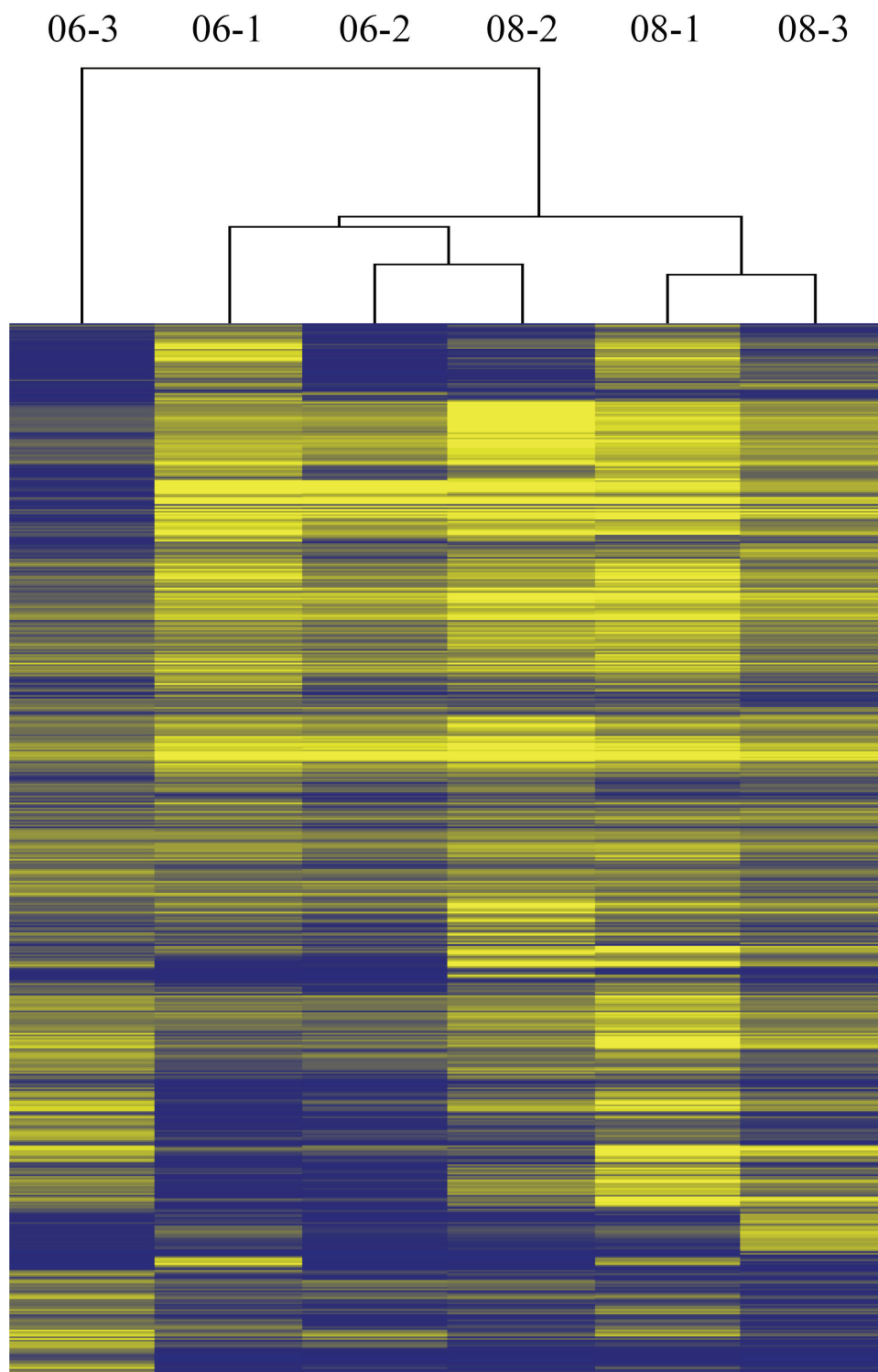


Figure 5.4 Hierarchical cluster analysis of soil slurry incubations. Soil slurries from each core segment were repeated in triplicate experiments and are represented as 06-1, 06-2, 06-3 for core FWB120-06-00 and 08-1, 08-2, 08-3 for FWB120-08-00.

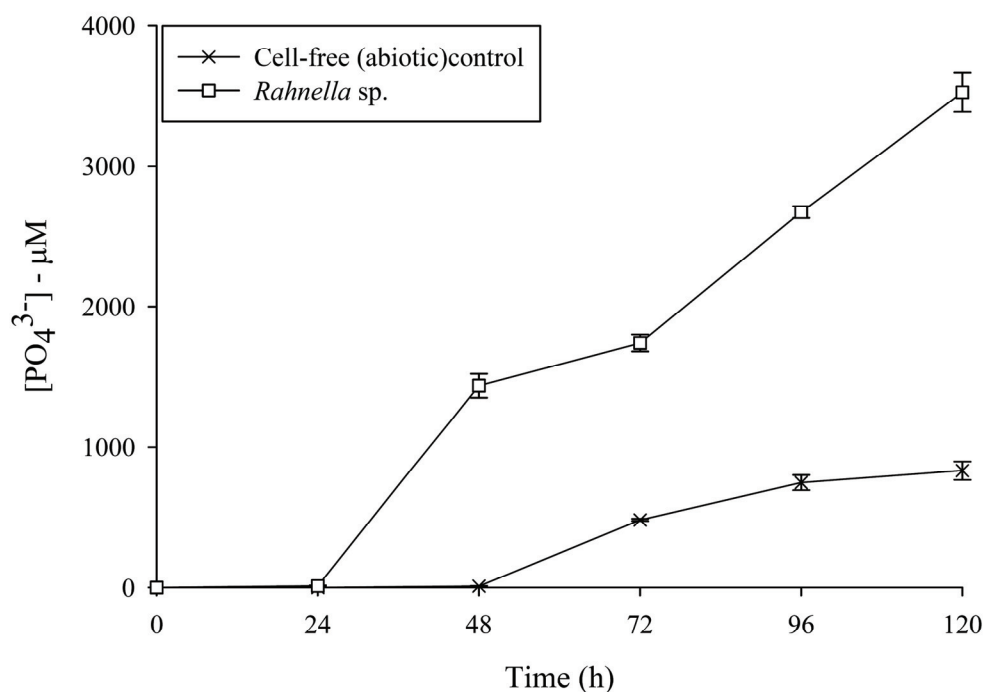


Figure 5.5 Hydrous ferric oxide slurry incubations. Incubations were conducted in synthetic groundwater (pH 7.0) amended with 10 mM glycerol (sole C source) 3.33 mM sodium tripolyphosphate (as sole P source). All incubations were performed under oxic conditions. Incubations containing the *Rahnella* sp. were inoculated to yield a final cell density of 10^7 cells/ml. Abiotic control incubations were cell-free. Error bars denote standard deviation of duplicate experiments.

5.5 Discussion

The remediation of metals and radionuclides present within subsurface soils and groundwater systems are current issues faced by the United States and Europe (Lloyd, 2005). Within the U.S. DOE legacy sites, radionuclide mobility [i.e., U(VI)] has spurred research in bioreduction as a remediation strategy (Lovley et al., 1991; Lovley and Phillips, 1992). Recent studies have demonstrated that reductively precipitated uranium can be reoxidized under anoxic conditions (Finneran et al., 2002; Senko et al., 2002;

Frazier et al., 2005; Wan et al., 2005). Therefore, complexation strategies that can sequester U(VI) irrespective of redox potential provide an alternative to bioreduction.

Phosphate-mediated biomineralization of U(VI) in pure culture studies have been demonstrated as a potentially effective approach for the remediation of uranium contaminated environments (Macaskie et al., 1992; Beazley et al., 2007; Martinez et al., 2007). Here we present culture independent data that demonstrates the presence of microbial taxa that are stimulated by the supplementation of 10 mM G3P in soil slurry incubations. Aerobic soil slurry incubations amended with G3P as the sole C and P source resulted in the hydrolysis of up to 91% of total amended organophosphate. Furthermore, G3P amended slurries stimulated 1084 phyla and demonstrated the robust microbial diversity extant within the contaminated ORFRC subsurface soils.

Analysis of aerobically incubated soil slurries via the high-density PhyloChip microarray provides a view of microbial diversity unmatched by traditional clone library studies from the ORFRC (Brodie et al., 2006; Akob et al., 2007). Additionally, our previous culture-dependent approach that identified *Arthrobacter*, *Bacillus*, and *Rahnella* spp. as the dominant isolates from Area 3 ORFRC subsurface soils further highlights the power of high-density 16S rRNA microarray diversity studies (Martinez et al., 2006b).

Although robust microbial diversity is demonstrated via the PhyloChip generated phylogeny (Fig. 5.2), replicate slurry incubations failed to cluster detected phyla through comparisons of species richness and hierarchical cluster analysis (Fig. 5.3 and Fig. 5.4). Furthermore, orthophosphate concentrations varying among replicate incubations and between the different soil samples indicate the heterogeneous distribution of bacterial phyla within the contaminated subsurface. Heterogeneity issues may be reflective of

subsurface groundwater flow fields that subject microbial communities to nutrients and/or elevated nitrate, metals, and radionuclides.

HFO slurry incubations provide insight into the abiotic contributions to phosphoester and phosphoanhydride hydrolysis within the subsurface. Within uncontaminated soils and aquatic environments, metal oxides in addition to microbial phosphatases have been shown to contribute to organophosphate and phosphoanhydride hydrolysis, thereby potentially influence phosphorus cycling (Baldwin et al., 1995; Baldwin et al., 1996; Baldwin et al., 2001; Inman et al., 2001). By examining the distribution of metal oxides in contaminated subsurface environments the abiotic control of metal and radionuclide solubility through metal oxide catalyzed phosphoester and phosphoanhydride hydrolysis can be defined. Furthermore, metal oxide phosphate hydrolysis can potentially provide a natural attenuation mechanism for the sequestration of metals and radionuclides.

The data obtained from these studies suggest a potential for high diversity in acid phosphatase gene expression during subsurface organophosphate stimulation of the microbial community. Thus, development non-specific acid phosphatase (NSAP) functional gene probes may provide a rapid method for assessing phosphatase gene expression and elucidate specific NSAP gene classes that may be optimal for *in situ* uranium phosphate complexation within the contaminated subsurface. Additionally, the influence of metal oxides within the subsurface may facilitate organophosphate hydrolysis of substrates (i.e., phytic acid) that may not be accessible to microorganisms which lack the appropriate phosphatases. The synergy between biotic and abiotic phosphate hydrolysis can not only promote the sequestration of metals and radionuclides

but can also provide a mechanism to neutralize low pH subsurface environments. This pH neutralization effect can further enhance microbial diversity by providing an environment for acid-sensitive species to thrive and potentially contribute to the sequestration of soluble uranium.

5.6 Experimental procedures

5.6.1 Sampling site

Contaminated soils were collected from the DOE Oak Ridge Field Research Center located in the Oak Ridge National Laboratory Reservation at Oak Ridge, Tenn. The contaminated soils are adjacent to the former S-3 waste ponds used during weapons production activities. The waste ponds and surrounding soils contain uranium (U) and other radionuclides, nitric acid, organics solvents and heavy metals (<http://www.esd.ornl.gov/orifrc/index.html>). In this study, contaminated subsurface soil samples were obtained from the saturated zone, where elevated U and nitrate concentrations have been reported (<http://www.esd.ornl.gov/orifrc/index.html>). Subsurface cores were collected on 18 July 2008 as previously described (Petrie et al., 2003). Subsurface samples were obtained from borehole FWB120 (Area 3; maximum depth, 23ft). These samples were handled aseptically and preserved under an argon atmosphere. Cores were shipped chilled overnight to Georgia Institute of Technology and processed for chemical and microbiological analysis immediately. Samples were incubated with deionized water to obtain pH and nitrate concentrations as previously described (Petrie et al., 2003). Subsurface core segments, FWB120-06-00 and FWB120-

08-00 had a pH of 3.7 and nitrate concentrations of 1.0 mM and 0.1 mM, respectively.

Uranium concentrations were obtained by the combining water extractable component to the acid extractable component. Acid extraction of uranium was performed by incubating 2g of soil (wet weight) in a 10 ml of 2% nitric acid for four days. Water and acid extracted uranium concentrations were analyzed via inductively coupled plasma-mass spectrometry (protocol described below). Combined water and acid extracted uranium concentrations of core segments FWB120-06-00 and FWB120-08-00 were 38 μ M and 23 μ M, respectively.

5.6.2 Hydrous ferric oxide synthesis

Hydrous ferric oxide (HFO) was synthesized as previously described (Schwertmann, 2000).

5.6.3 Subsurface strain and growth conditions

Nutrient broth (NB) agar (3 g beef extract, 5 g peptone, 15 g agar per liter) was used for the maintenance of the *Rahnella* sp. Y9602. Soil slurries utilizing ORFRC Area 3 soils were incubated in a final volume of 125 ml within a 500 ml erlenmeyer flask containing 2 g soil and pH buffered synthetic groundwater (SGW). SGW consisted of 50 mM MES (pH 5.5), 2 μ M FeSO₄, 5 μ M MnCl₂, 8 μ M Na₂MoO₄, 0.8 mM MgSO₄, 7.5 mM NaNO₃, 0.4 mM KCl, 7.5 mM KNO₃, 0.2mM Ca(NO₃)₂, and 10 mM glycerol-3-phosphate (Sigma) as the sole carbon and phosphorus source. Soil slurry incubations were repeated in triplicate experiments. Hydrous ferric oxide (HFO) slurry incubations were performed in a final volume of 125 ml within a 500 ml erlenmeyer flask containing

2 g HFO and pH 7.0 buffered SGW where 10 mM glycerol (Sigma) was the sole carbon source and 3.33 mM sodium tripolyphosphate (Sigma) was the sole phosphorus source. SGW pH 7.0 was buffered with 50 mM HEPES. HFO slurry incubations were repeated in duplicate experiments. All incubations were performed at 30°C. Slurries and liquid cultures were shaken at 200 rpm.

5.6.4 Phosphate measurement

For determination of phosphate and uranium concentrations, triplicate subsamples were removed and filtered (0.2 µm pore size, AcetatePlus; GE Water and Process Technologies). Phosphate concentrations were determined by spectrophotometry as previously described (Murphy and Riley, 1962).

5.6.5 Nucleic acid isolation, PCR amplification, and microarray analyses

Genomic DNA isolation for PCR amplification was performed by the bead mill homogenization method (Miller et al., 1999). The sequences of primers and PCR reaction conditions used for the amplification of *Bacteria*-specific 16S rDNA from isolated genomic DNA were followed as previously described (Brodie et al., 2006). Microarray hybridization and analysis of 16S rRNA PCR amplicons were conducted as previously described (Brodie et al., 2006).

5.7 Conclusions

Our studies indicate Area 3 ORFRC soils supplemented with 10 mM G3P liberated up to 9.1 mM orthophosphate during 10 day incubations. The resultant microbial diversity of ORFRC soil slurries determined by PhyloChip microarray analysis identified a total of 1084 taxa. HFO slurries inoculated with *Rahnella* sp. Y9602 yielded over 3.5 mM orthophosphate for incubations supplemented with 10 mM glycerol and 3.33 mM sodium tripolyphosphate as sole carbon and phosphorus sources, respectively. Abiotic (cell-free) HFO slurry incubations yielded over 0.8 mM orthophosphate over the same incubation period. These studies represent the first phylogenetic analysis of *in situ* microbial communities present within Area 3 ORFRC subsurface soils capable of contributing to uranium sequestration via organophosphate hydrolysis.

5.8 Acknowledgements

This research was supported by the Office of Science (BER), U.S. Department of Energy Grant No. DE-FG02-04ER63906. We would like to thank Justin Burns for assistance with the HFO studies and Dr. Cindy Wu for Phylochip analysis of Area 3 soil slurry studies.

CHAPTER 6

CONCLUSIONS

Global evidence for the microbially driven geochemical cycling of elements can be traced from over 3.5 billion years ago to present day (Schidlowski, 1988; Hedges and Keil, 1995; Shen et al., 2001; Newman and Banfield, 2002; Azam and Malfatti, 2007; Reeburgh, 2007). When considering the total estimate of prokaryotic cells extant within aquatic and terrestrial environments of $4\text{--}6 \times 10^{30}$, the scale of influence which microbial communities have becomes apparent (Whitman et al., 1998). Furthermore, the potential for rampant genetic exchange, estimated to be 10^{30} gene transfer events/day, in response to changing geochemical environments allows for microbial communities to continually adapt and sustain environmentally beneficial geochemical transformations including carbon sequestration and the cycling of essential and toxic metals (Heinemann and Roughan, 2000).

Microbial community analysis within mud volcano sediments demonstrates that methane and sulfate concentrations select for a microbial community structure that has been previously described in cold seep sediments and mud volcano sediments within the Barents Sea, Gulf of Mexico, Mediterranean Sea, and Pacific Ocean (Boetius et al., 2000; Michaelis et al., 2002; Mills et al., 2003; Niemann et al., 2006b). Specifically, the archaeal and bacterial 16S rRNA clone libraries were dominated by the *Euryarchaeota* and *Protoebacteria* phyla which carry out methanotrophic, sulfate-reducing, and sulfur-oxidizing metabolisms. Additionally, the comparison of RNA- and DNA-derived clone libraries suggested that methanotrophic ANME-2C clade archaeal species in low

abundance potentially have greater metabolic activity (on a per cell basis) when compared the ANME-2A clade at the 0-2cm sediment depth interval.

Culturable aerobic heterotrophic bacteria isolated from the metal and radionuclide ORFRC deep subsurface demonstrated low diversity as only *Arthrobacter*, *Bacillus*, and *Rahnella* spp. were isolated. Although low phylogenetic diversity was obtained through culture-dependent studies, the extent to which HGT has influenced these isolates is potentially vast as 20 % of a random subset of 50 metal resistant isolates demonstrated evidence for the transfer of P_{IB}-type ATPases. Additionally, the enhanced tolerance of *Bacillus* and *Rahnella* spp. to acid stress and soluble uranium oxidative stress relative to closely related type-strains suggest the ORFRC has selected for microbial communities with physiologies well adapted to such an environment.

The adaptations *Arthrobacter*, *Bacillus*, and *Rahnella* spp. have demonstrated to the low pH, high nitrate, and high uranium concentrations present within the ORFRC were further examined for potential use in the bioremediation of soluble uranium. Screening a subset of *Arthrobacter*, *Bacillus*, and *Rahnella* spp. for phosphatase activity indicated that only *Bacillus* and *Rahnella* spp. constitutively expressed NSAPs capable of hydrolyzing the organophosphate glycerol-3-phosphate (G3P). Biomineralization experiments utilizing pure cultures of *Bacillus* and *Rahnella* spp. growing in a simulated groundwater matrix with 10 mM G3P as the sole carbon and phosphorus source demonstrated the removal of 73% and 95% of soluble uranium, respectively. Interestingly, *Rahnella* spp. demonstrated a viable but non-culturable state following exposure to 200 μ M soluble uranium which was concomitant with a loss of phosphatase activity. Following a removal of >80% soluble uranium, culturability and phosphatase

activity of the ORFRC *Rahnella* spp. were restored. These data suggest that oxidative stress within the ORFRC subsurface may temporarily inhibit microbial activity but that biomineralization of uranium can promote the activity of extant microbial species by alleviating oxidative stress.

The majority of culture-dependent techniques fail to contribute to our understanding of the microbial diversity present in aquatic and terrestrial environments. Recent innovations in culture techniques have expanded the culturability of bacteria present aquatic and terrestrial environments. The use of techniques including low nutrient dilution to extinction, low nutrient gel encapsulation, and membrane diffusion chambers have yielded numerous *Acidobacteria*, *Actinobacteria*, *Bacteroidetes*, *Firmicutes*, *Proteobacteria*, *Spirochaete*, and *Verrucomicrobia* isolates (Connon and Giovannoni, 2002; Kaeberlein et al., 2002; Zengler et al., 2002; Bollmann et al., 2007). Although these methods yield viable cells, culturing can take up to 3 years for a small 200 µl volume of cells (Connon and Giovannoni, 2002).

Therefore, the need to rapidly access genomic DNA sequences and understand microbial community structure via culture-independent methods has spurred the development of current high-throughput DNA sequencing and high-density microarray technologies. The continued refinement of these technologies has contributed to the decrease in the cost per sample and thus allowing these technologies to become available to more researchers.

As an example application of these technologies, high-throughput DNA and protein sequence analysis have been utilized to describe the acid mine drainage (AMD) microbial community present within the Richmond Mine in Iron Mountain, California

(Tyson et al., 2004; Lo et al., 2007). Random shotgun sequencing of the uncultured microbial mats present within the AMD demonstrated the dominance of bacterial *Leptospirillum* sp. as well as archaeal *Ferroplasma* sp. Construction and analysis of the nearly completed genomes from AMD species allowed for the prediction of *Leptospirillum* and *Ferroplasma* spp. physiologies without a cultured representative as well as the influence of HGT within this environment. The benefits of high-throughput DNA sequencing may ultimately allow for the culturing of microorganisms which have been unculturable at one time. The comprehensive understanding of metabolic capabilities will aid in such culturing endeavours. Additionally, expanding the number of culturable microorganism can aid in the discovery of compounds with applications to biotechnology and industrial applications.

High-density microarrays, specifically the Affymetrix Phylochip, allow for the rapid and cost-effective analysis of archaeal and bacterial diversity at the subfamily level. The rapid assessment of microbial diversity is attained by the hybridization of 16S rDNA PCR amplicons to the high-density 25-mer oligo microarray which contains approximately 9,000 unique OTUs. The microbial community analysis of Area 2 ORFRC flowthrough columns permeated with 10.7 mM lactate at pH 7.2 for over 500 days was assessed to determine if shifts in community structure resulted in the reoxidation of bio-reduced uranium (Brodie et al., 2006). Although the metal reducing microbial community was maintained during the reoxidation of bio-reduced uranium and the electron acceptors responsible for uranium oxidation were not identified, this study demonstrated the enhanced sensitivity in determining microbial diversity when compared to traditional plasmid-based clone library construction. The great underestimation of

microbial diversity in the traditional plasmid-based clone libraries is demonstrated in this study. A total of 742 clones were gave rise to 63 unique OTUs in the traditional plasmid-based clone library compared to the 978 unique OTUs detected in the Phylochip analysis. The limitation of Phylochip diversity assessments is in the inability to obtain genus level sequences of the isolates that hybridized to the array but the speed and enhanced detection sensitivity demonstrate the strength of employing this technology.

6.1 Future directions

Issues relevant to sustaining an expanding human population on earth have become more evident with recent data indicating the magnitude by which anthropogenic activities have influenced global climate change and environmental pollution. In an effort to address such issues, a more comprehensive understanding of greenhouse gas influence on climate change as well as remediation strategies that can insure the supply of clean water and habitable land are essential. Thus, future microbial community structure and function studies within aquatic cold seep environments and metal-contaminated terrestrial subsurface systems can contribute to a greater understanding of *in situ* processes that promote carbon sequestration and influence the solubility of metals within subsurface soils and groundwater.

Currently, deep sea cold seep environments require long-term monitoring to better understand microbial community composition as well as studies that can address temporal and spatial changes in microbial community composition. The use of the previously described high throughput microarray technologies can provide more complete view of total microbial diversity as well as differentiate the metabolically active

prokaryotic fraction. Ongoing efforts to sequence the genomes of archaeal species that can anaerobically oxidize methane will further enhance our understanding of the dominant physiologies present in cold seeps. Additionally, a greater understanding of methane fluxes at depth originating from mud volcanoes and from destabilized methane hydrates are essential for accurately calculating deep sea contributions to the global methane budget.

Within the contaminated subsurface, changes in microbial activity can be driven by the percolation of rainwater. This migration of water will continually change the concentrations of oxygen, metals, oxyanions, nutrients, and ultimately microbial activity. As such, bioreduced and biomineralized chemical equilibria will be difficult to obtain. Therefore, to maintain steady state geochemical conditions that favor low solubility metals and radionuclides, a greater understanding of microbial community structure and metabolic responses to changes in nutrients and local geochemistry are required. Within subsurface environments similar to the ORFRC which are defined by low pH, high concentration of oxyanions, high concentrations of metal and radionuclides, and perturbations in redox potential via oxygenated rainwater do not support bioreduction strategies for radionuclide sequestration (Finneran et al., 2002; Senko et al., 2002; Frazier et al., 2005; Wan et al., 2005). Innovative bioremediation approaches that can neutralize the low pH groundwater and continuously deliver reactive phosphate are attractive alternatives to reductive precipitation. By employing a phosphate-mediated pH buffering system, soluble U(VI) can be sequestered as low solubility uranyl hydroxide and uranyl phosphate species. Unlike, uraninite mediated U-sequestration, U(VI) uranyl hydroxide and uranyl phosphate species are not prone to dissolution when changes in

redox potential are encountered in subsurface environments. Furthermore, thermodynamic modeling and recent anaerobic biomineralization assays utilizing our *Rahnella* sp. Y9602 indicate that uranium phosphate formation can occur in environments that support both aerobic and anaerobic respiration.

At present, the use of low nutrient dilution to extinction, low nutrient gel encapsulation, and membrane diffusion chambers to expand the culturable prokaryotic community in the Gulf of Mexico cold seep sediments as well as the ORFRC has yet to be conducted. By increasing the percentage of culturable prokaryotes in these unique extreme environments, a more comprehensive understanding of the microbial ecology as well as dominant physiologies can be attained. This culturing approach will allow investigators to be able to track changes in microbial community structure and the concomitant changes in physiologies when perturbations in environmental conditions (i.e., changes in nutrient availability, salinity, oxidants, etc.) are observed. Our current PhyloChip microarray analysis of G3P supplemented ORFRC soil slurries has provided valuable information regarding the diversity microbial taxa and the potential diversity of physiologies. By employing this approach with different growth substrates, optimal stimulation of microbial species that can promote metal and radionuclide sequestration can be ascertained. The application of innovative culturing techniques as well as high density microarray studies can be applied to microbial ecology studies in varying environments and undoubtedly enhance our understanding of microbial community dynamics.

REFERENCES

- Abe, F., and Horikoshi, K. (1998) Analysis of intracellular pH in the yeast *Saccharomyces cerevisiae* under elevated hydrostatic pressure: a study in baro- (piezo-) physiology. *Extremophiles* **2**: 223-228.
- Abe, F., Kato, C., and Horikoshi, K. (1999) Pressure-regulated metabolism in microorganisms. *Trends Microbiol* **7**: 447-453.
- Adams, M.W.W. (1993) Enzymes and proteins from organisms that grow near and above 100° C. *Annu Rev Microbiol* **47**: 627-658.
- Adcock, P.W., and Saint, C.P. (2001) Rapid confirmation of *Clostridium perfringens* by using chromogenic and fluorogenic substrates. *Appl Environ Microbiol* **67**: 4382-4384.
- Ahmad, A., Barry, J.P., and Nelson, D.C. (1999) Phylogenetic affinity of a wide, vacuolate, nitrate- accumulating *Beggiatoa* sp. from Monterey Canyon, California, with *Thioploca* spp. *Appl Environ Microbiol* **65**: 270-277.
- Akob, D.M., Mills, H.J., and Kostka, J.E. (2007) Metabolically active microbial communities in uranium-contaminated subsurface sediments. *FEMS Microbiol Ecol* **59**: 95-107.
- Alm, E.W., and Stahl, D.A. (2000) Critical factors influencing the recovery and integrity of rRNA extracted from environmental samples: use of an optimized protocol to measure depth-related biomass distribution in freshwater sediments. *J Microbiol Methods* **40**: 153-162.
- Altschul, S.F., Madden, T.L., Schaffer, A.A., Zhang, J.H., Zhang, Z., Miller, W., and Lipman, D.J. (1997) Gapped BLAST and PSI-BLAST: a new generation of protein database search programs. *Nucleic Acids Res* **25**: 3389-3402.
- Amy, P.S., Haldeman, D.L. (1997) Denizens of the deep. In *The microbiology of the deep terrestrial subsurface*. Amy, P.S., Haldeman, D.L. (ed). Boca Raton, FL: Lewis Publishers.
- Anderson, R.T., Vrionis, H.A., Ortiz-Bernad, I., Resch, C.T., Long, P.E., Dayvault, R. et al. (2003) Stimulating the *in situ* activity of *Geobacter* species to remove uranium from the groundwater of a uranium-contaminated aquifer. *Appl Environ Microbiol* **69**: 5884-5891.

- Appukuttan, D., Rao, A.S., and Apte, S.K. (2006) Engineering of *Deinococcus radiodurans* R1 for bioprecipitation of uranium from dilute nuclear waste. *Appl Environ Microbiol* **72**: 7873-7878.
- Arey, J.S., Seaman, J.C., and Bertsch, P.M. (1999) Immobilization of uranium in contaminated sediments by hydroxyapatite addition. *Environ Sci Technol* **33**: 337-342.
- Atlas, R.M.a.B., R. (1993) Microbial ecology: historical development. In *Microbial ecology: fundamentals and applications*. Brady, E.B. (ed). Redwood City, Ca: The Benjamin/Cummings Publishing Company.
- Axelsen, K.B., and Palmgren, M.G. (1998) Evolution of substrate specificities in the P-type ATPase superfamily. *J Mol Evol* **46**: 84-101.
- Axelsen, K.B., and Palmgren, M.G. (2001) Inventory of the superfamily of P-type ion pumps in *Arabidopsis*. *Plant Physiol* **126**: 696-706.
- Azam, F., and Malfatti, F. (2007) Microbial structuring of marine ecosystems. *Nat Rev Microbiol* **5**: 782-791.
- Baker-Austin, C., and Dopson, M. (2007) Life in acid: pH homeostasis in acidophiles. *Trends Microbiol* **15**: 165-171.
- Baker-Austin, C., Wright, M.S., Stepanauskas, R., and McArthur, J.V. (2006) Co-selection of antibiotic and metal resistance. *Trends Microbiol* **14**: 176-182.
- Baker, G.C., Smith, J.J., and Cowan, D.A. (2003) Review and re-analysis of domain-specific 16S primers. *J Microbiol Methods* **55**: 541-555.
- Baldwin, D.S., Beattie, J.K., and Jones, D.R. (1996) Hydrolysis of an organic phosphorus compound by iron-oxide impregnated filter papers. *Water Res* **30**: 1123-1126.
- Baldwin, D.S., Beattie, A.K., and Coleman, L.M. (2001) Hydrolysis of an organophosphate ester by manganese dioxide. *Environ Sci Technol* **35**: 713-716.
- Baldwin, D.S., Beattie, J.K., Coleman, L.M., and Jones, D.R. (1995) Phosphate ester hydrolysis facilitated by mineral phases. *Environ Sci Technol* **29**: 1706-1709.
- Banaszak, J.E., Rittmann, B.E., and Reed, D.T. (1999) Subsurface interactions of actinide species and microorganisms: Implications for the bioremediation of actinide-organic mixtures. *JRNC* **241**: 385-435.

- Banfield, J.F., Welch, S.A., Zhang, H.Z., Ebert, T.T., and Penn, R.L. (2000) Aggregation-based crystal growth and microstructure development in natural iron oxyhydroxide biomineralization products. *Science* **289**: 751-754.
- Barkay, T., and Schaefer, J. (2001) Metal and radionuclide bioremediation: issues, considerations and potentials. *Curr Opin Microbiol* **4**: 318-323.
- Barkay, T., Miller, S.M., and Summers, A.O. (2003) Bacterial mercury resistance from atoms to ecosystems. *FEMS Microbiol Rev* **27**: 355-384.
- Barlow, L.R.a.P., J.C. (2005) Suspensions to solutions: Characterizing contaminated land. In *Bioremediation: Applied microbial solutions for real-world environmental cleanup*. Atlas, R.M.a.P., J. (ed). Washington, DC: ASM Press, pp. 49-85.
- Basnakova, G., and Macaskie, L.E. (2001) Microbially-enhanced chemisorption of Ni^{2+} ions into biologically-synthesised hydrogen uranyl phosphate (HUP) and selective recovery of concentrated Ni^{2+} using citrate or chloride ion. *Biotechnol Lett* **23**: 67-70.
- Basnakova, G., Stephens, E.R., Thaller, M.C., Rossolini, G.M., and Macaskie, L.E. (1998) The use of *Escherichia coli* bearing a *phoN* gene for the removal of uranium and nickel from aqueous flows. *Appl Microbiol Biotechnol* **50**: 266-272.
- Beaber, J.W., Hochhut, B., and Waldor, M.K. (2004) SOS response promotes horizontal dissemination of antibiotic resistance genes. *Nature* **427**: 72-74.
- Beales, N. (2004) Adaptation of microorganisms to cold temperatures, weak acid preservatives, low pH, and osmotic stress: A review. *Compr Rev Food Sci Food Saf* **3**: 1-20.
- Beazley, M.J., Martinez, R.J., Sobecky, P.A., and Taillefert, M. (2007) Uranium biomineralization as a result of bacterial phosphatase activity: Insights from bacterial isolates from a contaminated subsurface. *Environ Sci Technol* **41**: 5701-5707.
- Becerra, A., Delaye, L., Islas, S., and Lazcano, A. (2007) The very early stages of biological evolution and the nature of the last common ancestor of the three major cell domains. *Annu Rev Ecol, Evol Syst* **38**: 361-379.
- Beiko, R.G., Harlow, T.J., and Ragan, M.A. (2005) Highways of gene sharing in prokaryotes. *Proc Natl Acad Sci U S A* **102**: 14332-14337.

- Benlloch, S., Lopez-Lopez, A., Casamayor, E.O., Ovreas, L., Goddard, V., Daae, F.L. et al. (2002) Prokaryotic genetic diversity throughout the salinity gradient of a coastal solar saltern. *Environ Microbiol* **4**: 349-360.
- Benyehuda, G., Coombs, J., Ward, P.L., Balkwill, D., and Barkay, T. (2003) Metal resistance among aerobic chemoheterotrophic bacteria from the deep terrestrial subsurface. *Can J Microbiol* **49**: 151-156.
- Berlutti, F., Casalino, M., Zagaglia, C., Fradiani, P.A., Visca, P., and Nicoletti, M. (1998) Expression of the virulence plasmid-carried apyrase gene (*apy*) of enteroinvasive *Escherichia coli* and *Shigella flexneri* is under the control of H-NS and the VirF and VirB regulatory cascade. *Infect Immun* **66**: 4957-4964.
- Bloch, E., Rachel, R., Burggraf, S., Hafenbradl, D., Jannasch, H.W., and Stetter, K.O. (1997) *Pyrolobus fumarii*, gen. and sp. nov., represents a novel group of archaea, extending the upper temperature limit for life to 113 degrees C. *Extremophiles* **1**: 14-21.
- Boetius, A., Ravensschlag, K., Schubert, C.J., Rickert, D., Widdel, F., Gieseke, A. et al. (2000) A marine microbial consortium apparently mediating anaerobic oxidation of methane. *Nature* **407**: 623-626.
- BoivinJahns, V., Ruimy, R., Bianchi, A., Daumas, S., and Christen, R. (1996) Bacterial diversity in a deep-subsurface clay environment. *Appl Environ Microbiol* **62**: 3405-3412.
- Bollmann, A., Lewis, K., and Epstein, S.S. (2007) Incubation of environmental samples in a diffusion chamber increases the diversity of recovered isolates. *Appl Environ Microbiol* **73**: 6386-6390.
- Bostick, W.D., Stevenson, R.J., Jarabek, R.J., and Conca, J.L. (1999) Use of apatite and bone char for the removal of soluble radionuclides in authentic and simulated DOE groundwater (Reprinted from Advances in Environmental Research, vol 3, pg 488-498, 2000). *Adv Environ Res* **3**.
- Boswell, C.D., Dick, R.E., Eccles, H., and Macaskie, L.E. (2001) Phosphate uptake and release by *Acinetobacter johnsonii* in continuous culture and coupling of phosphate release to heavy metal accumulation. *J Ind Microbiol Biotechnol* **26**: 333-340.
- Boswell, C.D., Dick, R.E., Macaskie, L.E. (1999) The effect of heavy metals and other environmental conditions on the anaerobic phosphate metabolism of *Acinetobacter johnsonii*. *Microbiology* **145**: 1711-1720.

- Bozal, N., Tudela, E., RosselloMora, R., Lalucat, J., and Guinea, J. (1997) *Pseudoalteromonas antarctica* sp. nov., isolated from an Antarctic coastal environment. *Int J Syst Bacteriol* **47**: 345-351.
- Brodie, E.L., DeSantis, T.Z., Joyner, D.C., Baek, S.M., Larsen, J.T., Andersen, G.L. et al. (2006) Application of a high-density oligonucleotide microarray approach to study bacterial population dynamics during uranium reduction and reoxidation. *Appl Environ Microbiol* **72**: 6288-6298.
- Brook, E.J., Sowers, T., and Orchardo, J. (1996) Rapid variations in atmospheric methane concentration during the past 110,000 years. *Science* **273**: 1087-1091.
- Brooks, J.M., Kennicutt, M.C., Fisher, C.R., Macko, S.A., Cole, K., Childress, J.J. et al. (1987) Deep-sea hydrocarbon seep communities - evidence for energy and nutritional carbon sources. *Science* **238**: 1138-1142.
- Brooks, S. (2001) Waste Characteristics of the Former S-3 Ponds and Outline of Uranium Chemistry Relevant to NABIR Field Research Center Studies.
- Bruno, J., Depablo, J., Duro, L., and Figuerola, E. (1995) Experimental study and modeling of the U(VI)-Fe(OH)₃ surface precipitation coprecipitation equilibria. *Geochim Cosmochim Acta* **59**: 4113-4123.
- Buck, E.C., Brown, N.R., and Dietz, N.L. (1996) Contaminant uranium phases and leaching at the Fernald site in Ohio. *Environ Sci Technol* **30**: 81-88.
- Buffett, B.A. (2000) Clathrate hydrates. *Annu Rev Earth Planet Sci* **28**: 477-507.
- Busenlehner, L.S., Pennella, M.A., and Giedroc, D.P. (2003) The SmtB/ArsR family of metalloregulatory transcriptional repressors: structural insights into prokaryotic metal resistance. *FEMS Microbiol Rev* **27**: 131-143.
- Butler, B.J., McCallum, K.L., and Inniss, W.E. (1989) Characterization of *Aquaspirillum arcticum* sp. nov., a new psychrophilic bacterium. *Syst Appl Microbiol* **12**: 263-266.
- Calderone, V., Forleo, C., Benvenuti, M., Thaller, M.C., Rossolini, G.M., and Mangani, S. (2004) The first structure of a bacterial class B acid phosphatase reveals further structural heterogeneity among phosphatases of the haloacid dehalogenase fold. *J Mol Biol* **335**: 761-773.

- Campbell, K.A. (2006) Hydrocarbon seep and hydrothermal vent paleoenvironments and paleontology: Past developments and future research directions. *Palaeogeogr, Palaeoclimatol, Palaeoecol* **232**: 362-407.
- Canchaya, C., Fournous, G., Chibani-Chennoufi, S., Dillmann, M.L., and Brussow, H. (2003) Phage as agents of lateral gene transfer. *Curr Opin Microbiol* **6**: 417-424.
- Cantafio, A.W., Hagen, K.D., Lewis, G.E., Bledsoe, T.L., Nunan, K.M., and Macy, J.M. (1996) Pilot-scale selenium bioremediation of San Joaquin drainage water with *Thauera selenatis*. *Appl Environ Microbiol* **62**: 3298-3303.
- Carlin, A., Shi, W., Dey, S., Rosen, B.P. (1995) The *ars* operon of *Escherichia coli* confers arsenical and antimonial resistance. *J Bacteriol* **177**: 981-986.
- Cavicchioli, R., Thomas, T., and Curmi, P.M.G. (2000) Cold stress response in Archaea. *Extremophiles* **4**: 321-331.
- Chanal, A., Chapon, V., Benzerara, K., Barakat, M., Christen, R., Achouak, W. et al. (2006) The desert of Tataouine: an extreme environment that hosts a wide diversity of microorganisms and radiotolerant bacteria. *Environ Microbiol* **8**: 514-525.
- Chapelle, F.H., and Lovley, D.R. (1990) Rates of microbial-metabolism in deep coastal-plain aquifers. *Appl Environ Microbiol* **56**: 1865-1874.
- Choi, I.G., and Kim, S.H. (2007) Global extent of horizontal gene transfer. *Proc Natl Acad Sci U S A* **104**: 4489-4494.
- Claus, D., and R. C. W. Berkeley (1986) Genus *Bacillus* Cohn, 174^{AL}. In *Bergey's manual of systematic bacteriology*, vol. 2. P. H. A. Sneath, N.S.M., M. E. Sharpe, and J. G. Holt (ed). Baltimore, Md.: Williams & Wilkins.
- Cleaves, H.J., and Chalmers, J.H. (2004) Extremophiles may be irrelevant to the origin of life. *Astrobiology* **4**: 1-9.
- Comeau, A.M., Chan, A.M., and Suttle, C.A. (2006) Genetic richness of vibriophages isolated in a coastal environment. *Environ Microbiol* **8**: 1164-1176.
- Connon, S.A., and Giovannoni, S.J. (2002) High-throughput methods for culturing microorganisms in very-low-nutrient media yield diverse new marine isolates. *Appl Environ Microbiol* **68**: 3878-3885.

- Coombs, J.M., and Barkay, T. (2004) Molecular evidence for the evolution of metal homeostasis genes by lateral gene transfer in bacteria from the deep terrestrial subsurface. *Appl Environ Microbiol* **70**: 1698-1707.
- Coombs, J.M., and Barkay, T. (2005) New findings on evolution of metal homeostasis genes: Evidence from comparative genome analysis of *Bacteria* and *Archaea*. *Appl Environ Microbiol* **71**: 7083-7091.
- Cox, M.M., and Battista, J.R. (2005) *Deinococcus radiodurans* - The consummate survivor. *Nat Rev Microbiol* **3**: 882-892.
- Craft, E.S., Abu-Qare, A.W., Flaherty, M.M., Garofolo, M.C., Rincavage, H.L., and Abou-Donia, M.B. (2004) Depleted and natural uranium: chemistry and toxicological effects. *J Toxicol Environ Health, Pt B Crit Rev* **7**: 297-317.
- Daly, M.J., Gaidamakova, E.K., Matrosova, V.Y., Vasilenko, A., Zhai, M., Venkateswaran, A. et al. (2004) Accumulation of Mn(II) in *Deinococcus radiodurans* facilitates gamma-radiation resistance. *Science* **306**: 1025-1028.
- DeLong, E.F. (1992) Archaea in coastal marine environments. *Proc Natl Acad Sci U S A* **89**: 5685-5689.
- Devos, D., and Valencia, A. (2001) Intrinsic errors in genome annotation. *Trends Genet* **17**: 429-431.
- Di Giulio, M. (2003) The universal ancestor and the ancestor of bacteria were hyperthermophiles. *J Mol Evol* **57**: 721-730.
- Dickens, G.R., Oneil, J.R., Rea, D.K., and Owen, R.M. (1995) Dissociation of oceanic methane hydrate as a cause of the carbon-isotope excursion at the end of the Paleocene. *Paleoceanography* **10**: 965-971.
- Dimitrov, L.I. (2002) Mud volcanoes-the most important pathway for degassing deeply buried sediments. *Earth-Sci Rev* **59**: 49-76.
- DOE (1995) Estimating the cold war mortgage: The 1995 baseline environmental management report, DOE/EM-0230. In. Energy, U.S.D.o. (ed). Washington, DC: U.S. Department of Energy.
- DOE (1997) Linking Legacies, DOE/EM-319. In. Energy, U.S.D.o. (ed). Washington, DC.

- DOE (2000) Status report on paths to closure. In. Energy, U.S.D.o. (ed). Washington, DC.
- DOE (2006). U.S. Department of Energy Office of Science. URL <http://www.lbl.gov/ERSP/index.html>
- DOE (2007) U.S. Department of Energy Highlights Fiscal Year 2007. In. Energy, U.S.D.o. (ed). Washington, DC.
- Doolittle, W.F. (1999) Phylogenetic classification and the universal tree. *Science* **284**: 2124-2128.
- Dykhuizen, R.S., Frazer, R., Duncan, C., Smith, C.C., Golden, M., Benjamin, N., and Leifert, C. (1996) Antimicrobial effect of acidified nitrite on gut pathogens: Importance of dietary nitrate in host defense. *Antimicrob Agents Chemother* **40**: 1422-1425.
- Edwards, R.A., and Rohwer, F. (2005) Viral metagenomics. *Nat Rev Microbiol* **3**: 504-510.
- Ehrlich, H.L. (1998) Geomicrobiology: its significance for geology. *Earth-Sci Rev* **45**: 45-60.
- Eichhubl, P., Greene, H.G., Naehr, T., and Maher, N. (2000) Structural control of fluid flow: offshore fluid seepage in the Santa Barbara Basin, California. *Journal of Geochemical Exploration* **69**: 545-549.
- Elias, D.A., Krumholz, L.R., Wong, D., Long, P.E., and Suflita, J.M. (2003) Characterization of microbial activities and U reduction in a shallow aquifer contaminated by uranium mill tailings. *Microb Ecol* **46**: 83-91.
- Etiope, G., and Milkov, A.V. (2004) A new estimate of global methane flux from onshore and shallow submarine mud volcanoes to the atmosphere. *Environ Geol* **46**: 997-1002.
- Felsenstein, J. (2006). PHYLIP (Phylogeny Inference Package) version 3.66. URL <http://evolution.genetics.washington.edu/phylip.html>
- Finneran, K.T., Housewright, M.E., and Lovley, D.R. (2002) Multiple influences of nitrate on uranium solubility during bioremediation of uranium-contaminated subsurface sediments. *Environ Microbiol* **4**: 510-516.

- Franklin, S.J. (2001) Lanthanide-mediated DNA hydrolysis. *Curr Opin Chem Biol* **5**: 201-208.
- Frazier, S.W., Kretzschmar, R., and Kraemer, S.M. (2005) Bacterial siderophores promote dissolution of UO₂ under reducing conditions. *Environ Sci Technol* **39**: 5709-5715.
- Fredrickson, J.K., Zachara, J.M., Kennedy, D.W., Duff, M.C., Gorby, Y.A., Li, S.M.W., and Krupka, K.M. (2000) Reduction of U(VI) in goethite (alpha-FeOOH) suspensions by a dissimilatory metal-reducing bacterium. *Geochim Cosmochim Acta* **64**: 3085-3098.
- Fredrickson, J.K., McKinley, J.P., Nierzwickibauer, S.A., White, D.C., Ringelberg, D.B., Rawson, S.A. et al. (1995) Microbial community structure and biogeochemistry of Miocene subsurface sediments - Implications for long-term microbial survival. *Mol Ecol* **4**: 619-626.
- Fredrickson, J.K., Zachara, J.M., Balkwill, D.L., Kennedy, D., Li, S.M.W., Kostandarithes, H.M. et al. (2004) Geomicrobiology of high-level nuclear waste-contaminated vadose sediments at the Hanford Site, Washington State. *Appl Environ Microbiol* **70**: 4230-4241.
- Freytag, J.K., Girguis, P.R., Bergquist, D.C., Andras, J.P., Childress, J.J., and Fisher, C.R. (2001) A paradox resolved: Sulfide acquisition by roots of seep tubeworms sustains net chemoautotrophy. *Proc Natl Acad Sci U S A* **98**: 13408-13413.
- Frost, L.S., Leplae, R., Summers, A.O., and Toussaint, A. (2005) Mobile genetic elements: The agents of open source evolution. *Nat Rev Microbiol* **3**: 722-732.
- Gadd, G.M. (2000) Bioremediation potential of microbial mechanisms of metal mobilization and immobilization. *Curr Opin Biotechnol* **11**: 271-279.
- Gadd, G.M. (2004) Microbial influence on metal mobility and application for bioremediation. *Geoderma* **122**: 109-119.
- Galtier, N., Tourasse, N., and Gouy, M. (1999) A nonhyperthermophilic common ancestor to extant life forms. *Science* **283**: 220-221.
- Garnova, E.S., Zhilina, T.N., Tourova, T.P., Kostrikina, N.A., and Zavarzin, G.A. (2004) Anaerobic, alkaliphilic, saccharolytic bacterium *Alkalibacter saccharofermentans* gen. nov., sp. nov. from a soda lake in the Transbaikal region of Russia. *Extremophiles* **8**: 309-316.

- Gavrilescu, M. (2004) Removal of heavy metals from the environment by biosorption. *Eng Life Sci* **4**: 219-232.
- Ghosal, D., Omelchenko, M.V., Gaidamakova, E.K., Matrosova, V.Y., Vasilenko, A., Venkateswaran, A. et al. (2005) How radiation kills cells: Survival of *Deinococcus radiodurans* and *Shewanella oneidensis* under oxidative stress. *FEMS Microbiol Rev* **29**: 361-375.
- Golyshina, O.V., Pivovarova, T.A., Karavaiko, G.I., Kondrat'eva, T.F., Moore, E.R.B., Abraham, W.R. et al. (2000) *Ferroplasma acidiphilum* gen. nov., sp. nov., an acidophilic, autotrophic, ferrous-iron-oxidizing, cell-wall-lacking, mesophilic member of the *Ferroplasmaceae* fam. nov., comprising a distinct lineage of the *Archaea*. *Int J Syst Evol Microbiol* **50**: 997-1006.
- Gonzalez, J.M., Sheckells, D., Viebahn, M., Krupatkina, D., Borges, K.M., and Robb, F.T. (1999) *Thermococcus waiotapuensis* sp. nov., an extremely thermophilic archaeon isolated from a freshwater hot spring. *Arch Microbiol* **172**: 95-101.
- Girguis, P.R., Orphan, V.J., Hallam, S.J., and DeLong, E.F. (2003) Growth and methane oxidation rates of anaerobic methanotrophic archaea in a continuous-flow bioreactor. *Appl Environ Microbiol* **69**: 5472-5482.
- Gogarten, J.P., and Townsend, J.P. (2005) Horizontal gene transfer, genome innovation and evolution. *Nat Rev Microbiol* **3**: 679-687.
- Green, B.A., Farley, J.E., Quinn, T., Deich, R.A., and Zlotnick, G.W. (1991) The e (P4) outer membrane protein of *Haemophilus influenzae*: biologic activity of anti-e serum and cloning and sequencing of the structural gene. *Infect Immun* **59**: 3191-3198.
- Guillaumont, R., Fanghänel, T., Fuger, J., and Grenthe, I., Neck, V., Palmer, D. A., Rand, M. H. (2003) *Chemical Thermodynamics 5: Update on the Chemical Thermodynamics of Uranium, Neptunium, Plutonium, Americium and Technetium*. Amsterdam: Elsevier.
- Haas, J.R., Dichristina, T.J., and Wade, R. (2001) Thermodynamics of U(VI) sorption onto *Shewanella putrefaciens*. *Chem Geol* **180**: 33-54.
- Hall, T.A. (1999) BioEdit: a user-friendly biological sequence alignment editor and analysis program for Windows 95/98/NT. *Nucl Acids Symp Ser* **41**: 95-98.
- Haney, C.J., Grass, G., Franke, S., and Rensing, C. (2005) New developments in the understanding of the cation diffusion facilitator family. *J Ind Microbiol Biotechnol* **32**: 215-226.

- Harrison, J.J., Ceri, H., and Turner, R.J. (2007) Multimetal resistance and tolerance in microbial biofilms. *Nat Rev Microbiol* **5**: 928-938.
- Heck, K.L., Belle, G.v., and Simberloff, D. (1975) Explicit calculation of the rarefaction diversity measurement and the determination of sufficient sample size. *Ecology* **56**: 1459-1461.
- Hedges, J.I., and Keil, R.G. (1995) Sedimentary organic matter preservation: an assessment and speculative synthesis. *Mar Chem* **49**: 81-115.
- Hein, J.R., Normark, W.R., McIntyre, B.R., Lorenson, T.D., and Powell, C.L. (2006) Methanogenic calcite, C-13-depleted bivalve shells, and gas hydrate from a mud volcano offshore southern California. *Geology* **34**: 109-112.
- Heinemann, J.A., and Roughan, P.D. (2000) New hypotheses on the material nature of horizontally mobile genes. *Ann N Y Acad Sci* **906**: 169-186.
- Hinrichs, K.U., Hayes, J.M., Sylva, S.P., Brewer, P.G., and DeLong, E.F. (1999) Methane-consuming archaeobacteria in marine sediments. *Nature* **398**: 802-805.
- Hinrichs, K.U., Hayes, J.M., Bach, W., Spivack, A.J., Hmelo, L.R., Holm, N.G. et al. (2006) Biological formation of ethane and propane in the deep marine subsurface. *Proc Natl Acad Sci U S A* **103**: 14684-14689.
- Holmes, D.S., and Quigley, M. (1981) A rapid boiling method for the preparation of bacterial plasmids. *Anal Biochem* **114**: 193-197.
- Horikoshi, K. (1999) Alkaliphiles: Some applications of their products for biotechnology. *Microbiol Mol Biol Rev* **63**: 735-750.
- Houghton, R.A. (2007) Balancing the global carbon budget. *Annu Rev Earth Planet Sci* **35**: 313-347.
- Hurt, R.A., Qiu, X.Y., Wu, L.Y., Roh, Y., Palumbo, A.V., Tiedje, J.M., and Zhou, J.H. (2001) Simultaneous recovery of RNA and DNA from soils and sediments. *Appl Environ Microbiol* **67**: 4495-4503.
- Huu, N.B., Denner, E.B.M., Ha, D.T.C., Wanner, G., and Stan-Lotter, H. (1999) *Marinobacter aquaeolei* sp. nov., a halophilic bacterium isolated from a Vietnamese oil-producing well. *Int J Syst Bacteriol* **49**: 367-375.
- Hwang, C., Wu, W.M., Gentry, T.J., Carley, J., Carroll, S.L., Schadt, C. et al. (2006) Changes in bacterial community structure correlate with initial operating

- conditions of a field-scale denitrifying fluidized bed reactor. *Appl Microbiol Biotechnol* **71**: 748-760.
- Inagaki, F., Sakihama, Y., Inoue, A., Kato, C., and Horikoshi, K. (2002) Molecular phylogenetic analyses of reverse-transcribed bacterial rRNA obtained from deep-sea cold seep sediments. *Environ Microbiol* **4**: 277-286.
- Inagaki, F., Suzuki, M., Takai, K., Oida, H., Sakamoto, T., Aoki, K. et al. (2003) Microbial communities associated with geological horizons in coastal subseafloor sediments from the Sea of Okhotsk. *Appl Environ Microbiol* **69**: 7224-7235.
- Indermuhle, A., Stocker, T.F., Joos, F., Fischer, H., Smith, H.J., Wahlen, M. et al. (1999) Holocene carbon-cycle dynamics based on CO₂ trapped in ice at Taylor Dome, Antarctica. *Nature* **398**: 121-126.
- Inman, M.P., Beattie, J.K., Jones, D.R., and Baldwin, D.S. (2001) Abiotic hydrolysis of the detergent builder tripolyphosphate by hydrous manganese dioxide. *Water Res* **35**: 1987-1993.
- Ishibashi, Y., Cervantes, C., and Silver, S. (1990) Chromium reduction in *Pseudomonas putida*. *Appl Environ Microbiol* **56**: 2268-2270.
- Ishikawa, K., Mihara, Y., Gondoh, K., Suzuki, E., and Asano, Y. (2000) X-ray structures of a novel acid phosphatase from *Escherichia blattae* and its complex with the transition-state analog molybdate. *EMBO J* **19**: 2412-2423.
- Istok, J.D., Senko, J.M., Krumholz, L.R., Watson, D., Bogle, M.A., Peacock, A. et al. (2004) In situ bioreduction of technetium and uranium in a nitrate-contaminated aquifer. *Environ Sci Technol* **38**: 468-475.
- Jannasch, H.W., and Mottl, M.J. (1985) Geomicrobiology of deep-sea hydrothermal vents. *Science* **229**: 717-725.
- Javaux, E.J. (2006) Extreme life on Earth - past, present and possibly beyond. *Res Microbiol* **157**: 37-48.
- Jeong, B.C., Poole, P.S., Willis, A.C., and Macaskie, L.E. (1998) Purification and characterization of acid-type phosphatases from a heavy-metal-accumulating *Citrobacter* sp. *Arch Microbiol* **169**: 166-173.
- Jeong, B.C., Macaskie, L.E. (1999) Production of two phosphatases by a *Citrobacter* sp. grown in batch and continuous culture. *Enzyme Microb Technol* **24**: 218-224.

- Johnsen, A.R., and Kroer, N. (2007) Effects of stress and other environmental factors on horizontal plasmid transfer assessed by direct quantification of discrete transfer events. *FEMS Microbiol Ecol* **59**: 718-728.
- Johnson, J.L. (1994) Similarity analysis of rRNAs. In *Methods for general and molecular bacteriology*. Gerhardt, P., Murray, R.G.E., Wood, W.A., and Krieg, N.R. (eds). Washington, D.C.: American Society for Microbiology, pp. 683-700.
- Joos, F., Spahni, R. (2008) Rates of change in natural and anthropogenic radiative forcing over the past 20,000 years. *Proc Natl Acad Sci U S A* **105**: 1425-1430.
- Jorgensen, B.B., and Boetius, A. (2007) Feast and famine - microbial life in the deep-sea bed. *Nat Rev Microbiol* **5**: 770-781.
- Joye, S.B., MacDonald, I.R., Montoya, J.P., and Peccini, M. (2005) Geophysical and geochemical signatures of Gulf of Mexico seafloor brines. *Biogeosciences* **2**: 295-309.
- Joye, S.B., Boetius, A., Orcutt, B.N., Montoya, J.P., Schulz, H., Erickson, M.J., and Lugo, S.K. (2004) The anaerobic oxidation of methane and sulfate reduction in sediments from Gulf of Mexico cold seeps. *Chem Geol* **205**: 219-238.
- Jukes, T.H.a.C., C.R. (1969) Evolution of protein molecules. In *Mammalian Protein Metabolism*. Munro, H.N. (ed). New York, NY: Academic Press, pp. 21-132.
- Kaeberlein, T., Lewis, K., and Epstein, S.S. (2002) Isolating "uncultivable" microorganisms in pure culture in a simulated natural environment. *Science* **296**: 1127-1129.
- Kallmeyer, J.a.B., A. (2004) Effects of temperature and pressure on sulfate reduction and anaerobic oxidation of methane in hydrothermal sediments of Guaymas Basin. *Appl Environ Microbiol* **70**: 1231-1233.
- Kassab, D.M., and Roane, T.M. (2006) Differential responses of a mine tailings *Pseudomonas* isolate to cadmium and lead exposures. *Biodegradation* **17**: 379-387.
- Keddie, R.M., M. D., Collins, and D. Jones (1986) Genus *Arthrobacter* Conn and Dimmick 1947. In *Bergey's manual of systematic bacteriology, vol. 2*. P. H. A. Sneath, N.S.M., M. E.Sharpe, and J. G. Holt (ed). Baltimore, Md.: Williams & Wilkins, pp. 1288-1301.

- Kennett, J.P., Cannariato, K.G., Hendy, I.L., and Behl, R.J. (2000) Carbon isotopic evidence for methane hydrate instability during quaternary interstadials. *Science* **288**: 128-133.
- Kennicutt, M.C., Brooks, J.M., Bidigare, R.R., Fay, R.R., Wade, T.L., and McDonald, T.J. (1985) Vent type taxa in a hydrocarbon seep region on the Louisiana Slope. *Nature* **317**: 351-353.
- Kikuchi, A., and Asai, K. (1984) Reverse gyrase - A topoisomerase which introduces positive superhelical turns into DNA. *Nature* **309**: 677-681.
- Kiyono, M.a.P.-H., H. (1999) The *merG* gene product is involved in phenylmercury resistance in *Pseudomonas* strain K-62. *J Bacteriol* **181**: 726-730.
- Klaus-Joerger, T., Joerger, R., Olsson, E., and Granqvist, C.G. (2001) Bacteria as workers in the living factory: metal-accumulating bacteria and their potential for materials science. *Trends Biotechnol* **19**: 15-20.
- Knittel, K., Boetius, A., Lemke, A., Eilers, H., Lochte, K., Pfannkuche, O. et al. (2003) Activity, distribution, and diversity of sulfate reducers and other bacteria in sediments above gas hydrate (Cascadia margin, Oregon). *Geomicrobiol J* **20**: 269-294.
- Koizumi, Y., Kojima, H., and Fukui, M. (2003) Characterization of depth-related microbial community structure in lake sediment by denaturing gradient gel electrophoresis of amplified 16S rDNA and reversely transcribed 16S rRNA fragments. *FEMS Microbiol Ecol* **46**: 147-157.
- Kopf, A.J. (2003) Global methane emission through mud volcanoes and its past and present impact on the Earth's climate. *Int J Earth Sci* **92**: 806-816.
- Kotegov, K.V., Pavlov, O.N. and Shvendov, V.P. (1968) Technetium. In *Advances in Inorganic Chemistry and Radiochemistry*. Emelius, H.J., Sharpe, A.G., Eds. (ed). New York, N.Y.: Academic Press, pp. 1-90.
- Krieg, N.R., and J. G. Holt (ed.) (1984) *Bergey's manual of systematic bacteriology*, vol. 1. Baltimore, Md.: Williams & Wilkins.
- Krumholz, L.R. (2000) Microbial communities in the deep subsurface. *Hydrogeol J* **8**: 4-10.
- Kuhlbrandt, W. (2004) Biology, structure and mechanism of P-type ATPases. *Nat Rev Mol Cell Biol* **5**: 282-295.

- Kumar, S., Tamura, K., and Nei, M. (2004) MEGA3: Integrated software for molecular evolutionary genetics analysis and sequence alignment. *Brief Bioinform* **5**: 150-163.
- Kvenvolden, K.A. (1999) Potential effects of gas hydrate on human welfare. *Proc Natl Acad Sci U S A* **96**: 3420-3426.
- Langmuir, D. (1997) *Aqueous Environmental Geochemistry*. Upper Saddle River, NJ: Prentice-Hall.
- Lanoil, B.D., Sassen, R., La Duc, M.T., Sweet, S.T., and Nealson, K.H. (2001) *Bacteria and Archaea* physically associated with Gulf of Mexico gas hydrates. *Appl Environ Microbiol* **67**: 5143-5153.
- Larbig, K.D., Christmann, A., Johann, A., Klockgether, J., Hartsch, T., Merkl, R. et al. (2002) Gene islands integrated into tRNA(Gly) genes confer genome diversity on a *Pseudomonas aeruginosa* clone. *J Bacteriol* **184**: 6665-6680.
- Lawrence, J.G., and Ochman, H. (1997) Amelioration of bacterial genomes: Rates of change and exchange. *J Mol Evol* **44**: 383-397.
- Lebranz, M., Druschel, G.K, Thomsen-Ebert, T, Gilbert, B, Welch, S.A, Kemner, K.M, Logan, G.A, Summons, R.E, de Stasio, G, Bond, P.L, Lai, B, Kelly, S.D, Banfield, J.F (2000) Formation of sphalerite (ZnS) deposits in natural biofilms of sulfate-reducing bacteria. *Science* **290**: 1744-1747.
- Lebrun, M., Audurier, A., and Cossart, P. (1994) Plasmid-borne cadmium resistance genes in *Listeria monocytogenes* are similar to *cadA* and *cadC* of *Staphylococcus aureus* and are induced by cadmium. *J Bacteriol* **176**: 3040-3048.
- LeDuc, D.L., and Terry, N. (2005) Phytoremediation of toxic trace elements in soil and water. *J Ind Microbiol Biotechnol* **32**: 514-520.
- Lee, Y.J., Wagner, I.D., Brice, M.E., Kevbrin, V.V., Mills, G.L., Romanek, C.S., and Wiegel, J. (2005) *Thermosediminibacter oceani* gen. nov., sp. nov. and *Thermosediminibacter litoriperuensis* sp. nov., new anaerobic thermophilic bacteria isolated from Peru Margin. *Extremophiles* **9**: 375-383.
- Legatzki, A., Grass, G., Anton, A., Rensing, C., and Nies, D.H. (2003) Interplay of the Czc system and two P-type ATPases in conferring metal resistance to *Ralstonia metallidurans*. *J Bacteriol* **185**: 4354-4361.

- Liebert, C.A., Hall, R.M., and Summers, A.O. (1999) Transposon Tn21, flagship of the floating genome. *Microbiol Mol Biol Rev* **63**: 507-+.
- Lin, L.H., Wang, P.L., Rumble, D., Lippmann-Pipke, J., Boice, E., Pratt, L.M. et al. (2006) Long-term sustainability of a high-energy, low-diversity crustal biome. *Science* **314**: 479-482.
- Lindell, D., Jaffe, J.D., Johnson, Z.I., Church, G.M., and Chisholm, S.W. (2005) Photosynthesis genes in marine viruses yield proteins during host infection. *Nature* **438**: 86-89.
- Line, M.A. (2002) The enigma of the origin of life and its timing. *Microbiology* **148**: 21-27.
- Liu, C.X., Zachara, J.M., Fredrickson, J.K., Kennedy, D.W., and Dohnalkova, A. (2002) Modeling the inhibition of the bacterial reduction of U(VI) by β -MnO₂(s). *Environ Sci Technol* **36**: 1452-1459.
- Llarch, A., Logan, N.A., Castellvi, J., Prieto, M.J., and Guinea, J. (1997) Isolation and characterization of thermophilic *Bacillus* spp. from geothermal environments on Deception Island, South Shetland Archipelago. *Microb Ecol* **34**: 58-65.
- Lloyd, J.R. (2002) Bioremediation of metals: The application of micro-organisms that make and break minerals. *Microbiol Today* **29**: 67-69.
- Lloyd, J.R. (2003) Microbial reduction of metals and radionuclides. *FEMS Microbiol Rev* **27**: 411-425.
- Lloyd, J.R., Thomas, G.H., Finlay, J.A., Cole, J.A., and Macaskie, L.E. (1999a) Microbial reduction of technetium by *Escherichia coli* and *Desulfovibrio desulfuricans*: Enhancement via the use of high-activity strains and effect of process parameters. *Biotechnol Bioeng* **66**: 122-130.
- Lloyd, J.R., Ridley, J., Khizniak, T., Lyalikova, N.N., and Macaskie, L.E. (1999b) Reduction of technetium by *Desulfovibrio desulfuricans*: Biocatalyst characterization and use in a flowthrough bioreactor. *Appl Environ Microbiol* **65**: 2691-2696.
- Lloyd, J.R., Anderson, R.T. and Macaskie, L.E. (2005) *Bioremediation of metals and radionuclides*. Washington, DC: American Society for Microbiology Press.

- Lo, I., Denef, V.J., VerBerkmoes, N.C., Shah, M.B., Goltsman, D., DiBartolo, G. et al. (2007) Strain-resolved community proteomics reveals recombining genomes of acidophilic bacteria. *Nature* **446**: 537-541.
- Logan, N.A., Lebbe, L., Hoste, B., Goris, J., Forsyth, G., Heyndrickx, M. et al. (2000) Aerobic endospore-forming bacteria from geothermal environments in northern Victoria Land, Antarctica, and Candlemas Island, South Sandwich archipelago, with the proposal of *Bacillus fumarioli* sp nov. *Int J Syst Evol Microbiol* **50**: 1741-1753.
- Lonsdale, P. (1977) Clustering of suspension-feeding macrobenthos near abyssal hydrothermal vents at oceanic spreading centers. *Deep-Sea Research* **24**: 857-863.
- Lopez, E., Elez, M., Matic, I., and Blazquez, J. (2007) Antibiotic-mediated recombination: ciprofloxacin stimulates SOS-independent recombination of divergent sequences in *Escherichia coli*. *Mol Microbiol* **64**: 83-93.
- Losekann, T., Knittel, K., Nadalig, T., Fuchs, B., Niemann, H., Boetius, A., and Amann, R. (2007) Diversity and abundance of aerobic and anaerobic methane oxidizers at the Haakon Mosby mud volcano, Barents Sea. *Appl Environ Microbiol* **73**: 3348-3362.
- Lovley, D.R., and Phillips, E.J.P. (1992) Bioremediation of uranium contamination with enzymatic uranium reduction. *Environ Sci Technol* **26**: 2228-2234.
- Lovley, D.R., and Coates, J.D. (1997) Bioremediation of metal contamination. *Curr Opin Biotechnol* **8**: 285-289.
- Lovley, D.R., Holmes, D.E., and Nevin, K.P. (2004) Dissimilatory Fe(III) and Mn(IV) reduction. *Adv Microb Physiol* **49**: 219-286.
- Lovley, D.R., Phillips, E.J.P., Gorby, Y.A., and Landa, E.R. (1991) Microbial reduction of uranium. *Nature* **350**: 413-416.
- Lundberg, J.O., Weitzberg, E., Cole, J.A., and Benjamin, N. (2004) Opinion - Nitrate, bacteria and human health. *Nat Rev Microbiol* **2**: 593-602.
- Lutsenko, S., and Kaplan, J.H. (1995) Organization of P-Type ATPases - Significance of structural diversity. *Biochemistry (Mosc)* **34**: 15607-15613.
- Macalady, J., and Banfield, J.F. (2003) Molecular geomicrobiology: genes and geochemical cycling. *Earth Planet Sci Lett* **209**: 1-17.

- Macaskie, L.E. (1991) The Application of Biotechnology to the Treatment of Wastes Produced from the Nuclear-Fuel Cycle - Biodegradation and Bioaccumulation as a Means of Treating Radionuclide-Containing Streams. *Crit Rev Biotechnol* **11**: 41-112.
- Macaskie, L.E., Blackmore, J.D., and Empson, R.M. (1988) Phosphatase overproduction and enhanced uranium accumulation by a stable mutant of a *Citrobacter* sp. isolated by a novel method. *FEMS Microbiol Lett* **55**: 157-161.
- Macaskie, L.E., Jeong, B.C., and Tolley, M.R. (1994) Enzymatically Accelerated Biomineralization of Heavy-Metals: Application to the Removal of Americium and Plutonium from Aqueous Flows. *FEMS Microbiol Rev* **14**: 351-367.
- Macaskie, L.E., Bonthron, K.M., Yong, P., and Goddard, D.T. (2000) Enzymically mediated bioprecipitation of uranium by a *Citrobacter* sp.: a concerted role for exocellular lipopolysaccharide and associated phosphatase in biomineral formation. *Microbiology* **146**: 1855-1867.
- Macaskie, L.E., Empson, R.M., Cheetham, A.K., Grey, C.P., and Skarnulis, A.J. (1992) Uranium bioaccumulation by a *Citrobacter* sp. as a result of enzymatically mediated growth of polycrystalline HUO_2PO_4 . *Science* **257**: 782-784.
- Macaskie, L.E., Yong, P., Doyle, T.C., Roig, M.G., Diaz, M., and Manzano, T. (1997) Bioremediation of uranium-bearing wastewater: Biochemical and chemical factors influencing bioprocess application. *Biotechnol Bioeng* **53**: 100-109.
- MacDonald, I.R. (1998) Stability and change in Gulf of Mexico Chemosynthetic Communities: Interim Report. In: Interior, U.S.D.o.t. (ed). New Orleans, LA: U.S. Department of the Interior.
- MacDonald, I.R., Buthman, D.B., Sager, W.W., Peccini, M.B., and Guinasso, N.L. (2000) Pulsed oil discharge from a mud volcano. *Geology* **28**: 907-910.
- Madigan, M.T., Martinko, J.M., Parker, J (2003) *Brock Biology of Microorganisms*. Upper Saddle River, NJ: Pearson Education.
- Mahillon, J., and Chandler, M. (1998) Insertion sequences. *Microbiol Mol Biol Rev* **62**: 725-774.
- Maidak, B.L., Cole, J.R., Parker Jr., C.T., Garrity, G.M., Larsen, N., Li, B. et al. (1999) A new version of the RDP (Ribosomal Database Project). *Nucleic Acids Res* **27**: 171-173.

- Malik, A. (2004) Metal bioremediation through growing cells. *Environ Int* **30**: 261-278.
- Marquis, R.E., and Bender, G.R. (1980) Isolation of a variant of *Streptococcus faecalis* with enhanced barotolerance. *Can J Microbiol* **26**: 371-376.
- Martinez, R.J., Mills, H.J., Story, S., and Sobecky, P.A. (2006a) Prokaryotic diversity and metabolically active microbial populations in sediments from an active mud volcano in the Gulf of Mexico. *Environ Microbiol* **8**: 1783-1796.
- Martinez, R.J., Wang, Y.L., Raimondo, M.A., Coombs, J.M., Barkay, T., and Sobecky, P.A. (2006b) Horizontal gene transfer of P_{IB}-type ATPases among bacteria isolated from radionuclide- and metal-contaminated subsurface soils. *Appl Environ Microbiol* **72**: 3111-3118.
- Martinez, R.J., Beazley, M., Taillefert, M., Arakaki, A., Skolnick, J., and Sobecky, P.A. (2007) Aerobic uranium(VI) bioprecipitation by metal resistant bacteria isolated from radionuclide and metal-contaminated subsurface soils. *Environ Microbiol* **9**: 3122-3133.
- Mayhew, L.E., Geist, D.J., and Childers, S.E. (2007) Microbial community comparisons as a function of the physical and geochemical conditions of Galapagos Island fumaroles. *Geomicrobiol J* **24**: 615-625.
- McLean, E.O. (1982) *Methods of soil analysis, part 2. Chemical and microbiological properties. Agronomy Monograph 9, 2nd ed.* Madison, WI: ASA-SSSA.
- Mergeay, M., Monchy, S., Vallaey, T., Auquier, V., Benotmane, A., Bertin, P. et al. (2003) *Ralstonia metallidurans*, a bacterium specifically adapted to toxic metals: towards a catalogue of metal-responsive genes. *FEMS Microbiol Rev* **27**: 385-410.
- Merroun, M.L., Raff, J., Rossberg, A., Hennig, C., Reich, T., and Selenska-Pobell, S. (2005) Complexation of uranium by cells and S-layer sheets of *Bacillus sphaericus* JG-A12. *Appl Environ Microbiol* **71**: 5532-5543.
- Methe, B.A., Nelson, K.E., Deming, J.W., Momen, B., Melamud, E., Zhang, X.J. et al. (2005) The psychrophilic lifestyle as revealed by the genome sequence of *Colwellia psychrerythraea* 34H through genomic and proteomic analyses. *Proc Natl Acad Sci U S A* **102**: 10913-10918.
- Metje, M., and Frenzel, P. (2007) Methanogenesis and methanogenic pathways in a peat from subarctic permafrost. *Environ Microbiol* **9**: 954-964.

- Michaelis, W., Seifert, R., Nauhaus, K., Treude, T., Thiel, V., Blumenberg, M. et al. (2002) Microbial reefs in the Black Sea fueled by anaerobic oxidation of methane. *Science* **297**: 1013-1015.
- Michalsen, M.M., Peacock, A.D., Spain, A.M., Smithgal, A.N., White, D.C., Sanchez-Rosario, Y. et al. (2007) Changes in microbial community composition and geochemistry during uranium and technetium bioimmobilization. *Appl Environ Microbiol* **73**: 5885-5896.
- Mieiro, C.L., Pato, P., Pereira, E., Mirante, F., Coutinho, J.A.P., Pinheiro, L.M. et al. (2007) Total mercury in sediments from mud volcanoes in Gulf of Cadiz. *Mar Pollut Bull* **54**: 1539-1544.
- Milkov, A.V. (2000) Worldwide distribution of submarine mud volcanoes and associated gas hydrates. *Mar Geol* **167**: 29-42.
- Milkov, A.V., and Sassen, R. (2001) Estimate of gas hydrate resource, northwestern Gulf of Mexico continental slope. *Mar Geol* **179**: 71-83.
- Milkov, A.V., and Etiope, G. (2005) Global methane emission through mud volcanoes and its past and present impact on the Earth's climate-a comment. *Int J Earth Sci* **94**: 490-492.
- Milkov, A.V., Sassen, R., Apanasovich, T.V., and Dadashev, F.G. (2003) Global gas flux from mud volcanoes: A significant source of fossil methane in the atmosphere and the ocean. *Geophys Res Lett* **30**.
- Miller, A.C., Stewart, M., Brooks, K., Shi, L., and Page, N. (2002) Depleted uranium-catalyzed oxidative DNA damage: absence of significant alpha particle decay. *J Inorg Biochem* **91**: 246-252.
- Miller, D.N., Bryant, J.E., Madsen, E.L., and Ghiorse, W.C. (1999) Evaluation and optimization of DNA extraction and purification procedures for soil and sediment samples. *Appl Environ Microbiol* **65**: 4715-4724.
- Mills, H.J., Martinez, R.J., Story, S., and Sobecky, P.A. (2004) Identification of members of the metabolically active microbial populations associated with *Beggiatoa* species mat communities from Gulf of Mexico cold-seep sediments. *Appl Environ Microbiol* **70**: 5447-5458.
- Mills, H.J., Martinez, R.J., Story, S., and Sobecky, P. (2005) Characterization of microbial community structure in Gulf of Mexico gas hydrates: comparative

- analysis of DNA- and RNA-derived clone libraries. *Appl Environ Microbiol* **71**: 3235-3247.
- Mills, H.J., Hodges, C., Wilson, K., MacDonald, I.R., and Sobecky, P.A. (2003) Microbial diversity in sediments associated with surface-breaching gas hydrate mounds in the Gulf of Mexico. *FEMS Microbiol Ecol* **46**: 39-52.
- Minton, K.W. (1994) DNA repair in the extremely radioresistant bacterium *Deinococcus radiodurans* *Mol Microbiol* **13**: 9-15.
- Mire, C.E., Tourjee, J.A., O'Brien, W.F., Ramanujachary, K.V., and Hecht, G.B. (2004) Lead precipitation by *Vibrio harveyi*: Evidence for novel quorum-sensing interactions. *Appl Environ Microbiol* **70**: 855-864.
- Miskin, I.P., Farrimond, P., and Head, I.M. (1999) Identification of novel bacterial lineages as active members of microbial populations in a freshwater sediment using a rapid RNA extraction procedure and RT-PCR. *Microbiology* **145**: 1977-1987.
- Moeseneder, M.M., Arrieta, J.M., and Herndl, G.J. (2005) A comparison of DNA- and RNA-based clone libraries from the same marine bacterioplankton community. *FEMS Microbiol Ecol* **51**: 341-352.
- Mongodin, E.F., Hance, I.R., DeBoy, R.T., Gill, S.R., Daugherty, S., Huber, R. et al. (2005) Gene transfer and genome plasticity in *Thermotoga maritima*, a model hyperthermophilic species. *J Bacteriol* **187**: 4935-4944.
- Moon, H.S., Komlos, J., and Jaffe, P.R. (2007) Uranium reoxidation in previously bioreduced sediment by dissolved oxygen and nitrate. *Environ Sci Technol* **41**: 4587-4592.
- Moreira, D., Rodriguez-Valera, F., and Lopez-Garcia, P. (2006) Metagenomic analysis of mesopelagic Antarctic plankton reveals a novel deltaproteobacterial group. *Microbiology* **152**: 505-517.
- Morita, R.Y. (1997) *Bacteria in Oligotrophic Environments*. New York, NY: Chapman & Hall.
- Moss, R.A., Bracken, K., and Zhang, J. (1997) Actinide (uranyl) hydrolysis of phosphodiesteres. *Chem Commun*: 563-564.
- Mountfort, D.O., Rainey, F.A., Burghardt, J., Kaspar, H.F., and Stackebrandt, E. (1998) *Psychromonas antarcticus* gen. nov., sp. nov., a new aerotolerant anaerobic,

- halophilic psychrophile isolated from pond sediment of the McMurdo Ice Shelf, Antarctica. *Arch Microbiol* **169**: 231-238.
- Moussard, H., Moreira, D., Cambon-Bonavita, M.A., Lopez-Garcia, P., and Jeanthon, C. (2006) Uncultured *Archaea* in a hydrothermal microbial assemblage: phylogenetic diversity and characterization of a genome fragment from a euryarchaeote. *FEMS Microbiol Ecol* **57**: 452-469.
- Mukhopadhyay, R., Rosen, B.P., Pung, L.T., and Silver, S. (2002) Microbial arsenic: from geocycles to genes and enzymes. *FEMS Microbiol Rev* **26**: 311-325.
- Muller, D., Lievremont, D., Simeonova, D.D., Hubert, J.C., and Lett, M.C. (2003) Arsenite oxidase *aox* genes from a metal-resistant beta-proteobacterium. *J Bacteriol* **185**: 135-141.
- Murphy, J., and Riley, J.P. (1962) A modified single solution method for determination of phosphate in natural waters. *Anal Chim Acta* **26**: 31-36.
- Naehr, T.H., Eichhubl, P., Orphan, V.J., Hovland, M., Paull, C.K., Ussler, W. et al. (2007) Authigenic carbonate formation at hydrocarbon seeps in continental margin sediments: A comparative study. *Deep-Sea Research Part II-Topical Studies in Oceanography* **54**: 1268-1291.
- Nakamura, Y., Itoh, T., Matsuda, H., and Gojobori, T. (2004) Biased biological functions of horizontally transferred genes in prokaryotic genomes. *Nat Genet* **36**: 760-766.
- Nakaya, R., Nakamura, A. and Murata, Y. (1960) Resistance transfer agents in *Shigella*. *Biochem Biophys Res Commun* **3**: 654-659.
- Nash, K.L., Jensen, M.P., and Schmidt, M.A. (1998) Actinide immobilization in the subsurface environment by in-situ treatment with a hydrolytically unstable organophosphorus complexant: Uranyl uptake by calcium phytate. *JALC* **271**: 257-261.
- Nauhaus, K., Boetius, A., Kruger, M., and Widdel, F. (2002) In vitro demonstration of anaerobic oxidation of methane coupled to sulphate reduction in sediment from a marine gas hydrate area. *Environ Microbiol* **4**: 296-305.
- Nazina, T.N., Kosareva, I.M., Petrunyaka, V.V., Savushkina, M.K., Kudriavtsev, E.G., Lebedev, V.A. et al. (2004) Microbiology of formation waters from the deep repository of liquid radioactive wastes Severnyi. *FEMS Microbiol Ecol* **49**: 97-107.

- Neff, J.M. (1997) Ecotoxicology of arsenic in the marine environment. *Environ Toxicol Chem* **16**: 917-927.
- Nemergut, D.R., Martin, A.P., and Schmidt, S.K. (2004) Integron diversity in heavy-metal-contaminated mine tailings and inferences about integron evolution. *Appl Environ Microbiol* **70**: 1160-1168.
- Nevin, K.P., and Lovley, D.R. (2000) Potential for nonenzymatic reduction of Fe(III) via electron shuttling in subsurface sediments. *Environ Sci Technol* **34**: 2472-2478.
- Newman, D.K., and Banfield, J.F. (2002) Geomicrobiology: How molecular-scale interactions underpin biogeochemical systems. *Science* **296**: 1071-1077.
- Niemann, H., Duarte, J., Hensen, C., Omoregie, E., Magalhaes, V.H., Elvert, M. et al. (2006a) Microbial methane turnover at mud volcanoes of the Gulf of Cadiz. *Geochim Cosmochim Acta* **70**: 5336-5355.
- Niemann, H., Losekann, T., de Beer, D., Elvert, M., Nadalig, T., Knittel, K. et al. (2006b) Novel microbial communities of the Haakon Mosby mud volcano and their role as a methane sink. *Nature* **443**: 854-858.
- Nies, A., Nies, D.H., and Silver, S. (1989) Cloning and expression of plasmid genes encoding resistances to chromate and cobalt in *Alcaligenes eutrophus*. *J Bacteriol* **171**: 5065-5070.
- Nies, D.H. (1992) Resistance to cadmium, cobalt, zinc, and nickel in microbes. *Plasmid* **27**: 17-28.
- Nies, D.H. (1999) Microbial heavy-metal resistance. *Appl Microbiol Biotechnol* **51**: 730-750.
- Nies, D.H. (2003) Efflux-mediated heavy metal resistance in prokaryotes. *FEMS Microbiol Rev* **27**: 313-339.
- Nogales, B., Moore, E.R.B., Abraham, W.-R., and Timmis, K.N. (1999) Identification of the metabolically active members of a bacterial community in a polychlorinated biphenyl-polluted moorland soil. *Environ Microbiol* **1**: 199-212.
- Nogales, B., Moore, E.R.B., Llobet-Brossa, E., Rossello-Mora, R., Amann, R., and Timmis, K.N. (2001) Combined use of 16S ribosomal DNA and 16S rRNA to study the bacterial community of polychlorinated biphenyl-polluted soil. *Appl Environ Microbiol* **67**: 1874-1884.

- Nomura, M., Gourse, R., and Baughman, G. (1984) Regulation of the synthesis of ribosomes and ribosomal components. *Annu Rev Biochem* **53**: 75-117.
- Norris, T.B., Wraith, J.M., Castenholz, R.W., and McDermott, T.R. (2002) Soil microbial community structure across a thermal gradient following a geothermal heating event. *Appl Environ Microbiol* **68**: 6300-6309.
- North, N.N., Dollhopf, S.L., Petrie, L., Istok, J.D., Balkwill, D.L., and Kostka, J.E. (2004) Change in bacterial community structure during in situ Biostimulation of subsurface sediment cocontaminated with uranium and nitrate. *Appl Environ Microbiol* **70**: 4911-4920.
- NRC (1999) Our common journey: A transition toward sustainability. In. Washington, DC, p. 384 pp.
- Nucifora, G., Chu, L., Misra, T.K., and Silver, S. (1989) Cadmium resistance from *Staphylococcus aureus* plasmid p1258 cadA gene results from a cadmium efflux ATPase. *Proc Natl Acad Sci U S A* **86**: 3544-3548.
- O'Sullivan, D., Ross, R.P., Twomey, D.P., Fitzgerald, G.F., Hill, C., and Coffey, A. (2001) Naturally occurring lactococcal plasmid pAH90 links bacteriophage resistance and mobility functions to a food-grade selectable marker. *Appl Environ Microbiol* **67**: 929-937.
- Onstott, T.C., Moser, D.P., Pfiffner, S.M., Fredrickson, J.K., Brockman, F.J., Phelps, T.J. et al. (2003) Indigenous and contaminant microbes in ultradeep mines. *Environ Microbiol* **5**: 1168-1191.
- Oren, A. (1999) Bioenergetic aspects of halophilism. *Microbiol Mol Biol Rev* **63**: 334-348.
- Orphan, V.J., House, C.H., Hinrichs, K.U., McKeegan, K.D., and DeLong, E.F. (2001a) Methane-consuming archaea revealed by directly coupled isotopic and phylogenetic analysis. *Science* **293**: 484-487.
- Orphan, V.J., House, C.H., Hinrichs, K.U., McKeegan, K.D., and DeLong, E.F. (2002) Multiple archaeal groups mediate methane oxidation in anoxic cold seep sediments. *Proc Natl Acad Sci U S A* **99**: 7663-7668.
- Orphan, V.J., Hinrichs, K.U., Ussler, W., 3rd, Paull, C.K., Taylor, L.T., Sylva, S.P. et al. (2001b) Comparative analysis of methane-oxidizing archaea and sulfate-reducing bacteria in anoxic marine sediments. *Appl Environ Microbiol* **67**: 1922-1934.

- Pan-Hou, H., Kiyono, M., Omura, H., Omura, T., and Endo, G. (2002) Polyphosphate produced in recombinant *Escherichia coli* confers mercury resistance. *FEMS Microbiol Lett* **207**: 159-164.
- Pancost, R.D., Damste, J.S.S., de Lint, S., van der Maarel, M., and Gottschal, J.C. (2000) Biomarker evidence for widespread anaerobic methane oxidation in Mediterranean sediments by a consortium of methanogenic archaea and bacteria. *Appl Environ Microbiol* **66**: 1126-1132.
- Pandit, S.B., Zhang, Y., and Skolnick, J. (2006) TASSER-Lite: An automated tool for protein comparative modeling. *Biophys J* **91**: 4180-4190.
- Paterson-Beedle, M., Macaskie, L.E., Lee, C.H., Hriljac, J.A., Jee, K.Y., and Kim, W.H. (2006) Utilisation of a hydrogen uranyl phosphate-based ion exchanger supported on a biofilm for the removal of cobalt, strontium and caesium from aqueous solutions. *Hydrometallurgy* **83**: 141-145.
- Pattanapitpaisal, P., Mabbett, A.N., Finlay, J.A., Beswick, A.J., Paterson-Beedle, M., Essa, A. et al. (2002) Reduction of Cr(VI) and bioaccumulation of chromium by Gram positive and Gram negative microorganisms not previously exposed to Cr-stress. *Environ Technol* **23**: 731-745.
- Paul, E.A. (2007) Soil microbiology, ecology, and biochemistry in perspective. In *Soil microbiology, ecology, and biochemistry*. Paul, E.A. (ed). Boston, MA: Academic Press, pp. 3-24.
- Paull, C.K., Hecker, B., Commeau, R., Freemanlynde, R.P., Neumann, C., Corso, W.P. et al. (1984) Biological communities at the Florida escarpment resemble hydrothermal vent taxa. *Science* **226**: 965-967.
- Payne, R.B., Gentry, D.A., Rapp-Giles, B.J., Casalot, L., and Wall, J.D. (2002) Uranium reduction by *Desulfovibrio desulfuricans* strain G20 and a cytochrome c3 mutant. *Appl Environ Microbiol* **68**: 3129-3132.
- Pearson, A.J., Bruce, K.D., Osborn, A.M., Ritchie, D.A., and Strike, P. (1996) Distribution of class II transposase and resolvase genes in soil bacteria and their association with mer genes. *Appl Environ Microbiol* **62**: 2961-2965.
- Peddie, C.J., Cook, G.M., and Morgan, H.W. (2000) Sucrose transport by the alkaliphilic, thermophilic *Bacillus* sp. strain TA2.A1 is dependent on a sodium gradient. *Extremophiles* **4**: 291-296.
- Pedone, E., Ren, B., Ladenstein, R., Rossi, M., and Bartolucci, S. (2004) Functional properties of the protein disulfide oxidoreductase from the archaeon *Pyrococcus*

furiosus - A member of a novel protein family related to protein disulfide-isomerase. *Eur J Biochem* **271**: 3437-3448.

Perriere, G., and Gouy, M. (1996) WWW-query: an on-line retrieval system for biological sequence banks. *Biochimie* **78**: 364-369.

Petrie, L., North, N.N., Dollhopf, S.L., Balkwill, D.L., and Kostka, J.E. (2003) Enumeration and characterization of iron(III)-reducing microbial communities from acidic subsurface sediments contaminated with uranium(VI). *Appl Environ Microbiol* **69**: 7467-7479.

Philp, J.C., Bamforth, S.M., Singleton, I., and Atlas, R.M. (2005) Environmental pollution and restoration: A role for bioremediation. In *Bioremediation: Applied microbial solutions for real-world environmental cleanup*. Atlas, R.M.a.P., J. (ed). Washington, DC: ASM Press.

Pikuta, E.V., Hoover, R.B., and Tang, J. (2007) Microbial extremophiles at the limits of life. *Crit Rev Microbiol* **33**: 183-209.

Pimenov, N., Savvichev, A., Rusanov, I., Lein, A., Egorov, A., Gebruk, A., Moskalev, L., Vogt, P. (1999) Microbial processes of carbon cycle as the base of food chain of Hakon Mosby Mud Volcano benthic community. *Geo-Mar Lett* **19**: 89-96.

Pimenov, N.V., Savvichev, A.S., Rusanov, II, Lein, A.Y., and Ivanov, M.V. (2000) Microbiological processes of the carbon and sulfur cycles at cold methane seeps of the North Atlantic. *Microbiology (Russ Acad Sci)* **69**: 709-720.

Powers, E.M. (1995) Efficacy of the Ryu nonstaining KOH technique for rapidly determining Gram reactions of food-borne and waterborne bacteria and yeasts. *Appl Environ Microbiol* **61**: 3756-3758.

Powers, L.G., Mills, H.J., Palumbo, A.V., Zhang, C.L., Delaney, K., and Sobecky, P. (2002) Introduction of a plasmid-encoded *phoA* gene for constitutive overproduction of alkaline phosphatase in three subsurface *Pseudomonas* isolates. *FEMS Microbiol Ecol* **41**: 115-123.

Price, P.B., and Sowers, T. (2004) Temperature dependence of metabolic rates for microbial growth, maintenance, and survival. *Proc Natl Acad Sci U S A* **101**: 4631-4636.

Quispel, A. (1998) Lourens G. M. Baas Becking (1895–1963), Inspirator for many (micro)biologists. *Int Microbiol* **1**: 69-72.

- Rai, D., Felmy, A.R., and Ryan, J.L. (1990) Uranium (IV) hydrolysis constants and solubility product of $\text{UO}_2 \cdot x\text{H}_2\text{O}(\text{am})$. *Inorg Chem* **29**: 260-264.
- Reeburgh, W.S. (2007) Oceanic methane biogeochemistry. *Chem Rev* **107**: 486-513.
- Reilly, T.J., Baron, G.S., Nano, F.E., and Kuhlenschmidt, M.S. (1996) Characterization and sequencing of a respiratory burst-inhibiting acid phosphatase from *Francisella tularensis*. *J Biol Chem* **271**: 10973-10983.
- Remonsellez, F., Orell, A., and Jerez, C.A. (2006) Copper tolerance of the thermoacidophilic archaeon *Sulfolobus metallicus*: possible role of polyphosphate metabolism. *Microbiology* **152**: 59-66.
- Renninger, N., Knopp, R., Nitsche, H., Clark, D.S., and Keasling, J.D. (2004) Uranyl precipitation by *Pseudomonas aeruginosa* via controlled polyphosphate metabolism. *Appl Environ Microbiol* **70**: 7404-7412.
- Rensing, C., Ghosh, M., and Rosen, B.P. (1999) Families of soft-metal-ion-transporting ATPases. *J Bacteriol* **181**: 5891-5897.
- Reyes, N.S., Frischer, M.E., and Sobecky, P.A. (1999) Characterization of mercury resistance mechanisms in marine sediment microbial communities. *FEMS Microbiol Ecol* **30**: 273-284.
- Riccio, M.L., Rossolini, G.M., Lombardi, G., Chiesurin, A., and Satta, G. (1997) Expression cloning of different bacterial phosphatase-encoding genes by histochemical screening of genomic libraries onto an indicator medium containing phenolphthalein diphosphate and methyl green. *J Appl Microbiol* **82**: 177-185.
- Riley, R.G., Zachara, J.M. and Wobber, F.J. (1992) Chemical contaminants on DOE lands and selection of contamination mixtures for subsurface science research, DOE/ER-0547T. In: Energy, U.D.o. (ed). Washington, DC.
- Rivera, M.C. (2007) Genomic analyses and the origin of the eukaryotes. *Chem Biodivers* **4**: 2631-2638.
- Rivera, M.C., and Lake, J.A. (2004) The ring of life provides evidence for a genome fusion origin of eukaryotes. *Nature* **431**: 152-155.
- Rivera, M.C., Jain, R., Moore, J.E., and Lake, J.A. (1998) Genomic evidence for two functionally distinct gene classes. *Proc Natl Acad Sci U S A* **95**: 6239-6244.

- Roh, Y., Lee, S.R., Choi, S.K., Elless, M.P., and Lee, S.Y. (2000) Physicochemical and mineralogical characterization of uranium-contaminated soils. *Soil & Sediment Contamination* **9**: 463-486.
- Rosen, B.P. (1996) Bacterial resistance to heavy metals and metalloids. *J Biol Inorg Chem* **1**: 273-277.
- Rosen, B.P. (2002) Transport and detoxification systems for transition metals, heavy metals and metalloids in eukaryotic and prokaryotic microbes. *Comparative Biochemistry and Physiology* **133**: 689-693.
- Rosenstein, R., Peschel, A., Wieland, B., and Gotz, F. (1992) Expression and regulation of the antimonite, arsenite, and arsenate resistance operon of *Staphylococcus xylosus* plasmid pSX267. *J Bacteriol* **174**: 3676-3683.
- Rossolini, G.M., Schippa, S., Riccio, M.L., Berlutti, F., Macaskie, L.E., and Thaller, M.C. (1998) Bacterial nonspecific acid phosphohydrolases: physiology, evolution and use as tools in microbial biotechnology. *Cell Mol Life Sci* **54**: 833-850.
- Rothschild, L.J., and Mancinelli, R.L. (2001) Life in extreme environments. *Nature* **409**: 1092-1101.
- Ruggiero, C.E., Boukhalfa, H., Forsythe, J.H., Lack, J.G., Hersman, L.E., and Neu, M.P. (2005) Actinide and metal toxicity to prospective bioremediation bacteria. *Environ Microbiol* **7**: 88-97.
- Russell, N.J. (2000) Toward a molecular understanding of cold activity of enzymes from psychrophiles. *Extremophiles* **4**: 83-90.
- Saitou, N., and Nei, M. (1987) The neighbor-joining method - A new method for reconstructing phylogenetic trees. *Mol Biol Evol* **4**: 406-425.
- Sanders, O.I., Rensing, C., Kuroda, M., Mitra, B. and Rosen, B.P. (1997) Antimonite is accumulated by the glycerol facilitator GlpF in *Escherichia coli*. *J Bacteriol* **179**: 3365-3367.
- Sani, R.K., Peyton, B.A., and Jandhyala, M. (2003) Toxicity of lead in aqueous medium to *Desulfovibrio desulfuricans* G20. *Environ Toxicol Chem* **22**: 252-260.
- Sassen, R., Milkov, A.V., Roberts, H.H., Sweet, S.T., and DeFreitas, D.A. (2003) Geochemical evidence of rapid hydrocarbon venting from a seafloor-piercing mud diapir, Gulf of Mexico continental shelf. *Mar Geol* **198**: 319-329.

- Sassen, R., Joye, S., Sweet, S.T., DeFreitas, D.A., Milkov, A.V., and MacDonald, I.R. (1999) Thermogenic gas hydrates and hydrocarbon gases in complex chemosynthetic communities, Gulf of Mexico continental slope. *Org Geochem* **30**: 485-497.
- Sato, T., Murakami, T., Yanase, N., Isobe, H., Payne, T.E., and Airey, P.L. (1997) Iron nodules scavenging uranium from groundwater. *Environ Sci Technol* **31**: 2854-2858.
- Schaetzl, R., Anderson, S. (2005) Basic concepts: soil morphology. In *Soils: genesis and geomorphology*. New York, NY: Cambridge University Press, pp. 9-31.
- Schecher, W.D.M., D. C. , User's Manual; Environmental , and Software:, R. (2001) MINEQL+: A Chemical Equilibrium Modeling System, Version 4.5 for Windows. In: Environmental Research Software.
- Schidlowski, M. (1988) A 3,800 million year isotopic record of life from carbon in sedimentary rocks. *Nature* **333**: 313-318.
- Schink, B. (1997) Energetics of syntrophic cooperation in methanogenic degradation. *Microbiol Mol Biol Rev* **61**: 262-&.
- Schippers, A., Neretin, L.N., Kallmeyer, J., Ferdelman, T.G., Cragg, B.A., Parkes, R.J., and Jorgensen, B.B. (2005) Prokaryotic cells of the deep sub-seafloor biosphere identified as living bacteria. *Nature* **433**: 861-864.
- Schlesinger, W.H. (2006) Global change ecology. *Trends Ecol Evol* **21**: 348-351.
- Schwertmann, U., Cornell, R.M. (2000) *Iron oxides in the laboratory: Preparation and characterization*. 2nd ed. New York: Wiley.
- Senko, J.M., Istok, J.D., Suflita, J.M., and Krumholz, L.R. (2002) *In situ* evidence for uranium immobilization and remobilization. *Environ Sci Technol* **36**: 1491-1496.
- She, Q., Singh, R.K., Confalonieri, F., Zivanovic, Y., Allard, G., Awayez, M.J. et al. (2001) The complete genome of the crenarchaeon *Sulfolobus solfataricus* P2. *Proc Natl Acad Sci U S A* **98**: 7835-7840.
- Shen, Y.A., Buick, R., and Canfield, D.E. (2001) Isotopic evidence for microbial sulphate reduction in the early Archaean era. *Nature* **410**: 77-81.

- Shiba, T. (1991) *Roseobacter litoralis* gen. nov., sp. nov. and *Roseobacter denitrificans* sp. nov., aerobic pink pigmented bacteria which contain bacteriochlorophyll A. *Syst Appl Microbiol* **14**: 140-145.
- Silver, S., and Misra, T.K. (1988) Plasmid mediated heavy metal resistances. *Annu Rev Microbiol* **42**: 717-743.
- Silver, S., and Phung, L.T. (2005) A bacterial view of the periodic table: genes and proteins for toxic inorganic ions. *J Ind Microbiol Biotechnol* **32**: 587-605.
- Simbahan, J., Kurth, E., Schelert, J., Dillman, A., Moriyama, E., Jovanovich, S., and Blum, P. (2005) Community analysis of a mercury hot spring supports occurrence of domain-specific forms of mercuric reductase. *Appl Environ Microbiol* **71**: 8836-8845.
- Sloan, E.D. (2003) Fundamental principles and applications of natural gas hydrates. *Nature* **426**: 353-359.
- Smalla, K. (2004) Culture-independent microbiology. In *Microbial Diversity and Bioprospecting*. Bull, A.T. (ed). Washington, DC: ASM Press, pp. 88-99.
- Smith, W.L., and Gadd, G.M. (2000) Reduction and precipitation of chromate by mixed culture sulphate-reducing bacterial biofilms. *J Appl Microbiol* **88**: 983-991.
- Sobecky, P.A., Mincer, T.J., Chang, M.C., and Helinski, D.R. (1997) Plasmids isolated from marine sediment microbial communities contain replication and incompatibility regions unrelated to those of known plasmid groups. *Appl Environ Microbiol* **63**: 888-895.
- Sobecky, P.A., Mincer, T.J., Chang, M.C., Toukdarian, A., and Helinski, D.R. (1998) Isolation of broad-host-range replicons from marine sediment bacteria. *Appl Environ Microbiol* **64**: 2822-2830.
- Sorensen, S.J., Bailey, M., Hansen, L.H., Kroer, N., and Wuertz, S. (2005) Studying plasmid horizontal transfer in situ: A critical review. *Nat Rev Microbiol* **3**: 700-710.
- Sowder, A.G., Clark, S.B., and Fjeld, R.A. (1996) The effect of silica and phosphate on the transformation of schoepite to becquerelite and other uranyl phases. *Radiochimica Acta* **74**: 45-49.
- Sowers, T., Alley, R.B., and Jubenville, J. (2003) Ice core records of atmospheric N₂O covering the last 106,000 years. *Science* **301**: 945-948.

- Springael, D., and Top, E.M. (2004) Horizontal gene transfer and microbial adaptation to xenobiotics: new types of mobile genetic elements and lessons from ecological studies. *Trends Microbiol* **12**: 53-58.
- Staley, J.T., and Konopka, A. (1985) Measurement of *in situ* activities of nonphotosynthetic microorganisms in aquatic and terrestrial habitats. *Annu Rev Microbiol* **39**: 321-346.
- Standing, D.a.K., K. (2007) The Soil Environment. In *Modern Soil Microbiology*. van Elsas, J.D., Jansson, J.K., and Trevors, J.T. (ed). Boca Raon, FL: CRC Press, pp. 1-22.
- Stephen, J.R., and Macnaughton, S.J. (1999) Developments in terrestrial bacterial remediation of metals. *Curr Opin Biotechnol* **10**: 230-233.
- Stetter, K.O. (1999) Extremophiles and their adaptation to hot environments. *FEBS Lett* **452**: 22-25.
- Steven, B., Leveille, R., Pollard, W.H., and Whyte, L.G. (2006) Microbial ecology and biodiversity in permafrost. *Extremophiles* **10**: 259-267.
- Suzuki, Y., and Banfield, J.F. (1999) Geomicrobiology of uranium. Uranium, Mineralogy, Geochemistry and the Environment. In *Reviews in Mineralogy*. Burns, P., Finch, R., Eds. (ed). Washington, D.C.: Mineralogy Society of America, pp. 393-424.
- Suzuki, Y., and Banfield, J.F. (2004) Resistance to, and accumulation of, uranium by bacteria from a uranium-contaminated site. *Geomicrobiol J* **21**: 113-121.
- Tamegai, H., Kato, C., and Horikoshi, K. (2004) Lateral gene transfer in the deep sea of mariana trench: Identification of *nar* gene cluster encoding membrane-bound nitrate reductase from *Pseudomonas* sp. strain MT-1. *DNA Seq* **15**: 338-343.
- Tatusova, T.A., and Madden, T.L. (1999) BLAST 2 SEQUENCES, a new tool for comparing protein and nucleotide sequences (vol 174, pg 247, 1999). *FEMS Microbiol Lett* **177**: 187-188.
- Teske, A., Wawer, C., Muyzer, G., and Ramsing, N.B. (1996) Distribution of sulfate-reducing bacteria in a stratified fjord (Mariager fjord, Denmark) as evaluated by most-probable-number counts and denaturing gradient gel electrophoresis of PCR-amplified ribosomal DNA fragments. *Appl Environ Microbiol* **62**: 1405-1415.

- Teske, A., Hinrichs, K.U., Edgcomb, V., de Vera Gomez, A., Kysela, D., Sylva, S.P. et al. (2002) Microbial diversity of hydrothermal sediments in the Guaymas Basin: evidence for anaerobic methanotrophic communities. *Appl Environ Microbiol* **68**: 1994-2007.
- Thomas, C.M., and Nielsen, K.M. (2005) Mechanisms of, and barriers to, horizontal gene transfer between bacteria. *Nat Rev Microbiol* **3**: 711-721.
- Thompson, J.D., Higgins, D.G., and Gibson, T.J. (1994) Clustal-W- Improving the sensitivity of progressive multiple sequence alignment through sequence weighting, position-specific gap penalties and weight matrix choice. *Nucleic Acids Res* **22**: 4673-4680.
- Thompson, J.D., Gibson, T.J., Plewniak, F., Jeanmougin, F., and Higgins, D.G. (1997) The CLUSTAL_X windows interface: flexible strategies for multiple sequence alignment aided by quality analysis tools. *Nucleic Acids Res* **25**: 4876-4882.
- Tian, W.D., and Skolnick, J. (2003) How well is enzyme function conserved as a function of pairwise sequence identity? *J Mol Biol* **333**: 863-882.
- Tian, W.D., Arakaki, A.K., and Skolnick, J. (2004) EFICAz: a comprehensive approach for accurate genome-scale enzyme function inference. *Nucleic Acids Res* **32**: 6226-6239.
- Torres, J., Brusoni, M., Peluffo, F., Kremer, C., Dominguez, S., Mederos, A., and Kremer, E. (2005) Phosphodiesterolytic activity of lanthanide (III) complexes with alpha-amino acids. *Inorg Chim Acta* **358**: 3320-3328.
- Totter, S., Harvie, D.R., Robinson, N.J. (2007) Molecular microbiology of heavy metals. In *Understanding how cells allocate metals*. Nies, D.H.a.S., S. (ed). Berlin: Springer-Verlag, pp. 3-35.
- Trimarco, E., Balkwill, D., Davidson, M., and Onstott, T.C. (2006) In situ enrichment of a diverse community of bacteria from a 4-5 km deep fault zone in South Africa. *Geomicrobiol J* **23**: 463-473.
- Tsai, K.J., Lin, Y.F., Wong, M.D., Yang, H.H.C., Fu, H.L., and Rosen, B.P. (2002) Membrane topology of the pl258 CadA Cd(II)/Pb(II)/Zn(II)-translocating P-type ATPase. *J Bioenerg Biomembr* **34**: 147-156.
- Tsuruta, T. (2002) Removal and recovery of uranyl ion using various microorganisms. *J Biosci Bioeng* **94**: 23-28.

- Tsuruta, T. (2004) Adsorption of uranium from acidic solution by microbes and effect of thorium on uranium adsorption by *Streptomyces levoris*. *J Biosci Bioeng* **97**: 275-277.
- Tsuruta, T. (2006) Removal and recovery of uranium using microorganisms isolated from Japanese uranium deposits. *J Nucl Sci Technol* **43**: 896-902.
- Tucker, M.D., Barton, L.L., and Thomson, B.M. (1998) Reduction of Cr, Mo, Se and U by *Desulfovibrio desulfuricans* immobilized in polyacrylamide gels. *J Ind Microbiol Biotechnol* **20**: 13-19.
- Turick, C.E., Graves, C., Apel, W.A. (1998) Bioremediation potential of Cr(VI)-contaminated soil using indigenous microorganisms. *Bioremediation* **2**: 1-6.
- Tyson, G.W., Chapman, J., Hugenholtz, P., Allen, E.E., Ram, R.J., Richardson, P.M. et al. (2004) Community structure and metabolism through reconstruction of microbial genomes from the environment. *Nature* **428**: 37-43.
- Uno, Y., Kiyono, M., Tezuka, T. and Pan-Hou, H. (1997) Phenylmercury transport mediated by *merT-merP* genes of *Pseudomonas* K-62 plasmid pMR26. *Biol Pharm Bull* **20**: 107-109.
- Utgikar, V.P., Tabak, H.H., Haines, J.R., and Govind, R. (2003) Quantification of toxic and inhibitory impact of copper and zinc on mixed cultures of sulfate-reducing bacteria. *Biotechnol Bioeng* **82**: 306-312.
- Valencia, A. (2005) Automatic annotation of protein function. *Curr Opin Struct Biol* **15**: 267-274.
- Valentine, D.L., and Reeburgh, W.S. (2000) New perspectives on anaerobic methane oxidation. *Environ Microbiol* **2**: 477-484.
- van der Maarel, M., Artz, R.R.E., Haanstra, R., and Forney, L.J. (1998) Association of marine archaea with the digestive tracts of two marine fish species. *Appl Environ Microbiol* **64**: 2894-2898.
- Van Dover, C.L., German, C.R., Speer, K.G., Parson, L.M., and Vrijenhoek, R.C. (2002) Marine biology - Evolution and biogeography of deep-sea vent and seep invertebrates. *Science* **295**: 1253-1257.
- van Elsas, J.D., and Bailey, M.J. (2002) The ecology of transfer of mobile genetic elements. *FEMS Microbiol Ecol* **42**: 187-197.

- van Waasbergen, L.G., Balkwill, D.L., Crocker, F.H., Bjornstad, B.N., and Miller, R.V. (2000) Genetic diversity among *Arthrobacter* species collected across a heterogeneous series of terrestrial deep-subsurface sediments as determined on the basis of 16S rRNA and *recA* gene sequences. *Appl Environ Microbiol* **66**: 3454-3463.
- Vandamme, P., and Coenye, T. (2004) Taxonomy of the genus *Cupriavidus*: a tale of lost and found. *Int J Syst Evol Microbiol* **54**: 2285-2289.
- Venkateswaran, K., Moser, D.P., Dollhopf, M.E., Lies, D.P., Saffarini, D.A., MacGregor, B.J. et al. (1999) Polyphasic taxonomy of the genus *Shewanella* and description of *Shewanella oneidensis* sp. nov. *Int J Syst Bacteriol* **49**: 705-724.
- Viamajala, S., Peyton, B.M., Sani, R.K., Apel, W.A., and Petersen, J.N. (2004) Toxic effects of chromium(VI) on anaerobic and aerobic growth of *Shewanella oneidensis* MR-1. *Biotechnol Prog* **20**: 87-95.
- Voroney, R.P. (2007) The Soil Habitat. In *Soil Microbiology, Ecology, and Biochemistry*. Paul, E.A. (ed). Boston, MA: Academic Press, pp. 25-49.
- Wade, R., and DiChristina, T.J. (2000) Isolation of U(VI) reduction-deficient mutants of *Shewanella putrefaciens*. *FEMS Microbiol Lett* **184**: 143-148.
- Walker, J.J., Spear, J.R., and Pace, N.R. (2005) Geobiology of a microbial endolithic community in the Yellowstone geothermal environment. *Nature* **434**: 1011-1014.
- Wall, J.D., and Krumholz, L.R. (2006) Uranium reduction. *Annu Rev Microbiol* **60**: 149-166.
- Wan, J.M., Tokunaga, T.K., Brodie, E., Wang, Z.M., Zheng, Z.P., Herman, D. et al. (2005) Reoxidation of bioreduced uranium under reducing conditions. *Environ Sci Technol* **39**: 6162-6169.
- Wanger, G., Southam, G., and Onstott, T.C. (2006) Structural and chemical characterization of a natural fracture surface from 2.8 kilometers below land surface: Biofilms in the deep subsurface. *Geomicrobiol J* **23**: 443-452.
- Wanner, B.L. (1996) Phosphorus assimilation and control of the phosphate regulon. In *Escherichia coli and Salmonella, Cellular and Molecular Biology, 2nd ed., vol. 1*. Neidhardt, F.C., Curtiss III, R., Ingraham, J.L., Lin, E.C.C., Low, K.B., Magasanik, B. et al. (eds) (ed). Washington, DC: ASM Press, pp. 1357-1381.

- Watanabe, K., Kodama, Y., Hamamura, N., and Kaku, N. (2002) Diversity, abundance, and activity of archaeal populations in oil-contaminated groundwater accumulated at the bottom of an underground crude oil storage cavity. *Appl Environ Microbiol* **68**: 3899-3907.
- WDCGG (2008). World Data Centre for Greenhouse Gases. URL <http://gaw.kishou.go.jp/wdcgg/>
- Weber, G., and Drickamer, H.G. (1983) The effect of high-pressure upon proteins and other biomolecules. *Q Rev Biophys* **16**: 89-112.
- Welch, T.J., Farewell, A., Neidhardt, F.C., and Bartlett, D.H. (1993) Stress response of *Escherichia coli* to elevated hydrostatic pressure. *J Bacteriol* **175**: 7170-7177.
- White, C., Sharman, A.K, Gadd, G.M (1998) An integrated microbial process for the bioremediation of soil contaminated with toxic metal. *Nat Biotechnol* **16**: 572-575.
- Whitman, W.B., Coleman, D.C., and Wiebe, W.J. (1998) Prokaryotes: The unseen majority. *Proc Natl Acad Sci U S A* **95**: 6578-6583.
- Wolff, E., and Spahni, R. (2007) Methane and nitrous oxide in the ice core record. *Philosophical Transactions of the Royal Society a-Mathematical Physical and Engineering Sciences* **365**: 1775-1792.
- Wu, W.M., Carley, J., Gentry, T., Ginder-Vogel, M.A., Fienen, M., Mehlhorn, T. et al. (2006) Pilot-scale in situ bioremediation of uranium in a highly contaminated aquifer. 2. Reduction of U(VI) and geochemical control of U(VI) bioavailability. *Environ Sci Technol* **40**: 3986-3995.
- Yakimov, M.M., Giuliano, L., Crisafi, E., Chernikova, T.N., Timmis, K.N., Golyshin, P.N. (2002) Microbial community of a saline mud volcano at San Biagio-Belpasso, Mt. Etna (Italy). *Environ Microbiol* **4**: 249-256.
- Yazzie, M., Gamble, S.L., Civitello, E.R., and Stearns, D.M. (2003) Uranyl acetate causes DNA single strand breaks in vitro in the presence of ascorbate (vitamin C). *Chem Res Toxicol* **16**: 524-530.
- Yong, P., and Macaskie, L.E. (1995) Enhancement of uranium bioaccumulation by a *Citrobacter* sp. via enzymatically mediated growth of polycrystalline $\text{NH}_4\text{UO}_2\text{PO}_4$. *J Chem Technol Biotechnol* **63**: 101-108.

- Yoon, K.P., Misra, T.K., and Silver, S. (1991) Regulation of the *cadA* cadmium resistance determinant of *Staphylococcus aureus* plasmid pI258. *J Bacteriol* **173**: 7643-7649.
- Yumoto, I., Yamazaki, K., Hishinuma, M., Nodasaka, Y., Suemori, A., Nakajima, K. et al. (2001) *Pseudomonas alcaliphila* sp. nov., a novel facultatively psychrophilic alkaliphile isolated from seawater. *Int J Syst Evol Microbiol* **51**: 349-355.
- Zatyka, M., and Thomas, C.M. (1998) Control of genes for conjugative transfer of plasmids and other mobile elements. *FEMS Microbiol Rev* **21**: 291-319.
- Zengler, K., Toledo, G., Rappe, M., Elkins, J., Mathur, E.J., Short, J.M., and Keller, M. (2002) Cultivating the uncultured. *Proc Natl Acad Sci U S A* **99**: 15681-15686.
- Zhang, C.L. (2002) Stable carbon isotopes of lipid biomarkers: analysis of metabolites and metabolic fates of environmental microorganisms. *Curr Opin Biotechnol* **13**: 25-30.
- Zhang, R.F., Wang, Y.L., and Gu, J.D. (2006) Identification of environmental plasmid-bearing *Vibrio* species isolated from polluted and pristine marine reserves of Hong Kong, and resistance to antibiotics and mercury. *Antonie Van Leeuwenhoek* **89**: 307-315.
- Zhilina, T.N., Garnova, E.S., Tourova, T.P., Kostrikina, N.A., and Zavarzin, G.A. (2001) *Halonatronum saccharophilum* gen. nov., sp. nov.: A new haloalkaliphilic bacterium of the order *Haloanaerobiales* from Lake Magadi. *Microbiology (Russ Acad Sci)* **70**: 64-72.
- Zubkov, M.V., Fuchs, B.M., Archer, S.D., Kiene, R.P., Amann, R., and Burkill, P.H. (2002) Rapid turnover of dissolved DMS and DMSP by defined bacterioplankton communities in the stratified euphotic zone of the North Sea. *Deep-sea Res (II Top Stud Oceanogr)* **49**: 3017-3038.

VITA

ROBERT J. MARTINEZ

MARTINEZ was born in Albany, New York. The eldest of three children, he attended Colonie Central High School in Albany, New York and received a B.A. in Biology with a specialization in Marine Science from Boston University in 1996. Prior to entering the graduate program at the Georgia Institute of Technology, he worked for five years examining integrin-mediated signal cascades in the laboratory of Dr. Susan E. LaFlamme at the Albany Medical College in Albany, New York. Within the laboratory of Dr. Patricia A. Sobecky at the Georgia Institute of Technology, he studied the microbial ecology of extreme environments within aquatic cold seep systems as well as metal- and radionuclide-contaminated terrestrial deep subsurface systems.